TESIS DE LA UNIVERSIDAD DE ZARAGOZA

2022

124

Francisco Merino Casallo

Cell Migration within 3D Microenvironments: an Integrative Perspective from the Membrane to the Nucleus

Director/es

García Aznar, José Manuel

Gómez Benito, María José

ISSN 2254-7606

Prensas de la Universidad Universidad Zaragoza

ISSN 2254-7606

Universidad Zaragoza
1542

Tesis Doctoral

CELL MIGRATION WITHIN 3D MICROENVIRONMENTS: AN INTEGRATIVE PERSPECTIVE FROM THE MEMBRANE TO THE NUCLEUS

Autor

Francisco Merino Casallo

Director/es

García Aznar, José Manuel
Gómez Benito, María José

UNIVERSIDAD DE ZARAGOZA
Escuela de Doctorado

Programa de Doctorado en Ingeniería Biomédica

2022

Mesenchymal Cell Migration within 3D Microenvironments:

an Integrative Perspective from the Membrane to the Nucleus

Universidad Zaragoza

Francisco Merino Casallo

Aragón Institute of Engineering Research (I3A)

University of Zaragoza

Faculty Advisors: J. M. García Aznar & M. J. Gómez Benito

A thesis submitted for the degree of

Doctor of Philosophy in Biomedical Engineering

Spring 2022

A mi familia

Las ideas no se muestran fecundas con quien las sugiere o las aplica por primera vez, sino con los tenaces que las sienten con vehemencia y en cuya virtualidad ponen toda su fe y todo su amor. Bajo este aspecto, bien puede afirmarse que las conquistas científicas son creaciones de la voluntad y ofrendas de la pasión.

Santiago Ramón y Cajal

Capítulo IV

Recuerdos de mi vida (1901-1904)

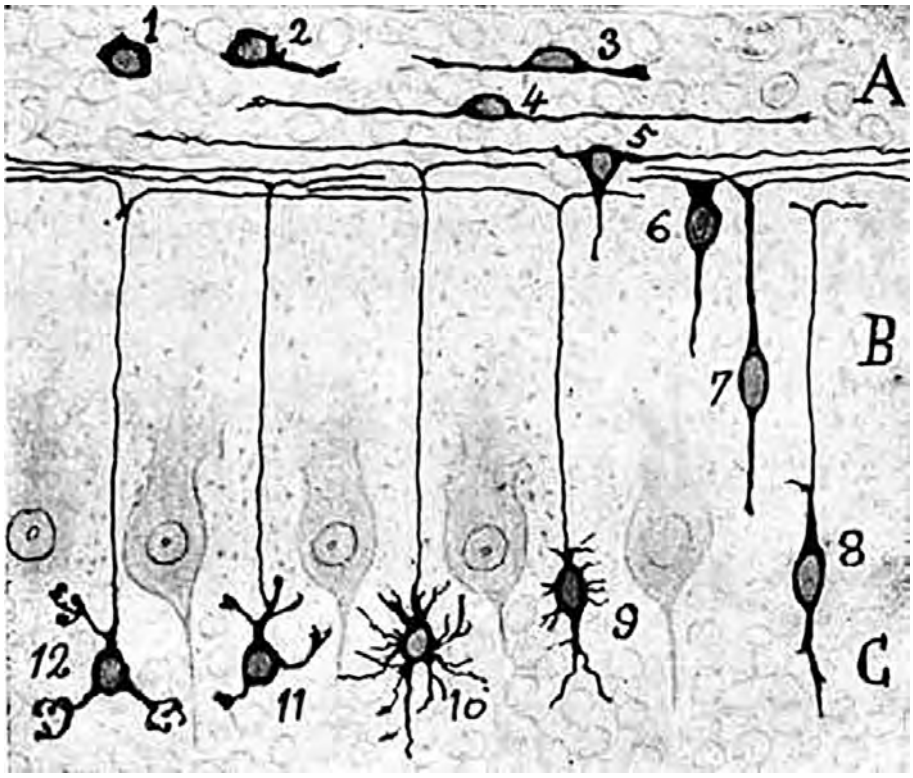

Migration and transformation of the granule cells of the cerebellum.
From Ramón y Cajal, 1917. Recuerdos de mi vida (1901-1904), Capítulo VIII.

Abstract

Cell migration is fundamental for life and development. Unfortunately, cell motility is also associated with some of the leading causes of morbidity and mortality, including immune, skeletal, and cardiovascular disorders as well as cancer metastasis. Cells rely on their ability to perceive and respond to external stimuli in many physiological and pathological processes (e.g., embryonic development, angiogenesis, tissue repair, and tumor progression). The global objective of this doctoral thesis was to investigate the migratory response of individual cells to biochemical and biophysical cues. In particular, the focus of this research was on the mechanisms enabling cells to perceive and internalize biochemical and biophysical cues and the influence of these stimuli on the migratory response of individual cells.

The first study aimed at establishing a methodology to facilitate the integration of theoretical studies with experimental data. By minimizing user intervention, the proposed framework based on Bayesian optimization techniques efficiently handled the otherwise tedious and error-prone calibration of in silico models. Afterward, an in silico model was built to investigate how biochemical and biophysical stimuli influence three-dimensional cell motion. This computational model integrated some of the main actors enabling cells to probe and respond to external cues, which may act at different scales and interact with each other. The results showed, on the one hand, that cells change their migratory behavior based on the slope of chemical gradients and the absolute concentration of chemical factors (e.g., growth factors) around them. On the other hand, these results revealed that cells' migratory response to matrix stiffness and density depends on their phenotype. Overall, this thesis highlights the dependence of three-dimensional cell migration on both cells' phenotype (i.e., nucleus size, deformability) and the properties of the surrounding microenvironment (e.g., chemical profile, matrix rigidity, confinement).

Resumen (Abstract in Spanish)

La migración celular es fundamental para la vida y el desarrollo. Desafortunadamente, la movilidad celular también está asociada con algunas de las principales causas de morbilidad y mortalidad, incluidos los trastornos inmunitarios, esqueléticos y cardiovasculares, así como la metástasis del cáncer. Las células dependen en su capacidad para percibir y responder a estímulos externos en muchos procesos fisiológicos y patológicos (p. ej., desarrollo embrionario, angiogénesis, reparación de tejidos y progresión tumoral). El objetivo global de esta tesis doctoral fue investigar la respuesta migratoria de células individuales a señales bioquímicas y biofísicas. En particular, el enfoque de esta investigación se centró en los mecanismos que permiten a las células percibir e internalizar señales bioquímicas y biofísicas y la influencia de estos estímulos en la respuesta migratoria de las células individuales.

El primer estudio tuvo como objetivo establecer una metodología para facilitar la integración de estudios teóricos con datos experimentales. Al minimizar la intervención del usuario, el sistema propuesto basado en técnicas de optimización Bayesiana gestionó de manera eficiente la calibración de los modelos *in silico*, que de otro modo sería tediosa y propensa a errores. Posteriormente, se construyó un modelo *in silico* para investigar cómo los estímulos bioquímicos y biofísicos influyen en el movimiento celular en tres dimensiones. Este modelo computacional integró algunos de los principales actores que permiten a las células percibir y responder a señales externas, que pueden actuar a diferentes escalas e interactuar entre sí. Los resultados mostraron, por un lado, que las células cambian su comportamiento migratorio en función de la pendiente de los gradientes químicos y la concentración absoluta de factores químicos (por ejemplo, factores de crecimiento) a su alrededor. Por otro lado, estos resultados revelaron que la respuesta migratoria de las células a la rigidez y densidad de la matriz depende de su fenotipo. En general, la tesis destaca la dependencia de la migración celular tridimensional al fenotipo de las células (es decir, el tamaño de su núcleo, la deformabilidad del mismo) y las propiedades del microambiente circundante (por ejemplo, el perfil químico, la rigidez de la matriz, el confinamiento).

List of Acronyms

1D One-Dimensional

2D Two-Dimensional

3D Three-Dimensional

AMT Amoeboid to Mesenchymal Transition

Arp2/3 Actin Related Protein 2/3

BM Basement Membrane

BO Bayesian Optimization

CAT Collective to Amoeboid Transition

Cdc42 Cell Division Control Protein 42 Homolog

DC Dendritic Cell

DNA Deoxyribonucleic Acid

EAT Epithelial to Amoeboid Transition

EC Endothelial Cell

ECM Extracellular Matrix

EGF Epidermal Growth Factor

EGFR Endothelial Growth Factor Receptor

EMT Endothelial to Mesenchymal Transition

Ena/VASP Enabled/Vasodilator-stimulated Phosphoprotein

FA Focal Adhesion

FAK Focal Adhesion Kinase

GAP GTPase-activating Protein

GEF Guanine Nucleotide Exchange Factor

GPCR G Protein-coupled Receptor

GTPases Guanosine Triphosphatases

HPC High Performance Computing

HSC Hematopoietic Stem Cell

IAC Integrin Adhesion Complex

IF Intermediate Filament

LINC Linker of Nucleoskeleton and Cytoskeleton

LOX Lysyl Oxidase

MAT Mesenchymal to Amoeboid Transition

mDia1 Diaphanous-related Formin-1

mDia2 Diaphanous-related Formin-2

MEC Mammary Epithelial Cells

ML Machine Learning

MMP Matrix Metalloproteinases

mRNA Messenger Ribonucleic Acid

MSC Mesenchymal Stem Cell

MT Microtubule

MTOC Microtubule-organizing Center

NCC Neural Crest Cell

NCP Neurocristopathies

NHDF Normal Human Dermal Fibroblasts

NPC Nuclear Pore Complex

PDGF Platelet-derived Growth Factor

PEG Polyethyleneglycol

PI(4,5)P_2 Phosphatidylinositol 4,5-bisphosphate

PI3K Phosphoinositide 3-kinase (also called Phosphatidylinositol 3-kinase)

PM Plasma Membrane

Rac1 Ras-related C3 Botulinum Toxin Substrate 1

rBM Reconstituted Basement Membrane

RhoA Ras Homolog Family Member A

RhoBTB1 Rho-related BTB Domain-containing Protein 1

ROCK Rho-associated Protein Kinase

ROI Region of Interest

RTK Receptor Tyrosine Kinase

Src Proto-oncogene Tyrosine-protein Kinase Src

SUN1/2 Sad1 and UNC84 Domains Containing 1 and 2

TAZ Tafazzin

TG2 Tissue Transglutaminase

TGFβ Transforming Growth Factor Beta

VEGF Vascular Endothelial Growth Factor

VEGFR Vascular Endothelial Growth Factor Receptor

YAP Yes-associated Protein

Contents

List of Figures

List of Tables

1 Introduction

Contents

1.1 Relevance of cell migration and its clinical significance

Cell migration is fundamental for life and development. Key physiological processes of multicellular organisms depend on cell migration, from embryonic development to the more specific bone formation and angiogenesis. For example, neural crest cells (NCC) migrate through prescribed regions of vertebrate embryos and contribute to tissue and organ formation (Figure 1.1a) [1, 2]. Also, migration of progenitor and stem cells (e.g., mesenchymal and hematopoietic stem cells; MSC and HSC) to the bone surface and throughout the bone matrix is a key step for bone formation and remodeling (Figure 1.1d). Once at their final location, these progenitor and stem cells differentiate into different cell types, which coordinately turn cartilage templates into an organized bone matrix. During angiogenesis, endothelial cells (EC) migrate from a pre-existing vascular bed to form new capillaries [3]. Indeed, ECs sprout out in response to signaling molecules secreted when tissues need more oxygen or become wounded (Figure 1.1b). Indeed, different types of ECs known as tip and stalk cells collaborate to create a vascular network with a tubular structure. Thus, cell motility is not only deeply involved in the development of multicellular organisms but also in their maintenance through protection and healing mechanisms.

Cells' ability to migrate is also critical during the immune response and tissue repair. For one, the migration and accurate positioning of dendritic cells (DCs; bone marrow-derived leukocytes) is fundamental for immune surveillance [4]. Moreover, the immune response depends on leukocyte recruitment to tissues under pathological conditions [5, 6]. During the initial inflammatory phase of acute traumatic injury, immune cells (e.g., lymphocytes, macrophages, neutrophils) clear dead cells, pathogens, and debris from the site of injury (Figure 1.1e) [7]. Afterward, reparative cells such as fibroblasts actively divide and migrate into the wound bed to deposit a disorganized provisional matrix tissue and promote wound contraction [7]. All these migratory events are tightly regulated, and minor perturbations may result in different pathological conditions.

Aberrant cell motility is associated with a wide array of pathologies. For example, minor perturbations in the regulators of NCC migration can lead to a wide variety of syndromes and diseases called Neurocristopathies (NCP; e.g., Branchio-Oculo-Facial Syndrome, Hirschsprung's Disease, Mowat-Wilson syndrome, and piebaldism) [8–11]. The broad spectrum of congenital malformations associated with NPCs affects a significant percentage of newborns. Also, abnormal motility of MSCs would drive a homeostatic imbalance of bone and may cause different skeletal disorders, including osteoporosis, fracture, and osteoarthritis [12]. By controlling the growth

and regression of blood capillaries, angiogenic therapies could improve the survival of poorly perfused essential tissues (e.g., heart, brain, skeletal muscle). These therapies could also free the body of unwanted tissues (i.e., tumors). Migration disorders of immune cells can be associated with autoimmune diseases (e.g., Crohn's disease, multiple sclerosis, rheumatoid arthritis, type I diabetes, and psoriasis) and chronic inflammation [13]. A dysregulated migration of DCs could lead to their abnormal activation or positioning [14]. Such behaviors would result in an imbalance of immune responses and even immune pathologies, including allergic and infectious diseases, as well as tumors. Cell migration is also linked to another leading cause of death: cancer metastasis (Figure 1.1c). The ability to block metastatic cells from leaving the primary tumor or intravasating into blood or lymph vessels would represent a huge step forward in our fight against cancer. These pathologies result in a huge socio-economic burden to our communities.

Pathologies associated with abnormal cell motility have a huge impact on our societies. For instance, cancer, heart diseases, and more than 70 of life's most threatening medical conditions could be cured by angiogenic therapies [15]. According to the Angiogenesis Foundation, angiogenic therapies could improve the lives of at least 1 billion people worldwide. In the United States, autoimmune diseases are a leading cause of death among young and middle-aged women [16]. The Autoimmune Association estimates that autoimmune diseases affect more than 24 million people in the United States, with roughly 80 % of all patients being women [17, 18]. Moreover, in 2001, the annual cost of treating autoimmune diseases in the United States was estimated at more than $100 billion. Globally, there were an estimated 19.3 million new cases of cancer in 2020 alone [19]. Accounting for about 90% of cancer deaths (9 million deceases worldwide in 2020), metastasis is the leading cause of cancer morbidity and mortality [20]. The economic burden of cancer in the United States and the European Union was estimated at $497.14 billion and €145.29 billion per year, respectively [21–23]. Remarkably, a dysregulation of DCs migration was also related to the coronavirus disease 2019 (COVID-19), which has caused the first pandemic of the 21st century with more than 350 million confirmed cases and 5.6 million deaths to date [24]. A comprehensive understanding of this biological process is therefore essential.

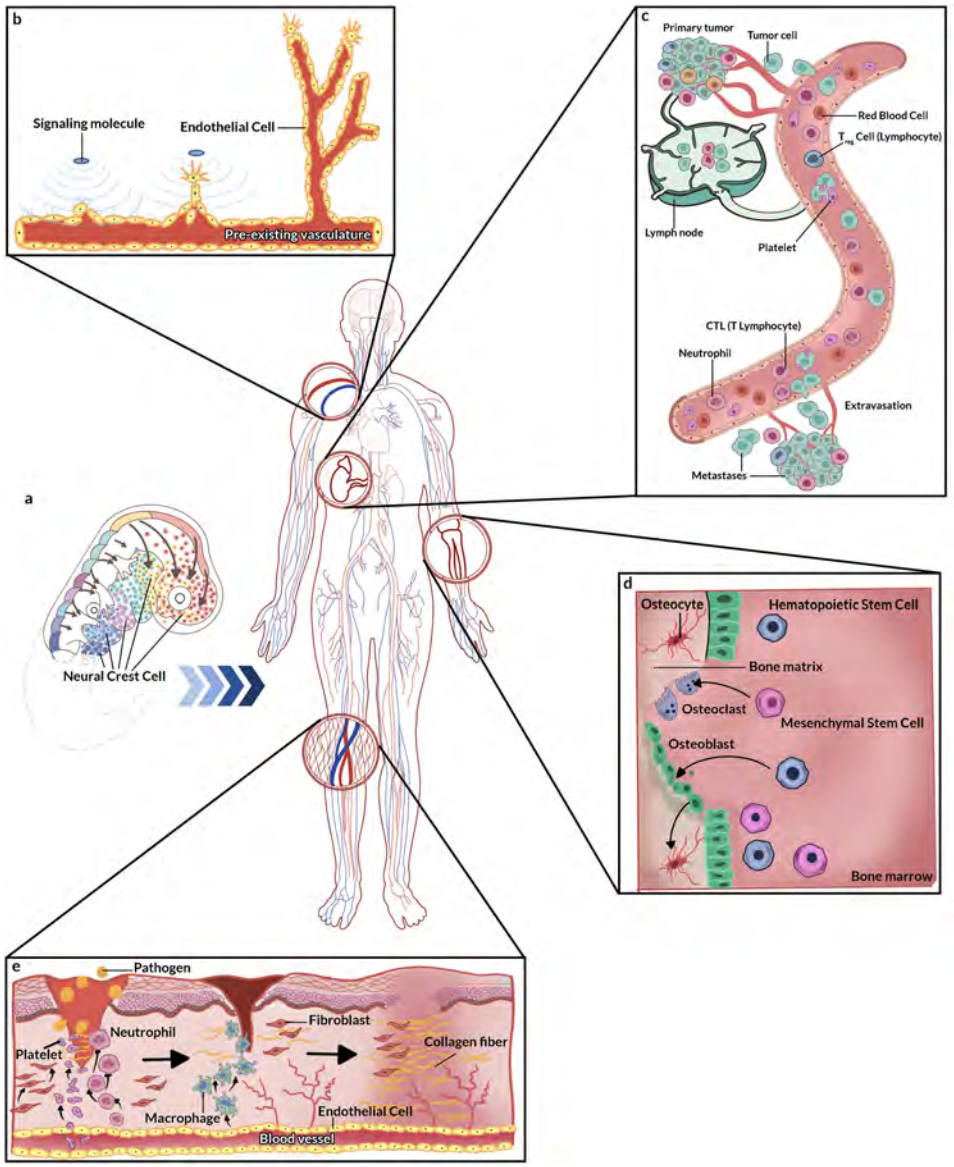

Figure 1.1: Clinical relevance of cell migration (a) Neural crest cells (NCC) migrate through prescribed regions of vertebrate embryos and contribute to tissue and organ formation. **(b)** During angiogenesis, endothelial cells (EC) migrate from a pre-existing vascular bed to form new capillaries. **(c)** Cell migration is also linked to some of the leading causes of death such as cancer metastasis. **(d)** Progenitor and stem cells (e.g., mesenchymal and hematopoietic stem cells; MSC and HSC) migrate to the bone surface and throughout the bone matrix during bone formation and remodeling, respectively. **(e)** Cell motility is fundamental for wound healing and tissue repair.

Biochemical cues and the biophysical properties of the surrounding microenvironment have a leading role in cells' migratory response during many of the aforementioned scenarios. For example, gradients of chemical factors throughout the extracellular matrix (ECM) guide the formation of new vessels during angiogenesis, and enable immune cells to locate foreign invaders. Unfortunately, angiogenesis also promotes invasive tumor growth and metastasis, and an excessive recruitment of leukocytes results in tissue damage and chronic inflammatory disease. Likewise, an heterogeneous biophysical profile of the matrix (e.g., differences in stiffness, density, composition, organization) is essential in physiological processes such as embryonic development [25]. Still, tweaking some of these properties (e.g., increasing matrix rigidity) may lead to pathological processes such as cancer dissemination. Hence, an in-depth knowledge of how these stimuli influence cell migration would drastically improve our life expectancy and quality of life. Such an exhaustive understanding of cell migration will require a collaborative effort between theoreticians and experimentalists.

CLINICAL CHALLENGE

Developing new therapies to control cell motility *in vivo*

The translation of migrating principles to therapeutic solutions would enable a cure for some of the leading causes of morbidity and mortality, improving the lives of billions of people worldwide. Some of these therapies could avoid congenital malformations affecting some newborns. Also, we could enhance bone regeneration and tempo-spatially restrict the growth and regression of blood capillaries. These therapeutic solutions could hinder the metastatic invasion of cancer cells. Further, they could allow for bioartificial organs.

1.2 Need for theoretical studies and computational models

Theoretical studies and computational models (also known as *in silico* models) can help us overcome some of the challenges of experimental research and advance our understanding of complex biological phenomena such as cell migration. For instance, theoretical studies and computational predictions connect experimental results to first principles. They can also describe the behavior of biological systems as a function of just a few variables—a scenario sometimes unattainable with current experimental techniques. Computational models allow us to efficiently quantify elements that may otherwise be technically difficult to measure experimentally. Also, *in silico* models enable us to carry out experiments that are extremely time-consuming, financially prohibitive, or otherwise technically impossible. Simulations

can be executed in high throughput computing (HPC) environments, and their results automatically analyzed. Furthermore, these models can be a valuable resource to design future experiments and predict their outcomes. For example, by identifying key parameters that play a central role in defining the overall behavior of the biological system. These studies could also drastically reduce the sample space of potential targets, allowing researchers to focus on a more manageable set of experiments. Therefore, theoretical research is a valuable asset for deciphering the intricacies of complex biological phenomena.

Unraveling the intricacies of some of the mechanisms involved in these biological processes can be extremely difficult. The multi-scale nature of these phenomena stands out as one of the main obstacles in this effort. At the atomic scale, researchers can study the structure and dynamic properties of different polymers (e.g., proteins, peptides, lipids) and their dependency on the features of the environment or ligand binding. Conversely, the molecular scale allows researchers to investigate signaling mechanisms regulating biological systems. The microscopic scale may include the cellular and multicellular or tissue scales, describing both single-cell and tissue behaviors and properties. Lastly, the macroscopic scale considers the dynamics of the gross organ or tumor behavior (e.g., their morphology, shape, vascularization). Further, elucidating multi-scale interactions and reciprocity can be remarkably challenging, particularly in large systems. Multi-scale models enable researchers to integrate players and events associated with different scales. Sustained advances and improvements in the computational power and data storage capabilities enhance the potential of *in silico* models. As a result, these computational replicas characterize and quantify biological systems much more accurately. Overall, multi-scale models have become an extremely valuable tool to investigate complex biological systems.

Over the last several decades, the research community has developed a wide variety of *in silico* models, aiming to further our knowledge of cell migration. Theoreticians and modelers may be interested in players and events occurring at a specific scale, such as the molecular or the microscopic one. Regarding the molecular scale, Borau and colleagues [26] studied the mechanosensing properties of the actomyosin network. Fatunmbi and colleagues [27] were interested in the recruitment of actin nucleating proteins at the membrane interface. Conversely, Hopkins and Camley [28] studied cells' ability to accurately process external signals in uncertain environments using an *in silico* model. At the microscopic scale, Aubry and colleagues [29] focused on the mechanical behavior of the cytoplasm and the nucleus during confined cell migration to study the link between cell morphology and the relationship between cell-channel and cell-substrate surface forces. Gonzalez-Valverde and Garcia-Aznar [30] were interested in epithelial

tissue mechanics associated with collective cell motility. Zheng and colleagues [31] studied the influence of ECM-mediated mechanical communication between cells on multicellular dynamics. Lastly, Gonçalves and Garcia-Aznar [32] established a relation between ECM density and individual cell migration. Still, the current trend is toward multi-scale models [33–36]. Notably, Fletcher and Osborne [37] reviewed the recent progress of the research community in multi-scale models of tissues. Hence, theoretical studies and computational models have enabled important advances in the quest for a comprehensive understanding of cell migration.

1.3 Motivation

Cell migration is an extremely complex phenomenon involving a wide variety of biological processes. Factors such as cell phenotype or the properties of the surrounding ECM regulate the activation of some of these processes. Note that cells produce the ECM to surround themselves with a scaffolding structure [38–40]. Therefore, cells can modulate the properties of their surrounding ECM. Different external cues, including chemical and biophysical stimuli from their microenvironment, influence cell migration [41], promoting cell invasion, immune cell motility, and facilitating tumor cell dissemination [42–45]. Notably, cells' phenotype, as well as their microenvironment, determine if and how cells migrate [46–49].

More than a century of research in the field [52–60] has allowed us to understand many of the intricacies of cell migration. However, because of its inherent complexity, plenty of unanswered questions still need to be addressed. Besides, much of what we know about cell migration (and of cell biology, for that matter) is based on cells cultured on Petri dishes or rigid flat sheets of plastic. Still, many are the differences between these two-dimensional (2D) substrates and the more physiological three-dimensional (3D) matrices (Figure 1.2). For one, soluble gradients are absent on plated cultures, whereas they may be present in 3D. While an apical-basal polarity is forced on 2D substrates, there is no prescribed polarity in 3D environments. Instead of the high stiffnesses (GPa range) associated with plated cultures, the stiffness of gels in 3D is in the lower kPa range. Also, 3D matrices are more pliable than 2D substrates. As a result, cells can alter ECM compliance more easily in 3D domains. Cells also behave differently within 3D matrices than on 2D substrates (Figure 1.2) [61–63], including during migration [41, 64, 65]. Although spreading and migration are unconstrained on the x-y plane on flat surfaces, they may be sterically hindered in 3D. Cells in 3D environments adopt a thinner and more elongated shape. They also follow a more persistent and direct trajectory than those on 2D surfaces. Adhesions are restricted to the x-y plane in 2D substrates but are distributed in

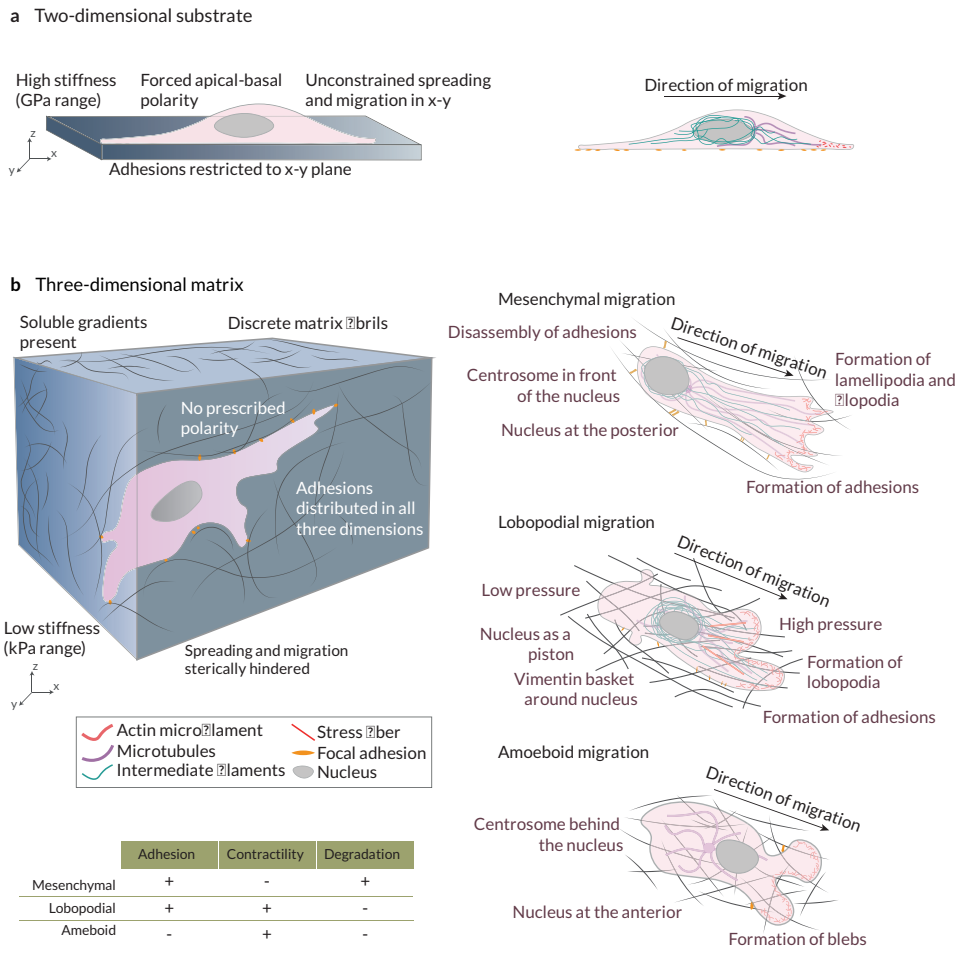

	Adhesion	Contractility	Degradation
Mesenchymal	+	-	+
Lobopodial	+	+	-
Ameboid	-	+	-

Figure 1.2: Cells in 2D vs 3D Cells in **(a)** 2D and **(b)** 3D microenvironments interact differently with their surroundings. Three modes of 3D migration have been identified so far: mesenchymal, amoeboid, and lobopodial migration. In mesenchymal migration, cells attach very strongly to the extracellular matrix through mature stress fiber-linked focal adhesions. These cells also exhibit a high matrix-degrading activity. The centrosome is in front of the nucleus and the cytoskeletal networks are polarized in the direction of migration. In contrast, amoeboid migration involves very few adhesions and low protease activity. Cells migrate through the formation of contraction-based blebs or use actin-driven protrusions to glide on the substrate. The centrosome is usually behind the nucleus during amoeboid migration. Lastly, during lobopodial migration, tightly adherent cells use actomyosin contractility, hydrostatic pressure, and nuclear pistoning to form bleb-like blunt protrusions called lobopodia. These cells exhibit very low protease activity. Adapted from [50, 51].

all three dimensions in these gels. Nuclear positioning is much more complex for cells migrating within 3D domains [66]. Another source of complexity in the study of cell migration is that its regulation depends on the biochemical and biophysical features of the pericellular space [67, 68]. Therefore, cells must integrate concurrent, potentially cooperative, or opposing inputs in their decision-making process [69–72]. These external cues can modulate cellular properties and events, from cell shape and polarity to cell-cell and cell-matrix interactions. Likewise, cells adjust their trajectory, speed, and mode of migration accordingly (Figure 1.2) [71, 73]. Even modest variations in the biochemical or biophysical stimuli can dramatically impact cells' migratory phenotype [74]. Thus, we still need to fill in some gaps in our knowledge of how cells (i) probe the surrounding environment, (ii) integrate these cues, as well as (iii) adapt and respond to them.

Replicating scenarios closer to *in vivo* conditions, though, is a challenging endeavor [63, 75–77]. For instance, if we focus on the mechanical response of *in vivo* environments, they have been identified as viscoelastic [78, 79] (they present properties observed in solids and fluids) and exhibit stress relaxation [80]. Interestingly, the impact of stress relaxation speed on 3D cell migration may be modulated by the material's steric hindrance [81]. Still, hydrogels used as synthetic substrates for 3D culture and tissue engineering *in vitro* are typically elastic. Measuring some features of these 3D matrices with the current technologies may be extremely difficult or even impossible [62, 79, 82–84]. Besides, in 3D domains, the underlying conditions must be more tightly controlled [51, 68, 85, 86]. Hence, studying cell migration under more physiologically relevant scenarios is not an easy task.

1.4 Research objectives

Global research objective

Investigate the influence of biochemical and biophysical stimuli from the surrounding microenvironment on mesenchymal migration within 3D matrices by combining *in vitro* and *in silico* models.

To achieve the global research objective of this doctoral thesis, three partial objectives were defined. The first goal of the research carried out by the Ph.D. candidate was to assess the suitability of Bayesian optimization techniques to integrate experimental data with theoretical studies and computational models. The second objective was to determine the influence of biochemical stimuli from the surrounding ECM on mesenchymal migration within 3D matrices. The third

goal was to establish how biophysical cues from the local microenvironment around cells regulate the motion of cells exhibiting a mesenchymal phenotype.

To address these objectives, three hypotheses have been defined and supported by the research presented in Chapter 3, Chapter 4, and Chapter 5 of this doctoral thesis.

Research hypothesis 1

A framework based on Bayesian optimization techniques enhances the integration of experimental data with *in silico* models.

Research hypothesis 2

A multi-scale computational framework that links intracellular signaling networks to cytoskeletal and nuclear dynamics predicts cells' migratory response to different biochemical stimuli.

Research hypothesis 3

A multi-scale computational framework that links cell-matrix adhesions to cytoskeletal and nuclear dynamics through mechanotransduction predicts cells' migratory response to different biophysical stimuli.

Testing these hypotheses enabled the candidate to tackle the aforementioned research objectives. Overall, the proposed research offers an integrative framework to improve our knowledge of cell migration within 3D environments. Moreover, this methodology combines experimental data with multi-scale computational models to shed some light on how cells internalize a variety of inputs and adapt their migratory behavior accordingly.

1.5 Outline

This thesis covers the research carried out by the candidate during his doctoral studies and is divided into six chapters. **Chapter 1** highlights the relevance of cell migration and its clinical significance, as well as the value of theoretical studies. It also presents the motivation and main objectives of the candidate's doctoral studies. **Chapter 2** reviews the literature on cell migration, including the main biological processes, events, and players involved. It also summarizes the current state of the art in *in silico* modeling of cell motility. **Chapter 3** introduces Bayesian optimization techniques and highlights their suitability to integrate experimental and theoretical works. The interest in using these techniques lies in their applicability to optimize expensive-to-evaluate functions, such as those assessing the response of *in silico* models to changes in their inputs. This allows for an efficient and

fully-automated workflow to calibrate computational models. **Chapter 4** presents a hybrid modeling approach for analyzing cell motion within 3D matrices. In particular, it studies mesenchymal-like migration guided by biochemical stimuli. This modeling approach focuses on how biochemical cues from the ECM trigger a signaling cascade to internalize such stimuli. As a result, cells remodel their cytoskeleton, generating pushing and pulling forces that enable cells to translocate their nucleus, which guides their trajectory. **Chapter 5** extends the modeling framework from **Chapter 4** to describe how biophysical cues from the surrounding microenvironment influence mesenchymal-like cell migration within 3D matrices. It pays special attention to the cell mechanics associated with the mesenchymal phenotype, that is, those related to the expansion and contraction of cellular protrusions, as well as nucleus translocation. This *in silico* model considers the heterogeneous nature of the ECM and relates the matrix rigidity and pore size to the contractile forces regulating cells' trajectories and speeds. Finally, **Chapter 6** presents the general conclusions and original contributions of this doctoral thesis. Further, this chapter introduces some possible future lines of research that would expand the capabilities of this modeling approach and other biological problems that can be simulated using these frameworks.

2

Unraveling cell migration: a literature review

Contents

This chapter is based on:

Francisco Merino-Casallo, Maria Jose Gomez-Benito, Silvia Hervas-Raluy, and Jose Manuel Garcia-Aznar. *Unravelling cell migration: defining movement from the cell surface.*

2.1 Mechano-chemo biology of cell biology

This chapter aims to give a global overview of our current understanding of cell migration and the different processes and players involved. We will start at the cell surface, where transmembrane receptors enable cells to sense external stimuli from their surroundings. Then, we will focus on the mechanics of cell motility. Different adhesive complexes, also located at the surface, allow cells to interact with one another and with the ECM. By binding to and interacting with all these players from the plasma membrane, the cytoskeleton can receive, process, and respond to signals from the outside. The cytoskeleton is also coupled to the nucleus. As a result, cells nuclei can adapt and react to the relayed signals initiated by external stimuli. Next, we will review different approaches to model some aspects of cell motility. Finally, we will discuss some of the current and future challenges for the research community. Note there are many excellent reviews about specific players or events associated with cell migration (e.g., [45, 46, 62, 71, 87]). We will refer the reader to some of them throughout the text.

2.1.1 Perceiving biochemical stimuli

Cells can change their migratory patterns and bias their trajectories in response to different biochemical stimuli, such as soluble ligands (chemotaxis) or cues fastened either to cell surfaces or to the substrate (haptotaxis) [39, 88–90]. Haptotaxis seems cell-type specific, dependent on cell-induced tractions, and therefore limited by substrate adhesiveness. Cells' ability to respond to biochemical stimuli (chemoattraction) is crucial in multicellular organisms. For instance, it allows the sperm to locate the egg during fertilization [91, 92]. Neural crest cells are guided toward their appropriate destination during embryogenesis [93–96]. Chemoattraction also enables immune cells to locate foreign invaders [97–99]. Hence, by allowing cells to read the biochemical profile of their surroundings and adapt their behavior accordingly, chemoattraction is essential for the proper functioning of multicellular organisms.

Biochemical cues

Cells can sense differences in concentrations of organic and inorganic substances. As a result, cells move toward and away from the gradients of these ligands, from bacterial peptides and ECM degradation products to chemokines and growth factors. Some of these proteins can exist in the fluid phase or immobilized (surface-bound). Several cell types can secrete chemokines into the surrounding environment. As a result, they can induce the migration of endothelial cells and promote angiogenesis.

Chemokines can also attract angiogenesis-promoting immune cells. Interestingly, cells can even create their own attractant gradients [87], which allow them to migrate collectively [100], and navigate complex routes using self-generated chemotaxis [101]. D'Alessandro and colleagues [102] recently demonstrated that on one-dimensional (1D) and 2D confined spaces, motile cells leave long-lived footprints along their way. Such footprints act as spatial memory of their path and determine their future trajectories. Thus, cells produce and respond to biochemical cues diffused into the matrix or surface-bound, guiding other cells and their future selves.

Secreted proteins can induce distinct cellular responses (e.g., their migratory phenotype). For example, different growth factors, including vascular endothelial (VEGF) and epidermal growth factor (EGF), as well as cytokines such as transforming growth factor beta (TGFβ), stimulate epithelial to mesenchymal transition (EMT). Such transition enables individual cancer cells to detach from an epithelial cluster and move freely, promoting tumor progression. Notably, TGFβ not only drives fibrosis, invasion, and metastasis [103, 104] but also induces highly motile amoeboid phenotypes [74]. Furthermore, Lopez-Luque and colleagues [105] demonstrated that some tumoral cells respond to TGFβ inducing and epithelial to amoeboid transition (EAT), after silencing epidermal growth factor receptors (EGFRs). Interestingly, metabolic challenges such as hypoxia can also induce collective to amoeboid transition (CAT) in cancer cells [106]. Independent works have pointed toward TGFβ promoting EMT. Still, some of these studies showed an atypical response to TGFβ, which stimulated different cell types to an incomplete EMT phenotype [107, 108]. Cells exhibiting such hybrid EMT phenotype, which promote metastasis, acquire mesenchymal features while maintaining cell-cell adhesions and therefore acting as collectives [109, 110]. These findings may suggest that, in the metastatic progress, the role of TGFβ strongly depends on context, including cell and cancer type. Ligand concentration may also influence other cell behaviors. For instance, low concentrations of platelet-derived growth factor (PDGF) can promote cell migration, whereas high concentrations may induce proliferation [111]. Hence, cells acting individually or as a collective can determine not only their own fate but also the fate of other cellular organisms.

For further insight into the principles of directed cell migration in general or in cancer see [112] and [113], respectively.

Internalization of biochemical stimuli

Biochemical cues bind to transmembrane receptors, triggering cascades of signaling pathways. As a result, the signals initiated by these receptors are transmitted across

the plasma membrane and inside the cytosol. There are several classes of these receptors (ion channel-linked receptors, enzyme-linked receptors, and G protein-coupled receptors), which bind to and sense different types of chemoattractants. Receptor tyrosine kinase (RTKs) are the enzyme-linked receptors with the largest population and the widest application, and detect many different growth factors (e.g., EGF, PDGF, and VEGF). In contrast, G protein-coupled receptor (GPCR) is the largest receptor superfamily in eukaryotic cells and recognizes many different ligands (e.g., chemokines, hormones, neurotransmitters, and photons). The spatial distribution of transmembrane receptors over the cell surface was initially considered homogeneous. Subsequent works discovered that the plasma membrane is divided into nanometre-scale domains that can be extended over macrodomains and exhibit different membrane receptor profiles. Some domains may have different amounts of the distinct cell surface receptors, including EGFRs and vascular endothelial growth factor receptors (VEGFRs) [114]. Also, those transmembrane receptors might be present in different configurations (monomeric, dimeric, higher-order oligomers, or clusters) even in the absence of ligands [115–117]. A high surface abundance of a particular transmembrane receptor may promote homodimerization and clustering. Conversely, a high surface abundance of distinct transmembrane receptors would promote heterodimer pairing. Other factors, such as the cytoskeleton organization and ligand stimuli, may bias such membrane receptor profile too (Figure 2.1) [111, 114, 118]. At the tissue scale, cells can establish larger macrodomains of the plasma membrane. In such scenarios, cell-cell contacts regulate membrane asymmetry, allowing cells to sense and respond to each other. Transmembrane receptors, which enable cells to probe and internalize external stimuli, are continually being synthesized, internalized, recycled, and degraded.

Cells degrade and recycle surface receptors through membrane trafficking using membrane-bound transport vesicles (Figure 2.1) [111, 119]. Different factors, such as ligand concentration, distinct types of stresses, and hypoxia, seem to influence the preferred internalization route of RTKs, that is, their sorting toward degradation or recycling. Different GPCR-interacting proteins and arrestins can also influence the GPCR internalization route [120]. Various studies showed that distinct RTK classes remain active during their internalization [111, 114, 117]. Indeed, in some cases, RTK and GPCR internalization is required for a complete signaling response [121, 122]. Whatsmore, transmembrane receptors can activate different effectors depending on whether they are at the plasma membrane or in endosomes. Changes in the spatial distribution generate variations in the internalized signals [111]. For instance, these signals can be localized and amplified over a specific area of the cell surface. Besides, an altered expression of transmembrane receptors can change

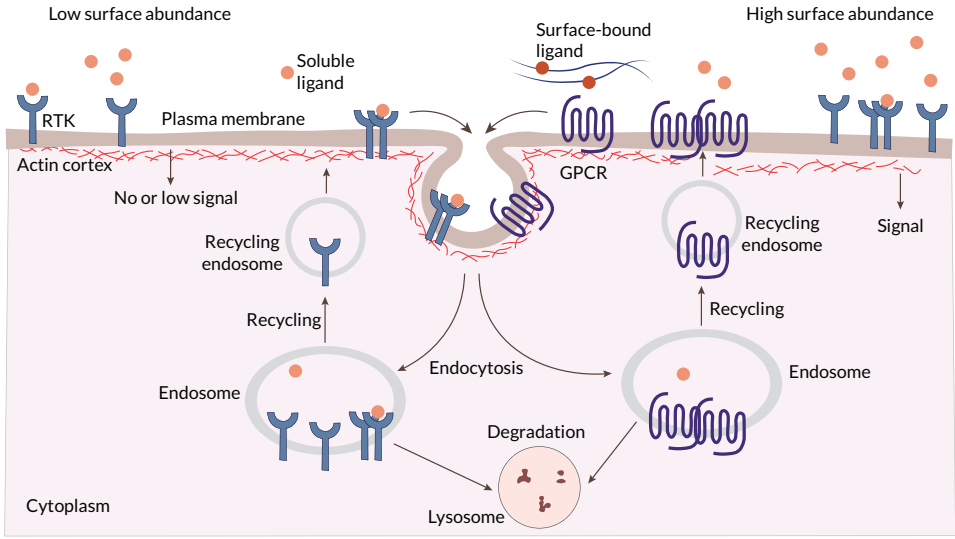

Figure 2.1: Sensing biochemical cues The surface abundance and distribution of transmembrane receptors, such as receptor tyrosine kinase (RTK) and G-protein-coupled receptor (GPCR), is a key regulatory step. Locally high surface levels of an individual surface receptor may promote homodimerization and/or clustering, and high surface abundance of two or more of these receptors may also increase heterodimer pairing. Distinct domains within the plasma membrane, as well as the closely apposed and dynamic cortical actin cytoskeleton, affect this key step in receptor activation. The surface abundance of transmembrane receptors is predominantly controlled by receptor endocytosis, which ultimately leads to receptor degradation or recycling. When localized in specific plasma membrane domains, stimulated (ligand-bound) or unstimulated (unbound) surface receptors are endocytosed or sequestered. Adapted from [114].

their spatial distribution, which may impact cell tracking, polarity, adhesion, and cytoskeletal organization during pathological processes (e.g., cancer development and progression) [114, 123, 124]. Thus, the internalization of transmembrane receptors allows for their dynamic organization over the plasma membrane and may be required for an appropriate signaling response.

Although some receptor classes access many of the same signaling pathways, their dynamics are significantly different. Each cell surface receptor may be activated by distinct ligands, triggering different signaling outcomes [125]. Some ligands can activate different RTKs too [116]. Interestingly, the activity of transmembrane receptors is even possible in the absence of ligands (basal activity). Ligand-bound GPCRs can also trigger the activation of unbound EGFRs through transactivation [126]. In addition, some ligands can bind different receptors together, mediating distinct biological responses. Besides, RTKs directly interact with the plasma membrane and the cytoskeleton. Altogether, surface receptors translate the biochemical profile of the ECM into biochemical signals inside the cell through many different interactions, occurring under a wide variety of circumstances.

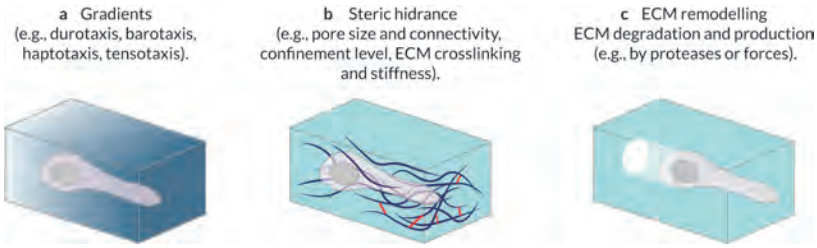

Figure 2.2: Extrinsic regulators of 3D cell migration. Different properties of the surrounding microenvironment can regulate or modulate cell migration. **(a)** The concentration of each extracellular matrix (ECM) component can vary locally creating, for example, gradients of stiffness (durotaxis) or ligand concentration (haptotaxis), biasing cell motility. **(b)** The presence and size of pores within the 3D environment—which can be altered by ECM crosslinking and may be dependent on ECM or tissue stiffness—and the level of confinement of cells mediated by the ECM modulate spatial obstruction of the substrate (steric hindrance) to cell migration. **(c)** Local remodeling (for example, by proteases or local force causing physical displacement of ECM components) can also influence cell motion. The features of the local microenvironment can be overlapping; for example, increasing the concentration of ECM components can increase local stiffness and alter the sizes of pores. Adapted from [41].

By initiating these downstream signaling, chemoattractants influence cells internal organization and their transcriptional regulation. As a result, these ligands may initiate changes in cell polarity. Thus, chemoattractants may bias influence cells' trajectories, enabling directed migration and different physiological processes, including immune response, wound repair, and tissue homeostasis.

For further review of specific aspects of cells' ability to probe and internalize biochemical cues see [111, 114, 116–118, 124, 125, 127–129].

2.1.2 Perceiving biophysical stimuli

Recently, much interest has focused on how biophysical factors, such as the stiffness and the microarchitecture of the ECM, influence cell migration. Still, our understanding of the role of these factors in cell motility is far from complete. Partially, at least, because many of these biophysical cues cannot be incorporated into and studied on flat surface assays. Indeed, 2D studies about the impact of biophysical stimuli in cell migration are limited to planar substrates with stiffness gradients [130], micropatterned barriers (e.g., slabs, micropillars, or microstencils) [131], and other nanometer- to micrometer-scale topographies (e.g., nanoscale ridges, needles, cones, sawtooth structures, or grooves) [132–135]. In 3D environments, cells use different modes of migration (e.g., mesenchymal, amoeboid, lobopodial, collective) based on the local ECM (Figure 1.2) [65, 76, 131]. For instance, macrophages use an amoeboid-like migration in porous substrates, whereas in dense

matrices such as Matrigel they use a mesenchymal-like one [97]. Furthermore, *in vitro* studies suggest that the speed of migrating macrophages is stiffness-dependent. Substrate stiffness can also guide cell migration (durotaxis) [46, 136, 137]. Indeed, mesoderm stiffening is required and sufficient to trigger the collective migration of neural crest cells during morphogenesis [138]. However, cells may also migrate toward softer environments to generate higher traction forces [139]. The biophysical properties of the tumor microenvironment contribute to cancer development and progression too [140–143]. For example, increasing substrate stiffness led to a switch from proteolytically-independent invasion to a proteolytically-dependent phenotype in breast cancer cells [144]. Substrate stiffening also promotes EMT by controlling the subcellular localization of downstream effectors [104]. Interestingly, ECM-induced EMT correlates with TGFβ activation by resident epithelial cells. Also, the inhomogeneity of 3D environments may promote clustered cells to switch to a single cell-dominated invasion [145]. Conversely, denser substrates and decreased porosity would lead to the opposite switch, from individual to collective cell migration. Thus, cells can sense the biophysical cues from the microenvironment and adapt their behavior accordingly.

We refer the curious reader to other excellent reviews focused on the specifics of how cells integrate biophysical cues from their surroundings and how they adapt to such external stimuli [41, 75, 78, 112, 135, 141, 142, 146–149].

Biophysical cues

Many biophysical cues from the surrounding microenvironment can influence cell migration. A list of the primary ECM features regulating or modulating cell migration may include at least the following: (i) ECM topology, (ii) the molecular composition of the ECM, and (iii) the local concentration of each ECM component (Figure 2.2) [41]. However, many other factors influence cell motility too, such as (i) ECM crosslinking, (ii) gradients of stiffness or ligand concentration, (iii) porosity and pore size within the ECM, (iv) ECM stiffness, (v) ECM (visco-)elastic behavior, and (vi) ECM confinement of cells. Whatsmore, some of these properties may be overlapping [150]. For example, collagen alignment can alter the ECM pore size and the micro-scale stiffness. Fibril diameter and intrafibrillar crosslinking control fibril bending stiffness independently, which correlates with matrix mechanical properties [151]. Increasing the concentration of Matrigel or ECM components (e.g., collagen) can also increase ECM stiffness and alter the size of its pores [41, 152]. Therefore, we must study how distinct architectural features (e.g., geometry, porosity, topology) affect cell behavior in these matrices. Lastly, during tumor progression, the organization and composition of the ECM are altered [43]. As

a result, tumoral tissue exhibits biophysical properties strikingly different than those of its healthy equivalent. In summary, a wide variety of biophysical features associated with the ECM affect cell motility.

The response of cells to ECM stiffness is cell-type specific [139, 146, 153, 154]. Still, there is ample evidence that substrate stiffness plays a role in cancer metastasis as tumoral tissue is stiffer than its normal counterpart [40, 137, 142, 155]. Increased stiffness may hinder cell migration due to an excessive steric hindrance [156, 157]. Besides, substrate rigidity in 3D may also impact cell-matrix interactions and intracellular activity [63]. Preliminary reports from Higgins and colleagues [158] suggest that decreased cell stiffness drives tumor-cell detachment and migration. On the other hand, in stiffened matrices, cells must either soften or remodel the surrounding environment to avoid migration arrest. Recent studies suggested that ECM rigidity and deformation mediate cell mechanosensing [159].

Fibers comprising the ECM are usually aligned in a specific direction, anisotropically. Moreover, in mammary tumors, aligned collagen fibers are oriented perpendicular to the tumor boundary [160]. Enhanced fiber alignment promotes a more directed cell polarization and migration [161]. Indeed, elongated cells respond more strongly to fiber alignment than those with a rounded morphology. Of note, cell-matrix adhesions and Rho-mediated actomyosin contractility modulate cell responses through the mesenchymal to amoeboid transition (MAT). Besides, the degree of fiber alignment regulates the transition rates between elongated and rounded morphologies. Notably, cells respond to ECM fiber alignment differently based on dimensionality. Fiber alignment modulates protrusion rate and orientation [162]. It also promotes the directed migration of cells [163]. For instance, recent *in vitro* studies suggest that, by aligning collagen fibers, cancer-associated fibroblasts may help tumor cells migrate toward blood vessels during the initial stage of metastasis.

When ECM pores are about the size of cells or slightly smaller, cells seem to migrate more effectively [74, 160]. However, if pores are significantly smaller than cells, their nuclei may impede cell migration because of their size, rigidity, and limited deformability [164]. On the other hand, pores bigger than the cell size may also impede migration as cells cannot develop protrusions and adhere to the ECM properly [165]. ECM architectures with narrow pores and short fibers seem to confine cells to a rounded shape and altered protrusion dynamics independently of substrate rigidity or bulk collagen density [166]. Hence, understanding the intricacies of how cells sense all these features may allow us, for example, to develop novel and effective techniques against metastasic diseases.

Tweaking the biophysical properties of the substrate *in vitro*

The ability to modify and customize the biophysical profile of the microenvironment is essential to understand how it affects cell migration. We already know how to tweak *in vitro* some of the biophysical properties of the ECM to study different setups. For example, the presence of polyethylene glycol (PEG) crowding agent during low-density collagen polymerization produces a more confined architecture [166]. Particularly, fiber length and pore size decrease to levels that more closely resemble high-density collagen matrices. However, the mechanical properties of such substrates are still those of low-density collagen matrices. In alginate-PEG hydrogels, PEG density modulates stress relaxation [167]. Mason and colleagues [168] tuned the mechanical properties of collagen-based scaffolds using non-enzymatic glycation of the collagen before polymerization. As a result, they produced collagen gels with a threefold increase in compressive modulus without significantly altering the matrix architecture. Matrigel, on the other hand, increases the stiffness and pore size of otherwise collagen-based hydrogels but decreases the number of pores [152]. Polymerization temperature also modulates network architecture [150]. Indeed, increasing polymerization temperature increases network connectivity and decreases pore size. Besides, aligned and random matrices were significantly stiffer at 25 °C than at 37 °C. Wisdom and colleagues [169] designed a series of hydrogels for 3D cell culture with modulated plasticities. Such hydrogels presented stiffness akin to that of tumoral tissue, equal concentrations of basement membrane (BM) ligands, nanoporosity analogous to BM, and limited susceptibility to cell-mediated degradation. Increasing covalent crosslinking of reconstituted basement membrane (rBM) matrices reduces mechanical plasticity and contributes to tissue stiffening too [40, 170]. Besides, even though Tissue transglutaminase (TG2)-mediated crosslinking does not prominently increase the shear modulus at low strains, it promotes earlier stiffening [171]. Hence, it is already possible to study the effects of many of these biophysical properties in isolation. Nonetheless, the scientific community is still interested in uncovering new ways of fine-tuning some of these properties, not only in isolation but also in aggregate [152, 172]. Next, we will describe the players and mechanisms allowing cells to sense such biophysical stimuli and how these cues influence cell migration.

Internalization of biophysical stimuli

Mechanotransduction enables cells to probe for biophysical features. It involves different membrane receptors (e.g., ion channels and growth factor receptors), and a wide range of proteins and assemblies, such as integrins and integrin adhesion

complexes (IACs) [159, 173–175]. Ion channels tightly control cellular voltage through the influx or efflux of ions, which trigger downstream signaling cascades [176–179]. They are activated by distinct stimuli, including ligands, temperature, and force (e.g., tensional stretch, shear stress, membrane tension).

Integrins are one of the primary transmembrane receptors that play a central role in cell-matrix interactions [179–182]. These receptors also act as biomechanical sensors of the microenvironment. As a result, integrins allow cells to sense haptotactic gradients composed of ECM components too [112]. Each integrin binds to specific ECM components and cell surface molecules with specific spatiotemporal distribution patterns in a given tissue [180, 183]. Distinct integrins can have overlapping ligand specificity. In such cases, integrins may synergize, antagonize, or complement their activities [184]. Moreover, every cell type has its specific integrin profile, and they can modulate it to adapt to new substrates [69]. Note that altered integrin expression is associated with several types of cancer and other diseases [180, 181, 185, 186].

Integrins are activated through biochemical interactions and by forces transmitted between intracellular and extracellular spaces (Figure 2.3) [179, 181, 182]. While activated, integrins have an increased affinity for ligand binding. In turn, extracellular binding and force application promote integrin clustering, triggering signaling pathways that couple integrins to the actin cytoskeleton [155, 181, 187, 188]. These integrin clusters, together with force-induced catch bonds, extend the lifetime of adhesion sites. Their targeted downstream effectors are essential for many processes such as cytoskeletal dynamics and cellular structure. Moreover, some of these processes are fundamental for maintaining cell polarity.

Integrin traffic not only regulates their spatial distribution (i.e., their cell-surface availability) but also IACs turnover [183, 189], based, among other factors, on biophysical stimuli [190]. The specifics of integrin trafficking pathways, though, depend on context and cell type [184]. As with other surface receptors (e.g., RTKs, and GPCR), endocytosis allow integrins to be efficiently recycled back to the plasma membrane or degraded by lysosomes (Figure 2.3). These processes are essential for regulating integrin function and therefore to cell migration and invasion in 3D substrates [189]. Interestingly, crosstalk with RTKs and other co-receptors modulate integrin functions in migrating cells [116, 174, 175, 191]. This crosstalk between integrins and growth factor receptors can enhance growth factor receptor activation and focal adhesion kinase (FAK) phosphorylation [174]. Whatsmore, mechanical stimuli can independently activate growth factor receptors without ligand-induced activation [135, 174, 184]. The dynamics of these processes allow for adhesion turnover, which is essential for mesenchymal cell migration.

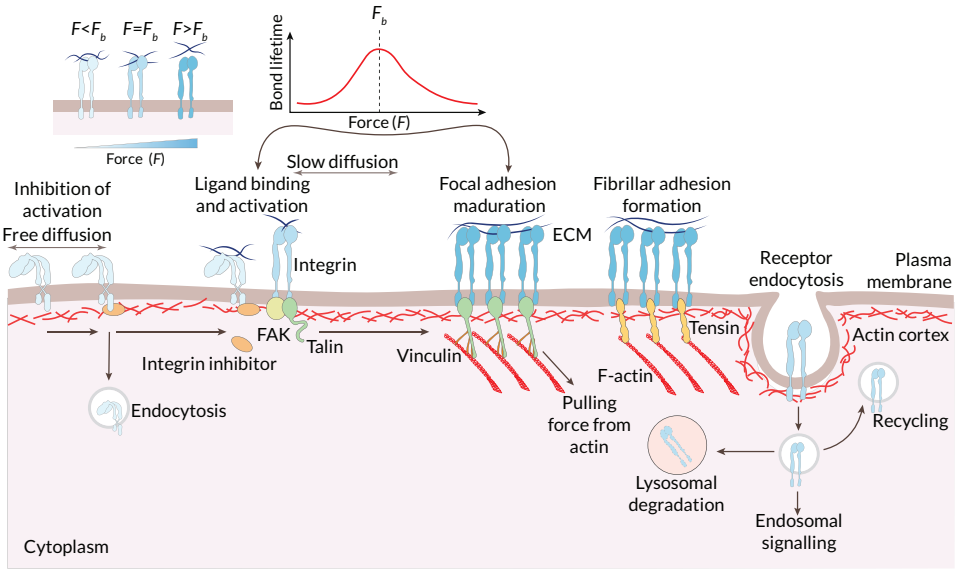

Figure 2.3: Sensing biophysical cues by means of the integrin dynamics. On the plasma membrane, different factors (e.g., the forces from the ECM) enable integrin activation and increased affinity for ligand binding. Inside-out signals regulate displacement of intracellular integrin inhibitors and allow talin to bind to integrins, tightly controlling integrin affinity for ECM ligands. In fibroblasts, recruitment of focal adhesion kinase (FAK) to integrins has been suggested to precede talin recruitment. Integrin activation is also promoted by an outside-in mechanism through ECM binding and force application that slows the diffusion of integrin dimers within the plasma membrane. Force application leads to integrin clustering and the initiation of integrin downstream signaling through the coupling of integrins via talin and vinculin to the actin cytoskeleton. Reciprocally, actin can pull on integrins, further contributing to force generation. In fibroblasts, focal adhesions can mature further to fibrillar adhesions where talin is replaced by tensin. Trafficking of integrins regulates their availability at the plasma membrane. Integrins are constantly endocytosed from the plasma membrane. They are then efficiently recycled, with a small subset of the receptors targeted to lysosomal degradation. Integrins can be endocytosed via multiple different routes depending on the cell type, adhesion status, and cellular signaling pathways that are activated. Force regulates integrin properties. Integrin–ligand binding follows a catch bond behavior. When force (F) applied to the ligand-bound integrin is below the optimal bond force (F_B), the strength (lifetime) of the bond increases with force. When F exceeds F_B, the bond lifetime decays with force. Mechanical force (F) acting on integrins through their ligands can favor integrin unbending and subsequent activation, thereby triggering outside-in integrin signaling. Activation increases catch bond behavior, further strengthening the bond. If a given F is applied to an adhesion site, further integrin clustering decreases the force applied to individual integrin dimers. This minimizes elastic energy since it decreases the applied strain, and could thus be promoted. Adapted from [182].

Integrin clustering initiates IACs formation [180, 183, 188, 192]. These IACs allow cells to adhere to their surrounding ECM, probing biophysical cues and transmitting forces. Of note, substrate stiffness and ligand spacing determine an optimal force threshold for IACs formation and coordination with downstream cascades [193]. During this initial stage of IACs formation, several proteins, such as tensin and talin, are recruited to nascent adhesions [160, 182, 194]. As a result, downstream effectors, including Ras-related C3 botulinum toxin substrate 1 (Rac1) and the Actin-related protein 2/3 (Arp2/3) complex, are activated, which induces protrusions formation. These nascent adhesions are also critical for ECM haptotaxis [112]. Integrin-mediated force transmission between cells and the ECM mature nascent adhesions to focal adhesions, recruiting other proteins such as paxillin, vinculin, and FAK [187, 195, 196]. In turn, FAK activates downstream pathways controlling different cell behaviors such as adhesion and motility [40, 172, 197]. Recently, nuclear paxillin was also associated with enhanced tumor angiogenesis, growth, and metastasis [198]. Focal adhesions may mature further to fibrillar adhesions in some cell types (e.g., fibroblasts, platelets) [182, 184]. These are long, thin, and centrally located adhesions, which enable fibronectin fibrillogenesis. Interestingly, mechanotransduction on stiffer surfaces alters EGFR organization and induces their clustering at focal adhesions [174]. Besides, IACs are not limited to actin-binding cell-ECM adhesions [184]. Instead, distinct proteins, when recruited to integrins, allow for specialized functions and connections with the cytoskeleton. The presence of Matrigel in collagen hydrogels increases the number and size of focal adhesions [152]. Focal adhesions also serve as signaling hubs where several signaling proteins group because of integrin activation and clustering [41]. Recent studies have demonstrated that focal adhesions also form nutrient-sensing hubs, which mediate, among others, spatially restricted growth factor receptor signaling and nutrient uptake [199]. Consequently, these macromolecular assemblies transmit mechanical forces and regulatory signals between cells and the ECM.

For more details about the main players and processes involved in the probe and internalization of biophysical cues, we refer the inquisitive reader to other comprehensive reviews [69, 117, 175, 176, 179–187, 190, 197, 200, 201].

2.1.3 Mechanics of cell migration

Cells rely on the coordination of four core biophysical processes to interact with and migrate through 3D environments: (i) adhesion, (ii) cytoskeletal, and (iii) nuclear dynamics, as well as (iv) matrix remodeling through cell-matrix interactions. The biophysical properties of the ECM modulate several of these biophysical processes. Migration through dense environments requires enhanced cytoskeletal remodeling

to displace the surrounding ECM and enable cells to squeeze themselves through narrower pores [106]. Cells also increase their protrusive activity to enhance matrix remodeling and the probe for cell tracks, which would enable a more efficient migration. As a result, cells increase their metabolism while migrating through dense environments to meet higher energy demands [202–204]. Multiple signaling mechanisms tightly regulate these processes [205, 206].

The Rho family of small guanosine triphosphatases (GTPases) is involved in many signaling pathways activated during cell migration [207, 208]. Rho GTPases such as Rho-related BTB domain-containing protein 1 (RhoBTB1) inhibit invasion [209]. Besides, an altered expression of several Rho GTPases appears in different human tumors and cancers [104, 206, 210–212]. Rho proteins are also involved in the epithelial to mesenchymal transition (EMT). As a result, they enable carcinoma cells to metastasize [206]. Hence, Rho GTPases are critical for cell motility.

The opposing actions of guanine nucleotide exchange factors (GEFs) and GTPase-activating proteins (GAPs) regulate the activity of Rho GTPases [104, 209, 211]. Such dynamic regulation depends on a coordinated and localized activation and inactivation of multiple proteins such as PI3K, FAK, and Src. Indeed, the ability of RhoGEFs and RhoGAPs to form complexes with such proteins is fundamental to spatiotemporal regulation of Rho GTPase activation in migration and invasion [205, 213]. Notice that cellular events can be regulated by integrated signaling networks instead of a specific signaling cascade. Therefore, the same stimuli in different cell contexts could promote distinct responses. The dynamics of such signaling events are thus varied and tightly regulated.

Distinct authors have reviewed in more detail specific players and events involved in the mechanics of cell motility (see [49, 65, 86, 104, 160, 172, 205–208, 210–212, 214–226]).

Next, we will summarize our current knowledge of the aforementioned four core biophysical processes enabling cells to interact with and migrate within 3D environments. In particular, we will highlight the roles of (i) cell-matrix and cell-cell adhesions; (ii) the cytoskeletal actin microfilaments, microtubules, and intermediate filaments; (iii) the nucleus; and (iv) cell-matrix interactions enabling matrix remodeling through alignment, degradation, deposition and crosslinking.

Adhesion dynamics

Different modes of migration depend on adhesive complexes. For example, individual fibroblasts may use mesenchymal migration mediated by cell-matrix adhesions during wound healing. However, collective migration used by neural crest cells during embryogenesis requires cell-cell junctions [87]. Besides, cell-matrix and cell-cell contacts play an important role in mechanotransduction [159, 174].

Cell-matrix adhesions for individual migration

Cell-matrix adhesions, essential for mesenchymal cell migration, support force transmission between extra- and intra-cellular spaces (Figure 2.4a). They also allow cells to probe the biophysical properties of the substrate. These adhesions are of particular importance in 3D scenarios where cells have to squeeze themselves across ECM pores. In 3D microenvironments, cell-matrix adhesions are longer and more elongated than the 2D counterpart. Indeed, fibroblasts seem to attach more strongly to the ECM in 3D domains than on flat surfaces. Still, integrin-mediated adhesions are not essential for 3D cell migration. More confining ECM architectures (i.e., smaller pores and shorter fibers) alter protrusion dynamics by reducing, but not eliminating, cell adhesions to the substrate [166]. Moreover, high confined spaces featuring low-adhesion properties abolish focal adhesions. Fast actomyosin retrograde flow allows cells to generate sufficient friction. As a result, cells switch to rapid amoeboid-like cell migration, propelling themselves forward. Active water transport through the cell membrane may induce an osmotic pressure gradient, which can also initiate and sustain friction-driven cell migration in 3D surroundings [160]. However, although cells can migrate without cell-matrix adhesions under specific circumstances, such adhesive complexes are fundamental for many biological responses.

Cells' ability to adhere to the substrate involves different players. Adaptor proteins, such as talin and vinculin, couple integrins located at IACs to actin microfilaments. As a result, cells' cytoskeleton binds to the substrate [155, 172, 227]. Adaptor proteins also interact with cells' cytoskeleton through intermediate filaments and microtubules [228]. However, the scientific community still lacks a detailed view of how adaptor proteins behave under different conditions. For example, Kluger and colleagues [229] recently unveiled that vinculin acts as a mechanosensitive logical gate, converting the input forces, pulling geometry (e.g., zipper-like vs. shear-like), and magnitude into distinct structural outputs. Mechanical forces generated during actin polymerization or by myosin motors initially exerted to actin microfilaments are transmitted to different adaptor proteins. Then, these forces are transmitted to transmembrane proteins, such as integrins, linking adaptor proteins to the surrounding ECM. According to the molecular clutch hypothesis, contractile forces are only optimally transmitted if the whole system (from actin microfilaments to these adaptor proteins) is engaged. Otherwise, the adhesion complex cannot maintain high force transmission because of an unstructured or fluidized, softened cytoskeleton [230]. Also, preliminary reports from Newman and colleagues [231] showed that IACs in protrusions enable actomyosin-mediated force transmission to

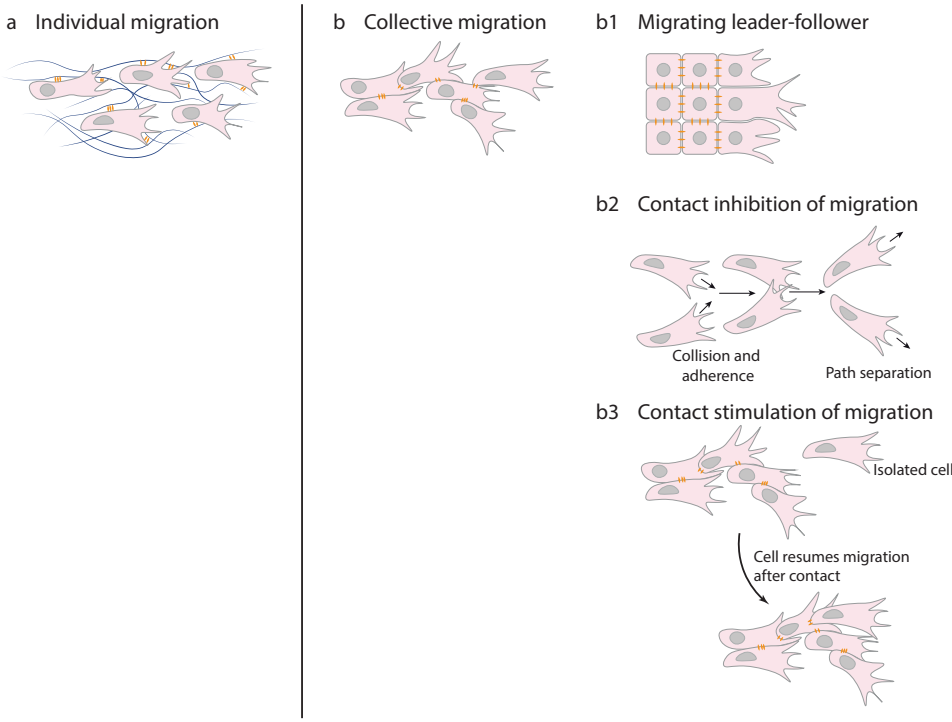

Figure 2.4: Cell adhesions. Non-migratory cells must be stimulated to migrate by transcription factors, growth factors, chemokines or physical forces. **(a)** They can migrate as loose cohorts of individually migrating cells. **(b)** Cells can also maintain cohesiveness by adherence using cell-cell adhesion molecules. **(b1)** When migrating collectively, cells can organize into leaders and followers, in which the leaders—established by signaling cues (for example, by diffusible growth and other factors) or by mechanical cues such as those generated by neighboring cells—provide guidance as long as the biochemical or biophysical signaling is maintained. Cohesive migration of cell populations can be supported by two types of cell-cell interactions: contact inhibition of migration or contact stimulation of migration. **(b2)** Contact inhibition of migration is a mechanism in which colliding cells migrate in new directions after collision rather than cohering; however, on a population level, this mechanism ensures that cells maintain similar polarities, thereby resulting in directionality of migration in collectives. **(b3)** Contact stimulation of migration provides a direct mechanism for maintaining cohesion. In this case, cells that migrate away from contact with their neighbors cease migrating and resume migration only after being contacted by another migrating cell. Adapted from [41].

the nucleus. The ECM is paramount for this mechanism because substrate rigidity directly controls when contractile forces are optimally transmitted. In fibrilar collagen substrates, effective cell adhesion may require proteolytic activity [166]. Thus, adaptor proteins and other proteins, different factors such as ECM stiffness, and processes (e.g., matrix degradation) play a part in cell-matrix adhesions.

Cell-cell adhesions for collective migration

Collective migration depends on cell-cell interactions coordinated with the actin cytoskeleton (Figure 2.4b) [48, 131]. By establishing attachments between cells and coupling their cytoskeletons, cells can sense and transmit forces between them [174]. These attachments also enable stress distribution between cells [47, 228]. As a result, cells can integrate external signals from and communicate over longer distances, which allows them to sense shallow biochemical and biophysical gradients [130]. Cell-cell coupling enables multicellular assemblies to migrate and rearrange during morphogenesis and tissue repair [131, 232]. These cohesive cell groups ensure the proper formation and repair of organs. Unfortunately, cell-cell adhesions can also drive cancer cell invasion [233]. Multicellular assemblies may display front-to-back polarity, where leading cells coordinate the migration at the front edge [131, 232, 234]. For instance, in epithelial monolayers exposed to an empty edge, leader cells drag follower cells by forming large lamellipodia and maintaining robust cell-cell adhesions with them (Figure 2.4b1). Therefore, cell-cell interactions and collective migration are critical for other fundamental biological processes.

Different cell-cell adhesion systems are fundamental for collective migration, including but not limited to adherens junctions and tight junctions [48, 174]. Adherens junctions are central hubs that control cell-cell cohesion and collective cell migration during tissue dynamics and remodeling [48]. Although usually associated with epithelial and endothelial tissues, adherens junctions may also transiently form in mesenchymal cells. Distinct mechanisms (e.g., endocytosis, cytoskeletal regulation) control adherens junctions' stability. Rho GTPases are also involved in these mechanisms [48, 131, 207]. Actin cytoskeleton coupling enables contractile forces transmission across adherens junctions [131, 174]. On the other hand, tight junctions form a central hub between cell-cell interactions and actin dynamics. The primary role of tight junctions is to function as paracellular gates restricting diffusion based on size and charge. Tight and adherens junctions seal the paracellular space and adhere epithelial cells to one another [235]. They also bind with the actomyosin cytoskeleton. Actomyosin dynamics are essential for the formation, structure, and function of junctions during epithelium homeostasis and

morphogenesis. Altogether, each cell-cell junctions have a different role, but all are essential for cells to migrate collectively.

Cells may also repolarize and change their trajectory upon contact with one another. An example of this phenomenon is contact inhibition of locomotion. This mechanism of cell repulsion moves cells away from cell-cell contacts (Figure 2.4b2) [52, 236–238], and can occur between cells of the same or different type.

Contact inhibition of locomotion is a multistep phenomenon, which initiates upon a collision. Colliding cells accelerate toward each other and form cadherin-based cell-cell adhesions. Then, their protrusive structures toward the contact collapse. Finally, cells develop new protrusions away from cell-cell contacts, separate, and move away. Note that cell-matrix adhesions play different roles in contact inhibition of locomotion (e.g., inducing lamellae paralysis upon collision and enabling separation by disassembling themselves near the contact afterward). Besides, cell-cell and cell-matrix adhesions directly crosslink to actin and regulate cytoskeleton dynamics. Cytoskeletal rearrangements are essential in contact inhibition of locomotion. In particular, the importance of actin microfilaments and microtubules has been demonstrated during the different stages of contact inhibition of locomotion. Small GTPases, which regulate cytoskeletal dynamics, play also a fundamental role in contact inhibition of locomotion. Rac1 activity, initially elevated in the leading edge of the cell, is suppressed near the contact upon collision. In contrast, Rho activity is stimulated around that contact region. Lastly, Rac1 activation is triggered in the edge driving cells repolarization and separation.

Contact inhibition of locomotion opposes cell propulsion [46]. When migrating collective, cells at the edge experience less contact inhibition of locomotion and therefore have more propulsion than those at the core of the cluster. In this scenario, edge cells also have stronger alignment interactions. Further, the collision properties of malignant tumoral cells may influence the alignment of cell motion.

A less recognized phenomenon where cells change their migratory phenotype upon contact with one another is contact stimulation of locomotion [41, 239]. Complementary to contact inhibition of locomotion, in contact stimulation of locomotion, cell-cell contacts stimulate collective migration (Figure 2.4b3). As a result, cells that race ahead of the migrating cohort lose contact with the rest and migrate poorly (if at all) when isolated. Only after restimulation by the group of migrating cells, do these isolated cells regain the initial migratory phenotype. Initially observed in neural crest cells by Thomas and Yamada [239], contact stimulation of locomotion has more recently been observed in prostate cancer cells [240] and myoblast-forming myotubes [241].

Interactions between different adhesive complexes and with other cellular components

Different adhesive complexes, such as cell-matrix and distinct cell-cell adhesions (e.g., adherens junctions, tight junctions), seem to communicate with each other [174, 242]. The regulation of cell-cell junction stability allows for different collective migration modes and patterns [46, 131, 174]. Furthermore, EMT depends on the regulation of cell-cell adhesions. The stability and strength of these adhesions modulate the degree of the transition. Cell junctions provide positional cues that guide the distribution of RTKs and their ligands [114]. They also transmit physical information, regulating RTKs more directly. Whatsmore, cell-cell contacts can inhibit RTK signaling. The interplay between cell-cell and cell-matrix interactions enables cell monolayers to self-organize, migrate, and evolve [153, 243]. This interplay regulates different phenomena such as tissue morphogenesis, EMT, wound healing, and tumor progression. Cell-cell and cell-matrix adhesion are not only interconnected [47]. Instead, the crosstalk between them affects downstream adhesion dynamics and signaling transduction [174]. For example, cadherins and integrins activate different Rho GTPases such as Rac, Ras homolog family member A (RhoA), and cell division control protein 42 homolog (Cdc42). At the same time, Rho GTPases intervene in regulating the formation of integrin-based focal adhesions and cadherin-based adherens junctions. Other studies have revealed pathways controlled by growth factor receptors and cadherins that regulate cell-cell adhesion and cell migration [244]. The coupling to common cytoskeletal and scaffolding structures is fundamental for the cadherin-integrin crosstalk. Therefore, tightly regulated adhesion dynamics are required to enable cell migration plasticity.

Cytoskeletal dynamics

To navigate through complex and constraining environments and overcome physical barriers, cells may remodel their cytoskeleton [39]. The cytoskeleton (Figure 2.5) is a dynamic network of fibrillar structures located in the cytoplasm of cells [245–247]. This fibrillar network allows cells to modulate their shape and migrate by creating a viscoelastic environment within themselves [50, 248]. In eukaryotes, the cytoskeleton comprises actin microfilaments, microtubules, and intermediate filaments. These three cytoskeletal components have starkly different stiffnesses and mechanical behaviors. Besides, they could often spread over the entire cell because of their length and straight shape [248]. Next, we will take a closer look at each of these cytoskeletal components and how they are involved in cell migration.

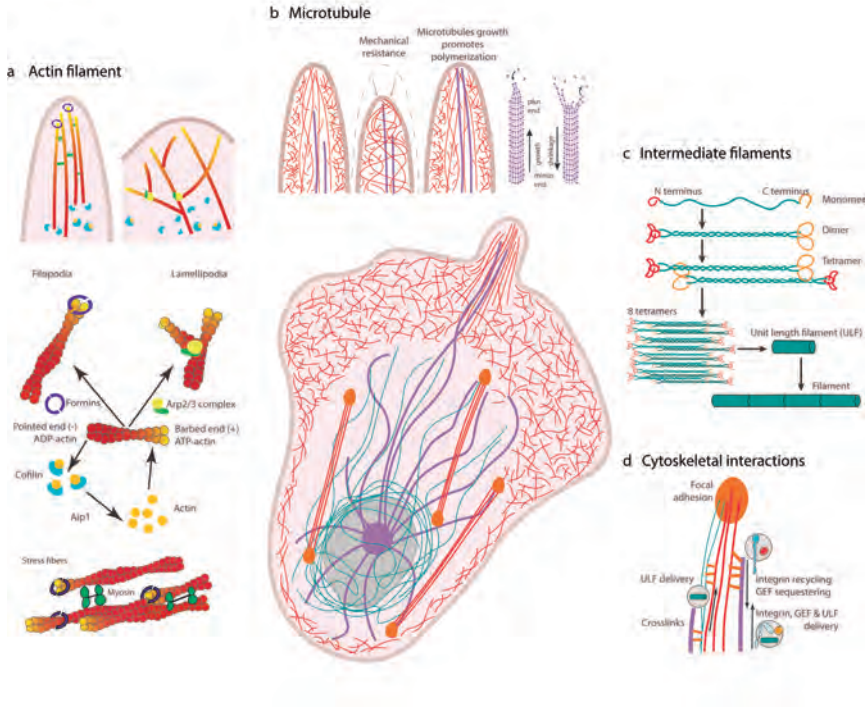

Figure 2.5: Cytoskeletal dynamics. **(a)** *Assembly and organization of the actin microfilament network.* The Arp2/3 complex nucleate branched actin microfilaments. Conversely, unbranched filaments may be nucleated *de novo* by the formins or generated from a preexisting Arp2/3-nucleated network. Actin filaments grow toward the plasma membrane, generating forces that move forward the leading edge. In filopodia, fascin is the main actin microfilament cross-linking/bundling protein. Cofilin triggers actin microfilament disassembly. **(b)** *Microtubule structure and functions.* Microtubules are anchored at the centrosome and grow toward the cell cortex. Microtubule stiffness paired with the viscosity of the cytoplasm allows them to resist large compressive forces. Microtubule assembly and disassembly result in pushing and pulling forces. Stiff microtubules may provide mechanical support against membrane retraction when actin polymerization is driving membrane protrusion. Also, the growth of microtubules leads to actin polymerization in protrusions. The binding of actin microfilaments and microtubules through crosslinks allows actin microfilaments to guide microtubule growth toward focal adhesions. **(c)** *Organization and assembly of intermediate filaments.* Monomers associate to form dimers, dimers then associates to form a staggered tetramer, eight tetramers associate to form a unit-length filament (ULF), ULFs anneal to form a thick filament, and further annealing of ULFs results in filament elongation, which is followed by compaction to achieve the final intermediate filament. By organizing into a cytoplasmic nuclear cage, intermediate filaments protect the nucleus against compressive forces. Intermediate filaments also provide mechanical support for the plasma membrane in contact sites with other cells and the ECM. **(d)** *Cytoskeletal interactions.* Both actin microfilaments and microtubules can act as transport tracks of ULFs and bind to intermediate filaments through crosslinks. Further, microtubules act as transport tracks, enabling the delivery and recycling or sequestering of integrins and other signaling molecules, such as guanine nucleotide exchange factors (GEFs). As a result, microtubules regulate different processes, such as mechanotransduction and actomyosin contractility.

Actin microfilaments

Actin (de)polymerization Cell migration depends, among others, on the dynamic formation and disassembly of actin microfilament networks (e.g., filopodia, lamellipodia, invadopodia), which differ in their structure and functionality (Figure 2.5a) [205, 249, 250]. These different actin-based structures are also located in specific subregions of the plasma membrane. Distinct external cues and downstream effectors are involved in actin dynamics. For one, the (dis)assembly of actin microfilaments and monomer recycling in lamellipodia are regulated by actin-binding proteins. Capping protein, cofilin, profilin, and cyclase-associated protein are some examples of actin-binding proteins. Kinase-phosphatase networks, small GTPases, and membrane phospholipids such as phosphatidylinositol 4,5-bisphosphate ($PI(4,5)P_2$) tightly regulate the activities of these actin-binding proteins [251]. Receptors located at the plasma membrane, including RTKs, can initiate signaling pathways where Rho GTPases may take part. Indeed, the Rac, Cdc42, and Rho subfamilies promote actin cytoskeleton reorganization: from the formation of actin-based structures and cell polarization to stress fiber formation and Rho-mediated contractility [218, 252]. For instance, different stimuli, including growth factors (e.g., PDGF, EGF) and integrin-mediated cell-matrix adhesions, activate Rac. In turn, Rac activation stimulates PI3K and the Arp2/3 complex [223]. Rac activation also creates a positive feedback loop that promotes active Rac accumulation at the cell front. Note that PI3K is paramount for distinct mechanotransduction pathways of, among others, the cardiovascular system [253]. Also, PI3K inhibition reverse fish keratocytes directed migration in electric fields (galvanotaxis) [254]. However, during collective migration, PI3K inhibition does not reverse the directed migration of large groups of these cells. Notably, smaller groups do not exhibit persistent directional migration.

The Arp2/3 complex initiates the growth of new actin microfilaments, branches of older actin microfilaments (Figure 2.5a). Interestingly, the Arp2/3 complex acts as an actin amplifier as it stimulates the production of its own drivers (positive fedback loop) [255]. Conversely, formins and enabled/vasodilator-stimulated phosphoprotein (Ena/VASP) proteins promote nucleation and elongation of unbranched actin microfilaments at the barbed end of actin microfilaments (Figure 2.5a) [206, 223, 256, 257]. Indeed, the formin Diaphanous-related formin-1 (mDia1) localizes at the leading edge of some cells (e.g., T-cells) and cooperates with the Arp2/3 complex to initiate lamellipodium formation. The activation of Cdc42 stimulates PI3K, the Arp2/3 complex, and Rho-associated protein kinase (ROCK)-mediated myosin

contractility [256]. Heavily branched actin microfilaments made up the cytoskeleton of lamellipodia (Figure 2.5a). Conversely, filopodia consist of tightly packed, parallelly aligned actin microfilaments, with fascin as their main cross-linking/bundling protein (Figure 2.5a) [206, 252]. Indeed, Rac1 and Cdc42 stimulate lamellipodia and filopodia formation, respectively [218, 252, 256]. As actin microfilaments grow, they push and protrude the plasma membrane forward [228]. By pushing the plasma membrane, actin microfilaments increase membrane tension, which may act as a long-range inhibitor for protrusions anywhere else under specific conditions [217]. Recent reports on flat surfaces showed that protrusion initiation requires local depletion of actin-plasma membrane links acting in coordination with actin polymerization [258]. The density of membrane-proximal actin microfilaments is low at the leading front and high at the rear [259]. Cells migrating in one, two, or three dimensions exhibit stable gradients of membrane-proximal actin microfilaments. By locally decreasing the density of membrane-proximal actin microfilaments through cofilin, cells may enable Rac-mediated protrusions onset, directing and promoting cell migration.

In contrast, ADF/cofilin, a family of actin-binding proteins, is associated with the rapid depolymerization of actin microfilaments (Figure 2.5a). Of note, ADF and Cofilin1 are also required to prevent over-accumulation of stress fibers and associated focal adhesions. They promote cortical actin flow as well as the leader bleb-based migration of constricted cells [260]. Also, they modulate nuclear shape, movement, and integrity [261].

Proteins involved in signaling pathways activated by extracellular cues, such as PI3K, Rac1, and FAK, influence actin dynamics in different ways, regulating protrusion formation, stabilization, length, and lifetime [262–264]. Interestingly, in 3D substrates, protrusive activity increases with collagen density [202]. Cells' dependency on ECM remodeling to migrate in dense environments could explain such behavior. Furthermore, substrate stress relaxation regulates filopodial protrusions (i.e., their lifetime, length, and number) and cell migration [265]. Overall, actin microfilaments dynamics, which are tightly regulated (in time and space), are fundamental for cell polarity and motility.

Contractile forces through the actin-myosin complex Rho/ROCK signaling, including the RhoA effector, promotes focal adhesion formation and actomyosin-mediated contractility upon integrin-ECM engagement [206, 223, 256, 266]. Rho/ROCK suppression triggers the amoeboid to mesenchymal transition (AMT). The serine/threonine kinase ROCK cooperates with mDia to assemble actomyosin bundles (e.g., stress fibers). Besides, Rac and ROCK negatively regulate each other [206]. Actomyosin contractility, together with Arp2/3-mediated actin polymerization,

generates a retrograde flow of actin microfilaments [267]. When engaged by focal adhesions, this retrograde flow of actin microfilaments promotes traction force. Focal adhesions transmit pulling forces generated by these bundles to the ECM. Moreover, as traction forces increase, so does the size of focal adhesions [268]. As a result, cells can propel themselves forward, not only reorienting and lengthening the surrounding substrate fibers but also increasing their density [269–271]. Of note, according to the molecular clutch hypothesis, such forces may not be optimally transmitted depending on substrate features (e.g., stiffness, viscoelasticity, and stored strain energy) [159, 265, 272]. An enhanced actomyosin activity and cell contractility enable cells to migrate against stiffness gradients [273]. Therefore, metastatic cells (e.g., mammary, lung, prostate) may exhibit an adurotactic behavior in their tumor-specific niche. However, less contractile cells tend to durotax on flat surfaces.

In collective migration, contractile actin cables may appear across neighboring cells [131]. The associated actomyosin structures are coupled through adherens junctions or tight junctions to propagate tension, for instance, during tissue repair. Notably, cells seem to migrate along stress orientations, minimizing shear stresses. The alignment of actin microfilaments influences how much tension can be generated by these myosin motors [266]. Besides, cortical tension presents a biphasic response on the level of connectivity. In networks too loosely connected, stresses do not propagate, but those densely connected are too rigid and, although stresses do propagate, such networks cannot actively be remodeled. As a result, cells may actively regulate the connectivity of their actin cortex while changing their shape. In summary, the Rho/ROCK signaling is essential for cells to exert actomyosin-generated contractile forces over the ECM.

Stress fibers are essential for adhesive-dependent migration, as they couple focal adhesions to the cytoskeleton and the nucleus [274–276]. Different stress fiber subtypes (based on their location, composition, and anchorage to focal adhesions) bear unique mechanical properties and structural roles [277]. Vignaud and colleagues [278] demonstrated that stress fibers are not independent structures with discrete connections between them. Instead, stress fibers are embedded entirely in a contractile cortical actin network. This cortical meshwork allows for contractile forces exerted by stress fibers to propagate across the entire cell, actively contributing to traction force transmission to focal adhesions. Consequently, the contraction of the cortical meshwork impacts the overall magnitude of cells' contractile energy. Interestingly, Tavares and colleagues [279] demonstrated that a transient accumulation of stress fibers increases cell rigidity before cells acquire malignant features. Later on, a higher Src contractility would disassemble stress fibers to facilitate cell migration.

Although initially stress fibers were thought to be an artifact of 2D culture, more recent publications indicated that contractile stress fibers are also fundamental *in vivo* [275]. For instance, transmembrane actin-dependent nuclear lines, stress fibers crossing the nuclear envelope and essential for nuclear movement, are also present in cells within 3D cultures [280]. Distinct cell types exhibit differences in stress fiber organization in 3D [281]. For example, pancreatic fibroblasts cultured in soft matrices displayed randomly organized stress fibers, while in those within stiffer ECMs, stress fibers presented a more organized pattern. Conversely, cancer-associated fibroblasts exhibited well-organized stress fibers. Still, mammary epithelial cells (MEC) within mechanically tunable 3D culture models did not present stress fibers [282], which may suggest that stress fibers formation is context-dependent. Indeed, amoeboid-like migration seem to lack stress fibers [50] and does not require Rac/Cdc42-driven actin polymerization [206]. Thus, mesenchymal migration requires stress fibers to transmit pulling forces across cells' cortical actin meshwork.

For further details about actin dynamics see [249, 251, 252, 257, 266, 275, 283, 284].

Microtubules

Microtubules are also involved in several processes associated with cell migration. For one, their ability to resist high compressive loads and generate pushing forces makes them a relevant contributor to protrusion formation and maintenance [285, 286] (Figure 2.5b). They can also generate pulling forces to move the cell nucleus and facilitate rapid and directional transport of specific cellular components based on cell polarity. Microtubules growth would activate Rac-mediated actin polymerization, whereas depolymerizing microtubules would increase actomyosin contractility via Rho activation [286–289]. Note that microtubule outgrowth promotes a reduction in focal adhesion size and disassembly [268, 288, 290]. Moreover, RhoA and formins such as Diaphanous-related formin-2 (mDia2) regulate microtubule stabilization. Bouchet and colleagues [291] showed that the elongated shape of mesenchymal cells and their migration in 3D environments (*in vitro* and *in vivo*) requires persistent microtubule growth at the cell cortex. Interestingly, substrate stiffness regulates the polarization of the microtubule network during cell migration [292]. Further, ECM stiffening stabilizes microtubules and reorganizes the microtubule network [287]. Therefore, the ability of microtubules to generate pushing and pulling forces supports protrusive structures and cell organization, and its dynamics—regulated by Rho signaling and the ECM—influence cell morphology and migration.

Regarding molecular trafficking to and from the plasma membrane, microtubule motors serve as cargo tracks for cytoskeletal regulators and components, from integrins, Cdc42, and Rac GTPases to intermediate filaments (Figure 2.5d) [285, 286, 288]. They also carry messenger ribonucleic acid (mRNA) encoding proteins involved in actin polymerization, such as the Arp2/3 complex. Microtubules participate in matrix metalloproteinase (MMP) exocytosis [285, 288, 289]. Different studies suggest that microtubules may further act as an endocytosis controller [285]. Microtubules anchored to the plasma membrane serve as tracks for the transport of exocytic vesicles to focal adhesion sites. Consequently, they allow for focal adhesion disassembly and promote their turnover. Hence, microtubule-based intracellular trafficking contributes to cell polarization, protrusion formation, and focal adhesion turnover during migration.

By interacting with other cytoskeletal networks and cross-linking proteins, microtubules are guided toward focal adhesion and establish stable anchorages in their vicinity (Figure 2.5d) [288, 293]. Formins mDia1 and mDia2 take part in the orientation and alignment of the microtubule and actin networks in different cell types. Intermediate filaments may also play a role in this process, but further studies are required to shed some light on this matter. The microtubule-anchoring machinery is crucial in regulating focal adhesion dynamics and cell migration in response to specific ECM components. Besides, this mechanism might be cell type-dependent and cue-specific. Microtubules can also affect Rho GTPase signaling and stress fiber assembly [172, 285, 288]. Recent studies on astrocytes depicted a novel crosstalk between actin and microtubules [294]. In particular, rigidity-dependent microtubule acetylation would alter the dynamics and distribution of focal adhesions, as well as actomyosin contractility. These interactions, downstream of integrin-mediated signaling, would promote mechanosensitive migration. Thus, actin microfilaments are crucial for cell migration because of their role in protrusions formation and stabilization, focal adhesion turnover and regulation, cell polarity, and membrane vesicle trafficking [50, 172, 288].

For more details about the MTs dynamics see [286, 289].

Intermediate filaments

Intermediate filaments play a leading role in reinforcing cell structure and organizing cells into tissues. They maintain the mechanical integrity of the cytoplasm and regulate the organization of cellular organelles. Although the intermediate filament structure is highly flexible, intermediate filaments are more stable than actin microfilaments and microtubules, which allows for their role as scaffolds.

Intermediate filaments can spread through the entire cell cytoplasm, encapsulating the nucleus (Figure 2.5c) [172, 295, 296]. The spatiotemporal localization of intermediate filaments is phosphorylation-dependent. Moreover, these phosphorylation events have a functional role in different cellular processes, including cell migration [296]. For instance, intermediate filaments promote the formation and maturation of focal adhesions, which stabilize FAK, and influence integrin clustering, recycling, and motility [296–298]. They also influence signaling pathways regulating actin dynamics, cell polarity, and cell migration.

Regarding intermediate filaments' structural role, they provide mechanical support for the plasma membrane in contact sites with other cells and the ECM (Figure 2.5) [295, 296]. They can also behave as an elastic and conductive network to transmit force and propagate mechanical stimuli within and between cells via adhesion complexes. Indeed, tensile forces reinforce stress fibers by a coordinated effort between Rho signaling and the intermediate filament network. Still, at larger forces and extensions, intermediate filaments deform in a plastic manner, stiffening and decreasing their diameter [295]. Besides, once organized into networks, intermediate filaments acquire viscoelastic properties based on the number of crosslinks and which intermediate filament proteins are involved.

Intermediate filaments may participate in protein traffic by interacting with microtubules and with intracellular compartments and regulators of membrane trafficking. They also assemble into the nuclear lamina—which binds to the inner nuclear membrane and the chromatin—and act as a nuclear scaffold and mechanosensor [299–301]. Moreover, the composition of the intermediate filament network is cell-type specific. It depends on the mode of migration and thus on the properties of the surrounding ECM. The intermediate filament network may be optimized to protect the cell and regulate the distribution of actomyosin pulling forces throughout the cell [297]. Additionally, recent studies suggest that intermediate filaments optimize collective cell migration by regulating actomyosin-generated forces [234, 302]. Hence, intermediate filaments play different roles in distinct cellular regions and influence several processes involved in cell motility.

We refer the inquisitive reader to some excellent reviews focused on specific details of IFs dynamics [295–298].

Interactions between different cytoskeletal networks and with other cellular components

Although often viewed as three separate entities, actin microfilaments, intermediate filaments, and microtubules cooperatively interact with each other [50,

293, 296]. For example, through multiple direct, indirect, and steric interactions, actin microfilaments and microtubules influence intermediate filaments organization (Figure 2.5d). Moreover, perturbing actin microfilaments, microtubules, or their associated molecular motors can trigger intermediate filaments collapse. Cross-linking proteins hold together actin microfilaments and myosin motors in stress fibers. In turn, stress fibers bind to the microtubule network enabling cytoskeleton contractility [172, 303]. Vimentin (one of the most abundant members of the intermediate filament family) stabilize microtubules by direct interactions, decreasing microtubule catastrophe and increasing the rescue of depolymerizing microtubules. Furthermore, actin seems to modulate microtubule dynamics and their lifetime based on the actin network architecture. Shanghvi-Shah and colleagues [296] also noted that cells use the available cytoskeletal network to facilitate adhesion and cohesion and balance intracellular tension and externally-derived stresses. More recently, Doss and colleagues [304] showed that, at least in 2D substrates, active and passive cytoskeletal stresses regulate cells' ability to respond to ECM stiffness. They also found that crosslinks and the relative cell-to-ECM elasticity modulate the organization of the actin cytoskeleton. Tension transmitted through the ligand-receptor axis is crucial for the organization of the actin cytoskeleton, at least in T cells [305]. Integrin-based adhesions mediate interactions between microtubules and the actomyosin network [268]. These interactions strongly influence focal adhesions too. The coupling between microtubules and integrins locally regulates Rho/ROCK signaling. It also modulates the formation of myosin filaments. In turn, these myosin filaments act as controllers of integrin-based adhesions. Microtubules disappear from trailing protrusions before or during their retraction [306]. Notably, microtubule depolymerization locally coordinates actomyosin contractility and competing protrusions when cells migrate within complex environments [307]. Other studies on flat surfaces showed that the architecture of the actin network defines the position of the centrosome, the main organizer of microtubules [308]. In particular, the centrosome is located at the geometric center of an inner space devoid of actin bundles. Nonetheless, the spatial distribution of cell adhesions regulates the anisotropy of the actin network. Therefore, this location may not be the geometric center of the cell. Besides, based on the level of actomyosin contraction, the nucleus may displace the centrosome from this position. Noteworthily, the cortical actomyosin network modulates the organization of components of the plasma membrane, and the plasma membrane composition can also regulate cytoskeletal dynamics [309]. Such dynamic interplay between plasma membrane organization and the actin cytoskeleton provides the cell with a stable yet flexible cell surface that can continuously adapt to the surrounding environment.

Cytoskeletal dynamics, initiated by cell migration, activate transcriptional coactivators Yes-associated protein (YAP) and Tafazzin (TAZ), triggering a transcriptional regulation program. Indeed, FAK controls YAP/TAZ nuclear translocation via the RhoA pathway, which is promoted by increasing ECM stiffness and faster stress relaxation [40, 206, 310, 311]. Interestingly, the nuclear transport of YAP and other transcriptional activators may not depend on contractility per se [61]. Rather, it would rely on contractile strain energy transmission to the nucleus and stress generation in the nuclear envelope. This transcriptional regulation program feeds back to modulate cell mechanics, maintain a responsive cytoskeletal equilibrium, and prevent migration arrest [312]. Cell spreading on flat substrates promotes stress fiber formation and YAP/TAZ nuclear shuttling through Rho GTPases. Once in the nucleus, YAP regulates cell mechanics by controlling focal adhesion assembly [313, 314]. Moreover, the activity of YAP/TAZ—which limits cytoskeletal tension and focal adhesion maturation—although not required for initiating cell migration, is essential for persistence cell motility [315]. Transcriptional co-factors YAP/TAZ are also required in and induce several steps of the invasion-metastasis cascade [316, 317]. Notably, YAP not only promotes focal adhesion assembly but also tumor invasiveness by regulating FAK phosphorylation in breast cancer [318]. Besides, YAP/TAZ activity also enhances TGFβ signaling, which drives substrate stiffening [40], and crosstalks with VEGF during angiogenesis [313]. Nevertheless, the role of YAP in mechanotransduction is context-dependent. Indeed, YAP does not mediate mechanotransduction in breast cancer [282] but does so in other *in vivo* contexts such as pancreatic cancer [75, 319].

In summary, all three cytoskeletal networks must act in coordination for an efficient cell migration [50]. They not only share common regulators, but each of them can also influence the other two through cytoskeletal crosslinks or signaling pathways. As a result, cells can adapt to an always-changing environment. Such crosstalks between actin microfilaments, intermediate filaments, and microtubules are involved in cell polarity, protrusions formation, cell adhesion, and contractility. Moreover, all three cytoskeletal components are associated with cancer by interacting with signaling pathways or through proteins that participate in their dynamics [256]. Overall, different signaling effectors tightly regulate the dynamics of the cytoskeleton. They can be dependent on cell type and the profile of the surrounding microenvironment. They are also fundamental for cell motility.

Nuclear dynamics

The nucleus is the largest, most complex, and organized organelle within the cell. It is also the most rigid. It comprises different structures such as the nuclear envelope,

the lamina network, and chromatin, a complex of DNA and proteins forming the chromosomes of eukaryotic cells (Figure 2.6). In 1D and 2D environments, establishing cell polarity and migration does not depend on the cell's nucleus [320]. Still, in 3D domains, it may be essential for proper cell contractility and migration [321]. For example, in confining viscoelastic environments, mesenchymal stem cells (MSCs) create migration paths through a nuclear piston [322]. Amoeboid cells often migrate with their nucleus in front of the microtubule-organizing center (MTOC) as well as the Golgi apparatus (Figure 1.2) [306, 307]. In this configuration, the nucleus would act as a mechanical gauge, enabling cells to distinguish between pores of different sizes. As a result, cells would preferentially migrate along the path of least resistance. Conversely, the posterior passage of the MTOC beyond an obstacle or through a gap would determine the future trajectory of the cell. Then, all but the leading protrusion should retract by cutting off their microtubule supply. Note that, in confined environments, the nucleus is the main source of steric hindrance for 3D migration [164]. Recent studies reported that HT1080 (fibrosarcoma) cells within confined 3D substrates show speed accelerations by nucleus deformation and recoil [321]. Nuclear dynamics can thus, also play a fundamental role in 3D cell migration.

Interactions between the nucleus and other cellular components

Cells cultured on rigid flat surfaces spread and flatten their nucleus [323]. Conversely, on soft 2D substrates and in 3D hydrogels, cells promote a rounded or elliptical nuclear shape. Confined spaces have low porosity and constraining micropores. Besides, sometimes cells need to cross physical barriers. In such scenarios, cells may deform and change the morphology of their nuclei (Figure 2.6) [301]. Cells would also attach to the ECM via integrins and focal adhesions, while stress fibers exert high contractile forces transmitted to the nucleus through nuclear anchorage proteins [300, 324]. The linker of nucleoskeleton and cytoskeleton (LINC) complex and the nuclear pore complex are some of the main players enabling nucleus-cytoskeleton interactions [320, 325, 326]. The LINC complex couples these two cellular components together, whereas the nuclear pore complex allows the transport of molecules across the nuclear envelope. Furthermore, the LINC complex is also essential for nuclear mechanotransduction and translocation [66, 300, 320, 327]. Note that the LINC complex includes two protein domains, which span the inner nuclear membrane and the outer nuclear membrane. Different proteins such as nesprins bind the cytoskeleton to the nucleus through proteins from the inner nuclear membrane Sad1 and UNC-84 domain containing 1 and 2 (SUN1/2) (Figure 2.6) [172, 228]. Indeed, by accumulating at the front of the nucleus during

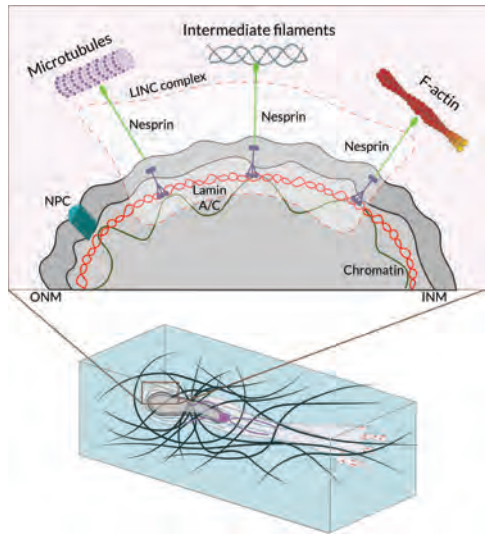

Figure 2.6: The nucleus during 3D cell migration. Mesenchymal cell migration within the extracellular matrix (ECM) requires multiple steps, including nuclear rotation and repositioning. Translocating the bulky nucleus of migrating cells through ECM barriers can become challenging unless the ECM is loose or highly pliable. Alternatively, the nucleus can be used to drive lobopodial cell migration, acting as a pressure-generating piston. Also, during amoeboid migration, cells can use the nucleus as a mechanical gauge or ruler by presenting it anteriorly to 'measure' the diameter of pores or passages in the ECM microenvironment. The cell then translocates through a passageway that is sufficiently wide to accommodate the bulky nucleus as the route of least resistance. The LINC complex is at the center of the nuclear-cytoskeletal coupling. On the cytoplasmic side, different nesprin isoforms connect the nucleus to the cytoskeleton. In the perinuclear space, nesprins bind SUN proteins, which span the inner nuclear membrane (INM) and interact with the nuclear lamina through lamin A. Emerin, a protein from the inner nuclear membrane, anchors SUN protein to lamin A and interacts directly with chromatin. NPC, nuclear pore complex. ONM, outer nuclear membrane. Adapted from [172].

confined cell migration, nesprins contribute to pulling it forward through narrow micropores and constrictions [324]. This nucleus-cytoskeleton coupling allows, for instance, microtubules to interact with proteins from the outer nuclear membrane, exerting mechanical forces onto them. In turn, proteins from the outer nuclear membrane relay these forces to the proteins from the inner nuclear membrane, the nuclear lamina, and chromatin [325]. These mechanical forces may alter the nuclear shape and induce nuclear envelope invaginations. Also, actin microfilaments located above the nucleus (perinuclear actin cap) align cells nuclei with the orientation of migration in some cell types (e.g., fibroblasts) [328]. As a result, cells can adapt and respond to external cues from the ECM.

Exerting high pushing and pulling forces may not be sufficient for cells to overcome these obstacles, though. Cells may also need to deform and change the

morphology of their nuclei to migrate (Figure 2.6) [301, 328]. Cells can modulate the ratios of lamins located in this organelle [300, 329–331]. As a result, cells contribute to the nucleus viscoelasticity by regulating the nuclear morphology and deformability. Mukherjee and colleagues [332] inhibited lamin A/C phosphorylation in HT-1080 fibrosarcoma cells, which increased their nuclei stiffness. Those cells migrate through 3 µm pores less efficiently than within 5 µm pores. They exhibited a dramatic change in nuclear circularity, suggesting that their nuclei underwent plastic deformation. Also, the proportion of nuclei with blebs after migrating through such pores increased threefold compared to the control group. Shiu and colleagues [333] showed that lamin A/C null fibroblasts exhibited a strongly reduced integrin clustering into the perinuclear region. The authors also reported an impaired YAP nuclear translocation.

Interestingly, Harada and colleagues [334] showed that 3D cell migration is biphasic in lamin-A levels. Moreover, partial loss of lamin-A is associated with several types of cancers (e.g., lung, breast, colon, ovarian, and prostate) [323]. While lamina dominates the mechanical resistance at large deformations, chromatin primarily governs such behavior for small ones [330]. Indeed, cells can change the balance of open and condensed chromatin within their nuclei [299, 331]. For instance, confined conditions in 3D induce chromatin decompaction and seem to decrease nuclear stiffness. Variations in substrate rigidity can also drive changes to the nucleus and chromatin state [301, 335]. Indeed, stiffer ECMs increase lamina-associated chromatin and the number of accessible chromatin sites. Such an event induces a tumorigenic phenotype in mammary epithelium. Interestingly, microtubules may also alter lamin phosphorylation and regulate chromatin dynamics [325]. The former, through the tension exerted onto the nucleus, while the latter by mediating the transport of specific molecular cargo within or to the nucleus. Microtubules not only interact with the nucleus through the LINC complex. They also force the transport of effector molecules and DNA repair proteins through nuclear pore complexes to influence chromatin and promote genome stability, respectively.

Constriction-induced deformation of the nucleus can have deleterious effects such as nuclear envelope rupture and excessive DNA damage (Figure 2.6) [300, 320, 336, 337]. Cells have some protective mechanisms against these events. The nuclear lamina is an organized meshwork of different lamins (i.e., intermediate filaments) underlying the nuclear envelope and separating the nucleus from the cytoplasm. Together with the cytoskeleton, it protects the nucleus against high nuclear stress [323]. Interestingly, Nava and colleagues [299] recently showed that persistent, high-amplitude stretch triggers a protective mechanism against DNA damage. As a result, the supracellular alignment of tissue redistributes stress before it reaches the

nucleus. Such tissue-scale mechanoadaptation involves a separate signaling cascade mediated by cell-cell contacts. This process allows cells to switch off the nuclear mechanotransduction and restore their initial chromatin state. Defects on nuclear dynamics are associated with the onset of devastating diseases [300].

Novel studies on MSCs showed that the nuclear envelope is wrinkled on soft 2D hydrogels [61]. However, on stiff 2D substrates (plastic or rigid glass), most cultured MSCs exhibited smooth nuclei, that is, little to no nuclear envelope wrinkling. A similar trend emerged in 3D systems, where MMP-degradability would determine the nuclear envelope morphology. Cell spreading would only happen after cytoskeletal tension removed nuclear envelope wrinkling in cells cultured on flat surfaces. Robust focal adhesion maturation would also require a taut nuclear envelope. In MMP-degradable hydrogels, MSCs exhibited prominent stress fibers and nuclear envelope wrinkling caused by actin impingement. Interestingly, a wrinkled nuclear envelope may also be associated with the chromatin-dominated regime of mechanical resistance. Conversely, a nuclear envelope with no wrinkles would indicate that the nucleus is under higher deformations and that lamins are the leading mechanical regulator of nucleus rigidity.

Recent works have proven the nucleus's ability to measure cellular shape variations [338, 339]. In particular, cell confinement below a threshold height deforms the nucleus. It also triggers actomyosin contractility, promoting fast amoeboid cell migration. As a result, cells might avoid getting stuck in their surroundings, of relevance during cancer cell invasion, and immune cells patrolling across peripheral tissues. It may also be paramount for progenitor cell motility within a highly crowded cell mass of a developing embryo. Hence, the dynamics of cells' nuclei allow them to migrate even across some of the most challenging 3D environments.

Different authors have reviewed specific aspects associated with nuclear dynamics (see [300, 301, 320, 323, 328, 331, 337, 340]).

ECM remodeling through cell-matrix interactions

Cells are continuously interacting with the ECM not only probing for cues, but also remodeling its structure [39, 47]. Such interactions between cells and their extracellular environment involve distinct mechanisms. The cell phenotype and the profile of the substrate determine which of these mechanisms are activated. For example, hydrogels with higher stress relaxation amplitudes seem to promote cell penetration and ECM remodeling [81]. This would enhance cell elongation, migration, and proliferation [81].

For further details on particular aspects of ECM remodeling see [40, 43, 143, 228, 341–346].

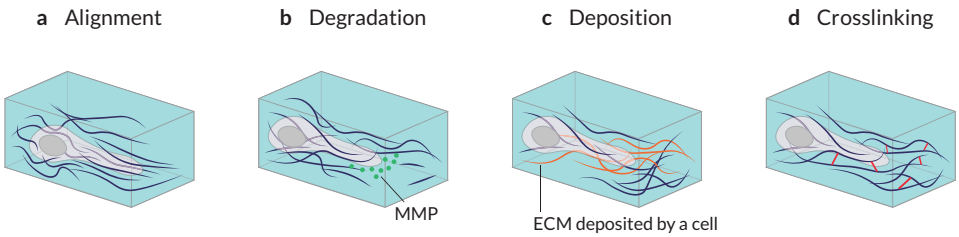

Figure 2.7: Matrix remodeling through cell-matrix interactions. (a) Mechanical forces exerted by cells can structurally remodel the surrounding matrix by stretching and aligning fibers of the extracellular matrix (ECM). **(b)** Cells may biochemically degrade a surrounding ECM by secreting various types of matrix metalloproteinases (MMPs). **(c)** Specific types of cells, such as fibroblasts, deposit additional ECM components on the surrounding matrix. This can lead to elevated matrix stiffness and smaller matrix pore size. **(d)** Cells can cross-link matrix fibers, resulting in the enhanced stiffness and elasticity of the ECM.

Aligning ECM fibers by exerting contractile forces

During migration, cells exert contractile forces to the ECM through focal adhesions, resulting in fiber alignment (Figure 2.7a) [152, 228, 270, 347]. For example, after migrating toward the injured area through chemotaxis, fibroblasts bring wound edges together by exerting pulling forces to their surroundings. Alignment in ECM fibers and microenvironment topography modulate, among others, the PI3K signaling pathway and promote cytoskeletal remodeling and cell polarization [347]. Interestingly, Matrigel-containing hydrogels increase alignment anisotropy around cells *in vitro*. The alignment of ECM fibrils allows for long-range communication between cells during angiogenesis and tissue repair. Fiber alignment also enhances the invasion of tumor cells [348]. The pushing and pulling behaviors of cells such as fibroblasts or human mesenchymal stem cells also induce ECM stiffening by fiber compaction [152, 228, 348, 349]. Substrate deformation gradually increases along a single axis during fibroblasts migrating in 3D domains, with higher and lower deformations at the leading and trailing edges, respectively [350]. Note that HT-1080 cells also exhibited this high frontal substrate prestrain found in fibroblasts. MDA-MB-231 cells, on the other hand, showed very similar displacements at the leading and rear edges. Moreover, during initial cell spreading within 3D matrices, fibroblasts seem to transmit anisotropic strain to the ECM to polarize. Chaudhuri and colleagues [80] highlighted the importance of matrix stress relaxation—which has recently been established as a key requirement for robust cell migration on soft substrates [265]—in cell-matrix interactions. Other works have shown a more versatile ECM because of the heterogeneity in crosslink unbinding kinetics [347, 351]. Predominantly permanent crosslinks increase tension sustainability. Conversely, high

levels of transient crosslinks increase plastic remodeling (i.e., nonelastic densification) during cell-matrix interactions. Therefore, a shift in the balance between permanent and transient crosslinks will bias ECM response to contractile cells. Other studies have shed some light on alternative strategies that facilitate cancer cell protease-independent invasion of basement membranes mediated by matrix mechanical plasticity [169, 343]. Cells' ability to mechanically remodel their surroundings is thus fundamental to many biological processes, including cell migration [39].

Degrading the ECM through cellular proteolytic activity

Cells can also degrade the surrounding environment and expand ECM pores by releasing MMPs (Figure 2.7b) [152, 352]. The properties of the microenvironment, including substrate composition, may influence cells' ability to align ECM fibers. For instance, in Matrigel-containing hydrogels, H1299 cancer cells require a more intense MMP activity to migrate than in collagen-only substrates. The former are stiffer and with fewer but larger pores than the latter. Matrix metalloproteinases act on several extracellular proteins (e.g., cytokines, antimicrobial peptides). Accordingly, they regulate, among others, different aspects of inflammation and immunity. Interestingly, Cdc42 and RhoA participate in MMPs trafficking to invadopodia tips [206, 218]. Cytoskeletal dynamics may also modulate MMPs transport [288]. A dysregulated MMP activity is also associated with cancer, fibrosis, and cardiovascular disease [40]. Besides MMPs, cells can use other proteases such as adamalysins and meprins to biochemically break down ECM components [160]. They do so by catalyzing proteolysis, which breaks down proteins into smaller polypeptides or single amino acids. Notice that, in the absence of proteolytic activity, and if the matrix is viscoelastic enough, cells may deform and expand nanometer-size pores and migrate through [78]. Further, after receptor-mediated internalization, endocytic cargo degradation enables cells to internalize and degrade ECM molecules in lysosomes. Indeed, collagen internalization is considered a key protection mechanism in liver fibrosis *in vivo* [346, 353]. Moreover, PI3K products have a role in membrane tension, influencing the endocytic response and membrane trafficking used by migrating cells (e.g., fibroblasts and neutrophils) [354]. Mechanical forces may alter the structure of some proteins, inhibiting/facilitating their interactions with the surrounding molecules [344]. As a result, strain suppresses the degradation of some ECM proteins, such as collagen [341]. Therefore, cells' ability to degrade the surrounding substrate is tension-dependent and involved different players, such as proteases and lysosomes.

Regulating ECM composition by synthesis, secretion, deposition and cross-linking of ECM components

Cells also regulate ECM composition by depositing and cross-linking some of its components (Figure 2.7c and Figure 2.7d). For instance, during morphogenesis, epithelial cells synthesize components of the basement membrane, such as collagen IV and laminin. Osteoblasts secret different ECM components (e.g., osteocalcin, osteopontin) during bone formation [355]. In the interstitial matrix, fibroblasts deposit several distinct ECM components within intact and wounded tissues [160]. Note that some of these secreted ECM proteins provide cell growth factors and cytokines, which may promote a chemotactic response. Other deposited components serve as physical scaffolds or mechanotransducers, promoting fibrils formation from collagen and fibronectin, and their cross-linking by enzymes. An example of ECM-modifying enzymes, lysyl oxidases (LOXs) covalently cross-link collagen fibrils, which is fundamental for the correct assembly of collagen fibers [38, 341, 342]. Tissue Transglutaminase (TG2) cross-links other ECM molecules, including fibronectin and collagen IV. Lysyl oxidases and TG2 are frequently overexpressed in cancer, increasing fibrosis, ECM stiffness, and cross-linking [140, 142]. Further, they promote tumorigenesis, metastasis, and affect mechanical properties and cell-matrix signaling. By depositing viscoelastic ECM components, cells can also remodel the surrounding microenvironment and promote cell migration in elastic degradable substrates [78]. Recent studies have shown that collagen endocytosis can also support fibril assembly at the plasma membrane [356]. Aberrant overexpression of growth factors such as TGFβ, PDGF, and VEGF may be associated with different pathologies [40, 181]. For instance, TGFβ overexpression promotes myofibroblasts differentiation, cell proliferation, and matrix production. At the same time, TGFβ signaling inhibits proteolytic activity, driving ECM stiffening. In response to substrate stiffening, cells exert higher contractile forces against the surrounding environment, which activates matrix production [345]. Moreover, by leveraging ECM remodeling through cell-matrix interactions, tumors create microenvironments that promote tumorigenesis and metastasis [342]. Interestingly, TGFβ controls many aspects of primary tumor growth and dissemination by inducing EMT and EMT-associated changes [104].

Interactions between different ECM remodeling mechanisms

Tissue homeostasis requires a balanced synthesis and degradation of structural proteins. Abnormal composition of the ECM because of the failed regulation of some of these processes is associated with different pathologies, such as fibrosis and

metastasis [97, 357]. For example, during the wound healing response fibroblasts end up undergoing apoptosis or become quiescent. However, during cancer and fibrotic diseases, the fibroblast response is sustained [40]. Fonta and colleagues [358] recently showed that in progressive diseases (e.g., cancer, viral infections of lymph nodes), tensional tissue homeostasis is perturbed by cell-matrix interactions. More recently, Perestrelo and colleagues [359] provided a comprehensive description of the changes in collagen network organization during pathological cardiac ECM remodeling. They also showed that underlying this reorganization, in cardiac fibroblasts, YAP is activated to rearrange the substrate in a profibrotic feed-forward loop. Note YAP activity also promotes the transcription of genes involved in cell-matrix interactions, ECM composition, and cytoskeleton integrity [172, 314, 360]. In summary, cells can interact with their surrounding microenvironment through a variety of mechanisms. Such cell-matrix interactions are fundamental for many cellular functions, including cell migration.

2.2 Theoretical studies and computational models

Computational models can help overcome some of the challenges of experimental research and advance the understanding of complex biological processes such as cell migration. Unraveling the intricacies of some of these mechanisms is getting increasingly expensive. It requires costly equipment and highly qualified professionals. Furthermore, as computational power and data storage capabilities increase, so does the use of *in silico* modeling tools. Mathematical models may offer valuable insights more efficiently, for example, by more easily isolating some specific mechanisms and behavioral patterns. They could even act as advisors and consultants for experimental researchers by fostering new hypotheses to be tested at the lab.

Over the last several decades, the research community has developed a wide variety of *in silico* models, aiming to further our knowledge on cell migration. Most of the mathematical models proposed are focused on cells migrating on flat surfaces, which is what we know best so far [31, 361–369]. However, there is an increasingly large number of *in silico* models replicating the more complex and physiologically relevant migration within 3D matrices [370–374]. Nonetheless, some of these computational models are 2D representations of 3D cell migration [375–377] or model a 3D cell moving on a flat substrate [378]. As a result, such works cannot replicate some hallmarks of cell motility within 3D matrices.

Next, we will present different *in silico* models classified according to different criteria based on the mode of migration, the scale, and the modeling approach.

2.2.1 Investigating different modes of migration

Mathematical models of cell motility can be classified according to the migratory strategy used by simulated cells (e.g., individual or collective). Sun and Zaman [379] reviewed models of cell migration and cytoskeletal dynamics associated with this cell motility. The authors analyzed differences between amoeboid and mesenchymal migration, as well as individual versus collective migration. Shatkin and colleagues [380] reviewed different theoretical approaches used to consider how the biophysical properties of the ECM modulate cell migration. In particular, they focused on mathematical models that improved our understanding of metastasic behaviors and durotaxis. The authors also reviewed *in silico* models of mesenchymal and amoeboid migration. Interestingly, the authors noted that none of the models included in their review considered all the variables involved in cell motility, which would likely be infeasible.

Individual migration

Some *in silico* models have tried to shed some light on individual cellular motility—which, for instance, allow leukocytes to patrol tissues looking for pathogens. In these cases, and depending on distinct factors (e.g., cell type, the properties of the environment), cells can use different migrating strategies.

Fibroblasts—which are essential for maintaining connective tissue homeostasis and tissue repair—are usually considered the prototypical mesenchymal cell. These are thin and elongated cells that migrate using protrusive structures that adhere to the ECM through numerous, robust, and dynamic focal adhesions. They also rely on MMPs proteolytic activity to degrade the surrounding ECM, expanding the pores through which they squeeze themselves. Myosin expression, which maintains polarized substrate prestrain during migration, is another essential component of the mesenchymal phenotype [350]. Note, however, that distinct cell types exhibit different degrees of mesenchymal features.

Different theoretical studies focused on modeling mesenchymal migration within 3D matrices [34, 381, 382]. For instance, Heck and colleagues [375] developed an *in silico* model of cells migrating through a degradable viscoelastic ECM. This computational model enabled them to provide new insights regarding the role of protrusions in this mode of migration. Bangasser and colleagues [154] proposed a model that predicted an optimal ECM stiffness for mesenchymal cell migration. Interestingly, altering the number of active molecular motors and clutches could shift this stiffness optimum. Afterward, the authors verified this prediction experimentally.

During amoeboid-like migration, cells have a limited proteolytic capacity and largely reduced adhesion that hinders their ability to pull and rearrange ECM fibers.

Several computational models focused on this protease-independent migration strategy [383]. For instance, Moure and Gomez [384] presented a computational model of amoeboid cells chemotaxing on 2D surfaces and within 3D matrices. Their modeling efforts unveiled an intricate interaction between the dynamics of chemotactic ligands and the geometry of the substrate. Such interplay would tightly regulate cell migration. Campbell and Bagchi [385] proposed an *in silico* model that predicted that cell deformability and protein diffusivity would alter swimming behavior and speed. In particular, increasing the former would increase the speed of migration and switch from a random to a persistent unidirectional motion.

Cells can also move within 3D environments using a lobopodial mode of migration [41, 44, 386].

Although this mode of migration was more recently proposed, a few *in silico* models already focus on it. Serrano-Alcalde and colleagues [387] presented a computational model to shed some light on the factors and mechanisms activating this mode of migration. Through finite element modeling, authors identified possible two mechanotransduction mechanisms that may regulate the switch from mesenchymal to lobopodial migration: the fluid flow velocity inside the cytoplasm and the pore pressure.

Collective models

Cells may also interact with their neighbors through cell-cell adhesions (e.g., tight junctions, cadherin-based adherens junctions, desmosomes). Collective migration is associated with development, regeneration, and tissue repair. During these events, cells can move as sheets adhered to the surrounding ECM. Tumoral cells also use this mode of migration while invading as sheets at the interface between tissues.

This cooperative mode of migration has been extensively studied using *in silico* models. Indeed, Alert and Trepat [388], as well as Camley and Rappel [389], recently reviewed the physical models developed by the research community to explain collective cell migration. Deutsch and colleagues [390] proposed BIO-LGCA, a cellular automaton, to analyze this mode of migration to predict the formation of clusters in adhesive interacting cells. Garcia-Gonzalez and Muñoz-Barrutia [391] were interested in studying how substrate stiffness influences collective migration. They developed a model to test different hypotheses regarding which mechanisms drive collective motion. The authors suggested that the main driver of non-symmetric collective motility is the induced cell polarization by substrate

stiffness gradients. Notably, Mayalu and colleagues [392] superposed single-cell computational models to predict multicellular behaviors. Neumann and colleagues [393] integrated experimental and computational data to create an *in silico* model of tube elongation. This computational model revealed that mammary morphogenesis can emerge by combining intercalation, interfacial tension dynamics, and high basal stress. Escribano and colleagues [394] developed a computational model that enabled them to compare single and collective migration. Their *in silico* model helped them understand why collective motion is much more efficient than single-cell migration.

2.2.2 Investigating at different scales

Mathematical models can also be classified according to their scale (i.e., subcellular, cellular, and tissue-level) [395, 396]. Of note, Buttenschon and Edelstein-Keshet [397] recently reviewed multi-scale models, coupling events from the intracellular to the cellular to the multicellular scales. Ferruzzi and colleagues [79] examined the experimental and modeling techniques available to study the structure and multi-scale mechanics of collagen networks. Conversely, Spill and colleagues [220] reviewed models and supported experimental findings of different aspects of mechanobiology—which are also related to cell migration—spanning different scales. Lastly, Cheng and colleagues [398] reviewed models from different scales proposed to improve our knowledge of how cells respond to biophysical stimuli.

Subcellular models

Subcellular models have tried to shed some light on specific processes involved in cell migration that may occur in some cellular regions. For instance, Borau and colleagues [26] focused on the mechanosensing properties of the actomyosin network. Fatunmbi and colleagues [27] focused on the recruitment of actin nucleating proteins at the membrane interface. In contrast, Hetmanski and colleagues [399] proposed a combination of distinct modeling approaches to study rear retraction dynamics of migrating cells within 3D substrates. Hobson and Stephens [400] reviewed the mechanical modeling of cell nuclei. Regarding chemotaxis, Hopkins and Camley [28] recently used *in silico* modeling to study cells' ability to accurately process external signals in uncertain environments. They argue that cells should adapt their cell surface receptor expression based on the surrounding environment. In particular, cells should only express multiple receptor types if they typically explore environments where ligand concentrations vary over orders of magnitude. Karagoz and colleagues [401] reviewed the computational models of integrin signaling. Also, LeRoux and colleagues [135] included a review of different mathematical

models proposed to improve our knowledge of the impact of mechanical stimuli on the plasma membrane and its complex mechanochemistry. Conversely, Oria and colleagues [193] proposed a general framework to explain how cells sense spatial and physical information at the nanoscale. They combined *in vitro* observations with a computational molecular-clutch model, in which individual integrin-matrix bounds respond to force loading by recruiting additional integrins (up to a maximum value). Interestingly, their results showed that, contrary to the by-then consensus, an increase in substrate stiffness or ligand density promoted adhesion growth. Lastly, Vignaud and colleagues [278] built a biophysical model to investigate the properties of an elastic network of actin fibers embedded in a cortical meshwork. One of the main novelties of this work was that stress fibers were not connected to the ECM but the adjacent cortical meshwork.

Cellular models

Cellular models may be interested in combining some of the aforementioned biological events to explain distinct aspects of cell motility and simulate the entire cell. For instance, Adebowale and colleagues [265] developed an *in silico* model that was able to replicate several observed experimental trends. First, how stress relaxation on viscoelastic substrates and stiffness on elastic ones influence cell migration speeds. Secondly, the impact of inhibition of adhesion, actin polymerization, and actomyosin contraction. In contrast, Cao and colleagues [378] proposed a computational model of cell migration integrating two continuum models: a biochemical activator-inhibitor system coupled with cell mechanics (cell membrane deformation and cell motion). Merino-Casallo and colleagues [35] developed an *in silico* model of 3D cell migration that integrated intracellular signaling with cell mechanics that replicated some of the main observations of *in vitro* experiments under different biochemical profiles. Also, Li and colleagues [372] proposed a 3D model of breast cancer cell migration, in which they included distinct modulating factors, such as fluid dynamics, autologous chemotaxis, substrate rigidity, and fibrillar structure, as well as cell-fiber and cell-flow interactions. Lastly, Moure and Gomez [33] recently studied the influence of myosin activity on cell polarization and how mechanical cues induce motion. In particular, their *in silico* model for keratocytes considered cell deformations, myosin-RhoA dynamics, and forces associated with the actomyosin network.

Tissue-level models

Tissue-level models represent collective cell motility. For example, Gonzalez-Valverde and Garcia-Aznar [30] proposed a hybrid model to simulate collective cell migration

in epithelial monolayers. Nosbisch and colleagues [402] developed a framework that enabled them to couple signal transduction mechanisms at the molecular level to individual and collective migration guided by chemoattractant gradients in tissues. Conversely, Peng and colleagues [36] proposed a multi-scale model of tumour invasive growth. This model considered the active interplay between the molecular mechanics of some proteolytic enzymes at the cell scale and the tissue-scale tumor dynamics. Sunyer and colleagues [130] found that multicellular clusters exhibited durotactic behaviors—even if their isolated constituent cells did not durotax—because of supracellular transmission of contractile forces. To explained the observed phenomenology, the authors proposed a continuum model integrating clutch-like cell-matrix dynamic at focal adhesions, long-range force transmission through cell-cell junctions, and actin polymerization at monolayer edges. Notably, Fletcher and Osborne [37] recently reviewed the progress in multi-scale modeling of multicellular tissues. They also highlighted some ongoing challenges associated with their definition, implementation, and validation.

2.2.3 Investigating through different modeling approaches

Mathematical models may also be classified depending on the modeling approach used (continuum, discrete, or hybrid) [396, 403].

Continuum models

Continuum models are based on the definition of constitutive laws to model processes and events (e.g., transport of biochemical substances, actomyosin contraction, or nuclear deformation). They rely on solving partial differential equations. The finite element method and other derived methods (e.g., smoothed-particle hydrodynamics) are some of the most applied techniques [332, 375, 404, 405]. Other authors have opted for the phase-field model [406]. These models have been extensively used to reproduce large-scale biological systems. However, as the number of biological processes included in these models increases, so does the complexity of the defined constitutive laws. For example, Ahmadzadeh and colleagues [407] developed a continuum model to determine how cells collaborate to elongate epithelial tubes. In this model, the authors included different aspects of cell migration, including cell adhesions, substrate rigidity, fiber realignment, strain stiffening, ECM ligand density, and pore size. In contrast, Arefi and colleagues [404] developed a finite-element model to simulate the extravasation process. They included the chemo-mechanics of the stress fibers and focal adhesions, as well as the contractile forces pulling the nucleus of tumor cells against the elastic resistance of

the endothelial cells. Banavar and colleagues [408] focused their attention on the role of genetically encoded mechanical feedback as a coordinator of cell morphogenesis and polarity. Also, Bennett and colleagues [409] developed a continuum model to explain the DNA damage occurring during constricted migration. Hervas-Raluy and colleagues [405] focused on the effects of actin and myosin in cell motility within confined environments, considering the different mechanical properties of the cytoplasm and the nucleus. Notably, Lee and colleagues [371] presented a combined *in silico* and *in vitro* model of macrophages migrating within 3D matrices in response to biophysical and biochemical factors. They coupled chemokine- and intermediate filament-mediated signaling cascades commonly regulated by Rho GTPases. Mackenzie, Rowlatt, and Insall [410] presented a finite element method to approximate systems of bulk-surface reaction-diffusion equations on 2D domains. They also used the proposed methodology to model individual migration guided by chemotaxis. Conversely, Moure and Gomez [406] reviewed phase-field models of individual and collective migration. Mukherjee and colleagues [332] used a continuum model to analyze the evolution of nuclear shape and stresses during the confined migration of a cell through a deformable ECM. Lastly, Serrano-Alcalde and colleagues [411] developed a continuum model to study the role of nuclear mechanics in cell deformation under different creeping flows.

Discrete models

In discrete models, the different agents involved are portrayed as separate units in the system. Therefore, it is more direct and intuitive to represent the spatial inhomogeneities and variability of biological systems. As a result, we can include more information in those models. Historically, discrete models were computationally expensive as they are representing every agent as an independent unit. They must also consider how those units interact with each other. However, computational costs have greatly decreased during the last several decades, which has dramatically alleviated this issue. Besides, the open-source community offers an increasing number of applications and libraries based on the discrete approach (e.g., PhysiCell, FLAME) [412–415].

Different authors have proposed agent-based models related to cell migration. For one, Feng and colleagues [416] integrated signaling networks, integrin dynamics, and substrate stiffness in a mechanochemical model of neutrophil migration. Reinhardt and Gooch [417] proposed a model focused on cell-matrix interactions. In particular, they studied the impact of different biophysical features of the substrate in ECM remodeling. Also, Drasdo, Van Liedekerke, and colleagues [418, 419] focused on different discrete modeling approaches (lattice and off-lattice) to simulate

different biological processes, including cell migration. Lastly, PhysiBoSS is a multi-scale agent-based modeling framework that combines intracellular signaling and multicellular behavior [420].

Hybrid models

Hybrid models combine continuum and discrete models to overcome their intrinsic limitations. Designing the interface between those models is their main issue, as they must share information with each other.

Different works have proposed a hybrid approach to replicate some of the biological processes associated with cell migration. For example, Gonçalves and Garcia-Aznar [32] proposed a hybrid model to simulate how the ECM density regulates the formation of tumor spheroids through cell motility. They modeled cells using a discrete center-based framework while a continuum model defined the ECM. Also, Gonzalez-Valverde and Garcia-Aznar focused on understanding how forces at cell-cell contact sites and the rigidity of epithelial monolayers modulate collective migration and topology [421]. In this case, an agent-based model defined cells whereas a continuum material model described the cell passive mechanics. Macnamara and colleagues [422] presented an *in silico* model to simulate cancer growth and migration within a 3D heterogeneous tissue. They used an agent-based model to simulate the behavior of cells and the tempo-spatial interactions between each other. The authors coupled this model to a finite-element solver to model the diffusion of oxygen from blood vessels to cells. Rens and Merks [362] proposed a hybrid model to explain the full range of cell shape and durotaxis from focal adhesion dynamics. They used an agent-based lattice model to represent cells. However, they calculated the planar stress in the ECM using a continuum model where they represented the substrate with a finite-element model. Lastly, Sfakianakis, Madzvamuse, and Chaplain [423] proposed a hybrid multi-scale model to describe cancer invasion of the ECM.

2.3 Summary

Chapter 2 has presented a detailed overview of cell migration. In particular, this chapter has focused on the mechanisms enabling cells to perceive and internalize biochemical and biophysical cues from the surrounding microenvironment. Chapter 2 has also paid special attention to how cells adapt and respond to these external stimuli. Note, however, that some of the findings mentioned in this chapter and others not included here may not translate to 3D (*in vitro* and *in vivo*)

systems. In summary, cell migration is essential for many physiological processes of multicellular organisms, including embryonic development, tissue repair, and the immune response. Unfortunately, aberrant cell motility also plays a prominent role in different pathological processes that can result in congenital malformations, skeletal, cardiovascular, and autoimmune disorders, as well as metastasis.

More than a century of research has allowed us to unravel, at least partially, some of the mechanisms involved in cell migration. However, we still lack a comprehensive understanding of how cells probe and respond to the surrounding microenvironment. From the signaling networks regulating cell migration to the cell mechanics allowing cells to adapt and respond to an ever-changing environment. An exhaustive knowledge of cell motility would dramatically improve our life expectancy and quality of life. It would enable novel advances in tissue engineering and regenerative medicine (e.g., creation of bioartificial organs). A comprehensive understanding of cell migration could also create new opportunities for selective, non-invasive, and effective medical treatments and therapies that would help to prevent or correct many pathologies, including some of the leading causes of morbidity and mortality.

Developing new methods and techniques to increase the scale and resolution of our experimental analyses is essential to uncover some of the remaining mysteries that lie ahead. Accordingly, we should aim for multidisciplinary studies considering the multi-scale nature of cell motion and integrating the different players and events involved in these migratory behaviors. *In silico* modeling has proven fundamental to advance our knowledge in many fields, including cell biology and motility. The integration of other computational tools (e.g., machine-learning [424, 425], Bayesian optimization [426–428], bioimage analysis [429–432]) in our workflows has demonstrated to be a very promising venue in our quest for a complete and detailed picture of cell migration.

The following chapters attempt to address some of the current deficits highlighted in this review using an integrative perspective. To facilitate the collaboration between theoreticians and experimentalists, Chapter 3 examines the feasibility of using Bayesian optimization techniques to integrate theoretical studies and *in silico* modeling with experimental data. Chapter 4 investigates how cells probe for biochemical stimuli and respond to them. Lastly, Chapter 5 studies the different mechanisms enabling cells to perceive biophysical cues and how such external signals bias cell's migratory behaviors.

3

Integrating experimental data with theoretical models

Contents

This chapter is partially based on:

Francisco Merino-Casallo, Maria Jose Gomez-Benito, Yago Juste-Lanas, Ruben Martinez-Cantin, and Jose Manuel Garcia-Aznar. *Integration of in vitro and in silico models using Bayesian optimization with an application to stochastic modeling of mesenchymal 3D cell migration.*

3.1 Need for the integration of experimental data and theoretical models

Experimental research has historically paved the way toward a comprehensive understanding of biological phenomena. By defining new protocols and engineering new equipment, experimentalists have been able to push forward the frontier of biological sciences. However, these novel developments can require vast amounts of time and money. Therefore, experimental researchers could take advantage of alternative approaches to overcome some of the current limitations of their discipline.

For the last couple of decades, the computational resources available to the research community have increased drastically. This improvement in computational power has enabled theoretical modelers to propose more complex *in silico* models. These computational models can now include a variety of players and events, which may interact with each other and act at distinct scales. As a result, theoretical studies and computational models have become a powerful tool to improve our knowledge of these biological systems and the perfect complement to experimental research.

Both disciplines have their own set of challenges. However, by acting in concert, they can complement each other. For example, experimentalists may test novel hypotheses proposed by theoreticians in the lab. Evaluating the predictions of theoretical models by direct observation in the lab is an essential part of the biological sciences. In contrast, theoretical studies and computational models may easily quantify elements that are technically challenging to quantitatively measure experimentally. *In silico* models could also carry out experiments that are currently very expensive or technically impossible in the lab. Hence, frameworks that enable the integration of experimental data with theoretical models can bring researchers closer to the next frontier of biological sciences.

Model calibration is fundamental for this integration between experimental data and theoretical models. This calibrating process enables theoreticians to find a set of values for the model parameters that provide a good characterization of the behavior of the system under study. As multi-scale models increase their complexity, they usually include more parameters. Accordingly, the calibration process becomes much more difficult. However, researchers still calibrate their *in silico* models through a process that requires frequent user interaction. The search space is usually too vast to be effectively navigated. Besides, there may be interactions or dependencies between some parameters. This process can be very tedious and error-prone, especially if *in silico* simulations take several hours to finish. Therefore, an automated workflow that integrates experimental data with theoretical models would be particularly valuable.

3.2 Relevance of Bayesian optimization and its methodological significance

The calibration process can be mapped to a nonlinear optimization problem whose objective is to find the combination of parameter values that best fits the experimental data (e.g., *in vitro*, *in vivo*). This mapping enables us to automate the tunning process. However, most nonlinear optimization solvers require too many iterations, gradient information of the target function (also known as the objective function), or are sensitive to local optima. Evaluating this target function may be very costly. In model calibration, the target function estimates the model fitness. Assessing the target function requires running simulations of these *in silico* models, which may take a long time (from several minutes to multiple days). Further, stochastic models require the execution of many simulations to capture the range of potential behaviors or outputs. Hence, by requiring too many iterations, these nonlinear optimization solvers could make the problem intractable.

More formally, we are looking for the optimal set of parameter values $\boldsymbol{x}^*$ satisfying:

$$\boldsymbol{x}^* = \underset{\boldsymbol{x}\in\chi}{\operatorname{argmax}}\, f(\boldsymbol{x}), \tag{3.1}$$

where $f(\boldsymbol{x})$ is the target function comparing the experimental data with the numerical results, and χ is the parameter domain.

Bayesian optimization, also called Efficient Global Optimization (EGO) [433] is a general-purpose black-box optimization methodology. The ability to reach global optimization after just a few iterations is one of the hallmarks of BO [434, 435]. Indeed, BO uses a probabilistic surrogate model of the target function $f(\boldsymbol{x})$ combined with optimal decision theory to drive the search toward the global optimum in fewer iterations than other popular nonlinear optimization alternatives, including Particle Swarm Optimization (PSO) [436], Covariance Matrix Adaptation Evolution Strategy (CMA-ES) [437], and Limited-memory Broyden-Fletcher-Goldfarb-Shanno (L-BFGS) [438]. In the case of BO, the surrogate model uses ML to capture previous iterations acting as a memory of the whole optimization process. Meanwhile, the decision component carefully selects the following query at each iteration. Besides, BO robustly handles noisy data and naturally adapts to discrete and irregular parameter domains, facilitating the exploration of noisy or irregular parameter spaces. Furthermore, BO efficiently scales with the parameter domain, promoting an efficient exploration of large parameter domains. Accordingly, BO is especially suitable for experimental design and the calibration of expensive processes [426, 439–441].

In model calibration, many metrics can be used as the target function, and some might be competing. We may be interested in optimizing several competing metrics. Then, we can redefine the problem as a multi-objective, multi-criteria optimization or Pareto optimization:

$$\boldsymbol{x}^* = \underset{\boldsymbol{x}\in\chi}{\operatorname{argmax}}(f_1(\boldsymbol{x}),\ f_2(\boldsymbol{x}),\ \ldots, f_n(\boldsymbol{x})), \tag{3.2}$$

where each $f_i(\boldsymbol{x})$ term is a competing target function comparing the experimental data with the numerical results. In this case, the objective may not be to find a single optimal set of parameters (parametrization). Instead, we could find ourselves in a Pareto optimality situation, where no individual criterion (target function $f_j(\boldsymbol{x})$) can get any better without getting at least another one (target function $f_k(\boldsymbol{x})$) worsening. Our objective would be to find the whole set of parametrizations (Pareto optimal points) associated with the Pareto frontier. Although this is a completely different problem, the seminal work of Knowles [442] extended the BO methodology to the multi-objective setup.

The BO methodology does not require specific knowledge about the target functions, making them easily exchangeable. Therefore, the same procedure applies to every target function (e.g., KL-divergence, Kolmogorov distance, or Root Mean Square Error). Metrics that are not directly related to the data, such as monetary cost and time, can also be included in this fitting process. In the presence of competing target functions, solutions along the Pareto set or frontier might follow a complex distribution. Finally, based on the specific circumstances, the expert user must balance these competing metrics by choosing the most convenient parametrization from the Pareto front a posteriori.

3.3 The Bayesian optimization procedure

The BO methodology consists of two main components: a probabilistic surrogate model of the target function $f(\boldsymbol{x})$ (statistical model) and an acquisition function α [434, 435]. On the one hand, the statistical model (a Gaussian Process) includes a prior distribution that captures our current beliefs about the behavior of the unknown target function and an observation model describing the data generation mechanism. On the other hand, the acquisition function assesses how optimal a sequence of queries is. These acquisition functions can take many forms (e.g., expected improvement, entropy search, knowledge gradient). Ideally, the acquisition function is maximized (or minimized) to select an optimal sequence of queries.

The BO procedure starts by initializing the statistical model, placing a Gaussian Process on $f(\boldsymbol{x})$. Secondly, we observe the target function $f(\boldsymbol{x})$ at n_0 points ($\boldsymbol{x_i}$),

which have been sampled from the parameter space χ either uniformly random or by low-discrepancy sequencing [443] (Figure 3.1 Step 1). Next, we update the prior based on the n_0 points ($\boldsymbol{x_i}$) and their associated output values ($y_i = f(\boldsymbol{x_i}), 0 \leq i \leq n_0$; observations) (Figure 3.1 Step 2). As a result, we produce a more informative posterior distribution (our current beliefs on the likely function $f(\boldsymbol{x})$ we are optimizing) over the space of target functions. We use the mean from the posterior as the function most likely to model the target function. Then, we apply the acquisition function α to guide the exploration of the parameter space χ. Acquisition functions trade off exploration and exploitation. Therefore, their optima are located where the uncertainty in the surrogate model is large (exploration) or where the model prediction is high (exploitation). Note that different acquisition functions take different approaches to define exploration and exploitation. Bayesian optimization algorithms choose the next query point ($\boldsymbol{x_{n+1}}$) by maximizing such acquisition functions (Figure 3.1 Step 3). Finally, we observe the target function at the new query point ($y_{n+1} = f(\boldsymbol{x_{n+1}})$; Figure 3.1 Step 4). We keep refining the statistical model with the latest sampled data ($\boldsymbol{x_{n+1}}$ and y_{n+1}) until we consume our budget of N function evaluations. As a result, we continue updating our posterior distribution (i. e., our current beliefs on $f(x)$). We also continue querying new data points through the acquisition function α. By iterating through this procedure, BO effectively navigates the parameter space while focusing on the global optima [434, 435, 444].

See [434, 435] for a more detailed explanation of the BO procedure, a list of software packages for BO, and a wide range of applications for this procedure.

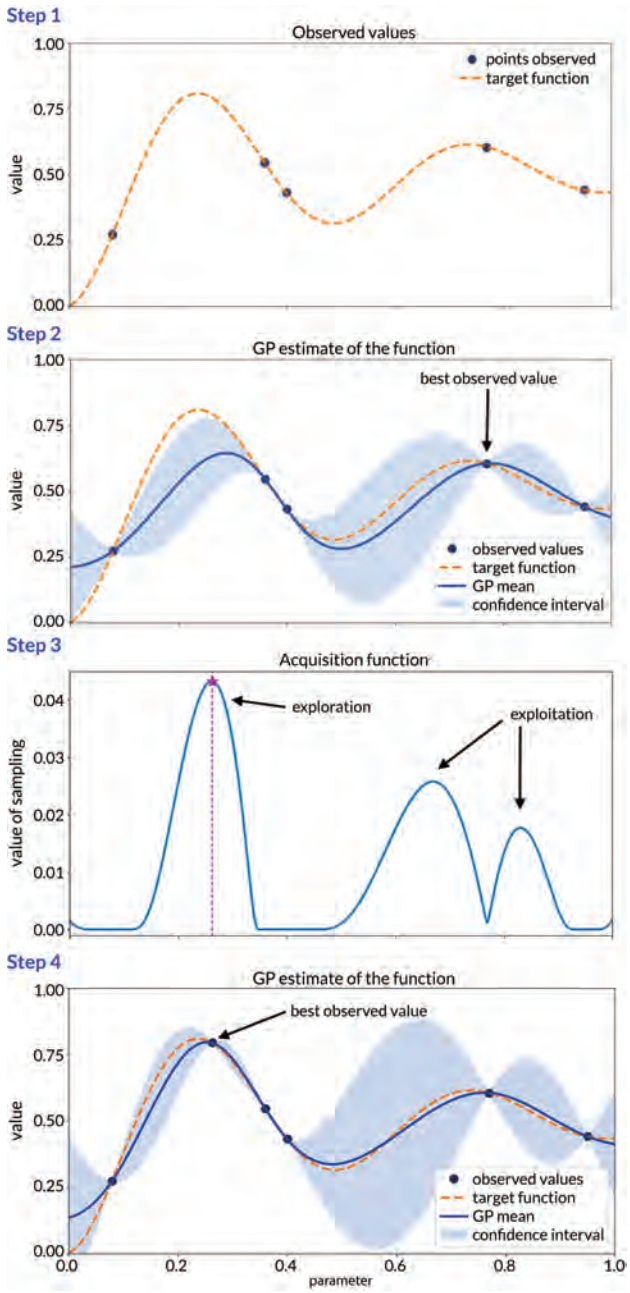

Figure 3.1: Illustration of the Bayesian optimization procedure First, we initialize the process by sampling the parameter space either randomly or low-discrepancy sequencing and getting these observations (**Step 1**). Secondly, we build a statistical model to approximate the target function based on the given parameter values and their associated output values (observations) (**Step 2**). Then, we use the maximal location of the acquisition function to figure out where to sample next in the parameter space (**Step 3**). Finally, we get an observation of the target function given the newly sampled data points (**Step 4**). Adapted from [445].

3.4 Defining an integrative methodology based on Bayesian optimization

Several software packages and platforms implement variants of the BO methodology [434, 435]. We first evaluated BayesOpt [447] for its performance. Still, we eventually chose the one provided by SigOpt[1] [448] for its support for parallelization and multi-objective optimization. Besides, SigOpt offers other valuable features, such as parameter constraints and an analysis of their impact. The former would allow us to discard areas of the search space that were not physically valid. The latter would help us better understand the influence of each parameter in the features evaluated by the defined target functions. Because of the stochastic nature of some of the processes involved in cell migration (e.g., intracellular signaling), we would have to run several simulations for each suggested parametrization to account for the intrinsic variability. Moreover, in some cases, we would be simulating N different scenarios (ECMs with distinct biophysical profiles), so we had to evaluate the statistical variability of each setting. In such cases, we opted to run M simulations per scenario (i.e., $N \times M$ simulations per suggested parametrization) and compute the defined target functions accordingly.

Figure 3.2 shows a global scheme of the implemented system doing the autonomous calibration. This system would run on our high-performance computing (HPC) environment. Nonetheless, it should run on any Linux-based HPC environment with minor modifications. First, the system would create a new experiment in SigOpt's platform with our specific requirements. These requirements would include: (i) the parameters to adjust and the boundaries of their space, (ii) any associated constraints, (iii) the defined target functions, (iv) the maximum number of valid observations (budget) to report back to SigOpt, and (v) the number of workers taking suggestions from SigOpt and reporting observations back to SigOpt. Once the experiment was created, as many as three workers would run in parallel. Each worker would start its main loop by asking SigOpt for a new suggestion (parametrization). Then, it would prepare the simulation environment (we would use a Conda virtual environment [2]). These workers would use HTCondor [446], a specialized workload management system for compute-intensive jobs, to distribute the execution of the $N \times M$ simulations required to evaluate the variability and fitness of SigOpt's suggestion. Once all simulations had finished, the workers would generate the *in silico* statistics associated with the features we were interested in. After retrieving the associated *in vitro* statistics, the chosen target functions

[1] https://sigopt.com/
[2] https://conda.io/

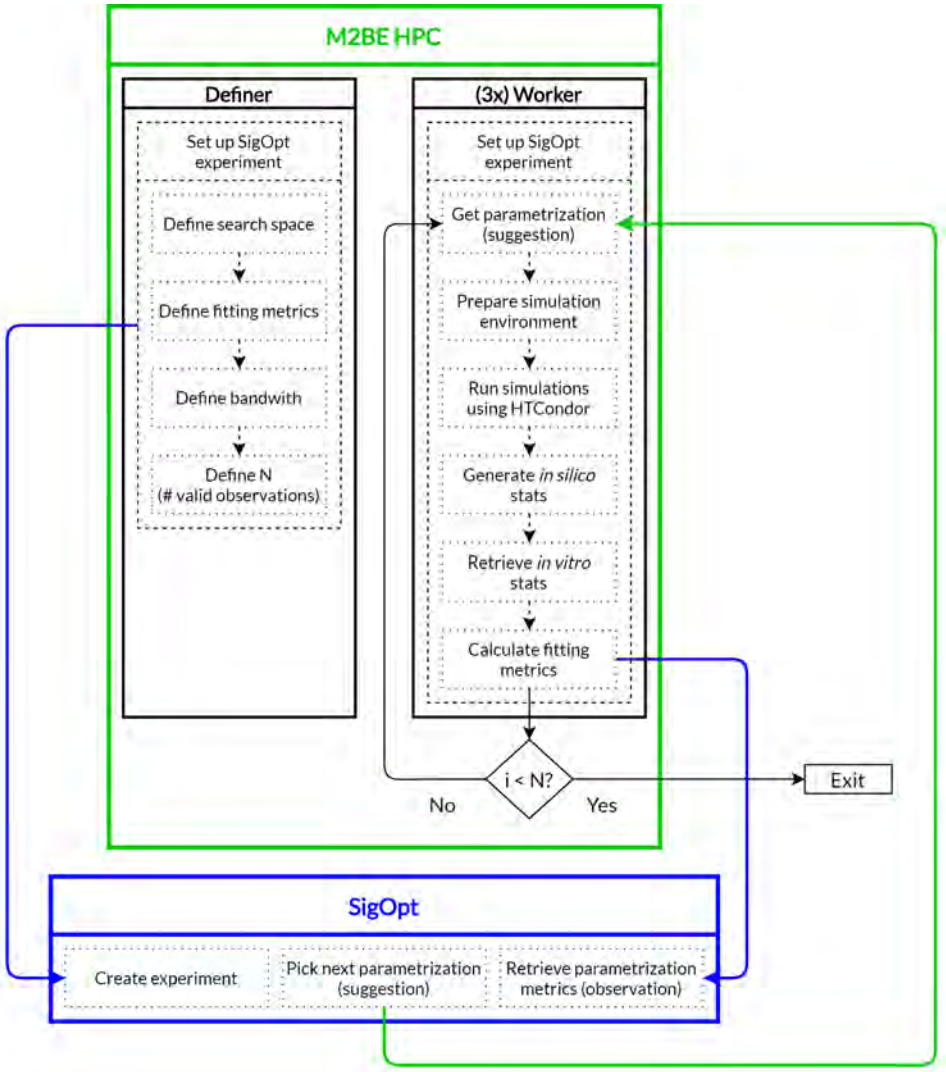

Figure 3.2: Global scheme of the integrative methodology In the M2BE high performance computing (HPC) environment, the master would set up the calibration system and send the details to SigOpt to create a new experiment. Then, also in the M2BE HPC, as many as three clients would start evaluating parametrizations suggested by SigOpt based on the definition of the already created experiment. Every iteration of the main algorithm would start by asking SigOpt for the next parametrization (also known as suggestion) using its API. Then, the client would set up the simulation environment, and run M simulations per case using HTCondor [446]. There may be several scenarios to simulate (e.g., cell migration within ECMs with different biochemical or biophysical profiles). Once all those simulations had finished, we would evaluate their numerical results. We may be interested in several features, which would require evaluating different target functions ($f_i(\boldsymbol{x})$). After retrieving the associated *in vitro* statistics, the defined target functions would be estimate and their values reported back to SigOpt. If this was the N-th observation reported to SigOpt (from a budget of N observations), we had already arrived at the end of the calibration process. Otherwise, we would ask SigOpt for another suggestion to analyze.

would be evaluated, and the observation reported back to SigOpt. If there would be more suggestions to analyze, the worker will start a new iteration of its main loop. Otherwise, their execution would finish.

See Chapter 4 and 5 for different examples of application of this integrative methodology.

3.5 Conclusions

Although theoretical modelers usually perform strong efforts to validate models comparing experimental data with numerical results, we still lack a full integration of both data types. However, this chapter presented a significant step toward this integration, showing a novel methodology that combines both modeling strategies (experimental and theoretical) using Bayesian optimization during the calibration process. The complexity of the calibration process of any model quickly increases with the number of parameters. Another factor that increases the complexity of the calibration process is the stochastic nature of some biological models, such as the one presented in the following chapters. Stochastic models require the execution of several simulations for each model parametrization to capture the variability of the results associated with the stochastic randomness. Moreover, if running each simulation takes more than a couple of minutes, an iterative approach for this calibration process becomes highly prone to inefficiencies.

When choosing the values for each model parameter using such an iterative approach, it is usually the case that researchers turn to the literature as their starting point. Then, they perform some manual tuning so that the numerical results approximately fit the experimental data. Generally, researchers start by modifying just a couple of parameters using some biologically relevant values. Then, they analyze how those parameters influence the model output based on the different values tested. Researchers iterate over this process by picking a couple of the remaining parameters in every iteration—ideally, the selected parameters in each iteration are related to each other. This iterative approach is very tedious because modifying some parameters may require the recalibration of others already calibrated. If the *in silico* model includes many parameters, researchers could start the calibration by performing a sensitivity analysis [449]. They would then focus on those parameters with a higher impact on the model output. Because of computational and time restrictions, this iterative step does not generally include more than a couple of rounds, even though it is becoming more and more common to have access to an HPC environment—which can reduce the required times to run those simulations by parallelizing them.

In this chapter, we proposed the application of BO to reduce these inefficiencies. Bayesian optimization has been applied to solve a wide range of problems such as machine learning applications [450], robot planning [451], simulation design [452], biochemistry [453], material design [454], and dynamical modeling of biological systems [455]. Interestingly, BO can also be applied to experimental design [426, 456] and offers an automated approach for model calibration. Interestingly, Bayesian methodologies may be appropriate even when the optimal parametrization is input-dependent [427] or changes over time [428]. Overall, BO minimizes the number of parametrizations to test on the *in silico* model and find a good enough fit for the experimental observations.

4

Cell migration biased by biochemical cues

Contents

This chapter is based on:

Francisco Merino-Casallo, Maria Jose Gomez-Benito, Yago Juste-Lanas, Ruben Martinez-Cantin, and Jose Manuel Garcia-Aznar. *Integration of in vitro and in silico models using Bayesian optimization with an application to stochastic modeling of mesenchymal 3D cell migration.*

4.1 Introduction

Directed cell migration (also known as cellular taxis), is critical for a myriad of physiological processes, including embryonic development [457, 458], angiogenesis [459, 460], bone formation [461], and tissue repair [462, 463]. Unfortunately, tactic movements are also involved in many pathological processes such as cancer metastasis [464–466]. Thus, investigating directed cell migration is still critical to acquire a comprehensive understanding of different biological processes involved in health and disease.

Directed cell migration is generally driven by asymmetric cues of tactic attractants or repellants in the surrounding environment, such as gradients of chemical ligands, stiffness, or electric current. Among these inducers of taxis, a chemical gradient of soluble ligands (chemotaxis) or surface-bound molecules (haptotaxis) in the ECM may lead cells toward regions with higher (or lower) concentrations of these chemoattractants (or chemorepellants). For instance, chemoattractant gradients, which may be species-specific [467–469], guide the sperm toward the egg during fertilization [91, 92]. During embryogenesis, neural crest cells are guided by chemoattractants toward their appropriate destination [470–472]. Chemoattraction also enables leukocytes recruitment into sites of inflammation and infection [58, 97, 98, 473]. Cells' ability to sense modest spatiotemporal variations on the concentration of these ligands is fundamental for living organisms.

Chemoattractive events may exhibit some context-specific features. For instance, they might occur only under a particular chemical profile within the ECM (e.g., composition, concentration, slope of the gradient). Such tactic events may also require specific transmembrane receptors to internalize the biochemical stimuli. Furthermore, they could depend on specific downstream effectors controlling cell polarization, cytoskeletal remodeling, or nuclear translocation. For example, different chemoattractant families contribute to neutrophil trafficking in a particular way, cooperating spatiotemporally, in a hierarchical manner, to orchestrate neutrophil migration [474]. An intravascular chemokine gradient would guide neutrophils from healthy tissue towards the site of inflammation. Later on, formyl peptides derived from dying cells could lead their final migratory step into the injured tissue. Understanding the intricacies of chemoattraction and the specific conditions triggering such motile responses are of the utmost importance.

Researchers have been investigating the mechanisms that enable chemoattraction for more than a century. In 1884, Pfeffer [475] reported his observations on the chemotactic response of fern spermatozoids and how they oriented to the gradients produced by diffusion of malate. Leber, who studied inflammatory reactions induced

in the cornea of rabbits, reported in 1888 [58] the first recorded observation of chemotaxis of leukocytes. At the turn of the century, Bloch included a list of all the substances believed to be chemotactic [56]. Strikingly, chemotaxis was not fully recognized as the leading driver of leukocyte accumulation *in vivo* until after the *in vitro* experiments of Boyden in 1962 [98]. In the 1960s, Julius Adler published pioneering works on bacterial chemotaxis and motility [476–479]. More recently, in 2013, Dona and colleagues [100] reported the first *in vivo* proof for self-directed tissue migration through a self-generated chemokine gradient during embryogenesis. Still, many questions remain unanswered nowadays.

Many different extrinsic and intrinsic factors regulate cell migration—and cellular taxis, for that matter. For instance, on 2D surfaces, cell motion has been widely studied and is typically characterized by a balance between counteracting traction and adhesion forces [130, 394]. However, cells generally migrate within 3D matrices, adopting different migratory strategies (individual: mesenchymal, amoeboid, or lobopodial; and collective). The cell phenotype and the properties of the surrounding environment (e.g., architecture, composition, presence of any tactic cue) may determine the specifics of the migratory process. Overall, the mechanisms governing cell migration within 3D matrices are far less well-understood owing to technical challenges and the variety of players and events that may act only under specific conditions.

In 3D environments, individual cells use different migratory strategies. When cells are unable to adhere to their surroundings, they modify their shape and squeeze through the ECM pores by using the amoeboid migration, which is very efficient. Cells such as neutrophils and T cells (immune system) use amoeboid migration, which allows for rapid cell locomotion (speed $\sim 10\,\mu\mathrm{m\,min^{-1}}$) [480–482]. Interestingly, cells seem to reach the highest speeds while migrating through pores of around cell size [74]. Conversely, if cells are tightly adherent and able to exert pulling forces on the surrounding ECM, they may switch to lobopodial migration. For instance, primary human fibroblasts use lobopodial migration when located within highly confining, linear elastic, crosslinked matrices [483]. Lastly, whenever cells' adhesion to the ECM and their proteolytic activity are high, cells use the mesenchymal migration, which is very inefficient. Different cell types, including fibroblasts (wound healing) and osteoblasts (bone formation), use mesenchymal migration, which leads to slow cell motion (speed $< 1\,\mu\mathrm{m\,min^{-1}}$) [165].

In vitro experiments trying to reproduce as accurately as possible the natural biological surroundings of organisms from *in vivo* studies have become increasingly sophisticated. These complex and sophisticated experiments require expensive lab work. As a result, *in silico* studies have stood out as a complementary asset to

acquire a comprehensive knowledge of such complex phenomena. Computer-based mathematical models allow for a myriad of controlled and reproducible experiments with much lower associated costs. The combination of both methodologies creates new research opportunities. *In silico* models enable the simulation of many different *in vitro* conditions, can directly obtain additional information that may not be available from experiments and propose new research hypotheses. On the other hand, *in vitro* experiments can evaluate these hypotheses to generate novel and valuable observations. Taken together, the integration of *in vitro* experiments with *in silico* experiments will enable a comprehensive understanding of many biological phenomena, including cell migration.

In this work, we present a mechano-chemical model of individual mesenchymal 3D migration. The main aim was to improve our knowledge of how cells sense biochemical stimuli, internalize these cues, and adapt their behavior accordingly. We assessed the computational resources required by the numerical simulations that determine the 3D migration trajectories to minimize the execution costs of simulations.

Recently, different authors [34, 379, 428] have dedicated their efforts to combine *in vitro* experiments and *in silico* models to elucidate the influence of specific factors on individual and collective cell migration. Also, by combining experiments with numerical models, Sunyer and colleagues [130] demonstrated that the stiffness variations sensed by cells at both edges of the cell monolayer promote directional migration. In this work, we applied the integrative methodology presented in Chapter 3 based on the Bayesian optimization to combine a multi-scale *in silico* model and experimental data. Accordingly, we were able to calibrate the parameters of the proposed *in silico* model autonomously.

4.2 Methods

In this section, we start by describing an *in silico* model of cell migration that continues past modeling efforts from the author's research group [382]. We present the mathematical definition and implementation of this multi-scale model. Then, we describe how we calibrated the parameters of this model applying the integrative methodology proposed in Chapter 3. As a result, we could integrate experimental measurements and numerical simulations consistently.

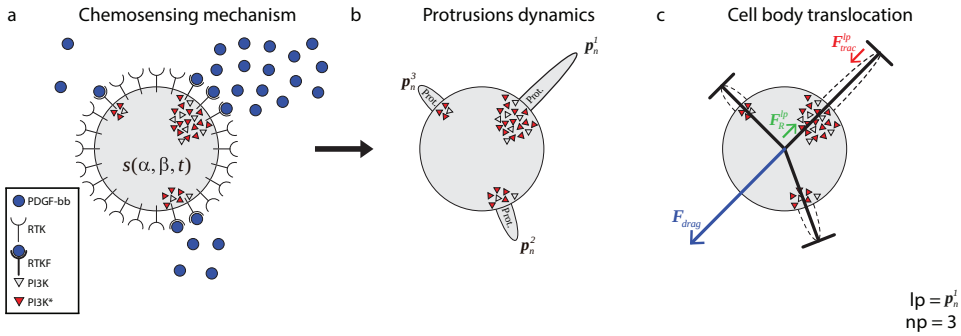

Figure 4.1: Global model scheme. **(a)** The chemosensing mechanism simulates how PDGFRs located in the cell membrane become activated by binding to PDGF-BB molecules (blue circles). This PDGFR activation, in turn, triggers the activation of PI3K molecules inside the cell (PI3K inactivated molecules as grey triangles and PI3K activated ones as red triangles). **(b)** Protrusions ($\boldsymbol{p}_n^i$) grow and stabilize on those areas with high concentration of PI3K activated molecules. **(c)** The longest protrusion generates a traction force ($\boldsymbol{F}_{trac}^{p_{longest}}$) when retracting, which exerts a reaction force ($\boldsymbol{F}_{R}^{p_{longest}}$) over the cell body. As a result of these reaction forces, the ECM generates a drag force ($\boldsymbol{F}_{drag}$) over the cell body.

4.2.1 Model description

The proposed *in silico* model to simulate mesenchymal cell migration within 3D matrices continues previous modeling efforts from our group [382] (Figure 4.1). Here, we start by describing the main aspects of this multi-scale model to improve our knowledge of the different modeling enhancements proposed. Then, we showcase the application of the integrative methodology presented in Chapter 3. This model assumes that mesenchymal cell migration within 3D matrices can be described as a three-stage process. In the initial stage, the cellular chemosensing mechanism allows cells to probe for biochemical cues located within their surroundings through different transmembrane receptors [88, 484]. Next, the second stage simulates how the activation of these transmembrane receptors triggers intracellular processes regulating the onset and growth of dendritic protrusions toward the surrounding ECM [485, 486]. These protrusions can appear and grow (pushing the matrix), as well as contract (pulling the matrix). Lastly, the third stage models how the dynamics of these protrusions regulate cell migration within 3D matrices [487–489] through the transmission of actomyosin-generated contractile forces from these protrusions to the nucleus, resulting in the nucleus translocation.

Next, these three main stages of mesenchymal cell migration within 3D matrices are described in greater detail. But first, the model of 3D cell behavior is defined.

Modeling 3D cell behavior

The 3D structure of the cell is geometrically modeled as a set of one-dimensional bars representing dendritic protrusions [382]. Those bars are located in a three-dimensional environment and diverge from a central connecting point representing the cell nucleus or centrosome. This central connecting point exists solely for modeling purposes as the point where all the bars are connected (Figure 4.1c).

Modeling the chemosensing mechanism

This stage models the spatiotemporal evolution of the signaling network enabling cells to probe for biochemical cues and respond accordingly (Figure 4.1a).

Signaling pathways can be extremely complex. Despite the depth of our molecular understanding of these pathways, a complete and precise definition of most of them remains elusive. Orchestrated cross-talks, feedback loops, and multi-component signaling are some of the intricate mechanisms hindering our progress in this endeavor. Also, a many different mediators and downstream effectors may or may not be actively involved in these signaling pathways based on context (i.e., cell phenotype and surrounding microenvironment). For instance, PI3K is considered one of the leading regulators of chemotactic migration guidance. Still, different redundant pathways to PI3K have been identified in distinct contexts (e.g., in CXCL8-mediated chemotaxis in neutrophils and in cAMP-mediated chemotaxis in Dictyostelium discoideum) [490, 491]. All in all, we opted to define a simplified signaling network based on our current knowledge of the signaling pathways enabling cells to sense and internalize biochemical stimuli. In particular, we focused on key signaling species and, to keep the model as simple as possible, discarded many intermediate reactions and unified others into a single 'common regulator' signaling node. The downstream signaling activity of the proposed signaling network would determine protrusions' location and their unconstrained length.

For clarity purposes, and owing to their pivotal role in regenerative processes [492–495], we focused on a specific context where NHDF cells migrate within collagen-based 3D matrices containing PDGF molecules. Note, however, that the proposed signaling network could be adapted to model other migratory contexts (i.e., other cell types and chemoattractants).

From a temporal perspective, the simplified signaling network proposed here, enabling cells to sense and internalize biochemical stimuli, is defined by Reactions 1 to 4. In this simplified model, one molecule of a chemoattractant (PDGF) activates the corresponding transmembrane receptor (PDGFR) by binding to it:

$$\mathrm{PDGFR} + \mathrm{PDGF} \xrightarrow{k_1} \mathrm{PDGFR_A}, \qquad \{1\}$$

where k_1 is the reaction rate coefficient, and $\mathrm{PDGFR_A}$ is an activated PDGFR. The unbinding of this chemoattractant molecule (PDGF) from the associated activated transmembrane receptor ($\mathrm{PDGFR_A}$) deactivates it:

$$\mathrm{PDGFR_A} \xrightarrow{k_2} \mathrm{PDGFR} + \mathrm{PDGF}, \qquad \{2\}$$

where k_2 is the reaction rate coefficient. One activated transmembrane receptor ($\mathrm{PDGFR_A}$) could, in turn, activate molecules of common regulators such as PI3K, located in the cytosol:

$$\mathrm{PDGFR_A} + \mathrm{PI3K} \xrightarrow{k_3} \mathrm{PI3K_A}, \qquad \{3\}$$

where k_3 is the reaction rate coefficient, and $\mathrm{PI3K_A}$ is an activated molecule of PI3K. Additionally, one $\mathrm{PI3K_A}$ could be naturally deactivated:

$$\mathrm{PI3K_A} \xrightarrow{k_4} \mathrm{PI3K}, \qquad \{4\}$$

where k_4 is the reaction rate coefficient.

Cellular consumption of chemoattractant molecules (PDGF) was considered negligible. Hence, the chemoattractant chemical profile did not change with time.

Based on Reactions 1 to 4, the time evolution of this simplified model could be computed as:

$$\begin{aligned}
\frac{\partial PDGFR}{\partial t} &= -k_1 PDGFR \cdot [PDGF] + k_2 PDGFR_A, \\
\frac{\partial PDGFR_A}{\partial t} &= k_1 PDGFR \cdot [PDGF] - k_2 PDGFR_A, \\
\frac{\partial PI3K}{\partial t} &= -k_3 PDGFR_A \cdot PI3K + k_4 PI3K_A, \\
\frac{\partial PI3K_A}{\partial t} &= k_3 PDGFR_A \cdot PI3K - k_4 PI3K_A,
\end{aligned} \qquad (4.1)$$

where k_1, k_2, k_3, and k_4 are the reactions rate coefficients. $PDGFR$ is the number of PDGF receptors, and $[PDGF]$ is the number of PDGF molecules. Conversely, $PDGFR_A$ is the number of activated PDGF receptors, $PI3K$ is the number of molecules of phosphoinositide 3-kinase, and $PI3K_A$ is the number of molecules of activated phosphoinositide 3-kinases. However, modeling a valid chemosensing mechanism not only requires knowing the time evolution of this simplified signaling network. Cells must also recognize the spatial orientation of chemical gradients.

From a spatial perspective, we assumed that initially, PDGFRs were uniformly distributed over the cell surface. Still, the activation density of transmembrane receptors depends on the distribution of PDGF all over the plasma membrane. The activation of PDGFRs preferentially occurs on areas of the cell surface surrounded

by a higher concentration of PDGF [114, 496]. Besides, over time, and based on external cues, the distribution of surface receptors such as PDGFR can be biased by endocytic membrane trafficking [114, 251, 497, 498]. Consequently, cells can sense the spatial distribution of PDGF and, therefore, gradients of these chemoattractants.

The proposed model of the chemosensing mechanism includes two sources of stochasticity: the evolution of the simplified signaling network (defined by Equation 4.1) and the activation of PDGFRs based on the concentration of chemoattractant molecules surrounding the cell. Therefore, the chemical reactions 1 to 4 are assumed to be stochastic processes described by a Poisson distribution [496]. This premise allows considering receptor activation over a domain with varying concentrations of PDGF as a multivariate non-homogeneous Poisson distribution. Therefore, we could model this activation of PDGFRs using the Inverse Method described by Saltzman and colleagues [499].

An approximate solution to the spatial activation of PDGFRs allowed us to evaluate the variation of $\mathrm{PI3K_A}$ in any specific location of the cytosol at any given time (t_k). To estimate this spatiotemporal variation we defined the variable $s(\alpha,\ \beta,\ t_k)$, which stores the spatial persistence of $\mathrm{PI3K_A}$ activation across time (t_k) in a location of the cell surface defined by coordinates ($\alpha,\ \beta$) (Figure 4.2). Based on *in vitro* observations of fibroblasts cultured in 3D collagen-based matrices [484, 500], the central region of the cell was considered a sphere with a 25-µm radius. The cell plasma membrane can be modeled as a flat surface defined by the polar coordinates α and β. The signal $s = s(\alpha,\ \beta,\ t_k)$ was evaluated at a fixed time t_k through the convolution function g with an area roughly the size of a protrusion section. As a result, we could assess the temporal evolution of the chemical signal at any given location.

The locations where cytosolic PI3K becomes preferentially activated at time t were estimated by:

$$s_t(\phi,\theta) = \int_0^{\pi}\int_0^{2\pi} d_{\mathrm{PI3K_A}}(u,v)\cdot g(\phi-u,\theta-v)\,\mathrm{d}u\,\mathrm{d}v, \tag{4.2}$$

where $d_{\mathrm{PI3K_A}}$ is the distribution of $\mathrm{PI3K_A}$ across the cell surface, ϕ and θ are the spherical coordinates (i.e., polar and azimuthal angles, Figure 4.2), and $g(\phi,\theta)$ is a circular convolution window approximately the size of a protrusion section ($\pi/18$ rad in diameter). However, it was also required to know how $\mathrm{PI3K_A}$ accumulates inside the cell over time. The persistence of $\mathrm{PI3K_A}$ at time t_k could be evaluated by sampling:

$$s = s(\phi,\theta,t_k) = \sum_{t=t_0}^{t_k} s_t(\phi,\theta), \tag{4.3}$$

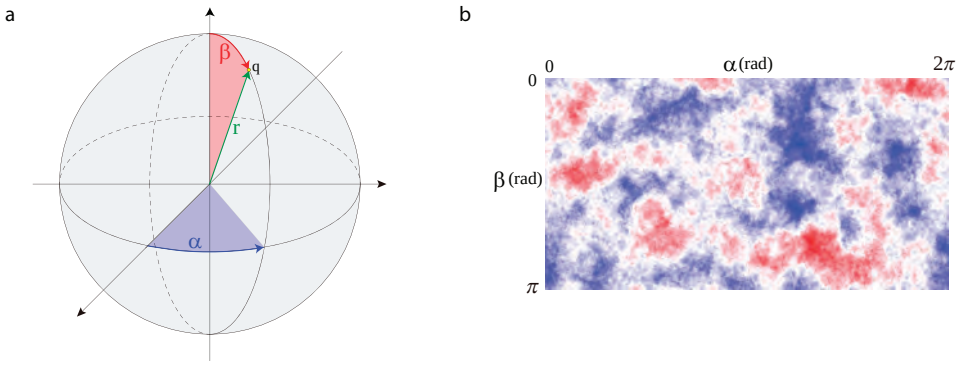

Figure 4.2: Signal spatial distribution. (a) Spherical coordinates (α, β) of point q. **(b)** s signal distribution example over the cell membrane.

at 1 Hz during 5 min intervals (from t_0 to t_k).

In the next section, we will explain in detail how the persistence of signal s determined the likely locations for protrusion formation and growth. Protrusions formation rate is roughly 0.002 Hz as measured *in vivo* [486]. Consequently, sampling the signal at 1 Hz was deemed adequate (according to signal sampling standards) as it is a higher frequency than the protrusion formation rate.

All in all, the methods described above enabled us to assess the spatiotemporal persistence of signal s (associated with cytoskeletal regulators such as PI3K_A) just below the plasma membrane. As a result, by focusing on signal peaks across the outer region of the cytosol (i.e., the one closer to the plasma membrane), we could pinpoint likely locations for protrusion formation and growth.

4.2.2 Modeling protrusion dynamics

The signal s and its variation (∂s), associated with regulators of actin-binding proteins such as PI3K, have a regulatory role in protrusions dynamics (Figure 4.1b) [486, 501–503]. For one, novel protrusions appear on locations with spatiotemporal persistence of these cytoskeletal regulators. Also, the intensity of s just below the plasma membrane determines if protrusions grow and stabilize or become smaller and even disappear. The former happens in locations with a strong s and buildup of PI3K_A. Conversely, the latter occurs in those regions with a weak s and small amounts of PI3K_A.

Protrusions were located using a set of signal thresholds (s_{birth}, $s_{reinforce}$, and s_{death}) over the spatiotemporal persistence of PI3K_A across the outer region of the cytosol (s; Equations 4.4 to 4.6). The search of peaks in signal s, where new protrusive structures would appear, was simplified through an internal parameter

s_{binary}. This internal parameter transformed s into a binary signal. Thus, while locating protrusions, any surface point where s was lower than s_{binary} became zero. Otherwise, the surface point became one. Once protrusions were located, we were interested in determining their length based on the intensity of the signal s in those regions of the outer cytosol.

Additionally, the stress-free (unconstrained) length variation of protrusions ($\partial L^f_{p_i}(s_{p_i},t)/\partial t$; i.e., their length variation when there is no ECM around them) depended on the signal variation in cytosolic regions where protrusions were located ($\delta s_{p_i}(t)$), Equations 4.4 to 4.6) [382]. During protrusion expansion, s_{birth} is the minimal amount of signal s for cells to develop new protrusive structures, as suggested by other authors [486, 496, 504, 505]. Consequently, we considered that novel protrusions can sprout longitudinally in locations of the cell surface where signal s was above s_{birth}:

$$\left.\frac{\partial L^f_{p_i}(s_{p_i},t)}{\partial t}\right|_{birth} = \begin{cases} \frac{\alpha_{exp} d\delta s_{p_i}(t)/dt}{\beta_{exp}+\delta s_{p_i}(t)} & \text{if } s_{p_i}(t) \geq s_{birth} \\ 0 & \text{otherwise} \end{cases}, \tag{4.4}$$

where $\delta s_{p_i}(t)$ is the variation of s in the surface location occupied by the i-th protrusion over time, and α_{exp}, β_{exp} are parameters regulating protrusion expansion. Furthermore, any pre-existing protrusion p_i became reinforced and grew if $s_{p_i}(t)$ was above $s_{reinforce}$. However, if s was below this threshold, the protrusion p_i became unstable and retracted:

$$\left.\frac{\partial L^f_{p_i}(s_{p_i},t)}{\partial t}\right|_{growth} = \begin{cases} \frac{\alpha_{exp} d\delta s_{p_i}(t)/dt}{\beta_{exp}+\delta s_{p_i}(t)} & \text{if } s_{p_i}(t) \geq s_{reinforce} \\ 0 & \text{otherwise} \end{cases}, \tag{4.5}$$

where $\delta s_{p_i}(t)$ is the variation of s in the surface location occupied by the i-th protrusion over time, and α_{exp}, β_{exp} are parameters regulating protrusion expansion. Note that the variation of s ($\delta s_{p_i}(t)$) is associated with the spatiotemporal persitence of the actin-binding regulator from the simplified signaling pathway associated with the chemosensing mechanism (Section 4.2.1). The spatiotemporal persistence of such an actin-binding regulator would modulate the actin polymerization rate. Indeed, the more persistent this actin-binding regulator is on a specific region just below the plasma membrane, the higher the polymerization rate in that region. Accordingly, the higher the polymerization rate on a specific region below the plasma membrane, the higher the stress-free (unconstrained) length increment of the protrusion located in that region. Therefore, we can establish a relationship between the unconstrained length variation of protrusions ($\partial L^f_{p_i}(s_{p_i},t)/\partial t$) and the actin polymerization rate.

During protrusions contraction, protrusions retracted in locations where s was above s_{death}. However, in those regions where s was below s_{death}, pre-existing

protrusive structures not only retracted but also disappeared:

$$\left.\frac{\partial L^f_{p_i}(s_{p_i},t)}{\partial t}\right|_{con} = \begin{cases} -\frac{\alpha_{con} d\delta s_{p_i}(t)/dt}{\beta_{con}+\delta s_{p_i}(t)} & \text{if } s_{p_i}(t) \geq s_{death} \\ -L^{con}_{p_i}(s_{p_i},t) & \text{otherwise} \end{cases}, \tag{4.6}$$

where $\delta s_{p_i}(t)$ is the variation of s in the surface location occupied by the i-th protrusion over time, α_{con}, β_{con} are parameters regulating protrusion contraction, and $L^{con}_{p_i}(s_{p_i},t)$ is the protrusion's length at the beginning of its contractile stage at time t.

We assumed a negative feedback loop for PI3K activation triggered by myosin motors during protrusions contraction, as suggested by [486]. Therefore, we considered a directly proportional decrease in $\delta s_{p_i}(t)$ to s_{p_i} during the contractile stage ($\delta s_{p_i}(t) < 0$, Equation 4.6). We also considered a time-dependent wear of $s_{p_i}(t)$, as time wears out the persistence of $\mathrm{PI3K_A}$, following a 30 min half-life decay [486].

Protrusions, as they form over the plasma membrane and grow toward the surrounding matrix, push and exert forces on the ECM. Consequently, the mechanical properties of the ECM act as a regulator for the extension or retraction of protrusions (Figure 4.3) [485]. This behavior was simulated by considering protrusions analogous to an elastic inclusion (ellipsoid) embedded in the ECM, applying Eshelby's analytical solution of ellipsoidal elastic inclusions inside an elastic, infinite body [506]. We considered that, during this second stage, protrusions grow and retract inside a collagen-based fibrous matrix, and they adhere to matrix fibers. Thus, we assumed the ECM behaves as a linear elastic material constraining protrusions growth. Indeed, during this growth, protrusions push to the ECM, deforming it, and the elastic properties of the matrix regulate this deformation. In this case, we quantified the growth of the protrusion and the deformation of the ECM applying Eshelby's theory, assuming the protrusion as an inclusion that is embedded within the matrix. Moreover, in all cases, we presumed infinitesimal deformations.

Eshelby's theory required us to define the tensor for the stress-free (unconstrained) expansion/retraction of the i-th protrusion as:

$$\begin{aligned} \dot{\boldsymbol{\varepsilon}}^f_{p_i,k} &= \dot{\varepsilon}^f_{p_i,k} \boldsymbol{e}_i \otimes \boldsymbol{e}_i, \\ \dot{\varepsilon}^f_{p_i,k} &= \frac{1}{L^k_{p_i}(s_{p_i},t_0)} \left.\frac{\partial L^f_{p_i}(s_{p_i},t)}{\partial t}\right|_k, \end{aligned} \tag{4.7}$$

where $\boldsymbol{e}_i$ represents the unit vector of the i-th protrusion longitudinal axis and k is *exp* (expansion) or *ret* (retraction). $\dot{\varepsilon}^f_{p_i,k}$ represents the stress-free expansion/retraction stretch rate field, $L^k_{p_i}(s_{p_i},t_0)$ is the length of the i-th protrusion at

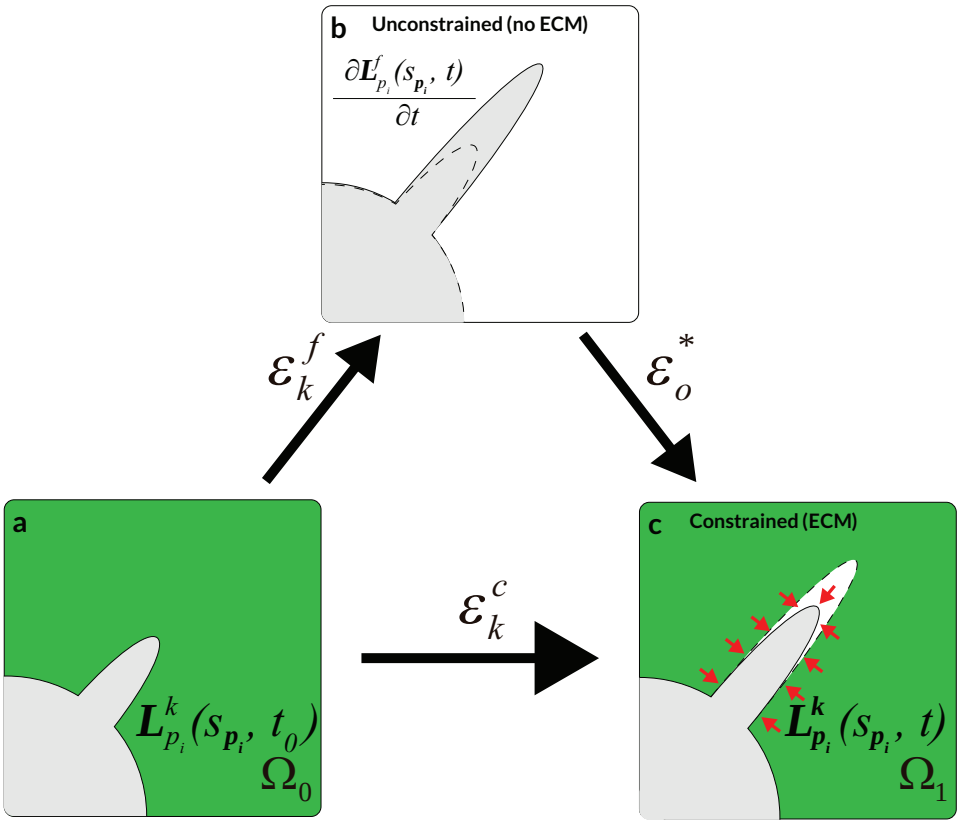

Figure 4.3: Protrusion dynamics using Eshelby's theory. Scheme of the three different configurations in protrusion dynamics based on Eshelby's description of ellipsoidal elastic inclusions (cell's protrusions) in an elastic, infinite body (the ECM). ε^{f}_{k} is the stress-free (unconstrained) expansion/retraction (ECM does not restrict protrusions deformation) Cauchy's strain tensor. ε^{*}_{0} is the compatibility Cauchy's strain tensor. ε^{c}_{k} represents the total deformation Cauchy's strain tensor. We assumed infinitesimal deformations.

the beginning of its expansive/contractile stage (t_0), and $\left.\frac{\partial L^{f}_{p_i}(s_{p_i},t)}{\partial t}\right|_{k}$ represents the stress-free (unconstrained) length variation of the i-th protrusion during the current expansive/contractile stage.

By using Eshelby's description of small ellipsoid inclusions (cell protrusions) inside an elastic, infinite body (the ECM), we could define (in Voigt notation) the second-order constrained strain rate field of the i-th protrusion as:

$$\dot{\tilde{\varepsilon}}^{c}_{p_i,k} = \boldsymbol{S}\left[\left(\boldsymbol{C}_I - \boldsymbol{C}_M\right)\boldsymbol{S} + \boldsymbol{C}_M\right]^{-1}\boldsymbol{C}_I\dot{\tilde{\varepsilon}}^{f}_{p_i,k} \tag{4.8}$$

where $\boldsymbol{S}$ represents the ellipsoid shape tensor, $\boldsymbol{C}_I$ is protrusions elasticity tensor, $\boldsymbol{C}_M$ represents the elasticity tensor of the surrounding matrix, and $\dot{\tilde{\varepsilon}}^{f}_{k}$ is the second-order stretch tensor $\dot{\varepsilon_k}^{f}$, which is Cauchy's strain tensor of the i-th protrusion stress-free

expansion/retraction (defined in Equation 4.7), in Voigt notation. Note that this modeling approach required us to consider the ECM a purely linear elastic material, and to focus only on the matrix rigidity when simulating protrusion dynamics.

We defined the constrained length variation rate of the i-th protrusion as:

$$\left.\frac{\partial L^c_{p_i}(s_{p_i},t)}{\partial t}\right|_k = L^k_{p_i}(s_{p_i},t)\dot{\varepsilon^c}_{p_i,k} \tag{4.9}$$

where $L^k_{p_i}(s_{p_i},t)$ is the length of the i-th protrusion at the beginning of its expansive/contractile stage, and $\varepsilon^c_{p_i,k}$ represents the constrained expansion/retraction stretch rate field. Finally, the length of the i-th protrusion at the end of its expansive/contractile stage (t_1) was computed as:

$$L^k_{p_i}(s_{p_i},t) = L^k_{p_i}(s_{p_i},t_0) + \int_{t_0}^{t_1} \left.\frac{\partial L^c_{p_i}(s_{p_i},t)}{\partial t}\right|_k dt \tag{4.10}$$

where $L^k_{p_i}(s_{p_i},t_0)$ is the length of the i-th protrusion at the beginning of its expansive/contractile stage t_0, and $\left.\frac{\partial L_{p_i}(s_{p_i},t)}{\partial t}\right|_k$ represents the constrained length variation of the i-th protrusion.

The length and number of protrusions depended on s. For instance, if s had a couple of regions where $PI3K_A$ had prominently accumulated over time (5 min), we could predict a few long protrusions. Conversely, if s was mainly homogeneous with modest variations, we should expect many small protrusions. However, these predictions could change based on the initial amount of PI3K (Table 4.1) and the parameters associated with s (s_{binary}, s_{birth}, $s_{reinforce}$, and s_{death}). Indeed, these parameters also regulate the length and number of protrusions at any given time t.

4.2.3 Modeling nucleus translocation

Finally, based on the experimental observations of how protrusions determine the nucleus translocation [352, 484, 507], it was assumed that the longest protrusion guides cell motion directly. The longest protrusion presents a larger adhesion surface and, consequently, adhesion proteins have a higher probability of connecting to the ECM. Every cell protrusion, except the longest one, becomes non-adherent and, therefore, they are all dragged by the cell during cell motion. The retraction of the longest protrusion generates a reaction force ($\boldsymbol{F}_R^{p_{longest}}$) supported by the nucleus. Thus, we could estimate the exerted drag force ($\boldsymbol{F}_{\text{drag}}$) by the ECM on the nucleus (Figure 4.1c) as:

$$\boldsymbol{F}_{drag} = -\boldsymbol{F}_R^{p_{longest}}, \tag{4.11}$$

where $\boldsymbol{F}_R^{p_{longest}}$ is the reaction force generated by the longest protrusion. As a result, both cell speed and position could be estimated at any given time t following the definition proposed by Borau and colleagues [508]. We assumed the nucleus is on the fluid component of the ECM and, therefore, we considered that the cell is moving through a fluid. Then, we could compute the drag force $\boldsymbol{F}_{drag}$ exerted by the matrix on the cell nucleus as:

$$\boldsymbol{F}_{drag} = -6\pi r\eta \boldsymbol{v}, \tag{4.12}$$

where r is the cell radius, η represents the ECM viscosity, and $\boldsymbol{v}$ is the cell speed. We assumed that there is a mechanical balance between the traction force of the adherent protrusion ($\boldsymbol{F}_{\text{trac}}^{p_{longest}}$), the longest one, and its corresponding reaction force ($\boldsymbol{F}_R^{p_{longest}}$) supported by the nucleus because of $\boldsymbol{F}_{trac}^{p_{longest}}$ (Figure 4.1c). Consequently, we could establish the following relationship:

$$\boldsymbol{F}_{trac}^{p_{longest}} = -\alpha_{adhesion} \cdot \boldsymbol{L}'^{,con}_{p_{longest}}(s_{p_{longest}}, t) = -\boldsymbol{F}_R^{p_{longest}}, \tag{4.13}$$

where $\boldsymbol{F}_{trac}^{p_{longest}}$ represents the contractile force of the longest protrusion, and $\alpha_{adhesion}$ is a constant that defines adhesion. $\boldsymbol{L}'^{,con}_{p_{longest}}(s_{p_{longest}}, t)$ is the length of the longest protrusion at the end of the contractile stage, and $\boldsymbol{F}_R^{p_{longest}}$ represents the reaction force supported by the cell nucleus because of the retraction force of the longest protrusion. All in all, we could define the associated force equilibrium as:

$$-6\pi r\eta \boldsymbol{v} + \alpha_{\text{adhesion}} \cdot \boldsymbol{L}'^{,con}_{p_{longest}}(s_{p_{longest}}, t) = 0, \tag{4.14}$$

where r is the cell radius, η is the ECM viscosity, and $\boldsymbol{v}$ is the cell speed. $\alpha_{adhesion}$ is a constant that defines adhesion, and $\boldsymbol{L}'^{,con}_{p_{longest}}(s_{p_{longest}}, t)$ is the length of the longest protrusion at the end of the contractile stage. Note that traction forces $\boldsymbol{F}_{trac}^{p_i}$ were assumed identical in magnitude to their corresponding reaction forces $\boldsymbol{F}_R^{p_i}$.

4.2.4 Numerical implementation

Our computational model was designed as a 3-stage process: chemosensing mechanism, protrusions dynamics, and the nucleus translocation (Figure 4.4). These three stages were implemented in Python using powerful packages and libraries for scientific computing such as NumPy [509] and SciPy [510] to maximize the model's performance.

The stochastic time evolution of the given set of reactions (R_1, R_2, R_3, and R_4) were numerically simulated using, initially, the Stochastic Simulation Algorithm (*SSA*; also known as the Gillespie Algorithm) [511, 512] in previous efforts from our group [382]. However, the SSA was considered too slow for our purposes and

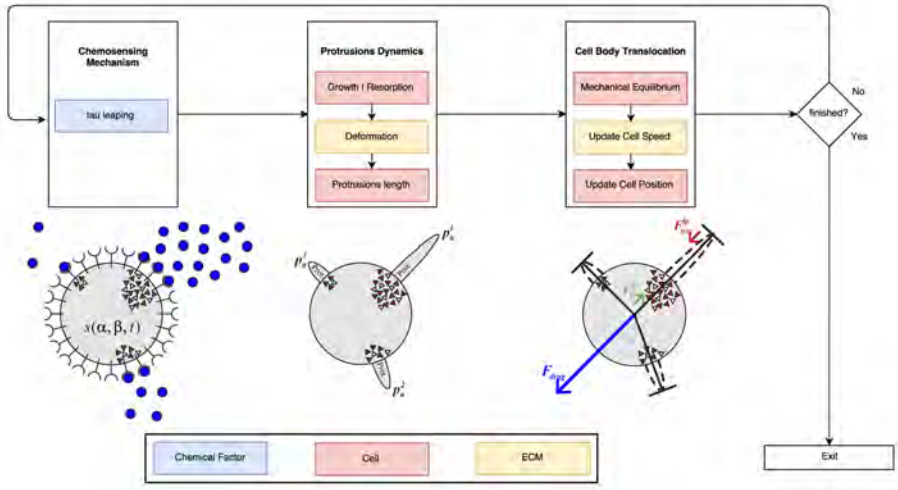

Figure 4.4: Numerical implementation. First, the chemosensing mechanism is simulated using the tau leaping algorithm. In this first stage, the concentration and gradient of the PDGF-BB is the main influence factor. During the second stage of the process, it is taken into account both ECM mechanical properties and cell mechanics in order to simulate protrusions development. Finally, the modeling of the cell body translocation is also influenced by the ECM mechanical properties (in particular, ECM viscosity) as well as cell mechanics. The blue boxes are associated with the chemical factor, the red ones with cell mechanics and the yellow ones with the ECM mechanical properties.

a faster alternative was proposed, the tau-leaping algorithm [513, 514]. The SSA computes an exact solution of the time evolution of a chemically reacting system. In contrast, the tau-leaping algorithm estimates a good enough[1] approximation [515, 516] by leaping over many reactions at once using Poisson random numbers.

The tau-leaping method attempt to accelerate stochastic simulations by approximating the frequency of each reaction being fired in the next specified time interval $[t, t+\tau)$. By comparison, the SSA focuses only on one reaction per time interval, which may be prohibitively small [517]. As long as the value of τ is small enough so the leap condition[2] is satisfied, it is possible to compute a good approximation of the evolution of any given chemically reacting system.

It is worth mentioning that neither the SSA nor the tau-leaping algorithm uses a fixed time step to simulate the evolution of biologically reacting systems like the

[1]The "good-enough" expression used here to describe the accuracy of the tau-leaping algorithm comes from previous works such as [515] where he states that "One acceleration strategy is to abandon absolute mathematical precision in favor of a good-enough approximation. Gillespie has also been a pioneer in this effort. One of his strategies is called 'tau-leaping'.". This statement is considered valid as long as the leap condition is satisfied, i.e. as long as the probability of each reaction taking place does not change significantly over the time leap.

[2]The leap condition is an accuracy-assuring restriction which states that during the time interval $[t,\ t+\tau)$ the probability of each reaction channel R_j being fired should remain approximately constant even though all reaction channels may be fired several times.

Reactant	Initial amount	Equation	Reference
PDGFR	4.275×10^3	(4.1)	[518]
$PDGFR_A$	0	(4.1)	Estimated
PI3K	75×10^3	(4.1)	[519]
$PI3K_A$	0	(4.1)	Estimated
k_1	$735\,\mathrm{nM}^{-1}\,\mathrm{s}$	(4.1)	[520]
k_2	$0.01\,\mathrm{s}^{-1}$	(4.1)	[520]
k_3	$4 \times 10^{-4}\,\mathrm{s}^{-1}$	(4.1)	[519]
k_4	$1\,\mathrm{s}^{-1}$	(4.1)	[519]

Table 4.1: Initial amounts of each reactant and reaction rates.

one presented in this work. Instead, they compute a new value τ in each iteration based on the current state of the system and a random variable.

The initial amounts of each reactant and the reaction rates (k_1, k_2, k_3, and k_4) used are included in Table 4.1.

Protrusion growth was then set based on the spatial distribution of $PI3K_A$ molecules and their amount in those locations. Protrusion final length was computed by applying Eshelby's solution of ellipsoidal elastic inclusions inside an elastic, infinite body. Next, mechanical equations were analytically solved using a computational algorithm. We assumed an elastic modulus of 104 Pa for the ECM based on previous experimental works of gels with a concentration of $2\,\mathrm{mg\,mL}^{-1}$ collagen type I [171, 352]. Lastly, the mechanical equilibrium associated with protrusion-generated forces was solved. Then, assuming that the longest protrusion is the one guiding cell motion, both cell speed and position were computed in the following time increment.

We decoupled the simulation of the chemosensing mechanism from the other two stages of the model (protrusions dynamics and nucleus translocation) because we were considering two different time scales in our model. Indeed, these chemical and mechanical events occur at different time scales. To accurately simulate the proposed signaling network, we opted for the iterative tau leaping algorithm with a variable associated time step τ in the range $[0.5, 1.5]$ seconds. However, to model protrusion dynamics and the nucleus translocation we used a different time step of 5 min. Indeed, signal s variations (Equation 4.3) between two consecutive time steps t and $t+\tau$ were very subtle. In contrast, protrusions required more noticeable variations of the chemical signal to change their current state. As a result, it was required to keep track of the signal s variation (∂s).

4.2.5 Development and quantification of *in vitro* experiments

Once we had numerically implemented the proposed model, we had to calibrate its parameters to optimize the predictive potential of this *in silico* model. We

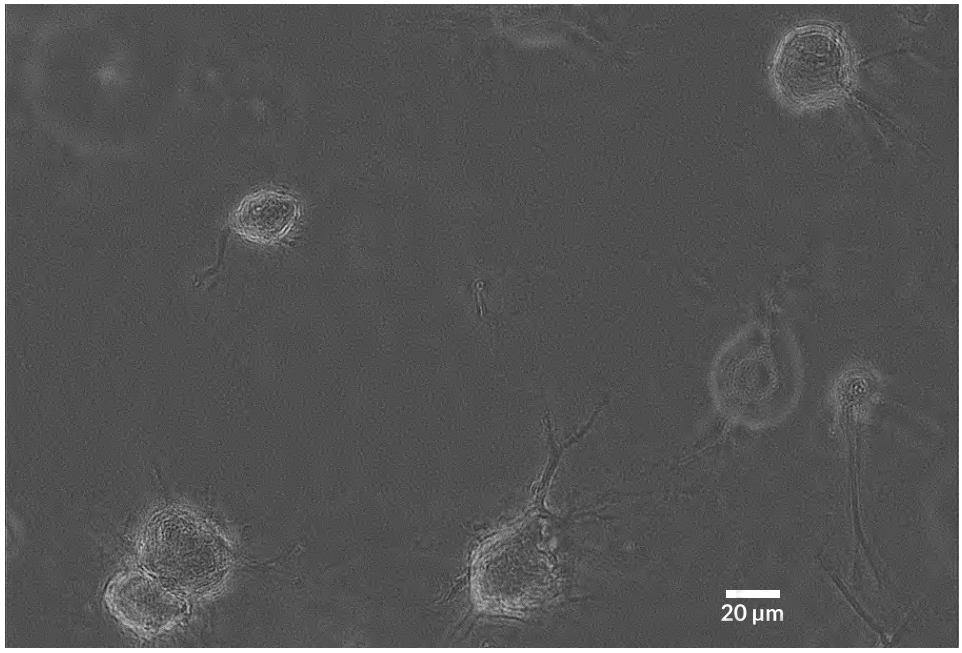

Figure 4.5: ***In vitro*** **experiments.** Norman Human Dermal Fibroblast (NHDF) cultured in 3D collagen-based fibrous matrix ($2\,\mathrm{mg\,mL^{-1}}$ collagen). Image was captured with a Nikon D-Eclipse Microscope with a Plan Fluor 200x magnification (20x Objective) and phase contrast.

calibrated the proposed multi-scale model by comparing the results of its simulations with experimental data. In particular, we focused on two different features to fit the model's parameters: the length of the longest protrusion and the number of protrusions of the migrating cell. As a result, we performed *in vitro* studies to get accurate experimental measurements of the length of the longest protrusion and the number of protrusions.

In vitro experiments were performed by culturing NHDF cells—human skin primary cells—within $2\,\mathrm{mg\,mL^{-1}}$ collagen gels at a concentration of 2.5×10^5 cells/mL, with temperature and atmospheric conditions maintained at 37 °C and 5 % CO_2, respectively. Immediately after the seeding, cells' evolution was monitored with multidimensional microscopy for 4 hours (from 0 to 4 h), every 5 minutes and 5 µm of the Z-axis, with 200x magnification (20x objective) and phase contrast (Figure 4.5). We chose a $2\,\mathrm{mg\,mL^{-1}}$ collagen concentration because it already implied a matrix pore size (1 µm) [521]. Individual cell protrusions were quantified by in-house Matlab algorithms [484]. For each image stack, the best Z was chosen to maximize accuracy and minimize the complexity of the manual analysis of the center of the cell and its protrusions. Single-cell analysis of four different samples was performed for the given collagen concentration ($2\,\mathrm{mg\,mL^{-1}}$).

FGM™-2 (Fibroblast Growth Medium-2) was used to support the growth of primary human fibroblasts. It contained a supplementation of GA-1000, recombinant human insulin 0.5%, HFGF-B GF, and 2% of Fetal Bovine Serum. Thus, these *in vitro* experiments only included a very low and fixed concentration of growth factors in the culture medium; they did not include any chemoattractant gradient.

4.2.6 Model calibration using Bayesian optimization

For our experiments, we decided to fit two competing metrics: the length of the longest protrusion (llp) as well as the number of protrusions (np) (Figure 4.1). The fitting of the *in silico* values to the *in vitro* measurements was computed using the Bhattacharyya coefficient (also known as BC), which has been widely used to compare the similarity or discrimination of two continuous or discrete distributions [522]. In fact, for discrimination, it corresponds to the upper bound of the Bayesian error when performing Bayesian hypothesis testing with symmetric cost functions and uninformative priors [523]. Note that Bayesian hypothesis testing already includes a penalization for model complexity and priors resulting in a regularization effect, being less sensitive to overfitting than classical hypothesis testing [524].

The proposed fitting metrics were defined as:

$$BC = \sum_{i=1}^{n} \sqrt{hist^{i}_{in\ vitro} \cdot hist^{i}_{in\ silico}}, \tag{4.15}$$

where $hist^i$ represents the value of the i-th histogram bin defined as the probability of occurrences in the range $(x_{i-1}, x_i]$. Note that histograms were used as discrete distributions.

The selection of metrics affects model calibration, so we carefully selected the metrics with a prominent influence on cell migration to the best of our knowledge. Moreover, these metrics were based on experimental measurements that we could accurately quantify. However, there were other measurements based on cell motion, such as the instant cell speeds, that were so low that we could not quantify them with the required accuracy. For those metrics, it was only possible to perform a qualitative analysis. Our proposed metrics were based on just two quantities measured in the experimental data. However, we considered that the length of the longest protrusion and cell speed are both fundamental in regulating the final 3D cell motion. In particular, experimental observations [352, 484, 507] suggest that the length of the longest protrusion has great influence over the cell speed whereas the number of protrusions has a great impact on the cell trajectory (whether it is random or directional).

Optimizing the BC function can be considered a form of Bayesian learning as we are trying to fit a model that best represents the distribution of the data and therefore maximizing the posterior. Similarly, optimizing the BC can be seen as a form of Bayesian hypothesis testing, where we are rejecting all the models with higher Bayesian error.

4.2.7 Model validation using different chemoattractant concentrations and gradients

After calibrating the numerical model, we had to validate it, testing their predictive ability to simulate different cell responses under different chemical gradients. This validation process allowed us to prove that the proposed model did not only accurately replicate the results used to calibrate it but also new ones so that there was no overfitting during the calibration process. In the previous calibration process, we used quantitative results related to the length of the longest protrusion and the number of protrusions of migrating NHDF cells from *in vitro* experiments without any chemoattractant gradient. However, the validation process of this *in silico* model was based on qualitative observations of migrating cells surrounded by a chemoattractant factor diffusing throughout the ECM [525, 526]. We simulated six different extracellular environments. Three of these environments included different PDGF gradients (10^{-1}, 10^{0}, 10^{1} $\mu M/mm$) but a fixed PDGF concentration at the initial cell's position of 0.8 µM. The other three environments included a fixed PDGF gradient (10^{0}µM mm^{-1}) but different PDGF concentrations at the initial cell's position (0.08, 0.8, and 8.0 µM. Twenty simulations were executed for each extracellular environment, using the same seeds used during the calibrating process. The comparison between *in vitro* and *in silico* results was based on qualitative observations of the velocity component in the direction of the chemotactic gradient (v_x).

We assumed a fixed growth factor profile without any induced modifications of the spatial gradient owing to the growth factor diffusion throughout the ECM. Thus, the chemoattractant chemical profile was assumed to be temporally stable as the inlets and outlets of our system kept a fixed growth factor profile during our 4-hour simulation.

4.3 Results

In this section, we start by showing the results from *in vitro* experiments and their quantification. Then, we showcase the suitability of the integrative methodology

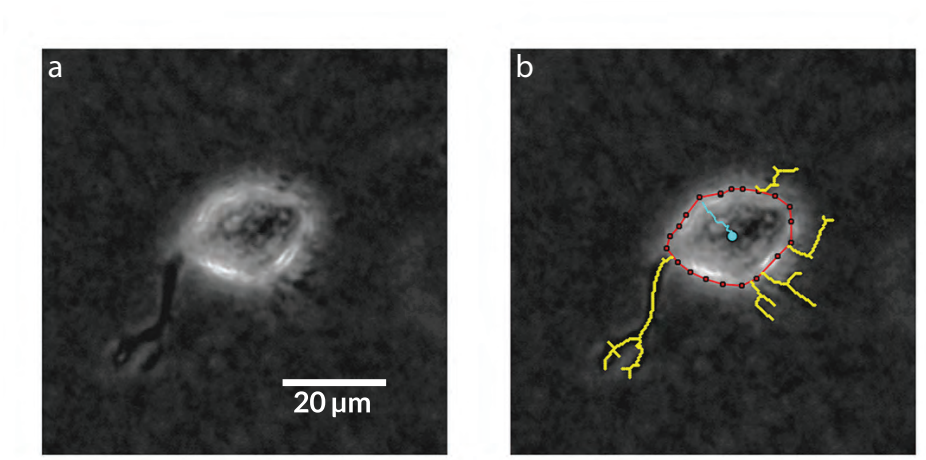

Figure 4.6: Image analysis. (a) Phase contrast example of a NHDF cell cultivated in a $2\,\mathrm{mg\,mL^{-1}}$ collagen gel, with 200x magnification (20x objective) acquired using multidimensional microscopy. **(b)** Protrusion analysis performed by in-house Matlab algorithms; red line delimits cell body, yellow lines represent the protrusions, and blue line shows cell body displacement. In this case, the longest protrusion is the green one and the number of protrusions is 5.

presented in Chapter 3 based on Bayesian optimization to calibrate *in silico* models using experimental data. Finally, we assess the potential of our calibrated numerical model under different chemoattractant concentrations and gradients.

The aforementioned *in vitro* experiments with NHDF cells allowed us to quantify both the length of every protrusion, as well as the number of protrusions generated at every checkpoint t ($t = 0,\ 5,\ 10,\ \ldots,\ 240$ *minutes*). Figure 4.6 shows an example of the images generated by multidimensional microscopy and the posterior protrusions analysis performed using in-house Matlab algorithms. However, the proposed *in silico* model focuses on the length of only the longest protrusion at each temporal checkpoint t, as explained in Section 4.2.3. Therefore, during the calibration process, the comparison between *in vitro* and *in silico* experiments was performed computing the BC associated with these two features (length of the longest protrusion and the number of protrusions generated by migrating cells).

During calibration, for every iteration in the optimization loop, we run 20 simulations replicating the *in vitro* scenario of a $2\,\mathrm{mg\,mm^{-1}}$ collagen ECM—to capture the stochastic nature of the proposed *in silico* model. Those 20 simulations used 20 different seeds to initialize the global random number generator of the proposed multi-scale model. After each simulations batch finished, a computer-based algorithm generated the associated histograms. These histograms (e. g. Figure 4.7

bottom) were compared with the *in vitro* histograms (Figure 4.7 top) using the following evaluation metrics BC_{llp} and BC_{np}:

$$\begin{aligned} BC_{llp} &= \frac{\sum_{i=1}^{N} BC_{llp}^{i}}{N},\ N = 20, \\ BC_{np} &= \frac{\sum_{i=1}^{N} BC_{np}^{i}}{N},\ N = 20, \end{aligned} \tag{4.16}$$

where BC_{llp}^{i} is the fitting metric evaluating the accuracy of the proposed *in silico* model regarding the longest protrusion for the i-th simulation. N represents the number of simulations executed (20). Lastly, BC_{np}^{i} is the fitting metric evaluating the accuracy of the proposed *in silico* model regarding the number of protrusions for the i-th simulation.

Computing both metrics based on the BC required to generate the associated histograms for the longest protrusion length and the total number of protrusions. Histograms associated with *in vitro* experiments using $2\,\mathrm{mg\,mL^{-1}}$ collagen gels showed how the protrusion length ranged from over 0 µm to almost 140 µm. However, the majority of the longest protrusions were 40-60 µm long (Figure 4.7 top left). The experimental data related to the number of protrusions exhibited high dispersion, ranging from 1 to 14 protrusions in each NHDF cell during the 4-hour *in vitro* experiments (Figure 4.7 top right). Figure 4.7 (bottom) includes the *in silico* histograms associated with the best parametrization suggested by SigOpt with metrics $BC_{llp} = 0.87$ and $BC_{np} = 0.81$. These histograms show how, although the length of the longest protrusions was between 0 µm and more than 150 µm, there was a peak in the interval 60-80 µm (Figure 4.7 bottom left). The experimental data related to the number of protrusions showed that there were usually about 9 to 12 in each NHDF cell during the 4-hour *in vitro* experiment (Figure 4.7 bottom right). When comparing measurements of the length of the longest protrusion, the mean values were 63.71 (*in vitro*) versus 65.98 (*in silico*), whereas the standard deviations were 31.20 (*in vitro*) versus 26.82 (*in silico*). For the measurements of the number of protrusions, the mean values were 7.57 (*in vitro*) versus 7.38 (*in silico*), whereas the standard deviations were 3.27 (*in vitro*) versus 4.00 (*in silico*).

Figure 4.9 shows the values of both metrics BC_{llp} and BC_{np} for every suggested parametrization by SigOpt. SigOpt was able to find parametrizations with higher values of the BC_{llp} (even above the 0.9 mark) than the BC_{np} (consistently below 0.8). Only 51 (17 %) of all the parametrizations suggested by SigOpt were considered invalid. Most valid parametrizations were higher than 0.7 for at least one metric (77.91 %). Moreover, 107 parametrizations were higher than 0.7 for both metrics (35.67 %). Overall, valid parametrizations got slightly better results for the metric related to the length of the longest protrusion (BC_{llp}, Figure 4.9).

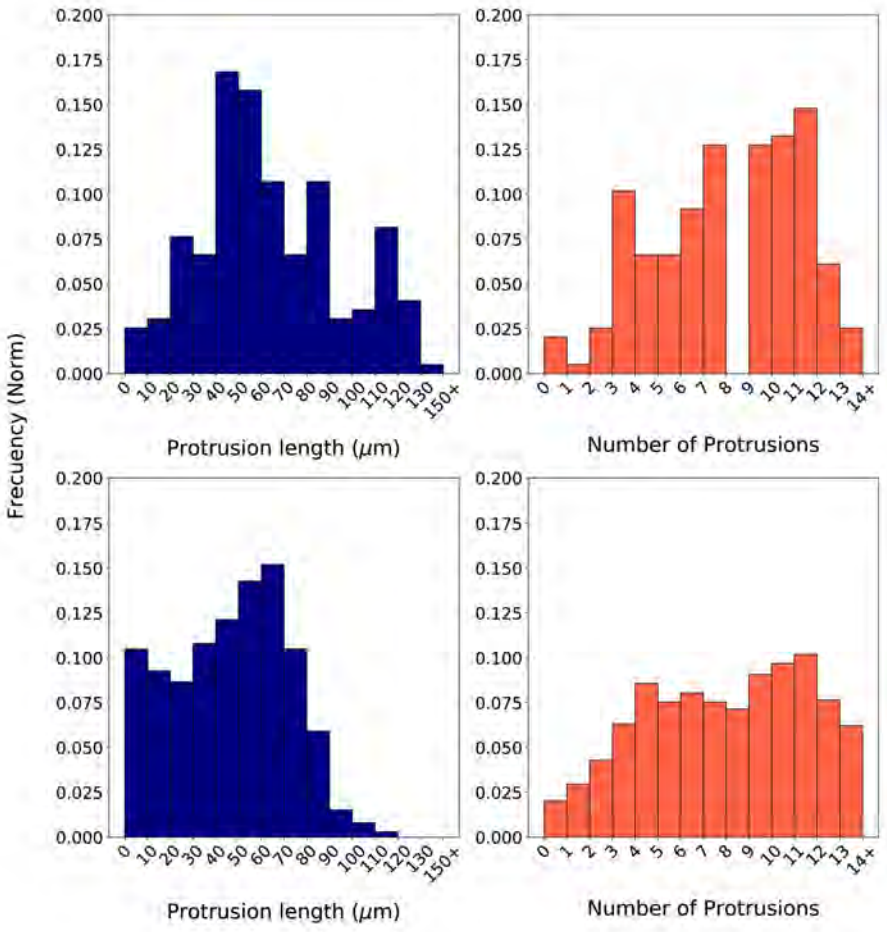

Figure 4.7: ***In vitro* vs *in silico*.** Normalized histograms associated with *in vitro* experiments (**top**) based on the length of the longest protrusion (measured in µm) (**left**) and on the number of protrusions (**right**). Normalized histograms associated with *in silico* experiments (**bottom**) based on the length of the longest protrusion (measured in µm) (**left**) and on the number of protrusions (**right**). *In silico* experiments were generated using one of the best parametrizations suggested by SigOpt with metrics $BC_{llp} = 0.87$ and $BC_{np} = 0.81$.

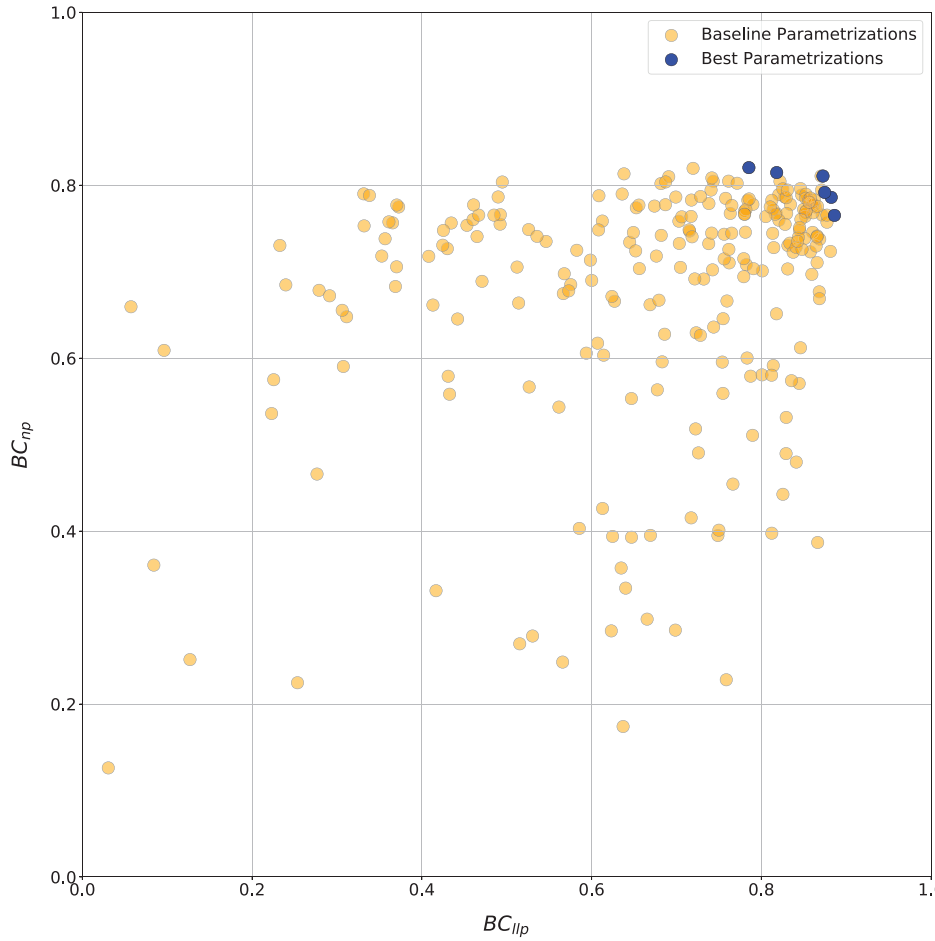

Figure 4.8: Optimization metrics for calibration. Values associated with metrics (BC_{llp} and BC_{np}) for the 300 model parametrizations suggested by SigOpt during the calibration process. Red circles are associated with every parametrization tested whereas the blue ones represent Pareto optimal points (parametrizations where one metric cannot be improved without another metric suffering) and form an approximate Pareto frontier.

Table 4.2 includes the nine parameters of the model that were calibrated. By establishing the boundaries of each parameter, we defined the parameter space. In this particular case, the parameter space included both continuous regions in the real space and discrete values for integer parameters. As a result, the calibration process became a mixed-integer programming problem, much harder to optimize than just real spaces (nonlinear optimization) or integer spaces (combinatorial optimization). For some parameters, we established a range based on the values used in [382]. Conversely, for others (e.g., E_{p_i}), we determined a range based on values found in the literature. In addition, for the parameters related to s

Parameter	Value	Equation	Range
E_{p_i}	1×10^7 Pa	(4.8)	$1 \times 10^i, i \in \{4, 5, \ldots, 10\}$
s_{birth}	85	(4.4)	$\mathbb{Z} \in [0,\ 100]$
$s_{reinforce}$	76	(4.5)	$\mathbb{Z} \in [0,\ 100]$
s_{death}	0	(4.6)	$\mathbb{Z} \in [0,\ 100]$
α_{exp}	$0.14\,\mathrm{mm\,s^{-1}}$	(4.4) and (4.5)	$\mathbb{R} \in [0.01,\ 0.2]$
β_{exp}	100	(4.4) and (4.5)	$\mathbb{R} \in [0.1,\ 100]$
α_{ret}	$0.05\,\mathrm{mm\,s^{-1}}$	(4.6)	$\mathbb{R} \in [0.01,\ 0.2]$
β_{ret}	54.86	(4.6)	$\mathbb{R} \in [0.1,\ 100]$
s_{binary}	62.5×10^3		$(12.5 + 2 \times j) \times 10^3, j \in \{0, 1, \ldots, 100\}$

Table 4.2: Model parameters calibrated using Bayesian optimization with SigOpt. The calibrated values are associated with the parametrization considered the best one, with computed metrics $BC_{llp} = 0.87$ and $BC_{np} = 0.81$. The given ranges have been established at the beginning of the calibration process and leave them unchanged.

signal (s_{birth}, $s_{reinforce}$, s_{death}, and s_{binary}), we analyzed the values of s at different time steps. These ranges should be biologically relevant. For example, the defined parameter space for E_{p_i} (protrusions elastic modulus) included the values given by Li and colleagues [527] and Mofrad and Kamm [528]. We also automatically discarded any parametrization with $s_{death} \geq s_{birth}$, $s_{death} \geq s_{reinforce}$, or $s_{reinforce} \geq s_{birth}$ because they are invalid from a biological perspective. Indeed, the minimal amount of signal required for the onset of new protrusions, s_{birth}, cannot be lower than the minimal amount of chemotactic signal s required to remain active and not disappear, s_{death}. Neither can the minimal amount of signal needed for reinforcing pre-existing protrusions, $s_{reinforce}$. The minimal amount of signal required for the onset of new protrusions, s_{birth}, cannot be lower than the minimal amount for the reinforcement of pre-existing protrusions either. Table 4.2 summarizes the parametrization selected as the optimal one after 300 iterations of the calibration process using SigOpt. For example, the best value for the elastic modulus was 1×10^7 Pa. The best parametrization, with metrics $BC_{llp} = 0.87$ and $BC_{np} = 0.81$, was selected because of the balance between both metrics.

Having a probabilistic surrogate model of the metrics enabled other types of data analysis during the optimization process. For instance, SigOpt also offers an analysis of the impact of each parameter on the metrics (see Figure 4.10). This analysis assesses how much the metric values change with variations of each parameter. This analysis gave us valuable insights into our model behavior. Although every parameter influences to some extent the metrics output, α_{exp}, a parameter that computes the stress-free (unconstrained) expansion/retraction stretch rate field during the protrusion dynamics stage, was the parameter with a higher impact (24.06 %). In second place came β_{exp} (15.25 %), also used to compute the stress-free

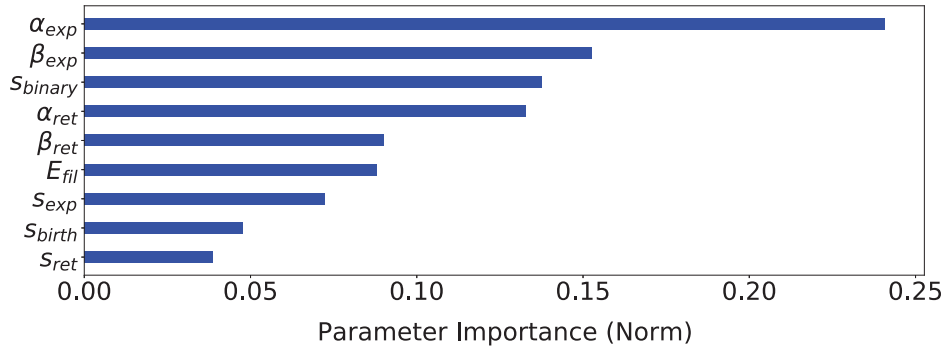

Figure 4.9: Parameter importance. Parameters sensitivity based on SigOpt analysis of each parameter importance on the proposed evaluation metrics.

expansion/retraction stretch rate field. The third most influential parameter on these metrics was s_{binary} (13.76 %), used to simplify the search of signal s peaks (where protrusions centroids located). Lastly, s_{birth} and $s_{reinforce}$ had the lowest impact on our evaluation metrics (4.76 % and 3.86 %, respectively).

Finally, we qualitatively validated the proposed *in silico* model based on observations of migrating cells surrounded by different chemoattractant gradients. Figure 4.8 (left) shows that as the PDGF gradient grew, the cell's speed in the direction of the chemotactic gradient increased too. Thus, cells follow a more directional trajectory, which agrees with experimental observations from [525]. However, Figure 4.8 (right) shows that as the PDGF concentration surrounding the cell increased, the cell's speed in the direction of the chemotactic gradient decreased. In this case, cells were following a more random trajectory. This fall in the effective speed of the cell may be associated with receptor saturation [526] and a phenotypic switch from migratory to proliferative [529].

4.4 Conclusions

Directed cell migration is critical for living organisms to grow and develop from a fertilized egg, protect themselves against foreign invaders, and repair damaged tissues. Therefore, healthy organisms depend on cells' ability to perceive tactic cues from their surroundings and respond accordingly. Cells tend to migrate mesenchymally within dense and highly adhesive 3D environments. In such scenarios, cells develop protrusive structures that hold on to the surrounding matrix and pull themselves forward, squeezing their nuclei through ECM pores.

Understanding cell migration is extremely difficult because of the wide array of modulating factors, such as temperature, architecture, and composition of the

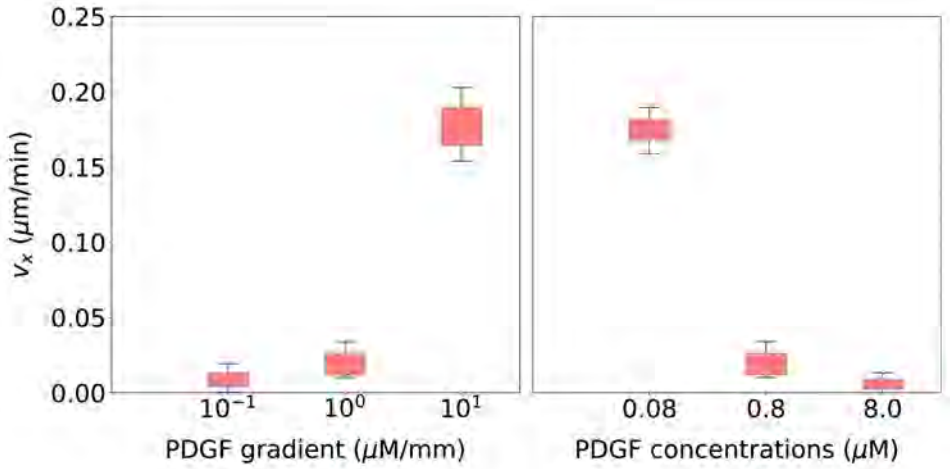

Figure 4.10: Model validation. Cell migration speed statistical analysis for 20 simulations using the parametrization selected during the calibration process and associated with six different extracellular environments. **Left**: three of these extracellular environments included different PDGF gradients (10^{-1}, 10^{0}, and 10^{1} µM mm^{-1}) but a fixed PDGF concentration at the initial cells positions (0.8 µM). **Right**: three extracellular environments included a fixed PDGF gradient (100 µM mm^{-1}) but different PDGF concentrations at the initial cells position (0.08, 0.8, and 8.0 µM).

ECM (e.g., density, pore size, stiffness) as well as the presence of tactic cues [41]. These factors regulate cell motion by acting through different intracellular signaling pathways (as triggers or downstream effectors), or in the dynamics of adhesions, the cytoskeleton, or the nucleus [47, 50, 205, 323].

According to our experimental observations [352, 484, 507], cells exhibiting a mesenchymal migratory phenotype within 3D matrices tend to present two different behaviors. They may increase the number of stable protrusions, in which case all protrusions are short. In contrast, they might decrease the number of stable protrusions, with some of them being notably longer. In the first case, protrusions compete against each other, resulting in no preferential movement. In the second case, cells usually present a defined trajectory in the direction of the longest protrusion.

We made several assumptions regarding the mechanical model of the ECM. First, we considered the matrix as an isotropic material. Nevertheless, the ECM is anisotropic because of the different fiber directions [171]. Second, we did not consider the inhomogeneities associated with the surrounding microenvironment [145]. Instead, we assumed a fixed rigidity for the matrix. Neither did we consider ECM remodeling in this *in silico* model. However, this is an acceptable approximation for preliminary studies of cell motion within collagen-based hydrogels, which allowed us to use Eshelby's theory.

Owing to the complexity of cell migration, *in silico* models have been widely used to improve our understanding of this fundamental biological process [225, 504, 530]. Intracellular signaling pathways regulating cell motion are one of the sources of complexity in cellular migratory behaviors. Cell motility can be considered a stochastic phenomenon because of its inherent variability. The evolution of intracellular signaling pathways highlights the stochastic nature of cell migration. The Stochastic Simulation Algorithm (SSA) [511, 512] has been widely used to numerically simulate the stochastic behavior of biochemical reactions. However, the SSA is considered too slow for many practical applications [514, 531]. This effect was evident in our specific case: even though the SSA offers an exact solution, simulations took too long to finish (an average of 10.77 hours of execution time for each 4-hour simulation of cell migration). The tau-leaping algorithm was considered a good fit for our purposes. It gave us a "good-enough" approximation (see Footnote 1 on page 81) of the temporal evolution of our signaling network, allowing us to optimize the numerical performance of our mechanochemical model (an average of 1.28 hours of execution time for each 4-hour simulation of cell migration). Thus, reducing the computational cost by almost an order of magnitude.

The complexity of the calibration process of any *in silico* model increases very quickly with the number of parameters. Another factor that notably increases the complexity of the calibration process is the stochastic nature of some biological models, such as the one presented in this chapter. Stochastic models require the execution of several simulations for each parametrization to capture the variation in the results associated with the stochastic randomness. Moreover, if executing each simulation takes more than a couple of minutes, a manual approach for this calibration process becomes highly prone to inefficiencies and human errors.

When choosing the values for each model parameter using such a manual approach, researchers usually turn to the literature as their starting point. Then, they perform some manual tuning so that results *in silico* approximately replicate the experimental data. Generally, researchers start by modifying just a couple of parameters using some values that are considered biologically relevant. Next, they analyze how those parameters influence the model output based on the different values tested. They iterate over this process by picking a couple of the remaining parameters in every iteration—ideally, the selected parameters in each iteration are related to each other. This manual approach is very tedious because modifying some parameters may require the recalibration of others already calibrated. If the *in silico* model includes many different parameters, researchers could start this tuning process by performing a sensitivity analysis [26, 394, 449, 532, 533] to focus on those parameters with a higher impact on the model output. Access to a High-Throughput Computing (HTC) environment—which can drastically reduce the

required elapsed times to run those simulations by parallelizing them—is becoming more common. Still, owing to computational and time restrictions, this manual step does not generally include more than a couple of iterations.

In most theoretical studies [30, 34, 384, 534–536] authors perform strong efforts to validate the proposed *in silico* models by comparing experimental data with the results of numerical simulations. Nevertheless, a complete integration of experimental and numerical results is still lacking. This work represents a relevant step forward in this direction by showcasing an example of application of the integrative methodology presented in Chapter 3. In particular, this autonomous framework integrates both modeling strategies (*in vitro* and *in silico*) by applying Bayesian optimization during the calibration process to reduce these inefficiencies.

Bayesian optimization, which has been applied to solve a wide range of problems such as machine learning applications [450], robot planning [451], simulation design [452], biochemistry [453], and dynamical modeling of biological systems [455], offers an automated approach for this calibration process. Furthermore, the Bayesian optimization technique can minimize the number of parametrizations evaluated to find a good enough fit for *in vitro* observations. In our case, from the 300 different parametrizations tested during the calibration process, only 6 (2 %) have the two metrics considered (BC_{llp} and BC_{np}) below 0.5. On the other hand, SigOpt suggests 107 parametrizations (35.67 %) with both metrics above 0.7.

This integrative methodology based on Bayesian optimization allowed us to identify the key parameters regulating the migration of NHDF cells embedded in a collagen-based matrix. In particular, this novel methodology was applied to calibrate a stochastic *in silico* model of a simplified signaling network based on the biochemical interaction between chemoattractants molecules (PDGF) and the associated transmembrane receptor (in this case, the PDGFR). This interaction, in turn, triggers a signaling cascade that enables cells to sense biochemical stimuli. Moreover, the calibration did not overfit the training data, that is, the experimental data used during the calibration process, as highlighted during the final validation process. To validate the selected parametrization, we simulated cell migration with a diffused chemoattractant factor throughout the ECM. Then, we qualitatively compared observations based on the cell's speed in the direction of the chemotactic gradient with results from previous experimental works [525, 526]. Our results agree with those from *in vitro* experiments, where cells followed a more directional motion as the chemoattractant gradient increased. However, when the chemoattractant concentration surrounding the cell reaches an upper bound, cells start to lose the ability to chemotax.

In conclusion, the tau-leaping algorithm allowed us to optimize the performance of the proposed *in silico* model by dramatically reducing the execution time required to simulate the spatiotemporal evolution of the defined signaling network. In addition, the integrative methodology proposed in Chapter 3 proved to enable theoreticians to calibrate their expensive-to-simulate *in silico* models in a very efficient and completely automatic way. As a result, this novel methodology will facilitate the development of *in silico* models, enabling researchers to acquire a more comprehensive understanding of cell migration.

5

Cell migration biased by biophysical cues

Contents

This chapter is based on:

Francisco Merino-Casallo, Maria Jose Gomez-Benito, Ruben Martinez-Cantin, and Jose Manuel Garcia-Aznar. *A mechanistic protrusive-based model for three-dimensional cell migration: an integrative approach.*

5.1 Introduction

Cell migration regulates the development and maintenance of multicellular organisms. Indeed, forming new tissues and organs during embryogenesis requires elaborate migratory patterns. During angiogenesis, endothelial cells migrate from pre-existing blood vessels to form new ones. Wound healing calls for the coordinated migration of several cell types, such as fibroblasts and epidermal cells. Cell migration is also associated with many diseases such as cancer, in which tumoral cells invade their surrounding tissue and other parts of the body during metastasis. Therefore, a comprehensive understanding of cell motility is crucial.

Cell migration is an extremely complex phenomenon involving many different biological processes and players. The specific cellular context—in particular, the cell phenotype and the properties of the surrounding microenvironment—determines if and how cells migrate [46–49, 225, 537]. Besides, distinct external cues may bias cells' trajectory and speed. These external signals span from chemicals (e.g., gradients of soluble or surface-bound factors) to mechanical ones, such as the extracellular matrix (ECM) architecture and stiffness. Nonetheless, how cells sense these external cues, adapt, and respond by establishing a specific migratory pattern is not fully understood yet.

Cell motion has been a subject of study for more than a century [59, 60, 475]. The focus of the research community has been primarily on how cells migrate on two-dimensional (2D) domains until recently. Studying migratory cells on flat surfaces has considerably increased our understanding of cell migration. Still, cell behavior on plated cultures does not accurately replicate how cells behave in three-dimensional (3D) *in vivo* conditions [65, 66, 538].

In such relevant settings, a variety of cell types can switch from one mode of migration to another based on their context [41, 76, 539]. Factors such as cell confinement, low adhesion, increased cellular contractility, and inhibited proteolytic activity promote lobopodial and amoeboid migration. Conversely, the main features of mesenchymal migration are prominent protrusions, high ECM adhesion, and proteolytic tissue remodeling.

The wide variety of actors, biological processes, and factors regulating cell migration calls for an integrative approach to unravel such complex phenomena [371, 381, 397]. Mathematical models have become a powerful tool to get valuable insights more efficiently. Simulators can also isolate specific mechanisms and behavior patterns more easily than their *in vitro* counterparts. Furthermore, *in silico* models may have a guiding role for experimental research by making predictions to test in the lab.

Over the last several decades, researchers have proposed many different computational models to increase our understanding of cell migration. Most of these theoretical models replicate cell motion on flat surfaces [31, 361–364]. Nonetheless, an increasing number of mathematical models focus on cell motility within more realistic 3D microenvironments [187, 370, 371, 383]. Different *in silico* models have tried to mimic the distinct modes of cell migration: individual [405, 540, 541] or collective [388, 389, 394, 420], amoeboid [384, 385, 542], mesenchymal [34, 375, 382], or even lobopodial [387]. Researchers usually focus on just one of the mechanisms involved in the migratory process (e.g., the biochemical [519, 543, 544], or the biophysical [372, 508, 545]). A few models even integrate a couple of them, such as the biochemical and biophysical mechanisms [379, 420, 546]. These models usually adopt one of the following modeling approaches: (i) discrete [536, 547, 548], (ii) continuum [411, 462, 534] or (iii) hybrid [30, 533, 549]. We would like to highlight the theoretical work of Kim and colleagues [34], in which authors defined a method to assess the ECM stiffness sensed by filopodia. The authors applied this method to model filopodial mechanosensing that resulted in guided cell migration within 3D environments.

The present work aimed to improve our knowledge of how and to what extent cell mechanics and ECM degradation regulate mesenchymal-like cell motility within 3D matrices. We created a new model that more accurately represents how the mechanical properties of cells and their surroundings influence their migratory patterns. By integrating biochemical and biomechanical stimuli, we could more accurately mimic how individual cells migrate through 3D dense microenvironments. In particular, our focus in this work was on cell-ECM interactions—which are deemed essential for mesenchymal migration. As a result, we could replicate how cells interact with their surroundings to sense external cues and modify their local microenvironment accordingly.

In the following sections, we will describe the different components of the proposed *in silico* model: from a simplified version of the chemosensing mechanism to the building blocks of the mechanism associated with cell-matrix interactions. In particular, we will emphasize how we modeled (i) protrusion dynamics, (ii) the ECM regulatory role on protrusion growth and retraction, (iii) how cells push their nucleus forward during mesenchymal migration, (iv) the formation and disassembly of cell-matrix adhesions, and (v) ECM degradation. Then, we will give a specific application for the proposed model. Next, we will highlight the main migratory behaviors predicted by this *in silico* model. Finally, we will give an overview of the presented model, its strengths and limitations, as well as the novelty and relevance of this work.

5.2 Methods

In this section, we will start by describing an *in silico* model of 3D mesenchymal cell migration that extends the proposed multi-scale model from Chapter 4 [35, 382]. We will present the mathematical definition and implementation of this multi-scale model. Then, we will illustrate the application of this *in silico* model, demonstrating the predictive capabilities by comparing the numerical results with experimental data.

5.2.1 Model description

Here, we start by describing the main aspects of this extended multi-scale model to better understand the novel modeling enhancements proposed. This model was built upon the assumption that the mesenchymal cell migration can be described as a three-stage process [112, 382]. First, the cell probes its surroundings for external cues such as gradients of chemoattractant through a variety of transmembrane receptors. Secondly, when these transmembrane receptors get activated by binding to such ligands, they initiate a cascade of signaling pathways that modulate the cellular migratory response. In particular, these signaling pathways regulate the dynamics of dendritic protrusions [250–252, 280]. Finally, these protrusive structures push and pull the ECM, allowing the cell to migrate throughout the ECM. Here, we established a relationship between the contractile forces exerted by these protrusions and the cell nucleus translocation.

The proposed model simulating mesenchymal cell migration within 3D matrices was built upon some of our previous works [35, 382]. However, we included several novel aspects to more accurately replicate the cell, the surrounding environment, and the interactions between each other. We will start by introducing the different building blocks of the proposed model of mesenchymal-like motility within dense environments. First, we will briefly describe the chemosensing mechanism that establishes protrusions locations and their stress-free (unconstrained) length variation. Secondly, we will present the ECM model that allowed us to consider the matrix as a heterogeneous entity. Next, we will describe how we modeled protrusions expansion and contraction, which enables the nucleus translocation through ECM pores. Then, we will define a model of matrix degradation that allows cells to enlarge narrow ECM pores. Lastly, we will give an overview of the numerical implementation of the proposed *in silico* model and an example of its application.

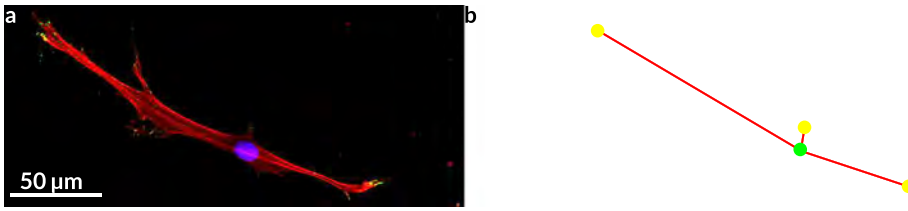

Figure 5.1: Cell 3D structure scheme. **(a)** Normal Human Dermal Fibroblast (NHDF) cultured in a 4 mg/ml collagen gel, stained for actin (red), vinculin (green), and nucleus (blue). Image were captured with a confocal microscope. (Adapted from [500]). **(b)** *In silico* model of a mesenchymal cell migrating within 3D matrices. Protrusions are considered as 1D deformable bars (yellow), and are all linked together in a central node representing the cell nucleus (green).

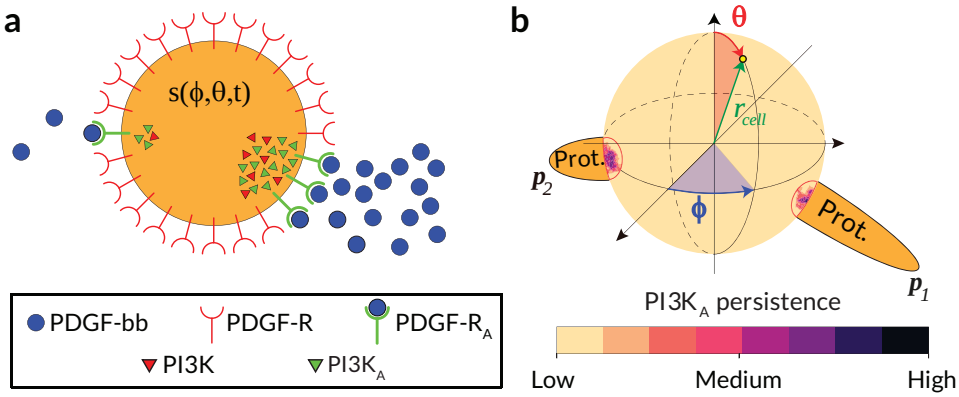

Figure 5.2: Cell signaling model scheme. **(a)** Two-dimensional representation of the modeled 3D chemosensing mechanism based on a simplified signaling pathway in which PDGF molecules activated their associated surface receptors (PDGFR) by binding to them. These activated PDGFR ($PDGFR_A$), in turn, activated messenger molecules of PI3K located in the cytosol. The spatial persistence of $PI3K_A$ ($s(\phi,\theta,t)$) has a regulatory role in protrusion dynamics. **(b)** Scheme of the regulatory role of $PI3K_A$ persistence in protrusion dynamics. The location of $s(\phi,\theta,t)$ peaks determined protrusions location (p_1 at $[\phi_{p_1},\theta_{p_1}]$ and p_2 at $[\phi_{p_2},\theta_{p_2}]$), while the signal variation ($\partial s(\phi,\theta,t)/\partial t$) influences protrusions stress-free (unconstrained) length variation.

Modeling cell behavior

We maintained the cell 3D structure proposed in Chapter 4. which simulated the cell body as a set of 1D deformable bars joined in a centroid (Figure 5.1b). This centroid represented the cell nucleus. These 1D bars were located in a 3D domain and simulated protrusions defining the cell body.

5.2.2 Chemosensing mechanism

The chemosensing mechanism enables cells to probe for biochemical cues in their surrounding ECM. The activation and deactivation of transmembrane receptors (e.g., RTKs, GPCRs) allow cells to perceive the biochemical profile of the ECM. These receptors embedded in the PM become activated by binding to different chemoattractant molecules (e.g., growth factors). When bound together, the activated receptors can activate downstream signaling molecules (e.g., phosphoinositide 3-kinases [PI3K]) located at the cytosol. As a result, the signal received in the PM is propagated inside the cell, regulating different cellular dynamics, including those of actin-based protrusions.

The spatiotemporal distribution of activated PI3K ($PI3K_A$) is closely related to protrusions dynamics and migratory patterns [486, 501–503]. Therefore, we modeled a simplified signaling network (Figure 5.2a). We were interested in the locations where (i) cytosolic PI3K was preferentially activated and (ii) $PI3K_A$ accumulated through time inside the cell. These features defined protrusions locations and directly influenced their expansion and contraction (Figure 5.2b).

We represented the PM of the cell as a spherical surface with a fixed radius (Figure 5.2b). The center of this sphere was the central node linking all protrusions in the proposed mechanical model (see Figure 5.4 and Figure 5.5).

More details on this chemosensing mechanism and the proposed signaling network are included in Subsection 4.2.1 (page 72).

5.2.3 Modeling the heterogeneous behavior of the ECM

In previous works [35, 382], we considered the ECM as a continuous and homogeneous entity. Nevertheless, this approximation is far from reality. The ECM internal structure builds upon a network of collagen fibers, which are interconnected by crosslinkers (Figure 5.3) [270, 551]. Still, the composition and microarchitecture of the ECM associated with each tissue are unique [552, 553]. Further, local variations in the biophysical properties of the matrix can dramatically impact different biological processes, including cell migration [145]. Indeed, cells can sense the local properties of their surrounding ECM, such as porosity, fiber alignment, and stiffness, and adapt their behavior accordingly [150, 355]. Thus, modeling physiological processes such as cell migration requires a good approximation of the ECM inhomogeneities.

A realistic model of how cells' local environment influences cell migration requires considering the ECM a heterogeneous entity. Accordingly, we opted to discretize the

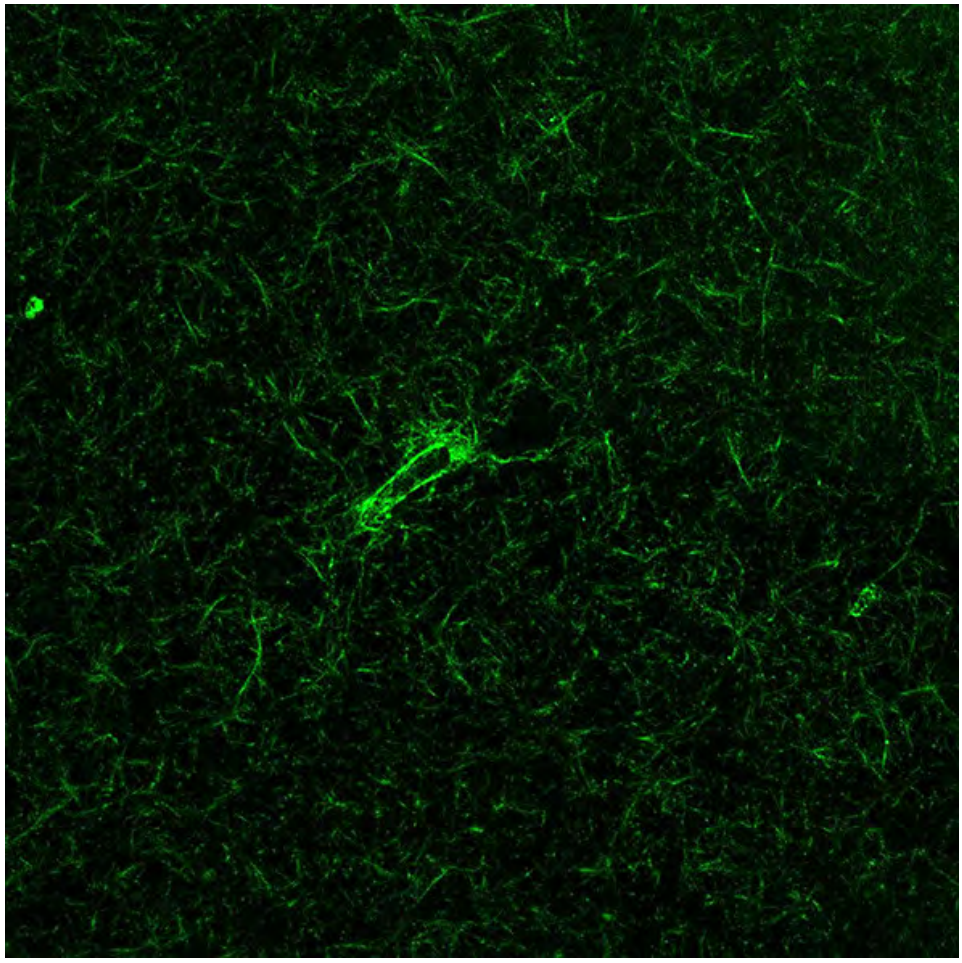

Figure 5.3: Confocal image in real-time of a Primary Human Osteoblast seeded in DQ-collagen I (green fluorescence) mixed with collagen I. Image reproduced with permission from Movilla N. [550].

extracellular domain in a set of voxels of a fixed size. This ECM representation allows to locally evaluate the biophysical properties of the cells' surrounding environment. Substrate stiffness influences some of the leading players in the cell-matrix interactive mechanism, such as actin (de)polymerization and actomyosin motors [554, 555]. Because of the ECM fibrillar interconnectivity, integrin-containing focal adhesions (FAs) allow cells to sense the stiffness of their local microenvironment [175, 182]. We assumed that the stiffness sensed by the cell through FAs is the stiffness of the ECM surrounding those adhesion complexes. The stiffness of the ECM is another factor regulating the protrusive stretch characteristics. Therefore, in this work, we paid special attention to the ECM stiffness.

To assess the local stiffness of ECM subdomains in our biophysical model, we used simple geometric elements. One or several of these elements made up what we called regions of interest (ROI). We opted for sphere-like elements with radius r_{ROI}.

We assumed a relationship between the porosity of the matrix and its stiffness, which may change based on the physical profile of the ECM. For collagen-based hydrogels, such relationship means that as the collagen concentration increases, so does its stiffness [171]. In contrast, the porosity of the matrix decreases [270].

5.2.4 Protrusions growth

Modeling cell mechanics during protrusion growth

In 3D microenvironments, actin polymerization contributes to protrusions formation and growth [266, 280]. Actin polymerization occurs much more rapidly at the barbed end of actin filaments, which most of the time points toward the PM. By polymerizing against the PM, actin filaments push this membrane and the surrounding ECM.

We defined a mechanical system based on nodes and elements (bars and springs) to simulate such expansive event. Unlike our previous works [35, 382], protrusions were considered as unidimensional elastic bars (p_i). The contact between these deformable bars and the surrounding matrix was simulated by means of springs. Conversely, the cell nucleus was considered the central node that connected all these elastic bars (Figure 5.4). The LINC complex connects the cell nucleus to the cytoskeleton, embedding it in a meshwork that can resist high compressive loads. Therefore, the displacements of the central node (the cell nucleus) were impeded. We located nodes at the tip of the protrusions and the cell nucleus (yellow circles in Figure 5.4).

We assigned a fixed rigidity to the 1D elastic bars. In contrast, the stiffness associated with the springs were calculated evaluating the rigidity of the surrounding ECM. Specifically, we assessed the rigidity of the ROIs associated with the areas that protrusions would traverse based on s_{p_i} ($\mathrm{ROI}^{\mathrm{exp}}$; Figure 5.4a, green and pink rectangles).

Location and stress-free (unconstrained) length variation

We assumed the persistence of activated actin-binding regulators such as PI3K ($\mathrm{PI3K_A}$) in the outer region of the cytosol (just below the cell surface) determines the protrusions location and their stress-free (unconstrained) length variation during their expansion. In locations where activated PI3K persistence increased, the corresponding i-th protrusion grew larger during the expansive stage. As a

result, the stress-free (unconstrained) expansion of protrusions depended on signal variations of PI3K$_{\mathrm{A}}$ (s) at those locations (s_{p_i}). Therefore, we computed the stress-free (unconstrained) length variation of each protrusion during its expansion based on these signal variations as:

$$\left.\frac{\partial L^f_{p_i}(s_{p_i},t)}{\partial t}\right|_{exp} = \begin{cases} \left.\frac{\partial L^f_{p_i}(s_{p_i},t)}{\partial t}\right|_{birth} & \text{if } p_i \text{ is new prot.} \\ \left.\frac{\partial L^f_{p_i}(s_{p_i},t)}{\partial t}\right|_{growth} & \text{otherwise} \end{cases}, \tag{5.1}$$

where s_{p_i} is the spatiotemporal variation of PI3K$_{\mathrm{A}}$ associated to the i-th protrusion, $\frac{\partial L^f_{p_i}(s_{p_i},t)}{\partial t}|_{birth}$ represents the stress-free (unconstrained) length variation of the i-th protrusion during its birth (defined in Equation 4.4 [page 76]), and $\frac{\partial L^f_{p_i}(s_{p_i},t)}{\partial t}|_{growth}$ is the stress-free (unconstrained) length variation of the i-th protrusion during its growth and stabilization (defined in Equation 4.5 [page 76]).

More details on how we established protrusions locations and their stress-free (unconstrained) expansion are included in Subsection 4.2.2 (page 75).

Simulating protrusion growth by actin polymerization

To simulate protrusions expansion because of actin polymerization, we applied forces to the aforementioned nodes located at both ends of protrusions (Figure 5.4b, left). The time variation of these forces was defined as:

$$\frac{\partial \boldsymbol{F}^{exp}_{p_i}(t)}{\partial t} = \frac{E_{p_i}A}{L^{exp}_{p_i}(s_{p_i},t_0)} \left.\frac{\partial L^f_{p_i}(s_{p_i},t)}{\partial t}\right|_{exp} \boldsymbol{e}_i, \tag{5.2}$$

where E_{p_i} represents the stiffness of the i-th protrusion, A is the area of the protrusion cross section, and $L^{exp}_{p_i}(s_{p_i},t_0)$ represents the length of the i-th protrusion at the beginning of its expansive stage (t_0). $\left.\frac{\partial L^f_{p_i}(s_{p_i},t)}{\partial t}\right|_{exp}$ is the stress-free (unconstrained) length variation of the i-th protrusion during its expansion (defined in Equation 5.1). Lastly, $\boldsymbol{e}_i$ is the unit vector in the direction of the longitudinal axis of the i-th protrusion.

Next, we computed the displacements of each node ($\boldsymbol{u}^i(t)$) (Figure 5.4b, right). We took into account the stiffness of the ECM surrounding the cell and the forces generated by protrusion's expansion. The length and relative position of each protrusion were updated using these computed displacements. Note that, as the displacements of the central node were impeded, only the nodes located at the protrusions tip would move.

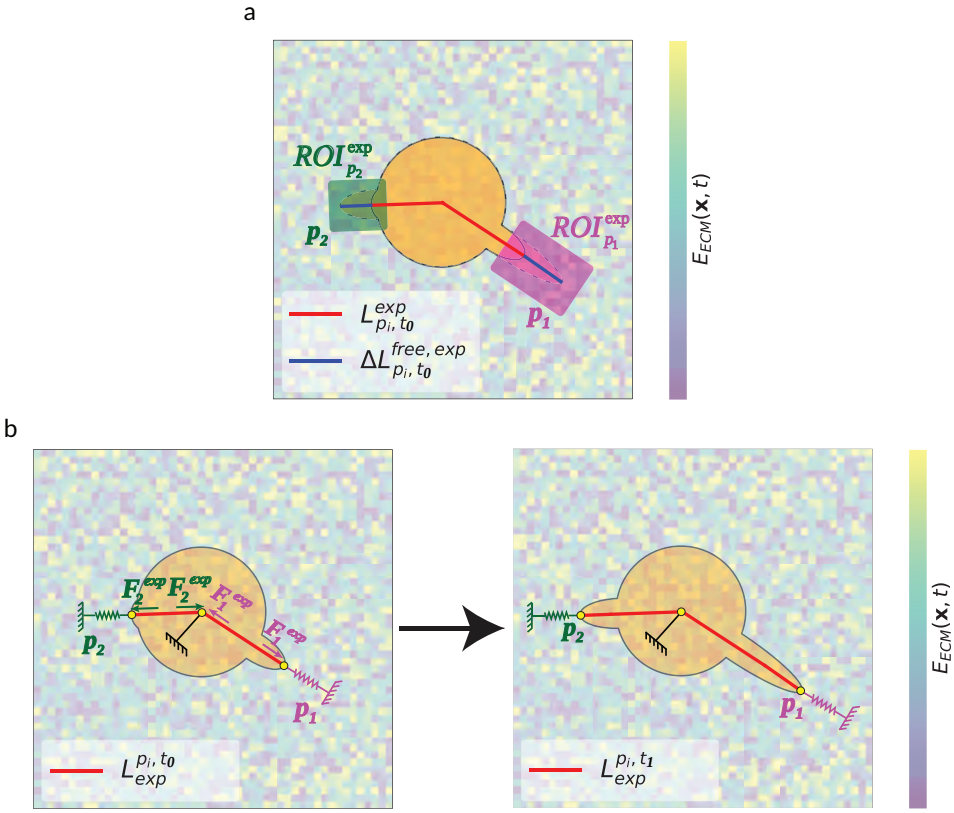

Figure 5.4: Two-dimensional representation of the 3D structure associated with protrusions expansion. Two protrusions, p_1 and p_2, are represented as unidimensional elastic bars, with a fixed rigidity. The cell nucleus is the central point connecting the bars, which represent cell's protrusions. We locate a node (yellow circles) at the location of the cell nucleus and at the tip of each protrusion. The contact between these deformable bars and the surrounding matrix was simulated by means of springs. **(a)** The stiffness of these springs was computed as the averaged Young's modulus of the corresponding region of interest ($ROI^{exp}_{p_1}$ and $ROI^{exp}_{p_2}$). **(b)** By binding cell nucleus to the cytoskeleton, the LINC complex embeds it in a meshwork that can resist high compressive loads. Therefore, the displacements of the central node were impeded. **(b, left)** Next, we applied forces to the nodes to simulate protrusions expansion because of actin polymerization. **(b, right)** Finally, we computed the displacements of each node. Note that only the nodes located at the protrusions tip would move.

5.2.5 Protrusions contraction

Modeling cell mechanics during protrusions contraction

Actin depolymerization and actomyosin motors play a key role in protrusions contraction. Actin depolymerization occurs much more rapidly at the pointed end of actin filaments, which most of the time face inside, away from the PM. Actomyosin motors generate traction forces in the cytoskeleton, which are then transmited to the cell nucleus by the LINC complex.

We defined a mechanical system based on nodes and elements (bars and springs) to simulate the contractile events. Protrusions were considered as unidimensional elastic bars (p_i), whereas FAs coupling the PM to the surrounding ECM were simulated by means of springs. The cell nucleus was considered the central node that connected all these elastic bars (Figure 5.5). We located nodes at the tip of the protrusions and the cell nucleus (yellow circles in Figure 5.5).

We assigned a fixed rigidity to the 1D elastic bars (the same rigidity than during the expansive stage). The stiffness associated with the springs were calculated evaluating the rigidity of the surrounding ECM. However, this time we assessed the rigidity of the ROIs associated with the protrusions adhesive regions ($\mathrm{ROI}^{\mathrm{con}}$; Figure 5.5A, green and pink rectangles). This adhesive region had a maximum length of 8 µm (in agreement with the 8 µm–16 µm range from [556]).

Unconstrained length variation

We assumed the protrusions length at the beginning of its contractile stage determines their stress-free (unconstrained) length variation during their contraction. Therefore, we defined the stress-free (unconstrained) length variation of each protrusion during its contraction accordingly. During protrusions contraction, in locations where s was above s_{death}, protrusions rectracted. However, in those regions where s was below s_{death}, pre-existing protrusive structures not only retracted but also disappeared:

$$\left.\frac{\partial L^f_{p_i}(s_{p_i},t)}{\partial t}\right|_{con} = \begin{cases} -cL^{con}_{p_i}(s_{p_i},t_0) & \text{if } s_{p_i}(t) \geq s_{death} \\ -L^{con}_{p_i}(s_{p_i},t_0) & \text{otherwise} \end{cases}, \tag{5.3}$$

where c is a parameter regulating protrusion contraction rate, and $L^{con}_{p_i}(s_{p_i},t_0)$ is the protrusion's length at the beginning of its contractile stage at time t_0. Notably, c could be associated with the contractility profile of the cell. This parameter c would depend on the cell-type and the specific properties of the surrounding ECM. Accordingly, we could establish a relationship between c and the number of motors

and clutches [154]. Interestingly, [273] recently suggested that increased contractility leads to mechanotype differences in weakly and strongly adherent cells.

A negative feedback loop for PI3K activation is generated by myosin motors during protrusions contraction, as suggested by [486]. Therefore, as in the proposed *in silico* model from Chapter 4, we assumed a directly proportional decrease in $\delta s_{p_i}(t)$ to s_{p_i} during the contractile stage ($\delta s_{p_i}(t) < 0$). We also considered a time-dependent wear of $s_{p_i}(t)$, as time wears out the persistence of $\mathrm{PI3K_A}$, following a 30 min half-life decay [486].

Note that the length and number of protrusions depends on signal s. For instance, if s has a couple of regions where $\mathrm{PI3K_A}$ has prominently accumulated over time (5 min), we could predict a few long protrusions. Conversely, if signal s is mainly homogeneous with small variations, we should expect many small protrusions. However, these predictions could change based on the initial amount of PI3K (Table 4.1), and the parameters associated with signal s (s_{binary}, s_{birth}, s_{growth}, and s_{death}). Indeed, these parameters also regulate the length and number of protrusions at any given time.

Simulating protrusion retraction by actin depolymerization and actomyosin motors

To simulate protrusions contraction because of actin depolymerization and actomyosin motors, we applied forces to the aforementioned nodes (Figure 5.5b, left). The time variation of these contractile forces were defined as:

$$\frac{\partial \boldsymbol{F}_{p_i}^{con}(t)}{\partial t} = (1-\mu)\frac{E_{p_i}A}{L_{p_i}^{con}(s_{p_i},t_0)}\frac{\partial L_{p_i}^{f}(s_{p_i},t)}{\partial t}\bigg|_{con}\boldsymbol{e}_i, \tag{5.4}$$

where μ is a friction term (defined below, in Equation 5.5), E_{p_i} represents the stiffness of the i-th protrusion, and A is the area of the protrusion cross section. $L_{p_i}^{con}(s_{p_i},t_0)$ is the length of the i-th protrusion at the beginning of its contractile stage (t_0). $\frac{\partial L_{p_i}^{f}(s_{p_i},t)}{\partial t}\Big|_{con}$ represents the stress-free (unconstrained) length variation of the i-th protrusion during its contraction (defined in Equation 5.3). Lastly, $\boldsymbol{e}_i$ is the unit vector in the direction of the longitudinal axis of the i-th protrusion

Including a friction term (μ) enabled our model to replicate the increasing difficulty that cells find to migrate within dense 3D environment because of steric hindrance. We computed this friction term (μ) by means of a phenomenological law that takes into account the drag that suffers the cell nucleus through ECM pores as:

$$\mu = \begin{cases} \left(\frac{E_{ECM}(\boldsymbol{x}_{p_i}^{sh},t)-E_{ECM}^{sq}}{E_{ECM}(\boldsymbol{x}_{p_i}^{sh},t)+E_{ECM}^{sq}}\right)^{\gamma_{fr}} & \text{if } E_{ECM}(\boldsymbol{x}_{p_i}^{sh},t) > E_{ECM}^{sq} \\ 0 & \text{otherwise} \end{cases}, \tag{5.5}$$

where E^{sq}_{ECM} represents a rigidity threshold, $E_{ECM}(\boldsymbol{x}^{sh}_{p_i}, t)$ is the ECM rigidity around the i-th protrusion shaft ($\boldsymbol{x}^{sh}_{p_i}$, the ECM region through which the nucleus would be squeezed), and γ_{fr} is a friction coefficient.

We assumed a relationship between the porosity of the matrix and its stiffness, which may change based on the physical profile of the ECM. In particular, for collagen-based hydrogels, we assumed an inverse relationship because, as the collagen concentration increases, so does its stiffness [171]. Conversely, the porosity of the matrix decreases [270]. Hence, we established a rigidity threshold E^{sq}_{ECM}, which is cell type-specific and may also change based on the physical profile of the ECM. Not only because cell types may exhibit a nucleus of a different size but also because nuclear deformability may change based on factors such as the matrix composition, which would modulate cell's nuclear lamin A/C ratio or induce chromatin decompaction. For example, inhibiting lamin A/C phosphorylation in HT-1080 fibrosarcoma cells increased their nuclei stiffness [332]. Conversely, confined conditions in 3D induce chromatin decompaction and seem to decrease nuclear stiffness [302, 557].

Protrusions adhered to stiffer, denser, more confined regions of the ECM would have to exert higher contractile forces to squeeze cells nuclei through. This friction term (μ) would act as a penalty term, biasing the migratory toward those regions that facilitate the translocation of cells nuclei through larger pores. Still, in some scenarios, this friction term may be negligible (even zero), that is, there might be no penalty for any region of the defined ECM. Indeed, in these scenarios, cells may exhibit highly deformable or small-enough nuclei to traverse ECM pores effortlessly. The biophysical properties of the matrix may not hinder cell migration through steric hindrance either.

In this work, we were focused on NHDF cells migrating in collagen-based hydrogels, so we calibrated this rigidity threshold (E^{sq}_{ECM}) accordingly. When the stiffness of the ECM around the i-th protrusion shaft ($E_{ECM}(\boldsymbol{x}^{sh}_{p_i}, t)$) is greater than this rigidity threshold, the porosity of the matrix would enable cells to migrate through pores effortlessly [558]. Otherwise, the ECM porosity would require cells to squeeze their nuclei to overcome the physical barrier that represents such small pores [301, 340]. By including γ_{fr} as a friction coefficient, we allow for a nonlinear response, which may be required to replicate the effect of the ECM steric hindrance [255]. Note that γ_{fr} may be equal to 1, which would translate into a linear response for the ECM steric hindrance.

Next, we computed the displacements of each node ($\boldsymbol{u}^i(t)$) (yellow circles in Figure 5.5b, right). Again, we took into account the stiffness of the ECM surrounding the cell and the forces generated by actomyosin motors. The cell nucleus was assumed

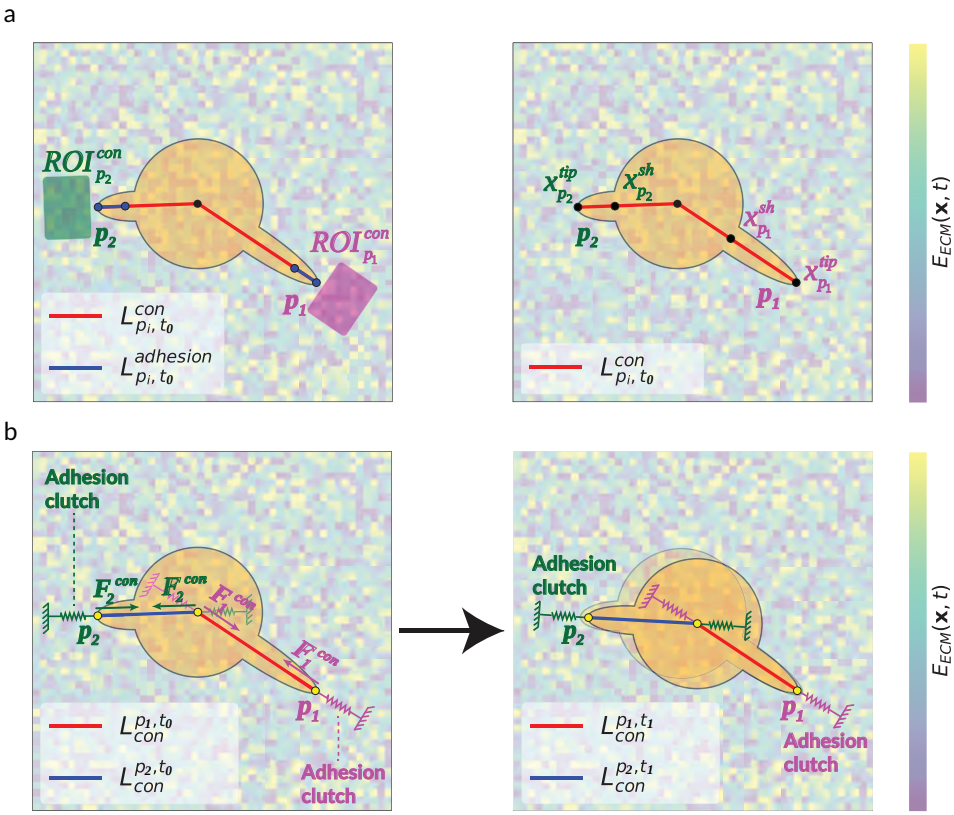

Figure 5.5: Two-dimensional representation of the 3D structure associated with protrusions contraction. Two protrusions, p_1 and p_2, are represented as unidimensional elastic bars, with a fixed rigidity. The cell nucleus is the central point connecting the bars, which represent cell's protrusions. We located a node (yellow circles) at the location of the cell nucleus and at the tip of each protrusion. Their adhesive region—which allows cells to probe the surroundings through focal adhesions—was modeled as a spring. **(a, left)** The stiffness of these springs was computed as the averaged Young's modulus of the corresponding region of interest ($\mathrm{ROI}^{\mathrm{con}}_{\mathrm{P1}}$ and $\mathrm{ROI}^{\mathrm{con}}_{\mathrm{P2}}$). During contraction, the ROIs did not overlap the space occupied by the cell's protrusions. Instead, they were located in front of them. This is where the ECM would received the maximum mechanical stimulus because of protrusions' contractions. **(a, right)** To compute the friction term (μ) associated with the contractile force of each protrusion ($F^{con}_{p_i}(t)$), we assessed the averaged Young's modulus around the shaft of the corresponding protrusion ($x^{sh}_{p_i}$). Conversely, to compute the reaction forces ($R_{p_i}(t)$) associated with each protrusion, we evaluated the average Young's modulus arount the tip of the corresponding protrusion ($x^{tip}_{p_i}$). *(continued)*

Figure 5.5: *(Continued from previous page)* **(b)** Also, we included adhesive clutches on FAs, which would determine protrusions adhesiveness to the surrounding ECM. We considered each protrusion connected to the cell nucleus through the cytoskeleton (and the LINC complex) as an isolated mechanical entity. Therefore, we solved the system associated with each mechanical entity independently. Each of these systems included a different spring connected to the central node, as the cell nucleus would move through a different region of the polarized cell's cytoplasm. We assumed that the stiffness of this region of the cytoplasm depended on the rigidity of the matrix around the adhesive region of each protrusion. We also assumed that the cell nucleus displacements happen in the same direction as one of the cell's protrusions. **(b, left)** Next, we applied forces to the nodes to simulate protrusions contraction because of actin depolymerization and actomyosin motors. **(b, right)** Finally, we computed the displacements of each node. The leading protrusion determining the cell trajectory was the one generating higher reaction forces.

to move through the cytoplasm of the cell. During the translocation of the cell nucleus, this organelle finds opposition from the cytoskeleton. Several authors have suggested that cells cortical stiffness depends on the rigidity of the surrounding ECM [559–563]. Therefore, we considered that the stiffness of this region of the cytoplasm depended on the rigidity of the matrix around the protrusions adhesive area. The length and relative position of each protrusion were updated using these computed displacements. However, based on experimental observations, we assumed that the cell nucleus displacements happen in the same direction as one of the cell's protrusions. We hypothesized cells would find lower opposition to push their nucleus forward through its cytoplasm than through the surrounding ECM. Thus, the position of the cell nucleus was determined by projecting the associated computed displacement over the direction vector of the nearest protrusion.

During mesenchymal-like migration, a leading protrusion determines cells' trajectories [350]. This leading protrusion is the one generating a higher deformation over the surrounding environment during the contractile stage. Consequently, we considered each protrusive structure connected to the cell nucleus through the cytoskeleton as an isolated mechanical entity. We solved the mechanical system associated to each protrusion and the cell nucleus individually. Then, we were able to determine the leading protrusion, that is, the one generating higher reaction forces—which we computed as:

$$\boldsymbol{R}_{p_i}(t) = \frac{E_{ECM}(\boldsymbol{x}_{p_i}^{tip}, t)A}{L_{p_i}^{con,adh}(t_1)}\boldsymbol{u}_{p_i}(t), \tag{5.6}$$

where $E_{ECM}(\boldsymbol{x}_{p_i}^{tip}, t)$ is the matrix rigidity around the i-th protrusion tip, A is the area of the protrusion cross section, $L_{p_i}^{adh}(t)$ is the length of the adhesive region of the i-th protrusion at the end of the contractile stage (t_1), and $\boldsymbol{u}_{p_i}(t)$ is the displacement vector of the i-th protrusion front.

Actomyosin force generation coordinates FA formation, reinforcement, and disassembly [312]. Hence, on the contractile stage of our model, we also included a simplified clutch model to simulate cell-matrix adhesions [154, 272] (Figure 5.5b). Regarding cell-ECM interactions, forces are transmitted only if molecular bonds establish a connection between: (i) ECM and integrins, and (ii) integrins and actin cytoskeleton. These bonds must be engaged to transmit contractile reaction forces generated by myosin motors located at the base of the protrusion to the surrounding ECM (Equation 5.7). Protrusions exerting contractile reaction forces too low or too high detach from the ECM. The bonds connecting the integrins to the ECM fibers, and integrins to the actin cytoskeleton, play an essential role here. Contractile reaction forces must be high enough for these bonds to be engaged. However, if those forces are too high, bonds linking integrins to the surrounding matrix will break. The contractile reaction forces that determined if the i-th protrusive node (located at the tip of the i-th protrusion, see Figure 5.5) was attached to the surrounding ECM was defined as:

$$p_i^{\text{attached}}(t) = \begin{cases} True & \text{if } R_{min} < \|\boldsymbol{R}_{p_i}(t)\| < R_{max} \\ False & \text{otherwise} \end{cases}, \tag{5.7}$$

where R_{min} and R_{max} are the lower and upper boundaries. If contractile reaction forces applied to the nodes located at the extremes of the 1D deformable bar associated to the i-th protrusion were smaller than R_{min} or bigger than R_{max}, then the corresponding bonds would not be engaged. We considered that only protrusions attached to the surrounding matrix could lead cell's migration. We also assumed that protrusions detached from the ECM retracted and subsequently disappeared.

5.2.6 ECM degradation

In dense 3D environments, cells switch to a mesenchymal-like migration based on protrusive and remodeling dynamics to overcome extracellular barriers that could, otherwise, impede cell migration [41, 321]. Cells generate tube-like geometries as they migrate through the ECM [160]. First, cell protrusions modify the ECM structure while expanding and contracting. Secondly, the cell body creates tracks while migrating through a dense 3D domain. Cells also cleave ECM collagen fibers by MMPs proteolytic activity. Even though MMPs are located all over the PM, the protrusive surface seems to have two differentiated subdomains—adhesive and proteolytic [556]. The former is located at the protrusive tip allowing cells to attach to the ECM, the latter along the shaft where ECM degradation occurs (Figure 5.6). Because of this proteolytic activity, ECM porosity increases—and ECM stiffness decreases accordingly—in the regions occupied by the cell and those nearby.

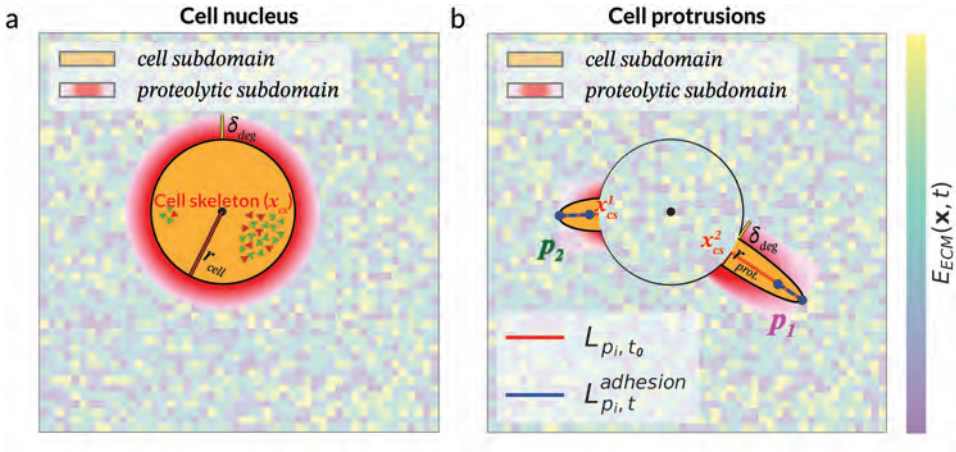

Figure 5.6: Two-dimensional representation of the ECM degradation model. A cell with two protrusions (p_1 and p_2) in which the center of the cell body is represented by a black circle. The protrusions' adhesive regions were depicted as blue dashes lines, and their boundaries as blue circles. The ECM was discretized and each squared region had an associated stiffness ($E_{ECM}(\boldsymbol{x}, t)$), represented as a colored square in the background. After a time interval, the ECM subdomain occupied by the cell ($d(\boldsymbol{x}, \boldsymbol{x_{cs}}) \leq r_{cell}$ in **(a)** and $d(\boldsymbol{x}, \boldsymbol{x_{cs}}) \leq r_{prot.}$ in **(b)**, in orange) would have a very low associated stiffness. For locations $\boldsymbol{x}$ closer to the central region of the cell, $r = r_{cell}$ **(a)**. For these locations, the proteolytic subdomain around the plasma membrane (PM) where MMPs are located and cleaving the ECM fibrilar network is delimited by $r' = r_{cell} + \delta_{deg}$. Conversely, locations $\boldsymbol{x}$ closer to one of cell's protrusions, $r = r_{prot.}$ **(b)**. In this case, the proteolytic subdomain surrounding the PM where MMP degradation activity occurs is delimited by $r' = r_{prot.} + \delta_{deg}$. These proteolytic subdomains were colored as red gradients. Note that the protrusion adhesive region does not degrade its surrounding microenvironment.

The stiffness variation on location $\boldsymbol{x}$ of the ECM domain because of degradation at time t was computed as:

$$\begin{aligned}
\frac{\partial E_{ECM}(\boldsymbol{x}, t)}{\partial t} &= \begin{cases} -K E_{ECM}(\boldsymbol{x}, t) & \text{if } d(\boldsymbol{x}, \boldsymbol{x_{cs}}) \leq r \\ -cl_{pm}(\boldsymbol{x}) v_{deg}(\boldsymbol{x}, t) & \text{if } r < d(\boldsymbol{x}, \boldsymbol{x_{cs}}) \leq r', \\ 0 & \text{otherwise} \end{cases} \\
cl_{pm}(\boldsymbol{x}) &= 1 - \frac{dist(\boldsymbol{x}, \boldsymbol{x_{pm}})}{\delta_{deg}}, \\
v_{deg}(\boldsymbol{x}, t) &= \alpha_{deg} \left(\frac{E_{ECM}(\boldsymbol{x}, t)}{E_{\mu}^{hydrogel}} \right)^{\beta_{deg}},
\end{aligned} \tag{5.8}$$

where $dist(\boldsymbol{x}, \boldsymbol{x_{cs}})$ is the distance from location $\boldsymbol{x}$ to the cell skeleton ($\boldsymbol{x_{cs}}$). Whenever $\boldsymbol{x}$ is closer to one of the cell's protrusions, r represents the radius of the protrusions section ($r_{prot.} = 3.5\,\mu m$). Conversely, when $\boldsymbol{x}$ is closer to the central region of the cell (represented as a sphere), r is the radius of this central region ($r_{cell} = 25\,\mu m$, based on experimental observations). $r'(= r + \delta_{deg})$ delimits the ECM

subdomain around the PM—where degradation occurs by MMPs proteolytic activity. We assumed a fixed δ_{deg}. K represents the mechanical damage rate generated by cells over the surrounding ECM as they migrate within the matrix generating tube-like geometries. We considered that locations occupied by the cell are matrix voids. Therefore, their stiffness was very low. $E_{ECM}(\boldsymbol{x}, t)$ is the stiffness in location $\boldsymbol{x}$ at time t. $cl_{pm}(\boldsymbol{x})$ assesses how close location $\boldsymbol{x}$ is from the PM ($cl_{pm}(\boldsymbol{x}) = 0$, if $\boldsymbol{x}$ is at the PM whereas $cl_{pm}(\boldsymbol{x}) = 1$, if $\boldsymbol{x}$ is at the frontier of the proteolytic subdomain). $v_{deg}(\boldsymbol{x}, t)$ determines the cell's degradation speed. $E_{\mu}^{hydrogel}$ represents the averaged stiffness of the microenvironment assessed by Valero and colleagues [171] based on the collagen concentration of the hydrogel where cells are embedded, and α_{deg} and β_{deg} are parameters regulating the MMPs cleave ratio. Matrix porosity increased—and ECM stiffness decreased accordingly—in those regions around the PM because of cells' proteolytic activity. Note that the stiffness of ECM locations in the proteolytic region ($r < d(\boldsymbol{x}, \boldsymbol{x_{cs}}) \leq r'$) did not decrease uniformly. Instead, the stiffness decreased more rapidly the closer these locations were to the PM (where MMPs locate) because of a diffusive phenomenon. The morphology of the cell body changed because of protrusions expansion and contraction. Hence, we updated the stiffness of the matrix surrounding the cell after computing the displacements of the nodes during the expansive and contractile stages.

5.2.7 Numerical implementation

This model was implemented in Python using powerful libraries such as NumPy [509], SciPy [510], and Scikit-learn [564] to maximize the performance of the model.

As in Chapter 4, we simulated the stochastic time evolution of this signaling network with the tau-leaping algorithm [513, 514]. This algorithm offers a good enough approximation (see Footnote 1 on page 81) [515, 516] of the exact solution given by the Stochastic Simulation Algorithm (SSA, also known as the Gillespie algorithm [511, 512]).

We computed the displacements of the cell nucleus and protrusive structures using the Direct Stiffness Method. Mechanical equations were numerically solved.

We modeled the ECM as a 3D matrix of voxels with 2 µm edges. As the cell migrate within the surrounding ECM, it modifies the stiffness of voxels that it occupies. Cells also reduce the stiffness of those regions close enough to be affected by cellular proteolytic activity, which degrades ECM fibers. Therefore, this proteolytic mechanism required to update the stiffness of up to hundreds of thousands of voxels per iteration. Consequently, the algorithm implementing this mechanism took advantage of the efficient management of arrays of NumPy

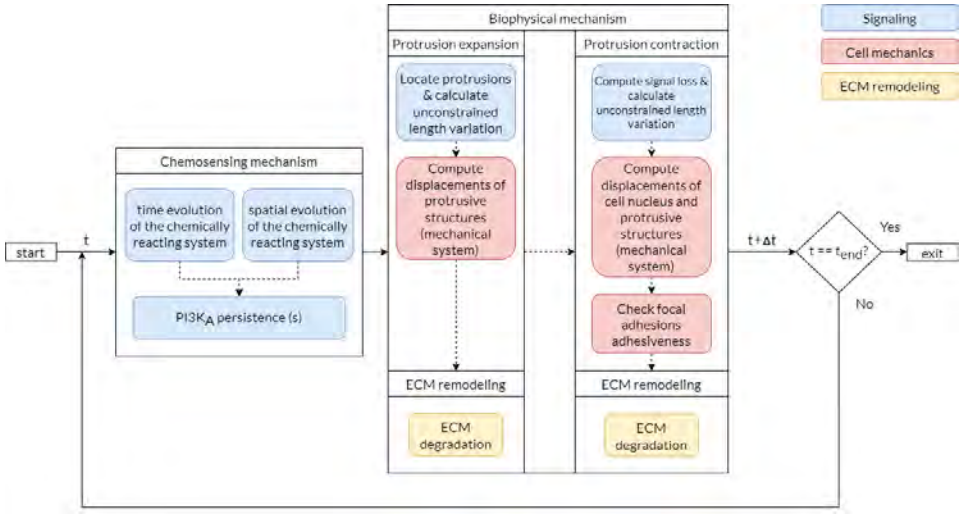

Figure 5.7: Global scheme of the proposed mathematical model of 3D cell migration. Every iteration of the main algorithm started by simulating the spatiotemporal evolution of the simplified signaling network associated to the chemosensing mechanism. The expansive stage began by determining protrusions locations and their stress-free (unconstrained) length variation based on the $PI3K_A$ persistence. Then, we computed the displacements of each protrusive structure of the defined mechanical system. This second stage finished updating the stiffness of the ECM subdomain surrounding the cell. The last stage of the main algorithm (i.e., the contractile one), started by computing the signal loss because of protrusions contraction and time wear at those locations. Next, we computed the displacements of the cell nucleus and each protrusive structure because of protrusions contraction. Afterward, we updated the stiffness of the ECM subdomain surrounding the cell. If we had already arrived at the end of the simulation (t_{end}), the algorithm finished. Otherwise, we began a new iteration of the main algorithm.

based on masks. To efficiently compute the distances from all those voxels to the cell skeleton, we used the k-dimensional trees (k-d trees) of Scikit-learn, which allows for k-nearest neighbors queries. Valero and colleagues [171] computed the averaged stiffness associated with ECMs with different collagen concentrations ($1.5\,\mathrm{mg\,mL^{-1}}$, $2.0\,\mathrm{mg\,mL^{-1}}$, $2.5\,\mathrm{mg\,mL^{-1}}$, $4.0\,\mathrm{mg\,mL^{-1}}$, and $6.0\,\mathrm{mg\,mL^{-1}}$). We used these experimental measurements to initialize this 3D matrix representing the stiffness of the different ECM subdomains. Afterward, we could compute the averaged stiffness of any region of interest (ROI) at time t—we selected 10-µm radius spherical elements to manage ROIs.

The simulation of the chemosensing mechanism was decoupled from the cell-matrix interactive mechanism as we were considering two different time scales [35, 381, 382]. Indeed, the chemical and physical phenomena occur at different time scales. To accurately simulate the proposed signaling network, we used the iterative tau-leaping algorithm with a variable time step of 0 5–1.5 s. Nevertheless,

to model the cell-matrix interactive mechanism, we used a different time step of 5 min. Besides, signal differences between two consecutive time steps were modest. In contrast, protrusions required more noticeable variations of the chemical signal to change their current state. As a result, we had to keep track of these cumulative variations in the chemical signal.

See Figure 5.7 for a global scheme of the proposed mathematical model of 3D cell migration.

5.2.8 Example of application

In this work, we developed a computational model able to simulate mesenchymal-like migration within 3D matrices under different mechanical conditions. To evaluate the predictive potential of this *in silico* model we replicated some previous *in vitro* experiments [507]. In particular, we simulated the experiments evaluating cellular behavior in response to hydrogels with different collagen concentrations, which consequently present distinct architectural properties (e.g., stiffness, porosity, pore size). In those experiments, Del Amo and colleagues [507] seeded NHDF cells in a 3D collagen matrix under step concentration gradients (Figure 5.8).

The authors used microfluidic chips with three symmetric and adjacent channels. As a result, they could tweak the mechanical properties of each channel separately. In particular, we were interested in those *in vitro* assays where each channel had a different stiffness (Figure 5.8): (i) assay with single-step gradient hydrogels, and collagen concentrations of $1.5\,\mathrm{mg\,mL^{-1}}$ (39.78 Pa), $2.0\,\mathrm{mg\,mL^{-1}}$ (119.56 Pa), and $2.5\,\mathrm{mg\,mL^{-1}}$ (185.18 Pa), respectively (*single assay*); and (ii) assay with double-step gradient hydrogels, and collagen concentrations of $2.0\,\mathrm{mg\,mL^{-1}}$ (119.56 Pa), $1.5\,\mathrm{mg\,mL^{-1}}$ (39.78 Pa), and $4.0\,\mathrm{mg\,mL^{-1}}$ (360.67 Pa), respectively (*double assay*). Thus, there was a stiffness interface between channels. Their results showed that, in the absence of chemical gradients, collagen concentration and mechanical interfaces did not bias the distribution of NHDF cells toward stiffer regions during the individual invasion experiment.

We assumed that voxels associated with each channel of the microfluidic device, which may contain a specific collagen concentration, initially present a fixed stiffness. For instance, all voxels associated with a channel containing a $1.5\,\mathrm{mg\,mL^{-1}}$ collagen concentration would initially present a 39.78 Pa stiffness.

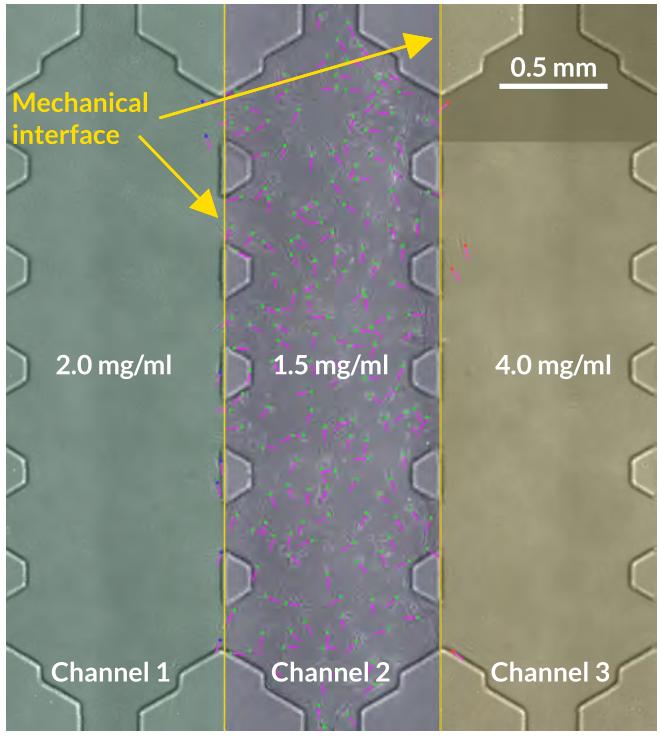

Figure 5.8: Initial distribution of Norman Human Dermal Fibroblast (NHDF) cultured in a microfluidic device with three different channels. Each channel may include collagen-based gels at different concentrations of collagen (e.g., 2.0 mg mL^{-1} in bottle green, 1.5 mg mL^{-1} in eggplant, and 4.0 mg mL^{-1} in mustard, respectively). Therefore, their associated stiffness may differ (e.g., 119.56 Pain bottle green, 39.78 Pa in eggplant, and 360.67 Pa in mustard, respectively). Yellow lines represent the channel boundaries (corresponding to collagen interfaces). Green dots represent centroids of cells located in the central channel. Conversely, the blue and red dots represent centroids of cells located in the lateral channels. Purple straight lines represent cell orientation. Images were captured with a Nikon D-Eclipse Microscope with a Plan Fluor 10x Objective. (Adapted from [507]).

5.3 Results

5.3.1 Fibroblasts do not durotax

First, we analyzed how cells sense and respond to different biophysical cues, such as ECM stiffness and pore size. In the considered *in vitro* assays, this would mainly happen at the mechanical interfaces between two channels. When cells get close enough to these mechanical interfaces, they may extend protrusions at both sides, which would allow them to attach to the different matrices and sense their biphysical differences. By initially locating cells in the different mechanical interfaces (i.e., in the interface between two channels, yellow lines in Figure 5.8) in our simulations, we focused on this phenomenon, right from the beginning. Thus,

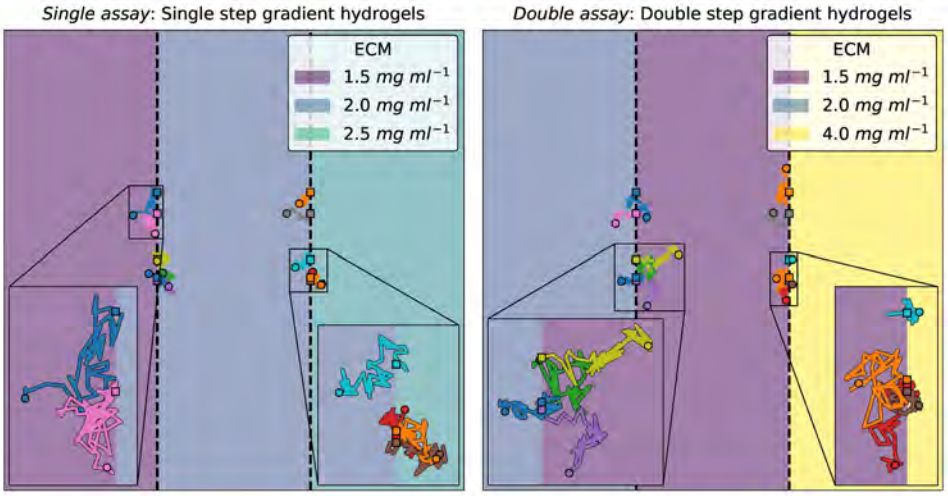

Figure 5.9: Cells trajectories over the three different channels of the microfluidic device used by Del Amo and colleagues [507], for the *in silico* model proposed in this work ($n = 12$). Cells' starting position is represented by squares whereas their final location is marked with circles. The ECM in each channel has different physical properties corresponding with different concentrations of collagen. Left: In the *single assay*, collagen concentrations were 1.5 mg mL^{-1}, 2.0 mg mL^{-1} and 2.5 mg mL^{-1}, respectively, with single step gradient hydrogels. Therefore, the associated stiffnesses would be 39.78 Pa, 119.56 Pa, and 185.18 Pa, respectively. Right: In the *double assay*, collagen concentrations were 2.0 mg mL^{-1}, 1.5 mg mL^{-1}, and 4.0 mg mL^{-1}, respectively, with double step gradient hydrogels. Hence, the associated stiffnesses would be 119.56 Pa, 39.78 Pa, and 360.67 Pa, respectively. We run simulations for 4 hours, with cells initially located at the interface between channels, using the base parametrization (see Table 5.1), with $\gamma_{fr} = 2.00$ and $E^{sq}_{ECM} = 25$ Pa.

we considered that simulating the first 4 hours of those *in vitro* assays, instead of the full 8 days, were enough for our specific interests.

We started by simulating the different scenarios (*single assay* and *double assay*, n = 12) described in Subsection 5.2.8 using the base parametrization (see Figure 5.9 and Table 5.1). For the *single assay* (with a single step gradient among the three channels, Figure 5.10 top), 66.7 % of the cells starting from the lower stiffness mechanical interface (between left and central channels) ended up in the channel with the lowest concentration of collagen (left channel, in purple, 1.5 mg mL^{-1} of collagen, 39.78 Pa, Figure 5.10 top). Conversely, 50 % of the cells starting from the stiffer mechanical interface (between the central and right channels) migrated toward the channel with an intermediate concentration of collagen (central channel, in blue, 2.0 mg mL^{-1} of collagen, 119.58 Pa, Figure 5.10 top). As a result, 33.3 % of all cells ended up in the channel with lowest collagen concentration (left channel, in purple, 1.5 mg mL^{-1} of collagen, 39.78 Pa, Figure 5.10 top), 41.7 %

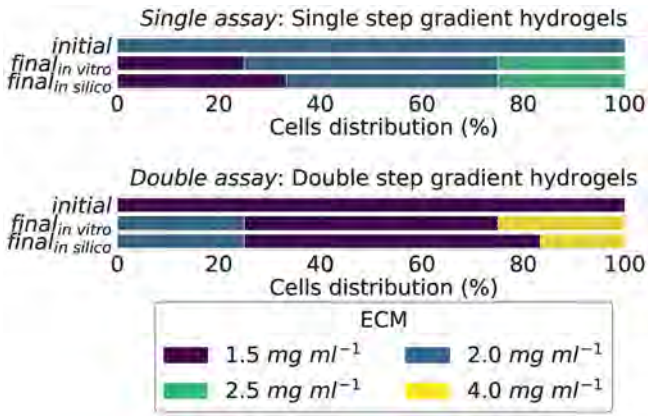

Figure 5.10: Cell distribution over the three different channels of the microfluidic device used in [507], for the *in vitro* model ($n \in [50, 100]$), and the *in silico* model ($n = 12$). The medium in each channel has different physical properties corresponding with different concentrations of collagen. Top: In the *single assay*, collagen concentrations were 1.5 mg mL^{-1}, 2.0 mg mL^{-1} and 2.5 mg mL^{-1}, respectively, with single step gradient hydrogels. Therefore, the associated stiffnesses would be 39.78 Pa, 119.56 Pa, and 185.18 Pa, respectively. Bottom: In the *double assay*, collagen concentrations were 2.0 mg mL^{-1}, 1.5 mg mL^{-1}, and 4.0 mg mL^{-1}, respectively, with double step gradient hydrogels. Hence, the associated stiffnesses would be 119.56 Pa, 39.78 Pa, and 360.67 Pa, respectively. We run simulations for 4 hours, with cells initially located at the interface between channels, using the base parametrization (see Table 5.1), with $\gamma_{fr} = 2.00$ and $E^{sq}_{ECM} = 25$ Pa.

in the channel with an intermedium collagen concentration (central channel, in blue, 2.0 mg mL^{-1} of collagen, 119.58 Pa), and 25.0 % in the channel with the highest collagen concentration (right channel, in green, 2.5 mg mL^{-1} of collagen, 185.18 Pa). For the *double assay* (with a double step gradient among the three channels, Figure 5.10 bottom), 50 % of the cells starting from the lower stiffness mechanical interface (between left and central channels) ended up in the channel with the lowest concentration of collagen (central channel, in purple, 1.5 mg mL^{-1} of collagen, 39.78 Pa, Figure 5.10 bottom). In contrast, 66.7 % of the cells starting from the stiffer mechanical interface (between central and right channels) migrated toward the channel with the lowest concentration of collagen (central channel, in purple, 1.5 mg mL^{-1} of collagen, 39.78 Pa, Figure 5.10 bottom). As a result, 58.3 % of all cells ended up in the channel with lowest collagen concentration (central channel, in purple, 1.5 mg mL^{-1} of collagen, 39.78 Pa, Figure 5.10 bottom), 25.0 % in the channel with an intermedium collagen concentration (left channel, in blue, 2.0 mg mL^{-1} of collagen, 119.58 Pa), and 16.7 % in the channel with the highest collagen concentration (right channel, in yellow, 4.0 mg mL^{-1} of collagen, 360.67 Pa). Together, these results showed that, in any of the simulated scenarios, cells exhibited a heterogeneous migratory pattern, with no clear bias based on collagen concentration or the architectural characteristics of the ECM.

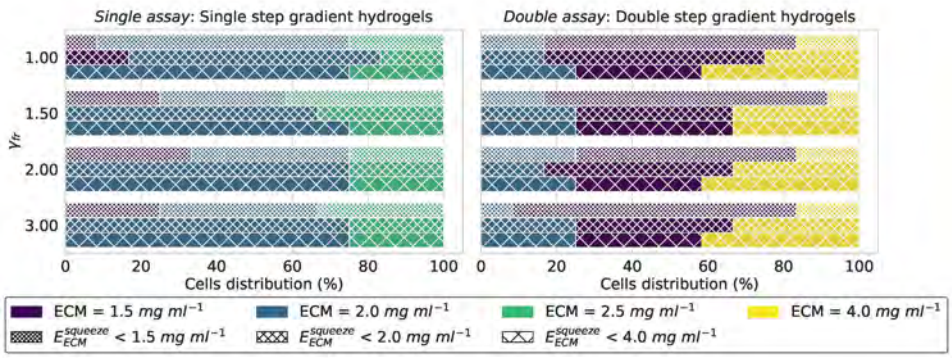

Figure 5.11: Final cell distribution over the three different channels of the microfluidic device used in [507], using the *in silico* model proposed in this work. The medium in each channel has different physical properties because the medium was polymerized with different concentrations of collagen. In the *single assay*, collagen concentrations were 1.5 mg mL^{-1}, 2.0 mg mL^{-1} and 2.5 mg mL^{-1}, respectively, with single step gradient hydrogels. Therefore, the associated stiffnesses would be 39.78 Pa, 119.56 Pa, and 185.18 Pa, respectively. In the *double assay*, collagen concentrations were 2.0 mg mL^{-1}, 1.5 mg mL^{-1}, and 4.0 mg mL^{-1}, respectively, with double step gradient hydrogels. Hence, the associated stiffnesses would be 119.56 Pa, 39.78 Pa, and 360.67 Pa, respectively. We run simulations for 4 hours, with cells initially located at the interface between channels, using different values of γ_{fr} (1.00, 1.50, 2.00, 3.00) and E_{ECM}^{sq} (25 Pa, 100 Pa, and 300 Pa). Note that $E_{ECM}^{sq} = 25$ Pa is below the stiffness associated with collagen-based hydrogels at 1.5 mg mL^{-1} of collagen (39.78 Pa), $E_{ECM}^{sq} = 100$ Pa is below the stiffness associated with collagen-based hydrogels at 2.0 mg mL^{-1} of collagen (119.56 Pa), and $E_{ECM}^{sq} = 300$ Pa is below the stiffness associated with collagen-based hydrogels at 4.0 mg mL^{-1} of collagen (360.67 Pa).

Table 5.1 includes the model's base parametrization used in 4-hour simulations, with cells initially located at the mechanical interfaces, to replicate some of the experimental observations from [507].

Overall, simulations managed to capture the general trends regarding cell distribution under these conditions (Figure 5.10). Both *in vitro* and *in silico* models exhibited a similar behavior regarding cell distribution throughout the three channels of the microfluidic device. In particular, most cells remain in the central channel, with a similar percentage of cells located in the lateral channels (50 % *in vitro* vs 58.3 % *in silico* for the *single assay* with single step gradient hydrogels, and 45 % *in vitro* vs 41.7 % *in silico* for the *double assay* with double step gradient hydrogels, Figure 5.10).

5.3.2 Steric hindrance hinders durotaxis

Next, we performed a sensitivity analysis focused on the parameters regulating the steric hindrance effect: (i) E_{ECM}^{sq} and (ii) γ_{fr}. Indeed, these parameters are

Parameter	Value	Equation	Range
α_{exp}	$8.81 \times 10^{-6}\,\mathrm{mm\,s^{-1}}$	(4.4) and (4.5)	$\mathbb{R} \in [0.01, 0.2]$
α_{deg}	$3.20 \times 10^{-4}\,\mathrm{Pa\,s^{-1}}$	(5.8)	$\mathbb{R} \in [10^{-5}, 10^{-3}]$
β_{exp}	62.46	(4.4) and (4.5)	$\mathbb{R} \in [0.1, 100]$
c	$1 \times 10^{-3}\,\mathrm{s^{-1}}$	(5.3)	$\mathbb{R} \in [10^{-4}, 10^{-2}]$
δ_{deg}	$8.9 \times 10^{-3}\,\mathrm{mm}$	(5.8)	$\mathbb{R} \in [0.001, 0.01]$
E_{p_i}	$1 \times 10^{3}\,\mathrm{Pa}$	(5.2) and (5.4)	$\mathbb{R} \in [10^{3}, 10^{7}]$
E^{sq}_{ECM}	$25\,\mathrm{Pa}$	(5.5)	$\mathbb{R} \in [25, 100, 300]$
γ_{fr}	2.00	(5.5)	$\mathbb{R} \in [1.25, 5.00]$
K	0.11	(5.8)	$\mathbb{R} \in [0.1, 0.4]$
s_{binary}	57.16×10^{3}		$\mathbb{R} \in [12.5, 212.5] \times 10^{3}$
s_{birth}	20.98	(4.4)	$\mathbb{R} \in [0.5, 100.0]$
s_{death}	5.77	(5.3)	$\mathbb{R} \in [0.5, 100.0]$
s_{growth}	15.45	(4.5)	$\mathbb{R} \in [0.5, 100.0]$
R_{min}	$1 \times 10^{-4}\,\mu\mathrm{N}$	(5.7)	$\mathbb{R} \in [10^{-4}, 10^{-3}]$
R_{max}	$0.085\,\mu\mathrm{N}$	(5.7)	$\mathbb{R} \in [0.01, 0.1]$

Table 5.1: Base parametrization for the proposed *in silico* model. The ranges associated to each parameter delimit the search space.

related to the ability of cells to squeeze themselves through ECM pores and migrate in such dense environments. As mentioned in Subsection 5.2.5, E^{sq}_{ECM} represents the minimum stiffness of the matrix for cells to struggle to squeeze their nuclei through narrow ECM pores. Higher values of E^{sq}_{ECM} would mean that cells migrate effortlessly through stiffer matrices. Therefore, the percentage of cells migrating toward stiffer regions should increase with higher values of E^{sq}_{ECM}. Note that for a fixed composition of collagen-based hydrogels, stiffer matrices are less porous and have narrower pores. For the *single assay* (with a single step gradient among the three channels), an $E^{sq}_{ECM} > 185.18\,\mathrm{Pa}$ meant that cells were always within ECMs with pores big enough for them to migrate effortlessly. In such scenarios ($E^{sq}_{ECM} = 300\,\mathrm{Pa}$ in Figure 5.11), most cells (75 %) migrated toward channels with higher concentrations of collagen, for all the values of γ_{fr} considered (1.00, 1.50, and 2.00). In contrast, an $E^{sq}_{ECM} < 39.78\,\mathrm{Pa}$ meant that cells were always within matrices with pores too narrow for an effortlessly migration. In this scenario ($E^{sq}_{ECM} = 25\,\mathrm{Pa}$ in Figure 5.11), all cells struggled to squeeze their nuclei while migrating through all channels, but at different degrees. Cells struggled less while migrating within the channel with lower collagen concentration (left channel, in purple, $1.5\,\mathrm{mg\,mL^{-1}}$, 39.78 Pa) than through the channel with higher collagen concentration (right channel, in green, $2.5\,\mathrm{mg\,mL^{-1}}$, 185.18 Pa, Figure 5.11). For the *double assay* (with a double step gradient among the three channels), an $E^{sq}_{ECM} > 360.67\,\mathrm{Pa}$ would mean that cells were always within matrices with pores big enough for them to

migrate effortlessly. Thus, in all simulated scenarios ($E^{sq}_{ECM} = \{25, 100, 300\}$ Pa in Figure 5.11), cells struggled to squeeze their nuclei through ECM pores, hindering their migration because of steric hindrance, at least in the channel with higher collagen concentration (right channel, in yellow, $4.0\,\mathrm{mg\,mL^{-1}}$, 360.67 Pa). In these cases, cells exhibited the same trend as in the *single assay* (with a single step gradient among the three channels), although a lower number of cells (≤ 66.7 %) migrated toward channels with higher concentrations of collagen (Figure 5.11).

γ_{fr} is another parameter that greatly influences the spatial distribution of cells in scenarios where matrices have different architectural properties. As γ_{fr} increases, so does the steric hindrance of the ECM encountered by cells, which more greatly hinders their migration. Hence, the number of cells migrating toward regions with higher concentrations of collagen should decrease. For example, we may focus on the *single assay*, with $E^{sq}_{ECM} = 25$ Pa. If $\gamma_{fr} = 1.00$, 33.3 % of the cells migrated toward regions with lower collagen concentrations (Figure 5.11). In contrast, if $\gamma_{fr} = 2.00$, 58.3 % of the cells migrated toward regions with lower collagen concentrations (Figure 5.11).

5.4 Conclusions

The proposed model builds upon an intracellular signaling network and a cell-matrix interactive mechanism based on cell mechanics and ECM degradation. These two building blocks have a leading role in 3D cell migration [41, 160, 321]. Furthermore, in this model, the local stiffness of the surrounding microenvironment influences cell mechanics. Indeed, the local stiffness of the surrounding ECM alters both the growth and retraction of cell protrusions and the cell nucleus translocation. In turn, ECM degradation dynamically changes the mechanical properties of the surrounding environment, reducing its stiffness and level of confinement. Matrix stiffness and confinement can influence migration speeds in 3D microenvironments [43, 146, 565]. We also included an approximation to the clutch model so that protrusions' adhesion to the ECM depends on their exerted contractile forces [272].

In our previous works [35, 382] (see Chapter 4), we considered protrusions analogous to an elastic inclusion (ellipsoid) embedded in the ECM and applied Eshelby's theory. We also assumed that the ECM was a continuous and homogeneous domain. Nonetheless, in this work, we introduced a new approximation to physically model how protrusions expand, contract, and retract based on deformable bars and springs. Additionally, we modeled the ECM as a heterogeneous entity. Furthermore, we included matrix degradation, which is considered an essential factor in 3D cell migration.

It is worth mentioning that Kim and colleagues [34] proposed an *in silico* model with shared features. For example, their computational model also considered the ECM as a heterogeneous entity. Furthermore, the authors modeled how cells integrate mechanical stimuli and how these external cues influence cell migration within 3D matrices. They also modeled matrix degradation by cellular proteolytic activity. Nonetheless, there are remarkable differences between their work and ours. Mainly, Kim and colleagues replicated experimental observations on flat surfaces where cells durotaxed [566]. They did not consider the effects associated with the steric hindrance of the ECM during cell motion, which may hinder durotaxis within 3D environments. Also, the complexity of their model, and therefore its computational requirements, greatly exceeds ours.

Cells change their mode of migration based on the physical and chemical properties of the surrounding ECM [41]. Carey and colleagues [567] reported that 3D type I collagen substrates promoted mesenchymal gene expression and an MT1-MMP-dependent invasive epithelial phenotype. Interestingly, this phenotype was sensitive to the architecture and mechanics of collagen-based matrices. In contrast, culture in 3D basement membrane (Matrigel) did not induce such a cellular response. More recently, Janmey and colleagues [146] also remarked that cells may change their stiffness based on the stiffness of the surrounding ECM.

The proposed model did not consider fiber alignment, which has been reported as a critical enabler of cancer dissemination [163, 568]. We assumed an isotropic distribution in each voxel of the 3D matrix representing the ECM. However, cells' ability to remodel the surrounding ECM affects fiber alignment [160]. Janmey and colleagues [146] recently noted that aligned fiber networks might be stiffer than unaligned matrix fibers. Therefore, further work is required to study how dynamic changes in the alignment of fibers by cells during their migration affect their migratory patterns.

The *in silico* model presented in this chapter considered that cells' cortical stiffness is associated with the rigidity of the surrounding environment, as suggested by independent works [559–563]. Likewise, Rianna and colleagues [569] showed that tumor cells soften during confined migration. However, other authors suggest that this long-established belief may be wrong [570]. Thus, future experimental works should try to confirm this new hypothesis, while prospective theoretical studies should consider this novel insight.

The presented model assumed a fixed ECM subdomain around the cell PM where the MMPs proteolytic activity occurs (defined by δ_{deg}). We opted for this assumption because we focused on migratory cells that do not stay at the same

location for long periods. Future works may consider establishing a dynamic proteolytic subdomain and analyze how this change impacts cells behavior.

In this work, we focused on the architectural properties of the surrounding matrix, initially established based on the ECM collagen concentration. Features such as ECM porosity and the pore size of the matrix are related to collagen concentration because matrices with high collagen concentrations usually exhibit narrow pores [270]. This was phenomenologically included in the proposed *in silico* model through the E^{sq}_{ECM} and γ^{fr} parameters. These features are linked to the inability of some cell types to migrate efficiently in dense microenvironments [160]. Matrix porosity is also modified during tumorigenesis by ECM synthesis and secretion as well as matrix-remodeling enzymes [43]. Consequently, future studies should further investigate how ECM porosity and the pore size of the matrix influence the migratory process.

Changes in membrane tension trigger different cellular responses to modulate cell surface area [135, 354]. For example, cells form and flatten PM folds to regulate membrane tension. As a result, cells are continuously remodeling their PM. However, the *in silico* model proposed in this work considered the cell membrane of the cell's central region containing its nucleus as the surface of a sphere with a fixed radius. Therefore, the volume of this central region remained fixed at $4.91\,\mathrm{mm}^3$. Protrusions, in contrast, were considered tube-like geometries with a steady cross-section but variable length. Therefore, the volume of the cell is not constant throughout our simulations. Indeed, as protrusions onset, grow, contract, and end up disappearing, their volume dynamically changes (around $3.85 \times 10^{-7}\,\mathrm{mm}^3$—$3.85 \times 10^{-5}\,\mathrm{mm}^3$). Still, we assumed this as a valid approximation for our purposes. Note that other authors did consider cell shape deformations [374, 406] at the cost of increasing the complexity of the proposed *in silico* models.

In 2D domains, cells can migrate toward the stiffer part of the substrate (a phenomenon known as durotaxis) [130]. Indeed, this durotactic behavior seems optimal within a given range of ECM stiffnesses [154, 571]. Still, as other authors pointed out [146, 394], factors such as pore size, porosity, fiber alignment, and matrix degradation regulate migration in 3D microenvironments [539, 572, 573]—even though they are not present or have less impact in 2D migration. Indeed, several authors have reported that 3D migration is impaired by steric hindrance [157, 352]. Nonetheless, cell response seems to depend on cell type and physiological or pathological conditions [146]. The proposed model replicated some of the observations associated with *in vitro* experiments of NHDF embedded in collagen-based matrices, in which durotaxis does not occur, probably because of steric hindrance. This was possible by including a friction term that opposes durotaxis

under specific conditions. In particular, this happens when ECM stiffness is high enough (and pore sizes low enough) that cells cannot squeeze their nuclei effortlessly through such narrow pores. As a result, these conditions hinder migration toward such confined environments. Without the E^{sq}_{ECM} and γ^{fr} parameters, associated with the ECM steric hindrance, our model always predicted a durotactic behavior (results not shown). Our model could replicate these experimental observations from Del Amo and colleagues [507] only by including these parameters. Notice that this behavior occurs even though cellular proteolytic activity is included in our model, which progressively reduces the stiffness of the surrounding environment (and increases the size of its pores accordingly).

Overall, the proposed model replicates some of the main hallmarks of mesenchymal-like migration within 3D matrices.

6

Toward a comprehensive knowledge of cell migration

Contents

6.1 Introduction

This chapter gathers together the main findings of the research carried out by the Ph.D. candidate during his doctoral studies. Section 6.2 outlines the results of the different research chapters (Chapter 3, Chapter 4, and Chapter 5). In particular, this section highlights how an integrative approach can result in a novel platform for rich, detailed, and multi-scale models that enable us to study and predict complex biological phenomena. Section 6.3 summarizes the implications for the field of cell biology in general and cell motility in particular. Next, Section 6.4 provides recommendations for further work, emphasizing potential enhancements for the integrative methodology and the *in silico* models presented in the previous chapters. Finally, Section 6.5 outlines the general conclusions of the studies included in this thesis.

6.2 Main achievements of the doctoral thesis

The research presented throughout this doctoral thesis investigated how different biochemical and biophysical stimuli influence cell migration within 3D matrices. Distinct building blocks were included in the *in silico* models to reveal the principles behind some of the main processes in cell migration, including intracellular signaling, cytoskeletal remodeling, nuclear displacement, and matrix degradation. The proposed *in silico* model predicted how chemical gradients of soluble ligands around cells bias their migratory patterns. More specifically, both the slope and the boundary concentrations (minimum and maximum) determined if cells followed a more directed or random trajectory. These building blocks also enabled the presented *in silico* model to predict different cellular responses to rigidity gradients within the surrounding ECM. In particular, cells durotaxed or exhibit an adurotactic behavior based on their nuclear phenotypes. Further, the proposed framework based on Bayesian optimization techniques greatly enhanced our ability to integrate experimental data with theoretical studies and computational models. The main contributions of the research carried out during the author's doctoral studies to test the hypotheses listed in Section 1.4 (Figure 6.1) are summarized below.

Research achievement 1
A fully automated workflow based on Bayesian optimization techniques promotes the integration of experimental data with *in silico* models.

The integrative framework based on Bayesian optimization techniques presented in Chapter 3 advances a synergistic research approach that couples experimental

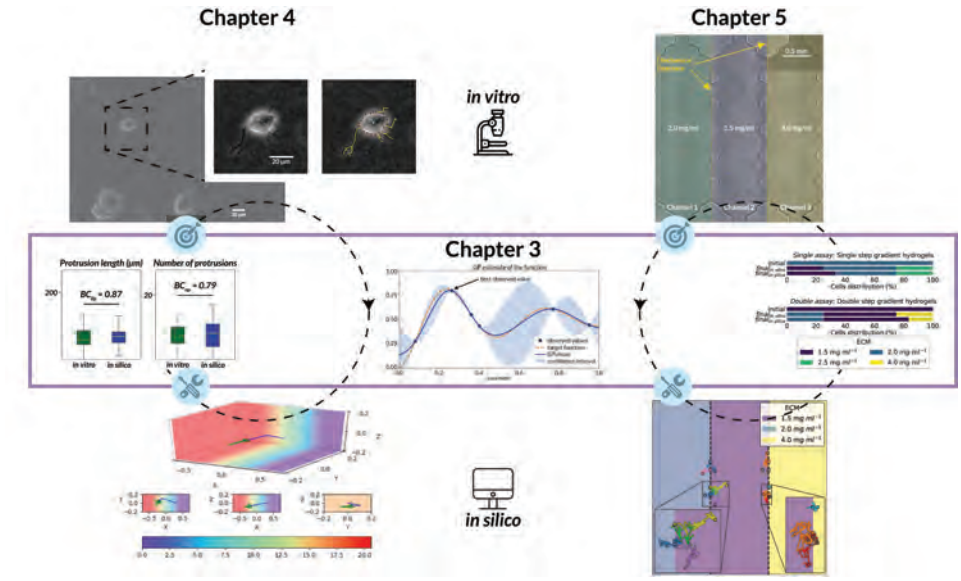

Figure 6.1: Illustration of the main results of this thesis An integrative methodology to investigate the migratory response of cells exhibiting a mesenchymal phenotype and cultured in 3D fibrous matrices to biochemical and biophysical stimuli.

data with theoretical studies and computational models. As a result, researchers can leverage the advantages of both disciplines. On the one hand, theoretical studies and computational models allow researchers to connect experimental results to first principles. They carry out very time-consuming, financially prohibited, and technically impossible experiments. On the other hand, experimental research enables us to form and test new or pre-existing hypotheses, validate theoretical predictions, and gather data for model calibration. Therefore, the proposed integrative framework is a valuable asset to acquire a comprehensive knowledge of complex phenomena such as cell migration.

Research achievement 2

A multi-scale *in silico* model coupling the spatiotemporal dynamics of intracellular signaling pathways with cytoskeletal and nuclear dynamics predicted cells' migratory response to different biochemical stimuli.

The multi-scale *in silico* model proposed in Chapter 4 predicted different migratory responses within 3D matrices to distinct biochemical stimuli. It demonstrated that both the slope of the chemical gradient and the chemoattractants concentrations influence cell motion. Cells tend to chemotax when surrounded by steep chemical gradients, whereas individual cells usually follow random trajectories when surrounded by shallow chemical gradients. However, cells may lose their

ability to chemotax when located in regions with very high concentrations of chemoattractants. Moreover, cells may exhibit different phenotypes based on the biochemical profile of the surrounding microenvironment. For instance, high PDGF concentrations enhance the proliferation of fibroblasts, whereas low PDGF concentrations promote their migratory response.

Research achievement 3

A multi-scale *in silico* model coupling cell-matrix adhesions with cytoskeletal and nuclear dynamics through mechanotransduction predicted cells' migratory response based on the biophysical profile of the surrounding matrix.

The expanded multi-scale *in silico* model emphasized how different biological processes, such as cell-matrix interactions and nuclear mechanics, lead to diverse migratory responses. In particular, it focused on how cells adapt and respond to matrix rigidity and porosity. Indeed, this multi-scale model predicted the regulatory role of cell nuclear deformability and the steric hindrance imposed by the surrounding ECM in the cells' ability to durotax.

Global achievement of the doctoral thesis

Clinical therapies to control cell motility *in vivo* and treat pathologies associated with aberrant cell migration requires a comprehensive knowledge of cell motion, which can only be acquired by integrating experimental data with theoretical studies and computational models. Understanding how local inhomogeneities in the surrounding microenvironment and intracellular dynamics regulate cells' migratory behaviors is fundamental for this endeavor.

Taken together, the results of this doctoral thesis highlight the importance of integrating experimental data with theoretical studies and computational models to acquire a comprehensive knowledge of complex phenomena. A novel framework was presented to lead this integrative endeavor. Also, these results highlight the fundamental role of multi-scale *in silico* models in unraveling the intricacies of cell migration. When investigating complex phenomena that involve different processes, events, and players, it is required not to consider isolated entities but interacting ones. When studying mesenchymal cell migration within 3D matrices, researchers must consider how intracellular signaling networks initiated by transmembrane receptors and adhesive complexes interact with the cytoskeletal components and the nuclear machinery. They also have to consider how cell-matrix interactions remodel the surrounding microenvironment. The proposed *in silico* model includes all these players and some of the main interactions driving the mesenchymal migratory behavior of individual cells.

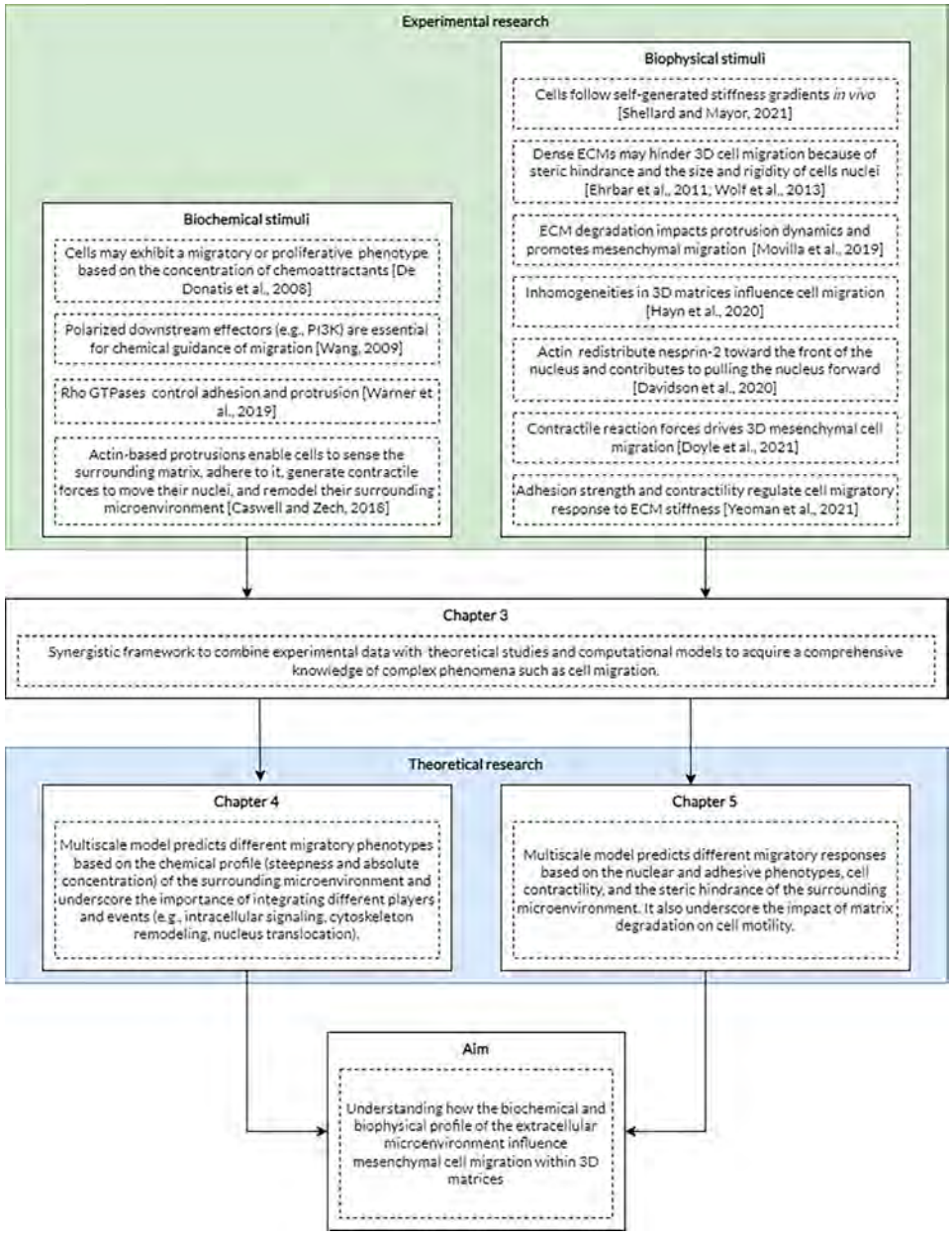

Figure 6.2: Implications for the field of cell migration Global scheme of the research carried out during the author's doctoral studies. The results and global aim of the research presented in throughout this doctoral thesis are highlighted in relation to the state-of-the-art of the field of cell migration.

6.3 Implications for the field of cell migration

Cell migration *in vivo* involves many different events, players, and processes. Some of them (e.g., cell-matrix adhesions, lamin A/C) only play an essential role in the migratory machinery of specific cell phenotypes (e.g., mesenchymal) or under particular conditions (e.g., dense matrices) [41, 45, 202]. Investigating cell migration within 3D microenvironments requires an integrative and multi-scale approach. Such an approach must include the different components involved in cell motility at different scales. It should also consider their interactions [215, 255, 574].

The research carried out by the author during his doctoral studies offers an integrative methodology and multi-scale *in silico* models that advanced the current understanding of cells' migratory response to biochemical and biophysical stimuli within 3D matrices (Figure 6.2).

Integration of experimental data with theoretical studies and computational models

Integrating experimental data with theoretical studies and computational models is fundamental for advancing scientific knowledge in many disciplines, including cell biology. Only such integration will enable us to acquire a comprehensive understanding of cell migration in the future.

The integrative methodology proposed in Chapter 3 promotes the collaborative efforts between experimentalists and theoreticians by integrating experimental data with theoretical studies and computational models. Furthermore, the predictive capabilities of the multi-scale *in silico* models presented in Chapter 4 and Chapter 5 resulted from applying the proposed methodology, which probes its suitability.

Biochemical stimuli influence cell behavior

Both the slope of the gradient and the absolute concentration of the chemoattractant determines cellular sensitivity to biochemical stimuli. For instance, De Donatis and colleagues [529] found that, in NIH3T3 fibroblasts, concentrations of PDGF as low as $1\,\mathrm{ng\,mL^{-1}}$ enabled a chemotactic behavior. Conversely, higher concentrations of PDGF ($> 5\,\mathrm{ng\,mL^{-1}}$) promoted a proliferative phenotype.

The *in silico* model proposed in Chapter 4 predicted a similar migratory response to gradients with different slopes and absolute concentrations of the chemoattractant. As a result, it emphasized the relevance of theoretical studies and computational models when investigating complex biological phenomena such as cell migration. Next, the reader will find a summary of the current (and still incomplete) knowledge

of how cells sense and respond to biochemical stimuli and the relevance of the research presented throughout this doctoral thesis.

Transmembrane receptors (e.g., RTKs and GPCRs) trigger signaling cascades that internalize external cues and enable cell migration guided by biochemical stimuli. Indeed, polarized downstream effectors such as PI3K are fundamental for chemical guidance [575]. Warner and colleagues recently reviewed our current understanding of the role of RhoGTPases in several processes associated with cell migration (e.g., lamellipodia and filopodia formation, cellular directionality, or stress fiber contractility). The authors also emphasized that some effectors (e.g., the Arp2/3 complex, PI3K) may be context-dependent. Indeed, they may not be a universal requirement for cell movement but only needed under specific conditions (i.e., specific cell phenotypes or within matrices with a particular composition). Likewise, Caswell and Zech [280] outlined the different roles of actin-based cell protrusions in migration and invasion within 3D matrices, acting as platforms for perceiving stimuli, adhering to the ECM, transmitting cell-matrix forces, and even remodeling the surrounding ECM.

The *in silico* model presented in Chapter 4 included a simplified version of the complex signaling networks involved in cell migration. Specifically, this computational model simulated how transmembrane receptors (e.g., RTKs and GPCRs) triggered intracellular signaling cascades after binding to chemoattractant molecules that promote actin-based protrusion formation and growth. These protrusive structures would exert RhoA-mediated contractile forces by actomyosin-based stress fibers. The LINC complex would, in turn, transmit these forces to the nucleus, resulting in its forward translocation. The results of Chapter 4 highlighted the importance of considering different actors, such as intracellular signaling, cytoskeleton remodeling, nuclear translocation, and their interactions when investigating cell migration.

Biophysical cues from the surrounding microenvironment influence cell migration

Historically, much attention has been paid to the impact of ECM stiffness on cell motility, especially on 2D substrates [69, 130, 566]. Interestingly, Shellard and Mayor [25] recently showed, for the first time, that durotaxis does occur *in vivo*. Wolf and colleagues [558] highlighted the importance of porosity and the size of ECM pores, as well as cells' ability to deform their nuclei when migrating within 3D matrices. In agreement with previous works [576], the authors also showed that in dense environments—where the steric hindrance of the ECM may impede migration—cells might depend on MMP-mediated matrix degradation to enlarge

narrow pores so they can squeeze their nuclei through them. Movilla and colleagues [381] further investigated the impact of ECM degradation on protrusion dynamics and cell migration. In particular, the authors showed a reduced migration speed and shorter cell protrusions in the presence of an MMP-inhibitor (Marimastat). Probably owing to cells' increased difficulty to deform the surrounding matrix and squeeze their nuclei through narrower pores. Still, matrix rigidity and pore size are not the only parameters characterizing the biophysical profile of the ECM. Hayn and colleagues [145] recently highlighted the relevance of the ECM structural inhomogeneities when investigating cell motility.

The *in silico* model proposed in Chapter 5 takes into account the stiffness, associated pore sizes, and inhomogeneities of collagen-based matrices to predict the migratory response of cells exhibiting a mesenchymal phenotype. Besides, the results presented in Chapter 5 highlight the influence of proteolytic activity, nuclear size, and deformability in cell migration. Altogether, the results from Chapter 5 emphasized the impact of proteolytic activity, both nucleus size and deformability, as well as matrix rigidity, pore size, and inhomogeneities on cell motion.

Independent works have investigated the biophysical mechanisms enabling force generation and transmission through the cell body from and to the surrounding ECM. Davidson and colleagues [324] showed that the actin cytoskeleton and myosin motors contribute to pulling the nucleus through narrow constrictions. Later on, Doyle and colleagues [350] demonstrated the existence of a dominant protrusion during mesenchymal motion through 3D matrices. This protrusion, which exerts the highest contractile reaction force over the surrounding ECM, drives the nucleus translocation and determines the migratory trajectory.

The *in silico* model proposed in Chapter 5 integrates these and other recent discoveries associated with mechanotransduction and force generation to investigate cell motion within 3D environments. As a result, it predicts different migratory responses of mesenchymal cells in 3D matrices depending on the biophysical profile of the ECM.

The seminal work of Zaman and colleagues [577] showed that 3D cell motion depends on multiple balances between integrin activity, adhesion ligand density, matrix rigidity, proteolytic activity, and steric hindrance. More recently, Yeoman and colleagues [273] demonstrated that adhesion strength and contractility regulate cells' migratory response to matrix rigidity. The authors saw that strongly adherent cells durotaxed while weakly adherent cells exhibited an adurotactic behavior. They also suggested that differences in intracellular actomyosin activity led to such distinct migratory behaviors.

Chapter 5 highlights the regulatory role of cells' ability to generate, distribute, and transmit mechanical forces over the different components of their body (e.g., cytoskeleton, nucleus) and to the surrounding environment.

6.4 Future lines of research

The research carried out by the Ph.D. candidate that resulted in this doctoral thesis provided a novel methodology to integrate experimental data with theoretical studies. It also presented an original *in silico* perspective to investigate the biological phenomenon of cell migration. As the scientific community proposes novel developments and presents new findings, the integrative framework and the *in silico* model introduced in this doctoral thesis could be extended. The integrative methodology could include other features and increase our knowledge of the principles regulating complex phenomena. The predictive potential of the proposed *in silico* model could be enhanced by considering additional possible scenarios (e.g., cells migrating through tracks or collectively via leader-follower dynamics) or by including new players or mechanisms (e.g., signaling molecules and proteins or nuclear deformability through lamins and chromatin). This section describes future lines of work to improve the integrative methodology presented in Chapter 3 and the *in silico* models proposed in Chapter 4 and Chapter 5. Also, this section suggests new approaches to overcome some of their current limitations.

6.4.1 Integrative methodology extension

Although the integrative methodology proposed in Chapter 3 already allows for a more tightly integration of experimental data with theoretical studies and computational models, several compelling ideas point toward different enhancements. For instance, multi-fidelity optimization could offer various sources of information with distinct levels of fidelity or accuracy [434]. Higher fidelity would give more accurate estimates of the fitting function but at a higher cost. Conversely, reduced fidelity would allow us to explore more regions of the parameter space but with lower accuracy.

Integrative methodology extension

A more feature-rich integrative methodology allowing for multi-fidelity enhances the integration of experimental data with *in silico* models.

6.4.2 Signaling model extension for case-specific applications

The *in silico* model presented in Chapter 4 and extended in Chapter 5 predicted different cellular migratory responses to biochemical and biophysical stimuli. The simplified signaling pathway included in this *in silico* model highlighted cells' sensitivity to the steepness of chemical gradients and the absolute concentration of

chemoattractants, which is particularly relevant when investigating physiological and pathological conditions (e.g., embryonic development, immune response, angiogenesis in cancer). Different intracellular signaling pathways play a crucial regulatory role in cell migration. For example, they modulate the internalization of external stimuli. These signaling pathways also influence cellular dynamics, from cell-matrix and cell-cell interactions to cytoskeletal and nuclear dynamics [178, 205, 206, 218]. Therefore, future studies should further investigate the impact of different signaling networks, such as Hippo [578, 579], Src/FAK [580–583], and TGFβ/PI3K/AKT [584–586], in cell migration.

Simulating the spatiotemporal evolution of the signaling model is the main bottleneck of the presented *in silico* models and one of the challenges signaling modelers are currently facing [587]. On the one hand, the tau-leaping algorithm [513, 514] enabled us to estimate the temporal evolution of the simplified signaling pathway included in the proposed *in silico* models. On the other hand, the Inverse Method described by Saltzman and colleagues [499] equipped these models with spatial resolution. Still, these methods were computationally intensive. The stochastic nature of the associated biological phenomenon amplifies this issue by requiring running batches of several simulations to get an accurate view of how cells behave in each specific scenario. Therefore, I consider of great interest to replace the current spatial model of the signaling network in 3D. In this regard, I find particularly relevant the work from Coulier, Hellander, and Hellander [588] proposing a multi-scale model where a compartment-based model approximates a detailed spatial stochastic model. Likewise, Hellander and Hellander [589] coupled mesoscopic simulations on meshes with different levels of granularity.

A more efficient spatial framework would enable the inclusion of an extended signaling network in these *in silico* models. For example, the signaling pathway could include biophysical factors as initiators or modulators of different processes involved in cell migration. I am especially interested in some of the published results [264] from the Reinhart-King lab at Vanderbilt University, where authors show that local ECM alignment directs cellular protrusion dynamics and migration through Rac1 and FAK. Still, many other factors involved in different signaling pathways may influence cell migration. For instance, mechanical cues exerted by the ECM, cell-matrix, and cell-cell adhesion complexes regulate metabolic pathways [574] and cytoskeletal activity [106, 287]. Notably, the cytoskeleton also modulates signaling pathways [590]. Extracellular signal-regulated kinases (ERK) play a relevant role in signaling events that regulate cell migration. For one, ERK modulates the rate and polarity of actin polymerization, regulating lamellipodia formation [591]. Also, ERK activation coordinates long-distance transmission of directional cues,

enabling collective cell polarization [592]. The Scar/WAVE complex is another player involved in pseudopod and lamellipodia formation, evolution, lifetime, and stability [263, 593–595]. Notably, forces generated by individual actin filaments mechanically control the dynamics of the WAVE complex [593].

Signaling model extension for case-specific applications

An efficient simulation of the spatiotemporal evolution of complex signaling networks in 3D remains one of the current challenges for signaling modelers. Given the impact of signaling cascades on a myriad of processes involved in cell migration, rich, detailed, and multi-scale models of cell motility should include extended signaling pathways. Based on the scenario(s) of interest, different biochemical and biophysical factors, as well as distinct downstream effectors, should be included. Simulating these extended signaling networks would only be feasible through efficient spatial models.

6.4.3 A more accurate *in silico* replica of the extracellular matrix

An accurate *in silico* replica of the ECM is essential to predict cell response in any specific scenario [39, 75, 142, 146, 160]. For one, the composition and microarchitecture of the ECM are widely variable among tissues [143, 552]. Mak [347] recently studied the impact of crosslink heterogeneity on ECM mechanics and remodeling. Also, Hayn and colleagues [145] highlighted the influence of local matrix inhomogeneity in cell migration. The physical cues in the tumor microenvironment have also been recognized as new hallmarks of cancer [342, 596]. Therefore, continuing our efforts to more accurately replicate *in silico* the surrounding microenvironment is another promising line of work.

Previous works from our lab and other groups have already made significant progress. For example, Olivares and colleagues [270] proposed an automated tool to reconstruct 3D collagen networks. Complementary tools to artificially generate matrices and tweak their biophysical properties (e.g., fiber alignment, pore size, or crosslinking) would also enable further studies on their impact on cell migration either in isolation or in combination with each other. These tools would also be valuable when modeling the aforementioned mechanisms studied by the Reinhart-King Lab, where the alignment of ECM fibers modulates cellular protrusion dynamics and migration [264]. They could also enable us to more accurately study the role of the cell nucleus in cell motility and the impact of ECM pore sizes and viscoelasticity in this biological phenomenon [322, 323]. In particular, when cells migrate within dense matrices, which may require them to squeeze their nucleus through narrow pores.

Modeling the entire *in vitro* domain (i.e., the geometry of the whole microchip) with high resolution represents another challenge for these *in silico* models. Using sparse 3D matrices to model these ECMs may be a suitable option, although initial efforts on this matter did not succeed. Still, a more concentrated effort may result in a different outcome.

Cells must quickly sense and adapt to the specific profile of the surrounding ECM to move and migrate through complex 3D environments. Therefore, an accurate replica of the *in vitro* and *in vivo* ECM is essential for a comprehensive understanding of cell migration.

A more accurate *in silico* replica of the extracellular matrix

An extended and enhanced *in silico* model of the ECM would drastically improve the predictive potential of the proposed computational models of 3D cell migration. Relevant models of cell motion must recapitulate the heterogeneity and complexity of the local microenvironment. The inclusion of distinct biochemical (soluble or surface-bound) and biophysical cues (e.g., stiffness, viscoelasticity, pore size, and fiber alignment) would enhance the predictive capabilities of the presented *in silico* models.

6.4.4 From individual migrants to migrating collectives

Collective cell migration is essential for organ formation, tissue regeneration, and wound healing. For instance, neural crest cells collectively migrate in embryos. During wound healing, sheets of epithelial cells move together as a unit. Unfortunately, it may also participate in many pathological processes. For example, cancer cells may collectively escape from the primary tumor and into a blood vessel and lymphatics [597–599]. Interestingly, cells migrate faster and more directionally in groups than as isolated individuals [130, 600, 601]. In cell collectives, the behavior of any individual cell depends on those connected, directly or indirectly, to it. As a result, cells migrate cooperatively and coordinately. Thus, extending the proposed *in silico* model by including cell-cell adhesions and other mechanisms involved in collective cell migration (e.g., contractile actin cables that appear across neighboring cells) would be of great interest.

During collective migration, each cell has its own identity but communicates with the rest of the group. The evolution of each cell could be simulated by individual processes, as in our current *in silico* model. Still, every cell must have an open communication channel. This modeling approach would take advantage of the computational resources available in HPC environments and their ability to distribute the execution of individual jobs over many different computing nodes at the same time.

From individual migrants to migrating collectives

Extending the proposed *in silico* models by including cell-cell interactions and other mechanisms involved in collective cell migration would enable the simulation of cells migrating in groups. As a result, these computational models would allow for a comprehensive knowledge of varied physiological and pathological phenomena, such as organ formation, tissue regeneration, and metastasis.

6.5 General conclusions

After more than a century investigating cell migration [602–606], we still lack a comprehensive knowledge of this critical phenomenon for life and development. Many questions about the activity and heterogeneous nature of the different actors involved in cell motion are still unanswered [607–610]. We are just beginning to uncover how cells perceive and internalize spatiotemporal information from their surroundings through distinct sensitivities of the cellular mechanosensors and their underlying transduction mechanisms [213, 611, 612]. Furthermore, technical limitations have hindered an in-depth investigation of other regulators of cell motility, such as cell metabolism [106, 215, 613, 614], cellular and ECM mechanical properties (e.g., viscoelasticity) [75, 78, 146, 615]. The collaborative effort of an army of specialists, including theoreticians and experimentalists, will be essential to uncover these mysteries.

The research community must several challenges to acquire novel and relevant knowledge of cell motion. Stark differences between 2D and 3D systems require the translation of studies to 3D *in vivo* scenarios [218], which may uncover distinct cellular behaviors [147, 616]. An interest in complex phenomena, including nonlinear responses [79, 552], feedback loops [617–619], competition between distinct components [249], and context-dependent responses [173, 620, 621], has recently emerged. This interest may uncover behaviors that would only arise from such complexity [255]. It is also imperative to study components at different scales and the interactions between multiple actors [309, 552, 622, 623], which will require novel quantitative tools [624–629] and more sophisticated experimental models [316, 630, 631].

The author's doctoral studies aimed to improve our knowledge of how biochemical and biophysical stimuli from the surrounding environment influence the migratory response of mesenchymal cells. The author undertook this endeavor from a theoretical perspective, developing *in silico* models of mesenchymal cells migrating within 3D matrices. Cells exhibiting a mesenchymal phenotype adopt an elongated morphology dependent on integrin-mediated cell-matrix adhesions and the presence

of high traction forces on both cell poles. In this context, cells develop protrusions, pushing the surrounding matrix and pulling themselves forward, squeezing their nuclei through the pores. Mesenchymal cells rely on surface proteases to digest and remodel the ECM. External cues from the surrounding microenvironment may bias the migratory behavior of these cells.

Experimental and theoretical studies complement each other, and their integration allows researchers to overcome many of their corresponding limitations. As a result, the convergence of both disciplines through integrative methodologies leads to a comprehensive knowledge of cell migration.

To facilitate the integration of experimental data with theoretical studies, an autonomous methodology based on Bayesian optimization techniques was proposed in Chapter 3, where I outlined the basis of this framework. Chapter 4 proved the suitability of this integrative methodology for calibrating *in silico* models by automating the whole process. Note that the calibration process has historically required frequent user interaction, making it error-prone. By using principles of statistical inference and decision theory, Bayesian optimization efficiently finds the global optimum of expensive-to-evaluate objective functions. In our case, this refers to computationally intensive models that take more than just a few minutes to run. Accordingly, Chapter 4 showcased how the proposed methodology facilitates the evaluation and enhancement of the accuracy and predictive capabilities of *in silico* models.

To increase our understanding of how biochemical stimuli influence cell migration within 3D matrices, an *in silico* model was proposed in Chapter 4. The signaling network that allows cells to internalize such external cues was recreated through a simplified signaling pathway. Downstream effectors of such signaling cascade regulate protrusion dynamics (i.e., formation, growth, and retraction). Consequently, the biochemical profile of the surrounding ECM modulates cells' migratory speed and trajectory. The modeling efforts were focused on restraining the computational requirements without any relevant loss in accuracy. Also, this was the first example of application for the proposed integrative methodology. By modeling intracellular signaling networks, cytoskeletal dynamics, and the interaction between them, this *in silico* model predicted different migratory responses based on the biochemical profile (gradient steepness and absolute concentration of the chemoattractant) of the surrounding matrix.

To better understand the impact of the biophysical stimuli on cell motility, the aforementioned *in silico* model was extended in Chapter 5. In this case, the focus was on the mechanosensing mechanism enabling cells to probe the biophysical profile of the surrounding ECM. As a result, a more detailed replica of the local

microenvironment was proposed, which allowed for a more accurate representation of cell mechanics. In particular, the modeling efforts aimed to investigate the role of matrix stiffness in protrusions growth and contraction and thus, in cells' migratory speed and trajectory. Contrary to what has been observed in 2D substrates, this computational model predicts a migratory behavior where the steric hindrance of 3D matrices hinders durotaxis. Hence, this extended *in silico* model would serve as a valuable framework to further investigate how different biophysical properties such as the microarchitecture of the ECM modulate cell motion within the more physiologically relevant 3D environments.

Overall, this doctoral thesis offers an integrative perspective to investigate the impact of different stimuli in cell migration within 3D environments. Specifically, the Ph.D. candidate integrates experimental data with advanced theoretical and computational techniques to evaluate distinct but relevant players and events involved in cell motion through 3D matrices. A novel methodology based on Bayesian optimization probed its suitability for integrating experimental data with theoretical studies, automating the calibration of *in silico* models. A hybrid modeling approach predicted different migratory behaviors based on the biochemical profile of the local environment. An extended version of this system exhibited a durotactic behavior if it did not consider the steric hindrance of 3D matrices nor the molecular clutch dynamics controlling cell mechanotransduction. Otherwise, the proposed *in silico* model could predict the lack of durotaxis in specific 3D environments. The integrative research methodology proposed in this doctoral thesis represents an innovative approach to improve our knowledge of many fields, including cell biology and migration. Moreover, the *in silico* modeling techniques serve as valuable assets to understand how distinct external cues from the local environment regulate cell motion. Future strategies could rely on these tools to advance our knowledge toward a comprehensive understanding of cell migration.

6.6 Conclusiones generales (General conclusions in Spanish)

Tras más de un siglo investigando la migración celular [602–606], todavía carecemos de un conocimiento exhaustivo de este fenómeno crítico para la vida y el desarrollo. Muchas preguntas sobre la actividad y la naturaleza heterogénea de los diferentes actores involucrados en el movimiento celular siguen sin respuesta [607, 608, 610]. Apenas estamos comenzando a descubrir cómo las células perciben e internalizan la información espaciotemporal de su entorno a través de distintas sensibilidades de los mecanosensores celulares y sus mecanismos de transducción subyacentes [213,

611, 612]. Además, las limitaciones técnicas han impedido una investigación en profundidad de otros reguladores de la motilidad celular, como el metabolismo celular [106, 215, 613, 614], o las propiedades mecánicas de la célula y de la matriz extracelular (p. ej., viscoelasticidad) [75, 78, 146, 615]. El esfuerzo colaborativo de un ejército de especialistas, incluidos teóricos y experimentadores, será fundamental para descubrir estos misterios.

La comunidad científica debe enfrentarse a varios desafíos para adquirir conocimientos novedosos y relevantes sobre el movimiento celular. Las marcadas diferencias entre los sistemas 2D y 3D requieren la traducción de los estudios a escenarios *in vivo* 3D [218], lo que puede desvelar comportamientos celulares distintos [147, 616]. Recientemente ha surgido un interés por los fenómenos complejos, incluidas las respuestas no lineales [79, 552], los bucles de retroalimentación [617–619], la competencia entre distintos componentes [249] y las respuestas dependientes del contexto [620, 621]. Este interés puede descubrir comportamientos que solo surgirían de dicha complejidad [255]. También es imperativo estudiar los componentes a diferentes escalas y las interacciones entre múltiples actores [309, 552, 622], lo que requerirá nuevas herramientas cuantitativas [624–629] y modelos experimentales más sofisticados [316, 630].

Los estudios de doctorado del autor tuvieron como objetivo mejorar el conocimiento de cómo los estímulos bioquímicos y biofísicos del entorno circundante influyen en la respuesta migratoria de las células mesenquimales. El autor emprendió este esfuerzo desde una perspectiva teórica, desarrollando modelos *in silico* de células mesenquimales que migran dentro de matrices 3D. Las células que exhiben un fenotipo mesenquimal adoptan una morfología alargada que depende de las adhesiones a la matriz extracelular a través de las integrinas y de la presencia de altas fuerzas de tracción en ambos polos celulares. En este contexto, las células desarrollan protrusiones, empujando la matriz circundante y tirando de sí mismas hacia adelante, apretujando sus núcleos a través de los poros. Las células mesenquimales dependen de las metaloproteinasas de matriz para digerir y remodelar la matriz extracelular. Las señales externas del microambiente circundante pueden sesgar el comportamiento migratorio de estas células. Los estudios experimentales y teóricos se complementan y su integración permite a los investigadores superar muchas de sus limitaciones correspondientes. Como resultado, la convergencia de ambas disciplinas a través de metodologías integradoras conduce a un conocimiento integral de la migración celular.

Para facilitar la integración de datos experimentales con estudios teóricos, en el Capítulo 3 se propuso una metodología autónoma basada en técnicas de optimización Bayesianas, donde se describen las bases de este marco. El Capítulo 4 demostró la

idoneidad de esta metodología integradora para calibrar modelos *in silico* mediante la automatización de todo el proceso. Tenga en cuenta que históricamente el proceso de calibración ha requerido una interacción frecuente del usuario, lo que lo hace propenso a errores. Mediante el uso de principios de inferencia estadística y teoría de decisiones, la optimización Bayesiana encuentra de manera eficiente el óptimo global de funciones objetivas costosas de evaluar. En nuestro caso, se trata de modelos computacionalmente intensivos que tardan más de unos minutos en ejecutarse. En consecuencia, el Capítulo 4 mostró cómo la metodología propuesta facilita la evaluación y mejora la precisión y las capacidades predictivas de los modelos *in silico*.

Para aumentar nuestra comprensión de cómo los estímulos bioquímicos influyen en la migración celular dentro de matrices 3D, se propuso un modelo *in silico* en el Capítulo 4. La red de señalización que permite a las células internalizar dichas señales externas se recreó a través de una vía de señalización simplificada. Los sucesivos efectores en dicha cascada de señalización regulan la dinámica de protrusión (es decir, su formación, crecimiento y retracción). En consecuencia, el perfil bioquímico de la matriz extracelular circundante modula la velocidad y la trayectoria migratoria de las células. Los esfuerzos de modelado se centraron en restringir los requisitos computacionales sin ninguna pérdida relevante en la precisión. Además, este fue el primer ejemplo de aplicación de la metodología integradora propuesta. Al modelar las redes de señalización intracelular, la dinámica del citoesqueleto y la interacción entre ellas, este modelo *in silico* predijo diferentes respuestas migratorias basadas en el perfil bioquímico (inclinación del gradiente y concentración absoluta del factor químico) de la matriz circundante.

Para comprender mejor el impacto de los estímulos biofísicos en la movilidad celular, el modelo *in silico* antes mencionado se amplió en el Capítulo 5. En este caso, la atención se centró en el mecanismo de detección mecánica que permite a las células percibir el perfil biofísico de la matriz extracelular circundante. Como resultado, se propuso una réplica más detallada del microambiente local, lo que permitió una representación más precisa de la mecánica celular. En particular, los esfuerzos de modelado tenían como objetivo investigar el papel de la rigidez de la matriz en el crecimiento y la contracción de las protrusiones y, por lo tanto, en la velocidad y trayectoria migratoria de las células. Al contrario de lo que se ha observado en sustratos 2D, este modelo computacional predice un comportamiento migratorio donde el impedimento estérico de las matrices 3D dificulta la durotaxis. Por lo tanto, este modelo *in silico* extendido serviría como un sistema valioso para investigar más a fondo cómo las diferentes propiedades biofísicas, como por ejemplo la microarquitectura de la matriz extracelular, modulan el movimiento celular dentro de los entornos 3D fisiológicamente más relevantes.

En general, esta tesis doctoral ofrece una perspectiva integradora para investigar el impacto de diferentes estímulos en la migración celular dentro de entornos 3D. Específicamente, el candidato a doctor ha integrado datos experimentales con técnicas teóricas y computacionales avanzadas para evaluar diferentes jugadores y eventos de relevancia involucrados en el movimiento celular a través de matrices 3D. Una metodología novedosa basada en la optimización Bayesiana probó su idoneidad para integrar datos experimentales con estudios teóricos, automatizando la calibración de modelos *in silico*. Un enfoque de modelado híbrido predijo diferentes comportamientos migratorios en función del perfil bioquímico del entorno local. Una versión extendida de este sistema exhibió un comportamiento durotáctico si no consideraba el impedimento estérico de las matrices 3D ni la dinámica del embrague molecular que controla la mecanotransducción celular. De lo contrario, el modelo *in silico* propuesto podría predecir la falta de durotaxis en entornos 3D específicos. La metodología de investigación integradora propuesta en esta tesis doctoral representa un enfoque innovador para mejorar nuestro conocimiento en muchos campos, incluida la biología y la migración celular. Además, las técnicas de modelado *in silico* sirven como activos valiosos para comprender cómo las distintas señales externas del entorno local regulan el movimiento celular. Las estrategias futuras podrían basarse en estas herramientas para avanzar en nuestro conocimiento hacia una comprensión integral de la migración celular.

Appendices

A

Variables for modeling cell migration biased by biophysical cues

Table A.1 includes the variables used in the *in silico* model presented in Chapter 5 and their descriptions.

Table A.1: The model's variables.

Symbol	Description
p_i	i-th protrusion
$d_{\mathrm{PI3K_A}}$	Distribution of $\mathrm{PI3K_A}$ across the cell surface
$g(\phi, \theta)$	Convolution window approximately the size of a protrusion section
s_{p_i}	$\mathrm{PI3K_A}$ spatio-temporal persistence at the location of the i-th protrusion
α_{exp} and β_{exp}	Parameters regulating protrusion expansion
$\frac{\partial s_{p_i}(t)}{\partial t}$	Time variation of s at the location of the i-th protrusion
s_{birth}, s_{growth} and s_{death}	Parameters regulating protrusion onset, growth, and complete retraction
$\frac{\partial L_{p_i}^{free}(s_{p_i},t)}{\partial t}\Big\vert_{exp}$	Unconstrained length variation of the i-th protrusion during its expansion at time t
$\frac{\partial L_{p_i}^{free}(s_{p_i},t)}{\partial t}\Big\vert_{birth}$	Unconstrained length variation of the i-th protrusion during its expansion for new protrusions at time t
$\frac{\partial L_{p_i}^{free}(s_{p_i},t)}{\partial t}\Big\vert_{growth}$	Unconstrained length variation of the i-th protrusion during its expansion for pre-existing protrusions at time t
c	Parameter regulating protrusion contraction

Continued on next page

Table A.1—continued from previous page

Symbol	Description
$L_{p_i}^{con}(s_{p_i}, t)$	Protrusions length at the beginning of its contractile stage at time t
$\frac{\partial L_{p_i}^{free}(s_{p_i},t)}{\partial t}\Big\vert_{con}$	Unconstrained length variation of the i-th protrusion during its contraction at time t
$\frac{\partial \boldsymbol{F}_{p_i}^{exp}(t)}{\partial t}$	Time variation of the expansive forces applied to the structural nodes at time t
E_{p_i}	Protrusions stiffness
A	Area of the section of the protrusions
$L_{p_i}^{exp}(s_{p_i}, t)$	Protrusions length at the beginning of its expansive stage at time t
$\boldsymbol{e}_i$	Unit vector in the direction of the longitudinal axis of the i-th protrusion
$\frac{\partial F_{p_i}^{con}(t)}{\partial t}$	Time variation of the contractile forces applied to the structural nodes at time t
μ	Friction term
$\boldsymbol{x}_{p_i}^{sh}$	Position of the shaft of the i-th protrusion
$E_{ECM}(\boldsymbol{x}_{p_i}^{sh}, t)$	ECM stiffness at the location of the shaft of the i-th protrusion at time t
E_{ECM}^{sq}	Rigidity threshold
γ_{fr}	Friction coefficient
$\boldsymbol{R}_{p_i}(t)$	Reaction forces generated by the i-th protrusion at time t
$\boldsymbol{x}_{p_i}^{tip}$	Position of the tip of the i-th protrusion
$E_{ECM}(\boldsymbol{x}_{p_i}^{tip}, t)$	ECM stiffness at the location of the tip of the i-th protrusion and time t
$L_{p_i}^{con,adh}(t)$	Length of the adhesion region of the i-th protrusion at the beginning of the contractile stage at time t
$\boldsymbol{u}^{p_i}(t)$	Displacement vector of the structural node located at the tip of the i-th protrusion
$p_i^{\text{attached}}(t)$	Adhesiveness of the i-th protrusion at time t
R_{min} and R_{max}	Lower and upper boundaries of the active region associated with the clutch model
$\frac{\partial E_{ECM}(\boldsymbol{x},t)}{\partial t}$	Time variation of the ECM stiffness at location $\boldsymbol{x}$ and time t
K	Mechanical damage associated with the matrix degradation as MMPs digest ECM proteins
$\boldsymbol{x_{cs}}$	Location of the cell skeleton
$d(\boldsymbol{x}, \boldsymbol{x_{cs}})$	Distance from location $\boldsymbol{x}$ to the cell skeleton ($\boldsymbol{x_{cs}}$)
r	Radius of the protrusions section or the central region of the cell (represented as a sphere)
$cl(\boldsymbol{x}, \boldsymbol{x_{cs}})$	Closeness from location $\boldsymbol{x}$ to location $\boldsymbol{x_{cs}}$
δ_{deg}	Delimits the ECM region where MMPs proteolytic activity occurs
α_{deg} and β_{deg}	Degradation coefficients

Continued on next page

Table A.1—continued from previous page

Symbol	Description
$E_{\mu}^{hydrogel}$	Averaged ECM stiffness assessed by Valero and colleagues [171] based on the collagen concentration of the hydrogel where cells are embedded

References

[1] Nicole Le Douarin and Chaya Kalcheim. "The Neural Crest". In: *The Neural Crest* (1999). DOI: 10.1017/CBO9780511897948.

[2] Marianne Bronner-Fraser. "Neural crest cell formation and migration in the developing embryo". In: *The FASEB Journal* 8.10 (1994), pp. 699–706. DOI: 10.1096/FASEBJ.8.10.8050668.

[3] Werner Risau. "Mechanisms of angiogenesis". In: *Nature* 386.6626 (1997), pp. 671–674. DOI: 10.1038/386671a0.

[4] David Alvarez, Elisabeth H. Vollmann, and Ulrich H. von Andrian. "Mechanisms and Consequences of Dendritic Cell Migration". In: *Immunity* 29.3 (2008), pp. 325–342. DOI: 10.1016/J.IMMUNI.2008.08.006.

[5] Marion Leick et al. "Leukocyte recruitment in inflammation: Basic concepts and new mechanistic insights based on new models and microscopic imaging technologies". In: *Cell and Tissue Research* 355.3 (2014), pp. 647–656. DOI: 10.1007/s00441-014-1809-9.

[6] Daniele D'Ambrosio and Francesco Sinigaglia. *Cell Migration in Inflammation and Immunity*. Ed. by Daniele D'Ambrosio and Francesco Sinigaglia. 1st ed. Humana Press, 2003. ISBN: 978-1-59259-435-1. DOI: 10.1385/1592594352.

[7] Feini Qu, Farshid Guilak, and Robert L. Mauck. "Cell migration: implications for repair and regeneration in joint disease". In: *Nature Reviews Rheumatology* 15.3 (2019), pp. 167–179. DOI: 10.1038/s41584-018-0151-0.

[8] T. Shawn Sato et al. "Neurocristopathies: Enigmatic appearances of neural crest cell– derived abnormalities". In: *Radiographics* 39.7 (2019), pp. 2085–2102. DOI: 10.1148/rg.2019190086.

[9] Guillermo A. Vega-Lopez et al. "Neurocristopathies: New insights 150 years after the neural crest discovery". In: *Developmental Biology* 444 (2018), S110–S143. DOI: 10.1016/J.YDBIO.2018.05.013.

[10] Paul A. Trainor. "Neural Crest Cells: Evolution, Development and Disease". In: *Neural Crest Cells: Evolution, Development and Disease* (2014), pp. 1–469. DOI: 10.1016/C2012-0-00698-9.

[11] Kristin E.Noack Watt and Paul A. Trainor. "Neurocristopathies: The Etiology and Pathogenesis of Disorders Arising from Defects in Neural Crest Cell Development". In: *Neural Crest Cells: Evolution, Development and Disease* (2014), pp. 361–394. DOI: 10.1016/B978-0-12-401730-6.00018-1.

[12] Peihong Su et al. "Mesenchymal Stem Cell Migration during Bone Formation and Bone Diseases Therapy". In: *International Journal of Molecular Sciences* 19.8 (2018), p. 2343. DOI: 10.3390/IJMS19082343.

[13] Doriane Vesperini et al. "Characterization of immune cell migration using microfabrication". In: *Biophysical Reviews* 13.2 (2021), pp. 185–202. DOI: 10.1007/S12551-021-00787-9.

[14] Juan Liu et al. “Dendritic cell migration in inflammation and immunity”. In: *Cellular & Molecular Immunology* 18.11 (2021), pp. 2461–2471. DOI: 10.1038/s41423-021-00726-4.

[15] Thomas H. Adair and Jean-Pierre Montani. “Angiogenesis”. In: *Colloquium series on integrated systems physiology: From molecule to function*. Vol. 2. 1. Morgan & Claypool Life Sciences, 2010, pp. 1–84. DOI: 10.4199/C00017ED1V01Y201009ISP010.

[16] S. J. Walsh and L. M. Rau. “Autoimmune diseases: a leading cause of death among young and middle-aged women in the United States”. In: *American Journal of Public Health* 90.9 (2000), pp. 1463–1466. DOI: 10.2105/AJPH.90.9.1463.

[17] *Research - Autoimmune Association*. URL: https://autoimmune.org/research/ (visited on 03/13/2022).

[18] American Association of Autoimmune Related Diseases. *The cost burden of autoimmune disease: the latest front in the war on healthcare spending*. 2011.

[19] Hyuna Sung et al. “Global cancer statistics 2020: GLOBOCAN estimates of incidence and mortality worldwide for 36 cancers in 185 countries”. In: *CA: A Cancer Journal for Clinicians* (2021), caac.21660. DOI: 10.3322/caac.21660.

[20] Xiangming Guan. “Cancer metastases: Challenges and opportunities”. In: *Acta Pharmaceutica Sinica B* 5.5 (2015), pp. 402–418. DOI: 10.1016/j.apsb.2015.07.005.

[21] A. B. Mariotto et al. “Projections of the Cost of Cancer Care in the United States: 2010-2020”. In: *JNCI: Journal of the National Cancer Institute* 103.2 (2011), pp. 117–128. DOI: 10.1093/jnci/djq495.

[22] Cathy J. Bradley et al. “Productivity Costs of Cancer Mortality in the United States: 2000–2020”. In: *JNCI: Journal of the National Cancer Institute* 100.24 (2008), pp. 1763–1770. DOI: 10.1093/jnci/djn384.

[23] Ramon Luengo-Fernandez et al. “Economic burden of cancer across the European Union: A population-based cost analysis”. In: *The Lancet Oncology* 14.12 (2013), pp. 1165–1174. DOI: 10.1016/S1470-2045(13)70442-X.

[24] *COVID-19 Map - Johns Hopkins Coronavirus Resource Center*. URL: https://coronavirus.jhu.edu/map.html (visited on 01/26/2022).

[25] Adam Shellard and Roberto Mayor. “Collective durotaxis along a self-generated stiffness gradient in vivo”. In: *Nature* 600.7890 (2021), pp. 690–694. DOI: 10.1038/s41586-021-04210-x.

[26] Carlos Borau et al. “Dynamic Mechanisms of Cell Rigidity Sensing: Insights from a Computational Model of Actomyosin Networks”. In: *PLoS ONE* 7.11 (2012). Ed. by Wilbur Lam, e49174. DOI: 10.1371/journal.pone.0049174.

[27] Ololade Fatunmbi et al. “A multiscale biophysical model for the recruitment of actin nucleating proteins at the membrane interface”. In: *Soft Matter* 16.21 (2020), pp. 4941–4954. DOI: 10.1039/d0sm00267d.

[28] Austin Hopkins and Brian A. Camley. “Chemotaxis in uncertain environments: Hedging bets with multiple receptor types”. In: *Physical Review Research* 2.4 (2020), p. 043146. DOI: 10.1103/PhysRevResearch.2.043146.

[29] D. Aubry et al. “A computational mechanics approach to assess the link between cell morphology and forces during confined migration”. In: *Biomechanics and Modeling in Mechanobiology* 14.1 (2014), pp. 143–157. DOI: 10.1007/S10237-014-0595-3.

[30] Ismael Gonzalez-Valverde and Jose Manuel Garcia-Aznar. "Mechanical modeling of collective cell migration: An agent-based and continuum material approach". In: *Computer Methods in Applied Mechanics and Engineering* 337 (2018), pp. 246–262. DOI: 10.1016/j.cma.2018.03.036.

[31] Yu Zheng et al. "Modeling multicellular dynamics regulated by extracellular-matrix-mediated mechanical communication via active particles with polarized effective attraction". In: *Physical Review E* 102.5 (2020), p. 052409. DOI: 10.1103/PhysRevE.102.052409.

[32] Ines G. Goncalves and Jose Manuel Garcia Aznar. "Extracellular matrix density regulates the formation of tumour spheroids through cell migration". In: *PLoS Computational Biology* 17.2 (2021), e1008764. DOI: 10.1371/JOURNAL.PCBI.1008764.

[33] Adrian Moure and Hector Gomez. "Influence of myosin activity and mechanical impact on keratocyte polarization". In: *Soft Matter* 16.22 (2020), pp. 5177–5194. DOI: 10.1039/d0sm00473a.

[34] Min-Cheol Kim et al. "Computational modeling of three-dimensional ECM-rigidity sensing to guide directed cell migration." In: *Proceedings of the National Academy of Sciences of the United States of America* 115.3 (2018), E390–E399. DOI: 10.1073/pnas.1717230115.

[35] Francisco Merino-Casallo et al. "Integration of in vitro and in silico Models Using Bayesian Optimization With an Application to Stochastic Modeling of Mesenchymal 3D Cell Migration". In: *Frontiers in Physiology* 9 (2018), p. 1246. DOI: 10.3389/fphys.2018.01246.

[36] Lu Peng et al. "A Multiscale Mathematical Model of Tumour Invasive Growth". In: *Bulletin of Mathematical Biology* 79.3 (2017), pp. 389–429. DOI: 10.1007/s11538-016-0237-2.

[37] Alexander G. Fletcher and James M. Osborne. "Seven challenges in the multiscale modeling of multicellular tissues". In: *WIREs Mechanisms of Disease* 14.1 (2022), e1527. DOI: 10.1002/wsbm.1527.

[38] Nikos K. Karamanos et al. "A guide to the composition and functions of the extracellular matrix". In: *The FEBS Journal* (2021), febs.15776. DOI: 10.1111/febs.15776.

[39] David A.Cruz Walma and Kenneth M. Yamada. "The extracellular matrix in development". In: *Development* 147.10 (2020). DOI: 10.1242/dev.175596.

[40] Marsha C. Lampi and Cynthia A. Reinhart-King. "Targeting extracellular matrix stiffness to attenuate disease: From molecular mechanisms to clinical trials". In: *Science Translational Medicine* 10.422 (2018). DOI: 10.1126/scitranslmed.aao0475.

[41] Kenneth M. Yamada and Michael Sixt. "Mechanisms of 3D cell migration". In: *Nature Reviews Molecular Cell Biology* 20.12 (2019), pp. 738–752. DOI: 10.1038/s41580-019-0172-9.

[42] Christopher Z. Eddy et al. "Morphodynamics facilitate cancer cells to navigate 3D extracellular matrix". In: *Scientific Reports* 11.1 (2021), pp. 1–10. DOI: 10.1038/s41598-021-99902-9.

[43] Matthew R. Zanotelli et al. "The Physical Microenvironment of Tumors: Characterization and Clinical Impact". In: *The Physics of Cancer*. Ed. by Bernard S. Gerstman. World Scientific Publishing Company, 2020, pp. 165–195. DOI: 10.1142/9789811223495_0008.

[44] Kenneth M. Yamada et al. “Extracellular matrix dynamics in cell migration, invasion and tissue morphogenesis”. In: *International Journal of Experimental Pathology* 100.3 (2019), pp. 144–152. DOI: 10.1111/iep.12329.

[45] Colin D. Paul, Panagiotis Mistriotis, and Konstantinos Konstantopoulos. “Cancer cell motility: lessons from migration in confined spaces”. In: *Nature Reviews Cancer* 17.2 (2017), pp. 131–140. DOI: 10.1038/nrc.2016.123.

[46] Adam Shellard and Roberto Mayor. “Rules of collective migration: From the wildebeest to the neural crest: Rules of neural crest migration”. In: *Philosophical Transactions of the Royal Society B: Biological Sciences* 375.1807 (2020). DOI: 10.1098/rstb.2019.0387.

[47] Chiara De Pascalis and Sandrine Etienne-Manneville. “Single and collective cell migration: The mechanics of adhesions”. In: *Molecular Biology of the Cell* 28.14 (2017). Ed. by Valerie Marie Weaver, pp. 1833–1846. DOI: 10.1091/mbc.E17-03-0134.

[48] Peter Friedl and Roberto Mayor. “Tuning collective cell migration by cell-cell junction regulation”. In: *Cold Spring Harbor Perspectives in Biology* 9.4 (2017), a029199. DOI: 10.1101/cshperspect.a029199.

[49] Marianne Lintz, Adam Muñoz, and Cynthia A. Reinhart-King. “The Mechanics of Single Cell and Collective Migration of Tumor Cells”. In: *Journal of Biomechanical Engineering* 139.2 (2017), p. 9. DOI: 10.1115/1.4035121.

[50] Shailaja Seetharaman and Sandrine Etienne-Manneville. “Cytoskeletal Crosstalk in Cell Migration”. In: *Trends in Cell Biology* 30.9 (2020), pp. 720–735. DOI: 10.1016/j.tcb.2020.06.004.

[51] Kayla Duval et al. “Modeling physiological events in 2D vs. 3D cell culture”. In: *Physiology* 32.4 (2017), pp. 266–277. DOI: 10.1152/physiol.00036.2016.

[52] Leo Loeb. “AMOEBOID MOVEMENT, TISSUE FORMATION AND CONSISTENCY OF PROTOPLASM”. In: *American Journal of Physiology-Legacy Content* 56.1 (1921), pp. 140–167. DOI: 10.1152/ajplegacy.1921.56.1.140.

[53] C. W.M. Poynter. “Some observations on wound healing in the early embryo”. In: *The Anatomical Record* 16.1 (1919), pp. 1–24. DOI: 10.1002/AR.1090160102.

[54] Shinichi Matsumoto. “Contribution to the study of epithelial movement. The corneal epithelium of the frog in tissue culture”. In: *Journal of Experimental Zoology* 26.3 (1918), pp. 545–564.

[55] Albert C Eycleshymer. “The closing of wounds in the larval Necturus”. In: *American journal of anatomy* 7.2 (1907), pp. 317–325.

[56] G Bloch. “Über Chemotaxis”. In: *Centralblatt für Allgemeine Pathologie und Pathologische Anatomie* 7 (1896), pp. 785–791.

[57] Julia B Platt. “Ectodermic origin of the cartilages of the head”. In: *Anatomischer Anzeiger* 8 (1893), pp. 506–509.

[58] T Leber. “Uber die Entstehung der Entzundung und die entzundungerregeden Scadliekeiten”. In: *Fortschr. Med* 4 (1888), p. 460.

[59] R Caton. “Contributions to the Cell-Migration Theory.” In: *Journal of Anatomy and Physiology* 5.Pt 1 (1870), pp. 35–420.7.

[60] William Addison. “Experimental and practical researches on the nature and origin of tubercles in the lungs”. In: *Provincial Medical and Surgical Journal* s1-4.20 (1842), pp. 403–407. DOI: 10.1136/bmj.s1-4.20.403.

[61] Brian D. Cosgrove et al. "Nuclear envelope wrinkling predicts mesenchymal progenitor cell mechano-response in 2D and 3D microenvironments". In: *Biomaterials* 270 (2021), p. 120662. DOI: 10.1016/j.biomaterials.2021.120662.

[62] Michael J. Harris, Denis Wirtz, and Pei Hsun Wu. "Dissecting cellular mechanics: Implications for aging, cancer, and immunity". In: *Seminars in Cell & Developmental Biology* 93 (2019), pp. 16–25. DOI: 10.1016/j.semcdb.2018.10.008.

[63] Jessica E. Kim et al. "Characterization of the mechanical properties of cancer cells in 3D matrices in response to collagen concentration and cytoskeletal inhibitors". In: *Integrative Biology* 10.4 (2018), pp. 232–241. DOI: 10.1039/C8IB00044A.

[64] Adrian Moure and Hector Gomez. "Dual role of the nucleus in cell migration on planar substrates". In: *Biomechanics and Modeling in Mechanobiology* 19.5 (2020), pp. 1491–1508. DOI: 10.1007/s10237-019-01283-6.

[65] Pei-Hsun Wu, Daniele M. Gilkes, and Denis Wirtz. "The Biophysics of 3D Cell Migration". In: *Annual Review of Biophysics* 47.1 (2018), pp. 549–567. DOI: 10.1146/annurev-biophys-070816-033854.

[66] Ruijun Zhu, Chenshu Liu, and Gregg G. Gundersen. "Nuclear positioning in migrating fibroblasts". In: *Seminars in Cell & Developmental Biology* 82 (2018), pp. 41–50. DOI: 10.1016/J.SEMCDB.2017.11.006.

[67] Pedro Barbacena et al. "Competition for endothelial cell polarity drives vascular morphogenesis". In: *bioRxiv preprint* (2021), p. 2021.11.23.469704. DOI: 10.1101/2021.11.23.469704.

[68] Kiersten E. Scott et al. "Emerging themes and unifying concepts underlying cell behavior regulation by the pericellular space". In: *Acta Biomaterialia* 96 (2019), pp. 81–98. DOI: 10.1016/j.actbio.2019.06.003.

[69] Jaime A. Espina, Cristian L. Marchant, and Elias H. Barriga. "Durotaxis: the mechanical control of directed cell migration". In: *FEBS Journal* (2021). DOI: 10.1111/febs.15862.

[70] Fan Zhang et al. "Mechanomics analysis of hESCs under combined mechanical shear, stretch, and compression". In: *Biomechanics and Modeling in Mechanobiology* 20.1 (2020), pp. 205–222. DOI: 10.1007/s10237-020-01378-5.

[71] Petra Kameritsch and Jörg Renkawitz. "Principles of Leukocyte Migration Strategies". In: *Trends in Cell Biology* 30.10 (2020), pp. 818–832. DOI: 10.1016/j.tcb.2020.06.007.

[72] Fernanda Bajanca et al. "In vivo topology converts competition for cell-matrix adhesion into directional migration". In: *Nature Communications* 10.1 (2019), pp. 1–17. DOI: 10.1038/s41467-019-09548-5.

[73] Veronika te Boekhorst, Luigi Preziosi, and Peter Friedl. "Plasticity of Cell Migration In Vivo and In Silico". In: *Annual Review of Cell and Developmental Biology* 32.1 (2016), pp. 491–526. DOI: 10.1146/annurev-cellbio-111315-125201.

[74] Florian Geiger et al. "Fiber stiffness, pore size and adhesion control migratory phenotype of MDA-MB-231 cells in collagen gels". In: *PLOS ONE* 14.11 (2019). Ed. by Jung Weon Lee, e0225215. DOI: 10.1371/journal.pone.0225215.

[75] Ovijit Chaudhuri et al. "Effects of extracellular matrix viscoelasticity on cellular behaviour". In: *Nature* 584.7822 (2020), pp. 535–546. DOI: 10.1038/s41586-020-2612-2.

[76] Colin D. Paul et al. “Probing cellular response to topography in three dimensions”. In: *Biomaterials* 197 (2019), pp. 101–118. DOI: 10.1016/J.BIOMATERIALS.2019.01.009.

[77] Michael Mak et al. “Integrated Analysis of Intracellular Dynamics of MenaINV Cancer Cells in a 3D Matrix”. In: *Biophysical Journal* 112.9 (2017), pp. 1874–1884. DOI: 10.1016/j.bpj.2017.03.030.

[78] Alberto Elosegui-Artola. “The extracellular matrix viscoelasticity as a regulator of cell and tissue dynamics”. In: *Current Opinion in Cell Biology* 72 (2021), pp. 10–18. DOI: 10.1016/j.ceb.2021.04.002.

[79] J. Ferruzzi et al. “Multi-scale Mechanics of Collagen Networks: Biomechanical Basis of Matrix Remodeling in Cancer”. In: *Studies in Mechanobiology, Tissue Engineering and Biomaterials*. Ed. by Yanhang Zhang. Vol. 23. Springer, 2020, pp. 343–387. DOI: 10.1007/978-3-030-20182-1_11.

[80] Ovijit Chaudhuri et al. “Hydrogels with tunable stress relaxation regulate stem cell fate and activity”. In: *Nature Materials* 15.3 (2016), pp. 326–334. DOI: 10.1038/nmat4489.

[81] Jonas Hazur et al. “Stress relaxation amplitude of hydrogels determines migration, proliferation, and morphology of cells in 3-D culture”. In: *Biomaterials Science* 10.1 (2021), pp. 270–280. DOI: 10.1039/D1BM01089A.

[82] Silvia Hervas-Raluy et al. “A new 3D finite element-based approach for computing cell surface tractions assuming nonlinear conditions”. In: *PLOS ONE* 16.4 (2021). Ed. by Fang-Bao Tian, e0249018. DOI: 10.1371/journal.pone.0249018.

[83] Manuel Gómez-González et al. “Measuring mechanical stress in living tissues”. In: *Nature Reviews Physics* 2.6 (2020), pp. 300–317. DOI: 10.1038/s42254-020-0184-6.

[84] Jian Zhang, Neil C. Chada, and Cynthia A. Reinhart-King. “Microscale Interrogation of 3D Tissue Mechanics”. In: *Frontiers in Bioengineering and Biotechnology* 7 (2019), p. 412. DOI: 10.3389/fbioe.2019.00412.

[85] Sefora Conti et al. “CAFs and cancer cells co-migration in 3D spheroid invasion assay”. In: *Methods in Molecular Biology*. Vol. 2179. Humana Press Inc., 2020, pp. 243–256. DOI: 10.1007/978-1-0716-0779-4_19.

[86] Sarah E. Shelton et al. “Engineering approaches for studying immune-tumor cell interactions and immunotherapy”. In: *iScience* 24.1 (2020), p. 101985. DOI: 10.1016/j.isci.2020.101985.

[87] András Szabó and Roberto Mayor. “Mechanisms of Neural Crest Migration”. In: *Annual Review of Genetics* 52.1 (2018), pp. 43–63. DOI: 10.1146/annurev-genet-120417-031559.

[88] Pere Roca-Cusachs, Raimon Sunyer, and Xavier Trepat. “Mechanical guidance of cell migration: lessons from chemotaxis”. In: *Current Opinion in Cell Biology* 25.5 (2013), pp. 543–549. DOI: 10.1016/J.CEB.2013.04.010.

[89] S. B. Carter. “Haptotaxis and the mechanism of cell motility”. In: *Nature* 213.5073 (1967), pp. 256–260. DOI: 10.1038/213256a0.

[90] H Harris. “Role of Chemotaxis in Inflammation”. In: *Physiological reviews* 34.3 (1954), pp. 529–562. DOI: 10.1152/physrev.1954.34.3.529.

[91] Charles J Brokaw. “Chemotaxis of bracken spermatozoids: Implications of electrochemical orientation”. In: *Journal of Experimental Biology* 35.1 (1958), pp. 197–212.

[92] C J Brokaw. "Chemotaxis of bracken spermatozoids: the role of bimalate ions". In: *Journal of Experimental Biology* 35.1 (1958), pp. 192–196.

[93] Marianne Bronner. "Riding the crest for 150 years!" In: *Developmental Biology* 444 (2018), S1–S2. DOI: 10.1016/j.ydbio.2019.03.001.

[94] Ross G Harrison et al. "Observations of the living developing nerve fiber". In: *The Anatomical Record* 1.5 (1907), pp. 116–128.

[95] S Ramon Y Cajal. "La rétine des vertébrés." In: *Cellule* 9 (1893), pp. 119–255.

[96] Wilhelm His. *Untersuchungen über die erste Anlage des Wirbelthierleibes: die erste Entwickelung des Hühnchens im Ei*. Vol. 1. Leipzig, Germany: Vogel, FCW, 1868.

[97] Nikhil Jain, Jens Moeller, and Viola Vogel. "Mechanobiology of Macrophages: How Physical Factors Coregulate Macrophage Plasticity and Phagocytosis". In: *Annual Review of Biomedical Engineering* 21 (2019), pp. 267–297. DOI: 10.1146/annurev-bioeng-062117-121224.

[98] Stephen Boyden. "The chemotactic effect of mixtures of antibody and antigen on polymorphonuclear leucocytes." In: *The Journal of experimental medicine* 115.3 (1962), pp. 453–466. DOI: 10.1084/jem.115.3.453.

[99] M. McCutcheon. "Chemotaxis in leukocytes." In: *Physiological reviews* 26.3 (1946), pp. 319–336. DOI: 10.1152/physrev.1946.26.3.319.

[100] Erika Donà et al. "Directional tissue migration through a self-generated chemokine gradient". In: *Nature* 503.7475 (2013), pp. 285–289. DOI: 10.1038/nature12635.

[101] Luke Tweedy et al. "Seeing around corners: Cells solve mazes and respond at a distance using attractant breakdown". In: *Science* 369.6507 (2020). DOI: 10.1126/science.aay9792.

[102] Joseph D'Alessandro et al. "Cell migration guided by long-lived spatial memory". In: *Nature Communications* 12.1 (2021), pp. 1–10. DOI: 10.1038/s41467-021-24249-8.

[103] J. Plou et al. "From individual to collective 3D cancer dissemination: roles of collagen concentration and TGF-β". In: *Scientific Reports* 8.1 (2018), pp. 1–14. DOI: 10.1038/s41598-018-30683-4.

[104] Hendrik Ungefroren, David Witte, and Hendrik Lehnert. "The role of small GTPases of the Rho/Rac family in TGF-β-induced EMT and cell motility in cancer". In: *Developmental Dynamics* 247.3 (2018), pp. 451–461. DOI: 10.1002/dvdy.24505.

[105] Judit López-Luque et al. "Downregulation of Epidermal Growth Factor Receptor in hepatocellular carcinoma facilitates Transforming Growth Factor-β-induced epithelial to amoeboid transition". In: *Cancer Letters* 464 (2019), pp. 15–24. DOI: 10.1016/J.CANLET.2019.08.011.

[106] Yusheng Wu et al. "Matrix-driven changes in metabolism support cytoskeletal activity to promote cell migration". In: *Biophysical Journal* 0.0 (2021). DOI: 10.1016/j.bpj.2021.02.044.

[107] Wenqian Li et al. "TGF-β1 in fibroblasts-derived exosomes promotes epithelial-mesenchymal transition of ovarian cancer cells". In: *Oncotarget* 8.56 (2017), pp. 96035–96047. DOI: 10.18632/ONCOTARGET.21635.

[108] Jingfang Gao et al. "TGF-β isoforms induce EMT independent migration of ovarian cancer cells". In: *Cancer Cell International* 14.1 (2014), pp. 1–10. DOI: 10.1186/S12935-014-0072-1.

[109] Mohit Kumar Jolly et al. “Hybrid epithelial/mesenchymal phenotypes promote metastasis and therapy resistance across carcinomas”. In: *Pharmacology & Therapeutics* 194 (2019), pp. 161–184. DOI: 10.1016/J.PHARMTHERA.2018.09.007.

[110] Ievgenia Pastushenko and Cédric Blanpain. “EMT Transition States during Tumor Progression and Metastasis”. In: *Trends in Cell Biology* 29.3 (2019), pp. 212–226. DOI: 10.1016/J.TCB.2018.12.001.

[111] Marta Miaczynska. “Effects of membrane trafficking on signaling by receptor tyrosine kinases”. In: *Cold Spring Harbor Perspectives in Biology* 5.11 (2013), a009035. DOI: 10.1101/cshperspect.a009035.

[112] Shuvasree SenGupta, Carole A. Parent, and James E. Bear. “The principles of directed cell migration”. In: *Nature Reviews Molecular Cell Biology* (2021), pp. 1–19. DOI: 10.1038/s41580-021-00366-6.

[113] Evanthia T. Roussos, John S. Condeelis, and Antonia Patsialou. “Chemotaxis in cancer”. In: *Nature Reviews Cancer* 11.8 (2011), pp. 573–587. DOI: 10.1038/nrc3078.

[114] Jessica B. Casaletto and Andrea I. McClatchey. “Spatial regulation of receptor tyrosine kinases in development and cancer”. In: *Nature Reviews Cancer* 12.6 (2012), pp. 387–400. DOI: 10.1038/nrc3277.

[115] Agata Faron-Górecka et al. “Understanding GPCR dimerization”. In: *Methods in Cell Biology* 149 (2019), pp. 155–178. DOI: 10.1016/BS.MCB.2018.08.005.

[116] Michael D. Paul and Kalina Hristova. “The RTK Interactome: Overview and Perspective on RTK Heterointeractions”. In: *Chemical Reviews* 119.9 (2019), pp. 5881–5921. DOI: 10.1021/acs.chemrev.8b00467.

[117] Carl Henrik Heldin et al. “Signals and receptors”. In: *Cold Spring Harbor Perspectives in Biology* 8.4 (2016), a005900. DOI: 10.1101/cshperspect.a005900.

[118] Ewan MacDonald, Bryan Savage, and Tobias Zech. “Connecting the dots: Combined control of endocytic recycling and degradation”. In: *Biochemical Society Transactions* 48.6 (2020), pp. 2377–2386. DOI: 10.1042/BST20180255.

[119] Nathan J. Pavlos and Peter A. Friedman. “GPCR Signaling and Trafficking: The Long and Short of It”. In: *Trends in Endocrinology & Metabolism* 28.3 (2017), pp. 213–226. DOI: 10.1016/J.TEM.2016.10.007.

[120] Stefanie L. Ritter and Randy A. Hall. “Fine-tuning of GPCR activity by receptor-interacting proteins”. In: *Nature Reviews Molecular Cell Biology* 10.12 (2009), pp. 819–830. DOI: 10.1038/nrm2803.

[121] Simon R. Foster and Hans Bräuner-Osborne. “Investigating Internalization and Intracellular Trafficking of GPCRs: New Techniques and Real-Time Experimental Approaches”. In: *Handbook of Experimental Pharmacology* 245 (2017), pp. 41–61. DOI: 10.1007/164_2017_57.

[122] Roshanak Irannejad and Mark Von Zastrow. “GPCR signaling along the endocytic pathway”. In: *Current Opinion in Cell Biology* 27.1 (2014), pp. 109–116. DOI: 10.1016/J.CEB.2013.10.003.

[123] Alfredo Ulloa-Aguirre et al. “Intracellular Trafficking of G Protein-Coupled Receptors to the Cell Surface Plasma Membrane in Health and Disease”. In: *Cellular Endocrinology in Health and Disease*. Academic Press, 2021, pp. 375–412. DOI: 10.1016/b978-0-12-819801-8.00018-1.

[124] Zhenfang Du and Christine M. Lovly. "Mechanisms of receptor tyrosine kinase activation in cancer". In: *Molecular Cancer* 17.1 (2018), pp. 1–13. DOI: 10.1186/S12943-018-0782-4.

[125] Raphael Trenker and Natalia Jura. "Receptor tyrosine kinase activation: From the ligand perspective". In: *Current Opinion in Cell Biology* 63 (2020), pp. 174–185. DOI: 10.1016/j.ceb.2020.01.016.

[126] Laura E. Kilpatrick and Stephen J. Hill. "Transactivation of G protein-coupled receptors (GPCRs) and receptor tyrosine kinases (RTKs): Recent insights using luminescence and fluorescence technologies". In: *Current Opinion in Endocrine and Metabolic Research* 16 (2021), pp. 102–112. DOI: 10.1016/J.COEMR.2020.10.003.

[127] Tao Gong et al. "DAMP-sensing receptors in sterile inflammation and inflammatory diseases". In: *Nature Reviews Immunology* 20.2 (2020), pp. 95–112. DOI: 10.1038/s41577-019-0215-7.

[128] Sofia De Oliveira, Emily E. Rosowski, and Anna Huttenlocher. "Neutrophil migration in infection and wound repair: Going forward in reverse". In: *Nature Reviews Immunology* 16.6 (2016), pp. 378–391. DOI: 10.1038/nri.2016.49.

[129] Joseph Schlessinger. "Cell signaling by receptor tyrosine kinases". In: *Cell* 103.2 (2000), pp. 211–225. DOI: 10.1016/S0092-8674(00)00114-8.

[130] Raimon Sunyer et al. "Collective cell durotaxis emerges from long-range intercellular force transmission". In: *Science* 353.6304 (2016), pp. 1157–1161. DOI: 10.1126/science.aaf7119.

[131] Benoit Ladoux and René Marc Mège. "Mechanobiology of collective cell behaviours". In: *Nature Reviews Molecular Cell Biology* 18.12 (2017), pp. 743–757. DOI: 10.1038/nrm.2017.98.

[132] Robert S. Fischer et al. "Contractility, focal adhesion orientation, and stress fiber orientation drive cancer cell polarity and migration along wavy ECM substrates". In: *Proceedings of the National Academy of Sciences of the United States of America* 118.22 (2021). DOI: 10.1073/PNAS.2021135118/VIDEO-7.

[133] Simon Lo Vecchio et al. "Collective Dynamics of Focal Adhesions Regulate Direction of Cell Motion". In: *Cell Systems* 10.6 (2020), 535–542.e4. DOI: 10.1016/J.CELS.2020.05.005/ATTACHMENT/FC003A7A-7624-4D48-902A-BD8AF79A3299/MMC2.PDF.

[134] Song Chen et al. "Actin Cytoskeleton and Focal Adhesions Regulate the Biased Migration of Breast Cancer Cells on Nanoscale Asymmetric Sawteeth". In: *ACS Nano* 13.2 (2019), pp. 1454–1468. DOI: 10.1021/acsnano.8b07140.

[135] Anabel Lise Le Roux et al. "The plasma membrane as a mechanochemical transducer". In: *Philosophical Transactions of the Royal Society B: Biological Sciences* 374.1779 (2019). DOI: 10.1098/rstb.2018.0221.

[136] Raimon Sunyer and Xavier Trepat. "Durotaxis". In: *Current Biology* 30.9 (2020), R383–R387. DOI: 10.1016/j.cub.2020.03.051.

[137] Brian J. DuChez et al. "Durotaxis by Human Cancer Cells". In: *Biophysical Journal* 116.4 (2019), pp. 670–683. DOI: 10.1016/j.bpj.2019.01.009.

[138] Elias H. Barriga et al. "Tissue stiffening coordinates morphogenesis by triggering collective cell migration in vivo". In: *Nature* 554.7693 (2018), pp. 523–527. DOI: 10.1038/nature25742.

[139] Aleksi Isomursu et al. “Negative durotaxis: cell movement toward softer environments”. In: *bioRxiv preprint* (2020), p. 2020.10.27.357178. DOI: 10.1101/2020.10.27.357178.

[140] Sarah T. Boyle, M. Zahied Johan, and Michael S. Samuel. “Tumour-directed microenvironment remodelling at a glance”. In: *Journal of Cell Science* 133.24 (2021), jcs247783. DOI: 10.1242/jcs.247783.

[141] Lianne Beunk et al. “Cancer invasion into musculature: Mechanics, molecules and implications”. In: *Seminars in Cell & Developmental Biology* 93 (2019), pp. 36–45. DOI: 10.1016/j.semcdb.2018.07.014.

[142] Fui Boon Kai, Allison P. Drain, and Valerie M. Weaver. “The Extracellular Matrix Modulates the Metastatic Journey”. In: *Developmental Cell* 49.3 (2019), pp. 332–346. DOI: 10.1016/j.devcel.2019.03.026.

[143] Andrea Malandrino et al. “Complex mechanics of the heterogeneous extracellular matrix in cancer”. In: *Extreme Mechanics Letters* 21 (2018), pp. 25–34. DOI: 10.1016/j.eml.2018.02.003.

[144] Anthony J. Berger et al. “Scaffold stiffness influences breast cancer cell invasion via EGFR-linked Mena upregulation and matrix remodeling”. In: *Matrix Biology* 85-86 (2020), pp. 80–93. DOI: 10.1016/j.matbio.2019.07.006.

[145] Alexander Hayn, Tony Fischer, and Claudia Tanja Mierke. “Inhomogeneities in 3D Collagen Matrices Impact Matrix Mechanics and Cancer Cell Migration”. In: *Frontiers in Cell and Developmental Biology* 8 (2020), p. 1224. DOI: 10.3389/fcell.2020.593879.

[146] Paul A. Janmey, Daniel A. Fletcher, and Cynthia A. Reinhart-King. “Stiffness Sensing by Cells”. In: *Physiological reviews* 100.2 (2020), pp. 695–724. DOI: 10.1152/physrev.00013.2019.

[147] Adam Shellard and Roberto Mayor. “Durotaxis: The Hard Path from In Vitro to In Vivo”. In: *Developmental Cell* 56.2 (2020), pp. 227–239. DOI: 10.1016/j.devcel.2020.11.019.

[148] Fabian Spill et al. “Impact of the physical microenvironment on tumor progression and metastasis”. In: *Current Opinion in Biotechnology* 40 (2016), pp. 41–48. DOI: 10.1016/J.COPBIO.2016.02.007.

[149] Guillaume Charras and Erik Sahai. “Physical influences of the extracellular environment on cell migration”. In: *Nature Reviews Molecular Cell Biology* 15.12 (2014), pp. 813–824. DOI: 10.1038/nrm3897.

[150] Paul V. Taufalele et al. “Fiber alignment drives changes in architectural and mechanical features in collagen matrices”. In: *PLOS ONE* 14.5 (2019). Ed. by Grace O’Connell, e0216537. DOI: 10.1371/journal.pone.0216537.

[151] Jiranuwat Sapudom et al. “Fibril bending stiffness of 3D collagen matrices instructs spreading and clustering of invasive and non-invasive breast cancer cells”. In: *Biomaterials* 193 (2019), pp. 47–57. DOI: 10.1016/j.biomaterials.2018.12.010.

[152] María Anguiano et al. “The use of mixed collagen-Matrigel matrices of increasing complexity recapitulates the biphasic role of cell adhesion in cancer cell migration: ECM sensing, remodeling and forces at the leading edge of cancer invasion”. In: *PLOS ONE* 15.1 (2020). Ed. by Daniel Bouvard, e0220019. DOI: 10.1371/journal.pone.0220019.

[153] Hayri E. Balcioglu et al. “A subtle relationship between substrate stiffness and collective migration of cell clusters”. In: *Soft Matter* 16.7 (2020), pp. 1825–1839. DOI: 10.1039/c9sm01893j.

[154] Benjamin L. Bangasser et al. “Shifting the optimal stiffness for cell migration”. In: *Nature Communications* 8.1 (2017), p. 15313. DOI: 10.1038/ncomms15313.

[155] Vasiliki Gkretsi and Triantafyllos Stylianopoulos. “Cell Adhesion and Matrix Stiffness: Coordinating Cancer Cell Invasion and Metastasis”. In: *Frontiers in Oncology* 8 (2018), p. 145. DOI: 10.3389/fonc.2018.00145.

[156] Julie Chang et al. “Increased Stiffness Inhibits Invadopodia Formation and Cell Migration in 3D”. In: *Biophysical Journal* 119.4 (2020), pp. 726–736. DOI: 10.1016/j.bpj.2020.07.003.

[157] Mar Cóndor et al. “Breast Cancer Cells Adapt Contractile Forces to Overcome Steric Hindrance”. In: *Biophysical Journal* 116.7 (2019), pp. 1305–1312. DOI: 10.1016/j.bpj.2019.02.029.

[158] Ghodeejah Higgins et al. “Decreased cell stiffness facilitates cell detachment and cell migration from breast cancer spheroids in 3D collagen matrices of different rigidity”. In: *bioRxiv preprint* (2021), p. 2021.01.21.427639. DOI: 10.1101/2021.01.21.427639.

[159] Valeria Panzetta, Sabato Fusco, and Paolo A. Netti. “Cell mechanosensing is regulated by substrate strain energy rather than stiffness”. In: *Proceedings of the National Academy of Sciences of the United States of America* 116.44 (2019), pp. 22004–22013. DOI: 10.1073/pnas.1904660116.

[160] Jing Li et al. “Roles of Interactions Between Cells and Extracellular Matrices for Cell Migration and Matrix Remodeling”. In: *Multi-scale Extracellular Matrix Mechanics and Mechanobiology*. Springer, 2020, pp. 247–282. DOI: 10.1007/978-3-030-20182-1_8.

[161] Jihan Kim et al. “The mechanics and dynamics of cancer cells sensing noisy 3D contact guidance”. In: *Proceedings of the National Academy of Sciences of the United States of America* 118.10 (2021). DOI: 10.1073/pnas.2024780118.

[162] Stephanie I. Fraley et al. “Three-dimensional matrix fiber alignment modulates cell migration and MT1-MMP utility by spatially and temporally directing protrusions”. In: *Scientific Reports* 5.1 (2015), p. 14580. DOI: 10.1038/srep14580.

[163] Arja Ray et al. “Enhanced Directional Migration of Cancer Stem Cells in 3D Aligned Collagen Matrices”. In: *Biophysical Journal* 112.5 (2017), pp. 1023–1036.

[164] Lena A. Lautscham et al. “Migration in Confined 3D Environments Is Determined by a Combination of Adhesiveness, Nuclear Volume, Contractility, and Cell Stiffness”. In: *Biophysical Journal* 109.5 (2015), pp. 900–913. DOI: 10.1016/J.BPJ.2015.07.025.

[165] Peter Friedl and Katarina Wolf. “Plasticity of cell migration: A multiscale tuning model”. In: *Journal of Cell Biology* 188.1 (2010), pp. 11–19. DOI: 10.1083/jcb.200909003.

[166] Daniel O Velez et al. “3D collagen architecture regulates cell adhesion through degradability, thereby controlling metabolic and oxidative stress”. In: *Integrative Biology* 11.5 (2019), pp. 221–234. DOI: 10.1093/intbio/zyz019.

[167] Sungmin Nam et al. “Varying PEG density to control stress relaxation in alginate-PEG hydrogels for 3D cell culture studies”. In: *Biomaterials* 200 (2019), pp. 15–24. DOI: 10.1016/j.biomaterials.2019.02.004.

[168] Brooke N. Mason et al. “Tuning three-dimensional collagen matrix stiffness independently of collagen concentration modulates endothelial cell behavior”. In: *Acta Biomaterialia* 9.1 (2013), pp. 4635–4644. DOI: 10.1016/j.actbio.2012.08.007.

[169] Katrina M. Wisdom et al. “Matrix mechanical plasticity regulates cancer cell migration through confining microenvironments”. In: *Nature Communications* 9.1 (2018), pp. 1–13. DOI: 10.1038/s41467-018-06641-z.

[170] Katrina M. Wisdom et al. “Covalent cross-linking of basement membrane-like matrices physically restricts invasive protrusions in breast cancer cells”. In: *Matrix Biology* 85-86 (2020), pp. 94–111. DOI: 10.1016/j.matbio.2019.05.006.

[171] Clara Valero et al. “Combined experimental and computational characterization of crosslinked collagen-based hydrogels”. In: *PLOS ONE* 13.4 (2018). Ed. by Dimitrios Zeugolis, e0195820. DOI: 10.1371/journal.pone.0195820.

[172] Fabiana Martino et al. “Cellular mechanotransduction: From tension to function”. In: *Frontiers in Physiology* 9 (2018), p. 824. DOI: 10.3389/fphys.2018.00824.

[173] Brenda Canales Coutiño and Roberto Mayor. “The mechanosensitive channel Piezo1 cooperates with semaphorins to control neural crest migration”. In: *Development* 148.23 (2021). DOI: 10.1242/DEV.200001/VIDEO-2.

[174] Ryan J. Leiphart et al. “Mechanosensing at Cellular Interfaces”. In: *Langmuir* 35.23 (2019), pp. 7509–7519. DOI: 10.1021/acs.langmuir.8b02841.

[175] James R.W. Conway and Guillaume Jacquemet. “Cell matrix adhesion in cell migration”. In: *Essays In Biochemistry* 63.5 (2019), pp. 535–551. DOI: 10.1042/EBC20190012.

[176] Sudong Kim et al. “Harnessing Mechanobiology for Tissue Engineering”. In: *Developmental Cell* 56.2 (2021), pp. 180–191. DOI: 10.1016/j.devcel.2020.12.017.

[177] Laurent Fattet et al. “Matrix Rigidity Controls Epithelial-Mesenchymal Plasticity and Tumor Metastasis via a Mechanoresponsive EPHA2/LYN Complex”. In: *Developmental Cell* 54.3 (2020), 302–316.e7. DOI: 10.1016/j.devcel.2020.05.031.

[178] Keith Burridge, Elizabeth Monaghan-Benson, and David M. Graham. “Mechanotransduction: from the cell surface to the nucleus via RhoA”. In: *Philosophical Transactions of the Royal Society B: Biological Sciences* 374.1779 (2019), p. 20180229. DOI: 10.1098/rstb.2018.0229.

[179] Jonathan D. Humphries et al. “Signal transduction via integrin adhesion complexes”. In: *Current Opinion in Cell Biology* 56 (2019), pp. 14–21. DOI: 10.1016/j.ceb.2018.08.004.

[180] Ivana Samaržija et al. “Integrin Crosstalk Contributes to the Complexity of Signalling and Unpredictable Cancer Cell Fates”. In: *Cancers* 12.7 (2020), p. 1910. DOI: 10.3390/cancers12071910.

[181] Michael Bachmann et al. “Cell adhesion by integrins”. In: *Physiological Reviews* 99.4 (2019), pp. 1655–1699. DOI: 10.1152/physrev.00036.2018.

[182] Jenny Z. Kechagia, Johanna Ivaska, and Pere Roca-Cusachs. “Integrins as biomechanical sensors of the microenvironment”. In: *Nature Reviews Molecular Cell Biology* 20.8 (2019), pp. 457–473. DOI: 10.1038/s41580-019-0134-2.

[183] Shailaja Seetharaman and Sandrine Etienne-Manneville. "Integrin diversity brings specificity in mechanotransduction". In: *Biology of the Cell* 110.3 (2018), pp. 49–64. DOI: 10.1111/boc.201700060.

[184] Megan R. Chastney, James R.W. Conway, and Johanna Ivaska. "Integrin adhesion complexes". In: *Current Biology* 31.10 (2021), R536–R542. DOI: 10.1016/j.cub.2021.01.038.

[185] Rafael Peláez et al. "Integrins: Moonlighting Proteins in Invadosome Formation". In: *Cancers* 11.5 (2019), p. 615. DOI: 10.3390/cancers11050615.

[186] Hellyeh Hamidi and Johanna Ivaska. "Every step of the way: integrins in cancer progression and metastasis". In: *Nature Reviews Cancer* 18.9 (2018), pp. 533–548. DOI: 10.1038/s41568-018-0038-z.

[187] Zhiqi Sun, Mercedes Costell, and Reinhard Fässler. "Integrin activation by talin, kindlin and mechanical forces". In: *Nature Cell Biology* 21.1 (2019). DOI: 10.1038/s41556-018-0234-9.

[188] Fatemeh Karimi et al. "Integrin Clustering Matters: A Review of Biomaterials Functionalized with Multivalent Integrin-Binding Ligands to Improve Cell Adhesion, Migration, Differentiation, Angiogenesis, and Biomedical Device Integration". In: *Advanced Healthcare Materials* 7.12 (2018), p. 1701324. DOI: 10.1002/adhm.201701324.

[189] Enoir Farage and Patrick T. Caswell. "Quantitative Analysis of Integrin Trafficking". In: *Methods in Molecular Biology*. Vol. 2217. Humana Press Inc., 2021, pp. 251–263. DOI: 10.1007/978-1-0716-0962-0_14.

[190] Paulina Moreno-Layseca et al. "Integrin trafficking in cells and tissues". In: *Nature Cell Biology* 21.2 (2019), pp. 122–132. DOI: 10.1038/s41556-018-0223-z.

[191] Marco A. Alfonzo-Méndez et al. "Dual clathrin and integrin signaling systems regulate growth factor receptor activation". In: *Nature Communications* 13.1 (2022), pp. 1–16. DOI: 10.1038/s41467-022-28373-x.

[192] Timo Baade et al. "Clustering of integrin β cytoplasmic domains triggers nascent adhesion formation and reveals a protozoan origin of the integrin-talin interaction". In: *Scientific Reports* 9.1 (2019), pp. 1–13. DOI: 10.1038/s41598-019-42002-6.

[193] Roger Oria et al. "Force loading explains spatial sensing of ligands by cells". In: *Nature* 552.7684 (2017), pp. 219–224. DOI: 10.1038/nature24662.

[194] Sangyoon J. Han et al. "Pre-complexation of talin and vinculin without tension is required for efficient nascent adhesion maturation". In: *eLife* 10 (2021). DOI: 10.7554/ELIFE.66151.

[195] Rajaa Boujemaa-Paterski et al. "Talin-activated vinculin interacts with branched actin networks to initiate bundles". In: *eLife* 9 (2020), pp. 1–26. DOI: 10.7554/eLife.53990.

[196] Rishita Changede et al. "Integrin nanoclusters can bridge thin matrix fibres to form cell–matrix adhesions". In: *Nature Materials* 18.12 (2019), pp. 1366–1375. DOI: 10.1038/s41563-019-0460-y.

[197] Elizabeth G Kleinschmidt and David D Schlaepfer. "Focal adhesion kinase signaling in unexpected places". In: *Current Opinion in Cell Biology* 45 (2017), pp. 24–30. DOI: 10.1016/J.CEB.2017.01.003.

[198] Kyunghee Noh et al. "The hidden role of paxillin: localization to nucleus promotes tumor angiogenesis". In: *Oncogene* 40.2 (2020), pp. 384–395. DOI: 10.1038/s41388-020-01517-3.

[199] Yoana Rabanal-Ruiz et al. “mTORC1 activity is supported by spatial association with focal adhesions”. In: *Journal of Cell Biology* 220.5 (2021). DOI: 10.1083/JCB.202004010.

[200] K.A. Jansen, P. Atherton, and C. Ballestrem. “Mechanotransduction at the cell-matrix interface”. In: *Seminars in Cell & Developmental Biology* 71 (2017), pp. 75–83. DOI: 10.1016/J.SEMCDB.2017.07.027.

[201] Nikki R. Paul, Guillaume Jacquemet, and Patrick T. Caswell. “Endocytic Trafficking of Integrins in Cell Migration”. In: *Current Biology* 25.22 (2015), R1092–R1105. DOI: 10.1016/J.CUB.2015.09.049.

[202] Jia shun Wu et al. “Plasticity of cancer cell invasion: Patterns and mechanisms”. In: *Translational Oncology* 14.1 (2021), p. 100899. DOI: 10.1016/J.TRANON.2020.100899.

[203] Jin Suk Park et al. “Mechanical regulation of glycolysis via cytoskeleton architecture”. In: *Nature* 578.7796 (2020), pp. 621–626. DOI: 10.1038/s41586-020-1998-1.

[204] Matthew R. Zanotelli et al. “Energetic costs regulated by cell mechanics and confinement are predictive of migration path during decision-making”. In: *Nature Communications* 10.1 (2019), pp. 1–12. DOI: 10.1038/s41467-019-12155-z.

[205] Campbell D. Lawson and Anne J. Ridley. “Rho GTPase signaling complexes in cell migration and invasion”. In: *Journal of Cell Biology* 217.2 (2018), pp. 447–457. DOI: 10.1083/jcb.201612069.

[206] Sepp Jansen et al. “Paving the Rho in cancer metastasis: Rho GTPases and beyond”. In: *Pharmacology & Therapeutics* 183 (2018), pp. 1–21. DOI: 10.1016/j.pharmthera.2017.09.002.

[207] Natasha S. Clayton and Anne J. Ridley. “Targeting Rho GTPase Signaling Networks in Cancer”. In: *Frontiers in Cell and Developmental Biology* 8 (2020), p. 222. DOI: 10.3389/fcell.2020.00222.

[208] Camilla Cerutti and Anne J. Ridley. “Endothelial cell-cell adhesion and signaling”. In: *Experimental Cell Research* 358.1 (2017), pp. 31–38. DOI: 10.1016/j.yexcr.2017.06.003.

[209] Raquel B. Haga et al. “RhoBTB1 interacts with ROCKs and inhibits invasion”. In: *Biochemical Journal* 476.17 (2019), pp. 2499–2514. DOI: 10.1042/BCJ20190203.

[210] Julius H. Svensmark and Cord Brakebusch. “Rho GTPases in cancer: friend or foe?” In: *Oncogene* 38.50 (2019), pp. 7447–7456. DOI: 10.1038/s41388-019-0963-7.

[211] Pontus Aspenström. “Activated Rho GTPases in Cancer—The Beginning of a New Paradigm”. In: *International Journal of Molecular Sciences* 19.12 (2018), p. 3949. DOI: 10.3390/ijms19123949.

[212] Xosé R. Bustelo. “RHO GTPases in cancer: known facts, open questions, and therapeutic challenges”. In: *Biochemical Society Transactions* 46.3 (2018), pp. 741–760. DOI: 10.1042/BST20170531.

[213] Paul M. Müller et al. “Systems analysis of RhoGEF and RhoGAP regulatory proteins reveals spatially organized RAC1 signalling from integrin adhesions”. In: *Nature Cell Biology* 22.4 (2020), pp. 498–511. DOI: 10.1038/s41556-020-0488-x.

[214] Jenna A Mosier, Yusheng Wu, and Cynthia A Reinhart-King. “Recent advances in understanding the role of metabolic heterogeneities in cell migration”. In: *Faculty Reviews* 10 (2021), p. 8. DOI: 10.12703/r/10-8.

[215] Jenna A. Mosier et al. "Cancer cell metabolic plasticity in migration and metastasis". In: *Clinical & Experimental Metastasis* 1 (2021), p. 3. DOI: 10.1007/s10585-021-10102-1.

[216] Valentina Rausch and Carsten G. Hansen. "The Hippo Pathway, YAP/TAZ, and the Plasma Membrane". In: *Trends in Cell Biology* 30.1 (2020), pp. 32–48. DOI: 10.1016/j.tcb.2019.10.005.

[217] Ewa Sitarska and Alba Diz-Muñoz. "Pay attention to membrane tension: Mechanobiology of the cell surface". In: *Current Opinion in Cell Biology* 66 (2020), pp. 11–18. DOI: 10.1016/j.ceb.2020.04.001.

[218] Harry Warner, Beverley J. Wilson, and Patrick T. Caswell. "Control of adhesion and protrusion in cell migration by Rho GTPases". In: *Current Opinion in Cell Biology* 56 (2019), pp. 64–70. DOI: 10.1016/J.CEB.2018.09.003.

[219] Shuh Narumiya and Dean Thumkeo. "Rho signaling research: history, current status and future directions". In: *FEBS Letters* 592.11 (2018), pp. 1763–1776. DOI: 10.1002/1873-3468.13087.

[220] Fabian Spill, Chris Bakal, and Michael Mak. "Mechanical and Systems Biology of Cancer". In: *Computational and Structural Biotechnology Journal* 16 (2018), pp. 237–245. DOI: 10.1016/j.csbj.2018.07.002.

[221] Francisco M. Vega and Anne J. Ridley. "The RhoB small GTPase in physiology and disease". In: *Small GTPases* 9.5 (2018), pp. 384–393. DOI: 10.1080/21541248.2016.1253528.

[222] G. A. Cardama et al. "Rho GTPases as therapeutic targets in cancer (Review)". In: *International Journal of Oncology* 51.4 (2017), pp. 1025–1034. DOI: 10.3892/ijo.2017.4093.

[223] Raquel B. Haga and Anne J. Ridley. "Rho GTPases: Regulation and roles in cancer cell biology". In: *Small GTPases* 7.4 (2016), pp. 207–221. DOI: 10.1080/21541248.2016.1232583.

[224] Richard G. Hodge and Anne J. Ridley. "Regulating Rho GTPases and their regulators". In: *Nature Reviews Molecular Cell Biology* 17.8 (2016), pp. 496–510. DOI: 10.1038/nrm.2016.67.

[225] Michael Mak et al. "Single-Cell Migration in Complex Microenvironments: Mechanics and Signaling Dynamics". In: *Journal of Biomechanical Engineering* 138.2 (2016), p. 021004. DOI: 10.1115/1.4032188.

[226] Denis Wirtz, Konstantinos Konstantopoulos, and Peter C. Searson. "The physics of cancer: The role of physical interactions and mechanical forces in metastasis". In: *Nature Reviews Cancer* 11.7 (2011), pp. 512–522. DOI: 10.1038/nrc3080.

[227] Krishna Chinthalapudi, Erumbi S. Rangarajan, and Tina Izard. "The interaction of talin with the cell membrane is essential for integrin activation and focal adhesion formation". In: *Proceedings of the National Academy of Sciences of the United States of America* 115.41 (2018), pp. 10339–10344. DOI: 10.1073/pnas.1806275115.

[228] Sjoerd Van Helvert, Cornelis Storm, and Peter Friedl. "Mechanoreciprocity in cell migration". In: *Nature Cell Biology* 20.1 (2018), pp. 8–20. DOI: 10.1038/s41556-017-0012-0.

[229] Carleen Kluger et al. "Different Vinculin Binding Sites Use the Same Mechanism to Regulate Directional Force Transduction". In: *Biophysical Journal* 118.6 (2020), pp. 1344–1356. DOI: 10.1016/j.bpj.2019.12.042.

[230] Ion Andreu et al. “The force loading rate drives cell mechanosensing through both reinforcement and cytoskeletal softening”. In: *Nature Communications* 12.1 (2021), p. 4229. DOI: 10.1038/s41467-021-24383-3.

[231] Daniel Newman et al. “3D matrix adhesion composition facilitates nuclear force coupling to drive invasive cell migration”. In: *bioRxiv preprint* (2021), p. 2021.05.17.443835. DOI: 10.1101/2021.05.17.443835.

[232] Eric Theveneau and Claudia Linker. “Leaders in collective migration: are front cells really endowed with a particular set of skills?” In: *F1000Research* 6 (2017), p. 1899. DOI: 10.12688/f1000research.11889.1.

[233] Anna Labernadie et al. “A mechanically active heterotypic E-cadherin/N-cadherin adhesion enables fibroblasts to drive cancer cell invasion”. In: *Nature Cell Biology* 19.3 (2017), pp. 224–237. DOI: 10.1038/ncb3478.

[234] Chiara De Pascalis et al. “Intermediate filaments control collective migration by restricting traction forces and sustaining cell-cell contacts”. In: *Journal of Cell Biology* 217.9 (2018), pp. 3031–3044. DOI: 10.1083/jcb.201801162.

[235] Torey R. Arnold, Rachel E. Stephenson, and Ann L. Miller. “Rho GTPases and actomyosin: Partners in regulating epithelial cell-cell junction structure and function”. In: *Experimental Cell Research* 358.1 (2017), pp. 20–30. DOI: 10.1016/j.yexcr.2017.03.053.

[236] Jugroop Singh et al. “Rules of contact inhibition of locomotion for cells on suspended nanofibers”. In: *Proceedings of the National Academy of Sciences of the United States of America* 118.12 (2021), e2011815118. DOI: 10.1073/PNAS.2011815118.

[237] Alice Roycroft and Roberto Mayor. “Michael abercrombie: Contact inhibition of locomotion and more”. In: *International Journal of Developmental Biology* 62.1-3 (2018), pp. 5–13. DOI: 10.1387/ijdb.170277rm.

[238] M. Abercrombie. “Contact inhibition in tissue culture”. In: *In Vitro* 6.2 (1970), pp. 128–142. DOI: 10.1007/BF02616114.

[239] L. A. Thomas and K. M. Yamada. “Contact stimulation of cell migration”. In: *Journal of Cell Science* 103.4 (1992), pp. 1211–1214. DOI: 10.1242/jcs.103.4.1211.

[240] Katarzyna Miekus et al. “Contact stimulation of prostate cancer cell migration: the role of gap junctional coupling and migration stimulated by heterotypic cell-to-cell contacts in determination of the metastatic phenotype of Dunning rat prostate cancer cells”. In: *Biology of the Cell* 97.12 (2005), pp. 893–903. DOI: 10.1042/BC20040129.

[241] Maik C. Bischoff et al. “Filopodia-based contact stimulation of cell migration drives tissue morphogenesis”. In: *Nature Communications* 12.1 (2021), pp. 1–18. DOI: 10.1038/s41467-020-20362-2.

[242] Anh Phuong Le et al. “Adhesion-mediated heterogeneous actin organization governs apoptotic cell extrusion”. In: *Nature Communications* 12.1 (2021), pp. 1–18. DOI: 10.1038/s41467-020-20563-9.

[243] Lakshmi Balasubramaniam et al. “Investigating the nature of active forces in tissues reveals how contractile cells can form extensile monolayers”. In: *Nature Materials* 20.8 (2021), pp. 1–11. DOI: 10.1038/s41563-021-00919-2.

[244] Thao Nguyen et al. "Enhanced cell–cell contact stability and decreased N-cadherin-mediated migration upon fibroblast growth factor receptor-N-cadherin cross talk". In: *Oncogene* 38.35 (2019), pp. 6283–6300. DOI: 10.1038/s41388-019-0875-6.

[245] Tim Hohmann and Faramarz Dehghani. "The Cytoskeleton—A Complex Interacting Meshwork". In: *Cells* 8.4 (2019), p. 362. DOI: 10.3390/cells8040362.

[246] Alexander D Bershadsky and Juri M Vasiliev. *Cytoskeleton*. 1st. Boston, MA: Springer Science & Business Media, 1988, p. 310. ISBN: 978-1-4684-5280-8. DOI: 10.1007/978-1-4684-5278-5.

[247] Nic Koltzoff. "Experimental Biology and the work of the Moscow Institute". In: *Science* 59.1536 (1924), pp. 497–502. DOI: 10.1126/science.59.1536.497.

[248] Adrian F. Pegoraro, Paul Janmey, and David A. Weitz. "Mechanical properties of the cytoskeleton and cells". In: *Cold Spring Harbor Perspectives in Biology* 9.11 (2017), a022038. DOI: 10.1101/cshperspect.a022038.

[249] Rachel S. Kadzik, Kaitlin E. Homa, and David R. Kovar. "F-Actin Cytoskeleton Network Self-Organization through Competition and Cooperation". In: *Annual Review of Cell and Developmental Biology* 36 (2020), pp. 35–60. DOI: 10.1146/annurev-cellbio-032320-094706.

[250] Tatyana Svitkina. "The actin cytoskeleton and actin-based motility". In: *Cold Spring Harbor Perspectives in Biology* 10.1 (2018). DOI: 10.1101/cshperspect.a018267.

[251] Yosuke Senju and Pekka Lappalainen. "Regulation of actin dynamics by PI(4,5)P2 in cell migration and endocytosis". In: *Current Opinion in Cell Biology* 56 (2019), pp. 7–13. DOI: 10.1016/J.CEB.2018.08.003.

[252] Jaakko Lehtimaki, Markku Hakala, and Pekka Lappalainen. "Actin filament structures in migrating cells". In: *Handbook of Experimental Pharmacology* 235 (2017), pp. 1–30. DOI: 10.1007/164_2016_28.

[253] Amanda Krajnik et al. "Phosphoinositide Signaling and Mechanotransduction in Cardiovascular Biology and Disease". In: *Frontiers in Cell and Developmental Biology* 8 (2020), p. 1588. DOI: 10.3389/fcell.2020.595849.

[254] Y. Sun et al. "PI3K inhibition reverses migratory direction of single cells but not cell groups in electric field". In: *bioRxiv preprint* (2020), p. 2020.08.05.238170. DOI: 10.1101/2020.08.05.238170.

[255] Robert Insall. "Actin in 2021". In: *Current Biology* 31.10 (2021), R496–R498. DOI: 10.1016/j.cub.2021.04.013.

[256] Carmen Ruggiero and Enzo Lalli. "Targeting the cytoskeleton against metastatic dissemination". In: *Cancer and Metastasis Reviews* (2021), pp. 1–52. DOI: 10.1007/s10555-020-09936-0.

[257] Simona Buracco, Sophie Claydon, and Robert Insall. "Control of actin dynamics during cell motility". In: *F1000Research* 8 (2019), p. 1977. DOI: 10.12688/f1000research.18669.1.

[258] Erik S. Welf et al. "Actin-Membrane Release Initiates Cell Protrusions". In: *Developmental Cell* 55.6 (2020), 723–736.e8. DOI: 10.1016/j.devcel.2020.11.024.

[259] Anjali Bisaria et al. "Membrane-proximal F-actin restricts local membrane protrusions and directs cell migration". In: *Science* 368.6496 (2020), pp. 1205–1210. DOI: 10.1126/science.aay7794.

[260] Maria F Ullo and Jeremy S Logue. “ADF and cofilin-1 collaborate to promote cortical actin flow and the leader bleb-based migration of confined cells”. In: *eLife* 10 (2021), e67856. DOI: 10.7554/eLife.67856.

[261] Georgios Kanellos et al. “ADF and Cofilin1 Control Actin Stress Fibers, Nuclear Integrity, and Cell Survival”. In: *Cell Reports* 13.9 (2015), pp. 1949–1964. DOI: 10.1016/j.celrep.2015.10.056.

[262] Shashi Prakash Singh and Robert H. Insall. “Adhesion stimulates Scar/WAVE phosphorylation in mammalian cells”. In: *Communicative & Integrative Biology* 14.1 (2021), pp. 1–4. DOI: 10.1080/19420889.2020.1855854.

[263] Shashi Prakash Singh et al. “Cell-substrate adhesion drives Scar/WAVE activation and phosphorylation by a Ste20-family kinase, which controls pseudopod lifetime”. In: *PLOS Biology* 18.8 (2020). Ed. by Cornelis Weijer, e3000774. DOI: 10.1371/journal.pbio.3000774.

[264] Shawn P. Carey et al. “Local extracellular matrix alignment directs cellular protrusion dynamics and migration through Rac1 and FAK”. In: *Integrative Biology* 8.8 (2016), pp. 821–835. DOI: 10.1039/C6IB00030D.

[265] Kolade Adebowale et al. “Enhanced substrate stress relaxation promotes filopodia-mediated cell migration”. In: *Nature Materials* 20.9 (2021), pp. 1–10. DOI: 10.1038/s41563-021-00981-w.

[266] Manasi Kelkar, Pierre Bohec, and Guillaume Charras. “Mechanics of the cellular actin cortex: From signalling to shape change”. In: *Current Opinion in Cell Biology* 66 (2020), pp. 69–78. DOI: 10.1016/j.ceb.2020.05.008.

[267] Patrick T. Caswell. “Letting Go to Move On: Membrane Detachment Initiates Protrusion”. In: *Developmental Cell* 55.6 (2020), pp. 671–672. DOI: 10.1016/j.devcel.2020.11.026.

[268] Nisha Bte Mohd Rafiq et al. “A mechano-signalling network linking microtubules, myosin IIA filaments and integrin-based adhesions”. In: *Nature Materials* 18.6 (2019), pp. 638–649. DOI: 10.1038/s41563-019-0371-y.

[269] Jiexiang Lin et al. “Mechanical roles in formation of oriented collagen fibers”. In: *Tissue Engineering - Part B: Reviews* 26.2 (2020), pp. 116–128. DOI: 10.1089/ten.teb.2019.0243.

[270] Vanesa Olivares et al. “Image-based Characterization of 3D Collagen Networks and the Effect of Embedded Cells”. In: *Microscopy and Microanalysis* 25.04 (2019), pp. 971–981. DOI: 10.1017/S1431927619014570.

[271] Jihan Kim et al. “Stress-induced plasticity of dynamic collagen networks”. In: *Nature Communications* 8.1 (2017), p. 842. DOI: 10.1038/s41467-017-01011-7.

[272] Alberto Elosegui-Artola, Xavier Trepat, and Pere Roca-Cusachs. “Control of Mechanotransduction by Molecular Clutch Dynamics”. In: *Trends in Cell Biology* 28.5 (2018), pp. 356–367. DOI: 10.1016/j.tcb.2018.01.008.

[273] Benjamin Yeoman et al. “Adhesion strength and contractility enable metastatic cells to become adurotactic”. In: *Cell Reports* 34.10 (2021), p. 108816. DOI: 10.1016/j.celrep.2021.108816.

[274] Anna M. Chizhik et al. “Dual-color metal-induced and Förster resonance energy transfer for cell nanoscopy”. In: *Molecular Biology of the Cell* 29.7 (2018). Ed. by Patricía Bassereau, pp. 846–851. DOI: 10.1091/mbc.E17-05-0314.

[275] Stacey Lee and Sanjay Kumar. "Actomyosin stress fiber mechanosensing in 2D and 3D [version 1; referees: 3 approved]". In: *F1000Research* 5 (2016), p. 2261. DOI: 10.12688/F1000RESEARCH.8800.1.

[276] Ariel Livne and Benjamin Geiger. "The inner workings of stress fibers - From contractile machinery to focal adhesions and back". In: *Journal of Cell Science* 129.7 (2016), pp. 1293–1304. DOI: 10.1242/jcs.180927.

[277] Yin Loon Lee and Brian Burke. "LINC complexes and nuclear positioning". In: *Seminars in Cell & Developmental Biology* 82 (2018), pp. 67–76. DOI: 10.1016/J.SEMCDB.2017.11.008.

[278] Timothée Vignaud et al. "Stress fibres are embedded in a contractile cortical network". In: *Nature Materials* (2020), pp. 1–11. DOI: 10.1038/s41563-020-00825-z.

[279] Sandra Tavares et al. "Actin stress fiber organization promotes cell stiffening and proliferation of pre-invasive breast cancer cells". In: *Nature Communications* 8.1 (2017), pp. 1–18. DOI: 10.1038/ncomms15237.

[280] Patrick T. Caswell and Tobias Zech. "Actin-Based Cell Protrusion in a 3D Matrix". In: *Trends in Cell Biology* 28.10 (2018), pp. 823–834. DOI: 10.1016/J.TCB.2018.06.003.

[281] Andreas Stylianou et al. "Collagen content and extracellular matrix cause cytoskeletal remodelling in pancreatic fibroblasts". In: *Journal of the Royal Society Interface* 16.154 (2019). DOI: 10.1098/RSIF.2019.0226.

[282] Joanna Y. Lee et al. "YAP-independent mechanotransduction drives breast cancer progression". In: *Nature Communications* 10.1 (2019), pp. 1–9. DOI: 10.1038/s41467-019-09755-0.

[283] Matthias Schaks, Grégory Giannone, and Klemens Rottner. "Actin dynamics in cell migration". In: *Essays in Biochemistry* 63.5 (2019), pp. 483–495. DOI: 10.1042/EBC20190015.

[284] Tea Vallenius. "Actin stress fibre subtypes in mesenchymal-migrating cells". In: *Open Biology* 3.JUN (2013). DOI: 10.1098/rsob.130001.

[285] Marileen Dogterom and Gijsje H. Koenderink. "Actin–microtubule crosstalk in cell biology". In: *Nature Reviews Molecular Cell Biology* 20.1 (2019), pp. 38–54. DOI: 10.1038/s41580-018-0067-1.

[286] Clare Garcin and Anne Straube. "Microtubules in cell migration". In: *Essays in Biochemistry* 63.5 (2019), pp. 509–520. DOI: 10.1042/EBC20190016.

[287] Stéphanie Torrino et al. "Mechano-induced cell metabolism promotes microtubule glutamylation to force metastasis". In: *Cell Metabolism* 33.7 (2021), 1342–1357.e10. DOI: 10.1016/j.cmet.2021.05.009.

[288] Shailaja Seetharaman and Sandrine Etienne-Manneville. "Microtubules at focal adhesions - a double-edged sword". In: *Journal of Cell Science* 132.19 (2019). DOI: 10.1242/jcs.232843.

[289] Benjamin P. Bouchet and Anna Akhmanova. "Microtubules in 3D cell motility". In: *Journal of Cell Science* 130.1 (2017), pp. 39–50. DOI: 10.1242/jcs.189431.

[290] Ashtyn Zinn et al. "The small GTPase RhoG regulates microtubule-mediated focal adhesion disassembly". In: *Scientific Reports* 9.1 (2019), pp. 1–15. DOI: 10.1038/s41598-019-41558-7.

[291] Benjamin P. Bouchet et al. “Mesenchymal Cell Invasion Requires Cooperative Regulation of Persistent Microtubule Growth by SLAIN2 and CLASP1”. In: *Developmental Cell* 39.6 (2016), pp. 708–723. DOI: 10.1016/j.devcel.2016.11.009.

[292] Matthew Raab and Dennis E. Discher. “Matrix rigidity regulates microtubule network polarization in migration”. In: *Cytoskeleton* 74.3 (2017), pp. 114–124. DOI: 10.1002/cm.21349.

[293] Morgan L. Pimm and Jessica L. Henty-Ridilla. “New twists in actin–microtubule interactions”. In: *Molecular Biology of the Cell* 32.3 (2021). Ed. by William Bement, pp. 211–217. DOI: 10.1091/mbc.E19-09-0491.

[294] Shailaja Seetharaman et al. “Microtubules tune mechanosensitive cell responses”. In: *Nature Materials* 21.3 (2021), pp. 366–377. DOI: 10.1038/s41563-021-01108-x.

[295] Sandrine Etienne-Manneville. “Cytoplasmic Intermediate Filaments in Cell Biology”. In: *Annual Review of Cell and Developmental Biology* 34.1 (2018), pp. 1–28. DOI: 10.1146/annurev-cellbio-100617-062534.

[296] Rucha Sanghvi-Shah and Gregory F. Weber. “Intermediate filaments at the junction of mechanotransduction, migration, and development”. In: *Frontiers in Cell and Developmental Biology* 5 (2017), p. 81. DOI: 10.3389/fcell.2017.00081.

[297] Emma J. Van Bodegraven and Sandrine Etienne-Manneville. “Intermediate filaments against actomyosin: the david and goliath of cell migration”. In: *Current Opinion in Cell Biology* 66 (2020), pp. 79–88. DOI: 10.1016/j.ceb.2020.05.006.

[298] Jonathan C.R. Jones et al. “Intermediate filaments and the plasma membrane”. In: *Cold Spring Harbor Perspectives in Biology* 9.1 (2017), a025866. DOI: 10.1101/cshperspect.a025866.

[299] Michele M. Nava et al. “Heterochromatin-Driven Nuclear Softening Protects the Genome against Mechanical Stress-Induced Damage”. In: *Cell* 181.4 (2020), 800–817.e22. DOI: 10.1016/j.cell.2020.03.052.

[300] Alexandra Sneider et al. “Recapitulation of molecular regulators of nuclear motion during cell migration”. In: *Cell Adhesion & Migration* 13.1 (2019), pp. 50–62. DOI: 10.1080/19336918.2018.1506654.

[301] Francisco J Calero-Cuenca, Cátia S Janota, and Edgar R Gomes. “Dealing with the nucleus during cell migration”. In: *Current Opinion in Cell Biology* 50 (2018), pp. 35–41. DOI: 10.1016/J.CEB.2018.01.014.

[302] Fengrong Wang et al. “Keratin 6 regulates collective keratinocyte migration by altering cell–cell and cell–matrix adhesion”. In: *Journal of Cell Biology* 217.12 (2018), pp. 4314–4330. DOI: 10.1083/jcb.201712130.

[303] Laura Schaedel et al. “Vimentin intermediate filaments stabilize dynamic microtubules by direct interactions”. In: *Nature Communications* 12.1 (2021), pp. 1–12. DOI: 10.1038/s41467-021-23523-z.

[304] Bryant L. Doss et al. “Cell response to substrate rigidity is regulated by active and passive cytoskeletal stress”. In: *Proceedings of the National Academy of Sciences of the United States of America* 117.23 (2020), pp. 12817–12825. DOI: 10.1073/pnas.1917555117.

[305] Sudha Kumari et al. “Cytoskeletal tension actively sustains the migratory T-cell synaptic contact”. In: *The EMBO Journal* 39.5 (2020), e102783. DOI: 10.15252/EMBJ.2019102783.

[306] Jörg Renkawitz et al. "Nuclear positioning facilitates amoeboid migration along the path of least resistance". In: *Nature* 568.7753 (2019), pp. 546–550. DOI: 10.1038/s41586-019-1087-5.

[307] Aglaja Kopf et al. "Microtubules control cellular shape and coherence in amoeboid migrating cells". In: *Journal of Cell Biology* 219.6 (2020). DOI: 10.1083/JCB.201907154.

[308] Ana Joaquina Jimenez et al. "Acto-myosin network geometry defines centrosome position". In: *Current Biology* 0.0 (2021). DOI: 10.1016/j.cub.2021.01.002.

[309] Joseph Mathew Kalappurakkal, Parijat Sil, and Satyajit Mayor. "Toward a new picture of the living plasma membrane". In: *Protein Science* 29.6 (2020), pp. 1355–1365. DOI: 10.1002/pro.3874.

[310] Nuria Barber-Pérez et al. "Mechano-responsiveness of fibrillar adhesions on stiffness-gradient gels". In: *Journal of Cell Science* 133.12 (2020), jcs.242909. DOI: 10.1242/JCS.242909.

[311] Dariusz Lachowski et al. "FAK controls the mechanical activation of YAP, a transcriptional regulator required for durotaxis". In: *The FASEB Journal* 32.2 (2018), pp. 1099–1107. DOI: 10.1096/fj.201700721R.

[312] Devon E. Mason et al. "YAP and TAZ limit cytoskeletal and focal adhesion maturation to enable persistent cell motility". In: *Journal of Cell Biology* 218.4 (2019), pp. 1369–1389. DOI: 10.1083/jcb.201806065.

[313] Antonio Totaro, Tito Panciera, and Stefano Piccolo. "YAP/TAZ upstream signals and downstream responses". In: *Nature Cell Biology* 20.8 (2018), pp. 888–899. DOI: 10.1038/s41556-018-0142-z.

[314] Giorgia Nardone et al. "YAP regulates cell mechanics by controlling focal adhesion assembly". In: *Nature Communications* 8 (2017), p. 15321. DOI: 10.1038/ncomms15321.

[315] Praful R. Nair and Denis Wirtz. "Enabling migration by moderation: YAP/TAZ are essential for persistent migration". In: *Journal of Cell Biology* 218.4 (2019), pp. 1092–1093. DOI: 10.1083/JCB.201902035.

[316] Francesca Zanconato, Michelangelo Cordenonsi, and Stefano Piccolo. "YAP and TAZ: a signalling hub of the tumour microenvironment". In: *Nature Reviews Cancer* 19.8 (2019), pp. 454–464. DOI: 10.1038/s41568-019-0168-y.

[317] Janine Warren, Yuxuan Xiao, and John Lamar. "YAP/TAZ Activation as a Target for Treating Metastatic Cancer". In: *Cancers* 10.4 (2018), p. 115. DOI: 10.3390/cancers10040115.

[318] Jie Shen et al. "Hippo component YAP promotes focal adhesion and tumour aggressiveness via transcriptionally activating THBS1/FAK signalling in breast cancer". In: *Journal of Experimental and Clinical Cancer Research* 37.1 (2018), pp. 1–17. DOI: 10.1186/s13046-018-0850-z.

[319] Tito Panciera et al. "Reprogramming normal cells into tumour precursors requires ECM stiffness and oncogene-mediated changes of cell mechanical properties". In: *Nature Materials* 19.7 (2020), pp. 797–806. DOI: 10.1038/s41563-020-0615-x.

[320] Cátia S. Janota, Francisco Javier Calero-Cuenca, and Edgar R. Gomes. "The role of the cell nucleus in mechanotransduction". In: *Current Opinion in Cell Biology* 63 (2020), pp. 204–211. DOI: 10.1016/j.ceb.2020.03.001.

[321] Marina Krause et al. “Cell migration through three-dimensional confining pores: speed accelerations by deformation and recoil of the nucleus”. In: *Philosophical Transactions of the Royal Society B: Biological Sciences* 374.1779 (2019), p. 20180225. DOI: 10.1098/rstb.2018.0225.

[322] Hong Pyo Lee et al. “The nuclear piston activates mechanosensitive ion channels to generate cell migration paths in confining microenvironments”. In: *Science Advances* 7.2 (2021), eabd4058. DOI: 10.1126/sciadv.abd4058.

[323] Yuntao Xia, Charlotte R. Pfeifer, and Dennis E. Discher. “Nuclear mechanics during and after constricted migration”. In: *Acta Mechanica Sinica/Lixue Xuebao* 35.2 (2019), pp. 299–308. DOI: 10.1007/s10409-018-00836-9.

[324] Patricia M Davidson et al. “Nesprin-2 accumulates at the front of the nucleus during confined cell migration”. In: *EMBO reports* 21.7 (2020), e49910. DOI: 10.15252/embr.201949910.

[325] Mitra Shokrollahi and Karim Mekhail. “Interphase microtubules in nuclear organization and genome maintenance”. In: *Trends in Cell Biology* 31.9 (2021), pp. 721–731. DOI: 10.1016/j.tcb.2021.03.014.

[326] Melanie Maurer and Jan Lammerding. “The Driving Force: Nuclear Mechanotransduction in Cellular Function, Fate, and Disease”. In: *Annual Review of Biomedical Engineering* 21 (2019), pp. 443–468. DOI: 10.1146/ANNUREV-BIOENG-060418-052139.

[327] Tasneem Bouzid et al. “The LINC complex, mechanotransduction, and mesenchymal stem cell function and fate”. In: *Journal of Biological Engineering* 13.1 (2019), pp. 1–12. DOI: 10.1186/s13036-019-0197-9.

[328] Patricia M. Davidson and Bruno Cadot. “Actin on and around the Nucleus”. In: *Trends in Cell Biology* 31.3 (2021), pp. 211–223. DOI: 10.1016/j.tcb.2020.11.009.

[329] Su Jin Heo et al. “Nuclear softening expedites interstitial cell migration in fibrous networks and dense connective tissues”. In: *Science Advances* 6.25 (2020), pp. 5083–5102. DOI: 10.1126/sciadv.aax5083.

[330] Marina Vortmeyer-Krause et al. “Lamin B2 follows lamin A/C- mediated nuclear mechanics and cancer cell invasion efficacy”. In: *bioRxiv preprint* (2020), p. 2020.04.07.028969. DOI: 10.1101/2020.04.07.028969.

[331] Marcel Dreger et al. “Novel contribution of epigenetic changes to nuclear dynamics”. In: *Nucleus* 10.1 (2019), pp. 42–47. DOI: 10.1080/19491034.2019.1580100.

[332] Abhishek Mukherjee et al. “Nuclear plasticity increases susceptibility to damage during confined migration”. In: *PLOS Computational Biology* 16.10 (2020). Ed. by Dennis E. Discher, e1008300. DOI: 10.1371/journal.pcbi.1008300.

[333] Jau Ye Shiu et al. “Nanopillar force measurements reveal actin-cap-mediated YAP mechanotransduction”. In: *Nature Cell Biology* 20.3 (2018), pp. 262–271. DOI: 10.1038/s41556-017-0030-y.

[334] Takamasa Harada et al. “Nuclear lamin stiffness is a barrier to 3D migration, but softness can limit survival”. In: *Journal of Cell Biology* 204.5 (2014), pp. 669–682. DOI: 10.1083/jcb.201308029.

[335] Ryan S. Stowers et al. “Matrix stiffness induces a tumorigenic phenotype in mammary epithelium through changes in chromatin accessibility”. In: *Nature Biomedical Engineering* 3.12 (2019), pp. 1009–1019. DOI: 10.1038/s41551-019-0420-5.

[336] Guilherme Pedreira de Freitas Nader et al. "Compromised nuclear envelope integrity drives TREX1-dependent DNA damage and tumor cell invasion". In: *Cell* 184.20 (2021), 5230–5246.e22. DOI: 10.1016/J.CELL.2021.08.035.

[337] Charlotte R. Pfeifer et al. "Nuclear failure, DNA damage, and cell cycle disruption after migration through small pores: A brief review". In: *Essays in Biochemistry* 63.5 (2019), pp. 569–577. DOI: 10.1042/EBC20190007.

[338] Valeria Venturini et al. "The nucleus measures shape changes for cellular proprioception to control dynamic cell behavior". In: *Science* 370.6514 (2020). DOI: 10.1126/science.aba2644.

[339] A. J. Lomakin et al. "The nucleus acts as a ruler tailoring cell responses to spatial constraints". In: *Science* 370.6514 (2020). DOI: 10.1126/science.aba2894.

[340] Marina Krause and Katarina Wolf. "Cancer cell migration in 3D tissue: Negotiating space by proteolysis and nuclear deformability". In: *Cell Adhesion & Migration* 9.5 (2015), pp. 357–366. DOI: 10.1080/19336918.2015.1061173.

[341] Karanvir Saini et al. "Tension in fibrils suppresses their enzymatic degradation – A molecular mechanism for 'use it or lose it'". In: *Matrix Biology* 85-86 (2020), pp. 34–46. DOI: 10.1016/j.matbio.2019.06.001.

[342] Juliane Winkler et al. "Concepts of extracellular matrix remodelling in tumour progression and metastasis". In: *Nature Communications* 11.1 (2020), pp. 1–19. DOI: 10.1038/s41467-020-18794-x.

[343] Julie Chang and Ovijit Chaudhuri. "Beyond proteases: Basement membrane mechanics and cancer invasion". In: *Journal of Cell Biology* 218.8 (2019), pp. 2456–2469. DOI: 10.1083/JCB.201903066.

[344] Karanvir Saini and Dennis E. Discher. "Forced Unfolding of Proteins Directs Biochemical Cascades". In: *Biochemistry* 58.49 (2019), pp. 4893–4902. DOI: 10.1021/acs.biochem.9b00839.

[345] Viola Vogel. "Unraveling the Mechanobiology of Extracellular Matrix". In: *Annual Review of Physiology* 80 (2018), pp. 353–387. DOI: 10.1146/annurev-physiol-021317-121312.

[346] Elena Rainero. "Extracellular matrix endocytosis in controlling matrix turnover and beyond: Emerging roles in cancer". In: *Biochemical Society Transactions* 44.5 (2016), pp. 1347–1354. DOI: 10.1042/BST20160159.

[347] Michael Mak. "Impact of crosslink heterogeneity on extracellular matrix mechanics and remodeling". In: *Computational and Structural Biotechnology Journal* 18 (2020), pp. 3969–3976. DOI: 10.1016/j.csbj.2020.11.038.

[348] Pardis Pakshir et al. "Dynamic fibroblast contractions attract remote macrophages in fibrillar collagen matrix". In: *Nature Communications* 10.1 (2019). DOI: 10.1038/s41467-019-09709-6.

[349] Oleg V. Kim et al. "Quantitative structural mechanobiology of platelet-driven blood clot contraction". In: *Nature Communications* 8.1 (2017), p. 1274. DOI: 10.1038/s41467-017-00885-x.

[350] Andrew D. Doyle et al. "3D mesenchymal cell migration is driven by anterior cellular contraction that generates an extracellular matrix prestrain". In: *Developmental Cell* 0.0 (2021). DOI: 10.1016/j.devcel.2021.02.017.

[351] Andrea Malandrino et al. “Dynamic filopodial forces induce accumulation, damage, and plastic remodeling of 3D extracellular matrices”. In: *PLOS Computational Biology* 15.4 (2019). Ed. by Scott L. Diamond, e1006684. DOI: 10.1371/journal.pcbi.1006684.

[352] N. Movilla et al. “Degradation of extracellular matrix regulates osteoblast migration: A microfluidic-based study.” In: *Bone* 107 (2018), pp. 10–17. DOI: 10.1016/j.bone.2017.10.025.

[353] Zhijin Chen et al. “Targeted drug delivery to hepatic stellate cells for the treatment of liver fibrosis”. In: *Journal of Pharmacology and Experimental Therapeutics* 370.3 (2019), pp. 695–702. DOI: 10.1124/jpet.118.256156.

[354] Joseph Jose Thottacherry et al. “Mechanochemical feedback control of dynamin independent endocytosis modulates membrane tension in adherent cells”. In: *Nature Communications* 9.1 (2018), pp. 1–14. DOI: 10.1038/s41467-018-06738-5.

[355] Gabriele Nasello et al. “Primary human osteoblasts cultured in a 3D microenvironment create a unique representative model of their differentiation into osteocytes”. In: *Frontiers in Bioengineering and Biotechnology* 8 (2020), p. 336. DOI: 10.3389/FBIOE.2020.00336.

[356] Joan Chang et al. “The endosome is a master regulator of plasma membrane collagen fibril assembly”. In: *bioRxiv preprint* (2021), p. 2021.03.25.436925. DOI: 10.1101/2021.03.25.436925.

[357] Zhi Hua Zhou et al. “Reorganized collagen in the tumor microenvironment of gastric cancer and its association with prognosis”. In: *Journal of Cancer* 8.8 (2017), pp. 1466–1476. DOI: 10.7150/JCA.18466.

[358] Charlotte M. Fonta et al. “Fibronectin fibers are highly tensed in healthy organs in contrast to tumors and virus-infected lymph nodes”. In: *Matrix Biology Plus* 8 (2020), p. 100046. DOI: 10.1016/j.mbplus.2020.100046.

[359] Ana Rubina Perestrelo et al. “Multiscale Analysis of Extracellular Matrix Remodeling in the Failing Heart”. In: *Circulation Research* 128.1 (2021), pp. 24–38. DOI: 10.1161/circresaha.120.317685.

[360] Fernando Calvo et al. “Mechanotransduction and YAP-dependent matrix remodelling is required for the generation and maintenance of cancer-associated fibroblasts”. In: *Nature Cell Biology* 15.6 (2013), pp. 637–646. DOI: 10.1038/ncb2756.

[361] Yuqiang Fang et al. “An Active Biomechanical Model of Cell Adhesion Actuated by Intracellular Tensioning-Taxis”. In: *Biophysical Journal* 118.11 (2020), pp. 2656–2669. DOI: 10.1016/j.bpj.2020.04.016.

[362] Elisabeth G. Rens and Roeland M.H. Merks. “Cell Shape and Durotaxis Explained from Cell-Extracellular Matrix Forces and Focal Adhesion Dynamics”. In: *iScience* 23.9 (2020), p. 101488. DOI: 10.1016/j.isci.2020.101488.

[363] Diego A. Vargas et al. “Modeling of Mechanosensing Mechanisms Reveals Distinct Cell Migration Modes to Emerge From Combinations of Substrate Stiffness and Adhesion Receptor–Ligand Affinity”. In: *Frontiers in Bioengineering and Biotechnology* 8 (2020), p. 459. DOI: 10.3389/fbioe.2020.00459.

[364] Cole Zmurchok et al. “Membrane Tension Can Enhance Adaptation to Maintain Polarity of Migrating Cells”. In: *Biophysical Journal* 119.8 (2020), pp. 1617–1629. DOI: 10.1016/j.bpj.2020.08.035.

[365] Jingchen Feng et al. "Cell motility, contact guidance, and durotaxis". In: *Soft Matter* 15.24 (2019), pp. 4856–4864. DOI: 10.1039/c8sm02564a.

[366] Abdel Rahman Hassan, Thomas Biel, and Taeyoon Kim. "Mechanical Model for Durotactic Cell Migration". In: *ACS Biomaterials Science and Engineering* 5.8 (2019), pp. 3954–3963. DOI: 10.1021/acsbiomaterials.8b01365.

[367] Florian Thüroff et al. "Bridging the gap between single-cell migration and collective dynamics". In: *eLife* 8 (2019), e46842. DOI: 10.7554/eLife.46842.

[368] Yu Zheng et al. "Modeling cell migration regulated by cell extracellular-matrix micromechanical coupling". In: *Physical Review E* 100.4 (2019), p. 043303. DOI: 10.1103/PhysRevE.100.043303.

[369] Vivi Andasari et al. "Computational model of wound healing: EGF secreted by fibroblasts promotes delayed re-epithelialization of epithelial keratinocytes". In: *Integrative Biology* 10.10 (2018), pp. 605–634. DOI: 10.1039/C8IB00048D.

[370] Maurício Moreira-Soares et al. "Adhesion modulates cell morphology and migration within dense fibrous networks". In: *Journal of Physics Condensed Matter* 32.31 (2020), p. 314001. DOI: 10.1088/1361-648X/ab7c17.

[371] Sharon Wei Ling Lee et al. "Integrated in silico and 3D in vitro model of macrophage migration in response to physical and chemical factors in the tumor microenvironment". In: *Integrative Biology* 12.4 (2020), pp. 90–108. DOI: 10.1093/INTBIO/ZYAA007.

[372] Ang Li et al. "Are the Effects of Independent Biophysical Factors Linearly Additive? A 3D Tumor Migration Model". In: *Biophysical Journal* 117.9 (2019), pp. 1702–1713. DOI: 10.1016/J.BPJ.2019.09.037.

[373] P. Van Liedekerke et al. "A quantitative high resolution computational cell model to unravel the mechanics in living tissues". In: *Computer Methods in Biomechanics and Biomedical Engineering* 22.sup1 (2019), S367–S369. DOI: 10.1080/10255842.2020.1714947.

[374] Benjamin Winkler, Igor S. Aranson, and Falko Ziebert. "Confinement and substrate topography control cell migration in a 3D computational model". In: *Communications Physics* 2.1 (2019), p. 82. DOI: 10.1038/s42005-019-0185-x.

[375] Tommy Heck et al. "The role of actin protrusion dynamics in cell migration through a degradable viscoelastic extracellular matrix: Insights from a computational model". In: *PLoS Computational Biology* 16.1 (2020), e1007250. DOI: 10.1371/journal.pcbi.1007250.

[376] Ondrej Maxian, Alex Mogilner, and Wanda Strychalski. "Computational estimates of mechanical constraints on cell migration through the extracellular matrix". In: *PLoS Computational Biology* 16.8 (2020), e1008160. DOI: 10.1371/journal.pcbi.1008160.

[377] Jie Zhu and Alex Mogilner. "Comparison of cell migration mechanical strategies in three-dimensional matrices: a computational study". In: *Interface Focus* 6.5 (2016), p. 20160040. DOI: 10.1098/rsfs.2016.0040.

[378] Yuansheng Cao et al. "A minimal computational model for three-dimensional cell migration". In: *Journal of the Royal Society Interface* 16.161 (2019). DOI: 10.1098/rsif.2019.0619.

[379] Meng Sun and Muhammad H. Zaman. "Modeling, signaling and cytoskeleton dynamics: integrated modeling-experimental frameworks in cell migration". In: *Wiley Interdisciplinary Reviews: Systems Biology and Medicine* 9.1 (2017), e1365. DOI: 10.1002/wsbm.1365.

[380] Gabriel Shatkin et al. “Computational models of migration modes improve our understanding of metastasis”. In: *APL Bioengineering* 4.4 (2020), p. 41505. DOI: 10.1063/5.0023748.

[381] Nieves Movilla et al. “Matrix degradation regulates osteoblast protrusion dynamics and individual migration”. In: *Integrative Biology* 11.11 (2019), pp. 404–413. DOI: 10.1093/intbio/zyz035.

[382] F. O. Ribeiro et al. “Computational model of mesenchymal migration in 3D under chemotaxis”. In: *Computer Methods in Biomechanics and Biomedical Engineering* 20.1 (2017), pp. 59–74. DOI: 10.1080/10255842.2016.1198784.

[383] Eric J. Campbell and Prosenjit Bagchi. “A computational study of amoeboid motility in 3D: the role of extracellular matrix geometry, cell deformability, and cell–matrix adhesion”. In: *Biomechanics and Modeling in Mechanobiology* 20.1 (2021), pp. 167–191. DOI: 10.1007/s10237-020-01376-7.

[384] Adrian Moure and Hector Gomez. “Three-dimensional simulation of obstacle-mediated chemotaxis”. In: *Biomechanics and Modeling in Mechanobiology* 17.5 (2018). DOI: 10.1007/s10237-018-1023-x.

[385] Eric J. Campbell and Prosenjit Bagchi. “A computational model of amoeboid cell swimming”. In: *Physics of Fluids* 29.10 (2017), p. 101902. DOI: 10.1063/1.4990543.

[386] Ryan J. Petrie et al. “Nonpolarized signaling reveals two distinct modes of 3D cell migration”. In: *Journal of Cell Biology* 197.3 (2012), pp. 439–455. DOI: 10.1083/jcb.201201124.

[387] Francisco Serrano-Alcalde, José Manuel García-Aznar, and María José Gómez-Benito. “Cell biophysical stimuli in lobodopodium formation: a computer based approach”. In: *Computer Methods in Biomechanics and Biomedical Engineering* 24.5 (2020), pp. 496–505. DOI: 10.1080/10255842.2020.1836622.

[388] Ricard Alert and Xavier Trepat. “Physical Models of Collective Cell Migration”. In: *Annual Review of Condensed Matter Physics* 11.1 (2020), pp. 77–101. DOI: 10.1146/annurev-conmatphys-031218-013516.

[389] B A Camley and W-J Rappel. “Physical models of collective cell motility: from cell to tissue”. In: *Journal of Physics D: Applied Physics* 50.11 (2017), p. 113002. DOI: 10.1088/1361-6463/aa56fe.

[390] Andreas Deutsch et al. “BIO-LGCA: A cellular automaton modelling class for analysing collective cell migration”. In: *PLOS Computational Biology* 17.6 (2021), e1009066. DOI: 10.1371/JOURNAL.PCBI.1009066.

[391] Daniel Garcia-Gonzalez and Arrate Muñoz-Barrutia. “Computational insights into the influence of substrate stiffness on collective cell migration”. In: *Extreme Mechanics Letters* 40 (2020), p. 100928. DOI: 10.1016/j.eml.2020.100928.

[392] Michaëlle N. Mayalu, Min Cheol Kim, and H. Harry Asada. “Multi-cell ECM compaction is predictable via superposition of nonlinear cell dynamics linearized in augmented state space”. In: *PLoS Computational Biology* 15.9 (2019), e1006798. DOI: 10.1371/journal.pcbi.1006798.

[393] Neil M. Neumann et al. “Coordination of Receptor Tyrosine Kinase Signaling and Interfacial Tension Dynamics Drives Radial Intercalation and Tube Elongation”. In: *Developmental Cell* 45.1 (2018), 67–82.e6. DOI: 10.1016/j.devcel.2018.03.011.

[394] Jorge Escribano et al. "A hybrid computational model for collective cell durotaxis". In: *Biomechanics and Modeling in Mechanobiology* 17.4 (2018), pp. 1–16. DOI: 10.1007/s10237-018-1010-2.

[395] Adrian Moure and Hector Gomez. "Phase-field model of cellular migration: Three-dimensional simulations in fibrous networks". In: *Computer Methods in Applied Mechanics and Engineering* 320 (2017), pp. 162–197. DOI: 10.1016/J.CMA.2017.03.025.

[396] Nicola Bellomo et al. "On the interplay between mathematics and biology. Hallmarks toward a new systems biology." In: *Physics of Life Reviews* 12 (2015), pp. 44–64. DOI: 10.1016/j.plrev.2014.12.002.

[397] Andreas Buttenschön and Leah Edelstein-Keshet. "Bridging from single to collective cell migration: A review of models and links to experiments". In: *PLOS Computational Biology* 16.12 (2020), e1008411. DOI: 10.1371/journal.pcbi.1008411.

[398] Bo Cheng et al. "Cellular mechanosensing of the biophysical microenvironment: A review of mathematical models of biophysical regulation of cell responses". In: *Physics of Life Reviews* 22-23 (2017), pp. 88–119. DOI: 10.1016/J.PLREV.2017.06.016.

[399] Joseph H. R. Hetmanski et al. "Combinatorial mathematical modelling approaches to interrogate rear retraction dynamics in 3D cell migration". In: *PLOS Computational Biology* 17.3 (2021). Ed. by David Umulis, e1008213. DOI: 10.1371/journal.pcbi.1008213.

[400] Chad M. Hobson and Andrew D. Stephens. "Modeling of Cell Nuclear Mechanics: Classes, Components, and Applications". In: *Cells* 9.7 (2020), p. 1623. DOI: 10.3390/cells9071623.

[401] Zeynep Karagöz et al. "Towards understanding the messengers of extracellular space: Computational models of outside-in integrin reaction networks". In: *Computational and Structural Biotechnology Journal* 19 (2021), pp. 303–314. DOI: 10.1016/j.csbj.2020.12.025.

[402] Jamie L. Nosbisch et al. "Mechanistic models of PLC/PKC signaling implicate phosphatidic acid as a key amplifier of chemotactic gradient sensing". In: *PLOS Computational Biology* 16.4 (2020). Ed. by Stacey Finley, e1007708. DOI: 10.1371/journal.pcbi.1007708.

[403] Ismael Gonzalez-Valverde. "Modeling and simulation of multi-cellular systems using hybrid FEM/Agent-based approaches". PhD thesis. Zaragoza, Spain: University of Zaragoza, 2018.

[404] S. M.Amin Arefi et al. "A biomechanical model for the transendothelial migration of cancer cells". In: *Physical biology* 17.3 (2020), p. 036004. DOI: 10.1088/1478-3975/ab725c.

[405] S. Hervas-Raluy, J. M. Garcia-Aznar, and M. J. Gomez-Benito. "Modelling actin polymerization: the effect on confined cell migration". In: *Biomechanics and Modeling in Mechanobiology* 18.4 (2019), pp. 1177–1187. DOI: 10.1007/s10237-019-01136-2.

[406] Adrian Moure and Hector Gomez. "Phase-Field Modeling of Individual and Collective Cell Migration". In: *Archives of Computational Methods in Engineering* 28.2 (2021), pp. 331–344. DOI: 10.1007/s11831-019-09377-1.

[407] Hossein Ahmadzadeh et al. “Modeling the two-way feedback between contractility and matrix realignment reveals a nonlinear mode of cancer cell invasion.” In: *Proceedings of the National Academy of Sciences of the United States of America* 114.9 (2017), E1617–E1626. DOI: 10.1073/pnas.1617037114.

[408] Samhita P. Banavar et al. “Coordinating cell polarization and morphogenesis through mechanical feedback”. In: *PLOS Computational Biology* 17.1 (2021). Ed. by David Umulis, e1007971. DOI: 10.1371/journal.pcbi.1007971.

[409] Rachel R. Bennett et al. “Elastic-Fluid Model for DNA Damage and Mutation from Nuclear Fluid Segregation Due to Cell Migration”. In: *Biophysical Journal* 112.11 (2017), pp. 2271–2279. DOI: 10.1016/j.bpj.2017.04.037.

[410] John Mackenzie, Christopher Rowlatt, and Robert Insall. “A Conservative Finite Element ALE Scheme for Mass-Conservative Reaction-Diffusion Equations on Evolving Two-Dimensional Domains”. In: *SIAM Journal on Scientific Computing* 43.1 (2021), B132–B166. DOI: 10.1137/19M1298585.

[411] Francisco Serrano-Alcalde, José Manuel García-Aznar, and María José Gómez-Benito. “The role of nuclear mechanics in cell deformation under creeping flows”. In: *Journal of Theoretical Biology* 432 (2017), pp. 25–32. DOI: 10.1016/J.JTBI.2017.07.028.

[412] Arnau Montagud, Miguel Ponce-de-Leon, and Alfonso Valencia. “Systems biology at the giga-scale: Large multiscale models of complex, heterogeneous multicellular systems”. In: *Current Opinion in Systems Biology* 28 (2021), p. 100385. DOI: 10.1016/J.COISB.2021.100385.

[413] John Metzcar et al. “A Review of Cell-Based Computational Modeling in Cancer Biology”. In: *JCO Clinical Cancer Informatics* 3 (2019), pp. 1–13. DOI: 10.1200/cci.18.00069.

[414] Ahmadreza Ghaffarizadeh et al. “PhysiCell: An open source physics-based cell simulator for 3-D multicellular systems”. In: *PLOS Computational Biology* 14.2 (2018), e1005991. DOI: 10.1371/JOURNAL.PCBI.1005991.

[415] Simon Coakley et al. “Exploitation of high performance computing in the FLAME agent-based simulation framework”. In: *Proceedings of the 14th IEEE International Conference on High Performance Computing and Communications, HPCC-2012 - 9th IEEE International Conference on Embedded Software and Systems, ICESS-2012*. Liverpool, UK, 2012, pp. 538–545. ISBN: 9780769547497. DOI: 10.1109/HPCC.2012.79.

[416] Shiliang Feng et al. “Mechanochemical modeling of neutrophil migration based on four signaling layers, integrin dynamics, and substrate stiffness”. In: *Biomechanics and Modeling in Mechanobiology* 17.6 (2018), pp. 1611–1630. DOI: 10.1007/s10237-018-1047-2.

[417] James W. Reinhardt and Keith J. Gooch. “An Agent-Based Discrete Collagen Fiber Network Model of Dynamic Traction Force-Induced Remodeling”. In: *Journal of Biomechanical Engineering* 140.5 (2018), p. 051003. DOI: 10.1115/1.4037947.

[418] Dirk Drasdo, Andreas Buttenschön, and Paul Liedekerke. “Agent-Based Lattice Models of Multicellular Systems”. In: *Numerical Methods and Advanced Simulation in Biomechanics and Biological Processes*. Ed. by Miguel Cerrolaza, Sandra J. Shefelbine, and Diego Garzón-Alvarado. Elsevier Ltd, 2018. Chap. 12, pp. 223–238. ISBN: 978-0-12-811718-7. DOI: 10.1016/C2016-0-01393-1.

[419] Paul Liedekerke, Andreas Buttenschön, and Dirk Drasdo. "Off-Lattice Agent-Based Models for Cell and Tumor Growth". In: *Numerical Methods and Advanced Simulation in Biomechanics and Biological Processes*. Ed. by Miguel Cerrolaza, Sandra J. Shefelbine, and Diego Garzón-Alvarado. Elsevier Ltd, 2018. Chap. 14, pp. 245–267. ISBN: 978-0-12-811718-7. DOI: 10.1016/C2016-0-01393-1.

[420] Gaelle Letort et al. "PhysiBoSS: A multi-scale agent-based modelling framework integrating physical dimension and cell signalling". In: *Bioinformatics* 35.7 (2019), pp. 1188–1196. DOI: 10.1093/bioinformatics/bty766.

[421] Ismael Gonzalez-Valverde and Jose Manuel Garcia-Aznar. "An agent-based and FE approach to simulate cell jamming and collective motion in epithelial layers". In: *Computational Particle Mechanics* 6.1 (2019), pp. 85–96. DOI: 10.1007/s40571-018-0199-2.

[422] Cicely K. Macnamara et al. "Computational modelling and simulation of cancer growth and migration within a 3D heterogeneous tissue: The effects of fibre and vascular structure". In: *Journal of Computational Science* 40 (2020), p. 101067. DOI: 10.1016/j.jocs.2019.101067.

[423] Nikolaos Sfakianakis, Anotida Madzvamuse, and Mark A.J. J Chaplain. "A Hybrid Multiscale Model for Cancer Invasion of the Extracellular Matrix". In: *Multiscale Modeling & Simulation* 18.2 (2020), pp. 824–850. DOI: 10.1137/18M1189026.

[424] Jiaye He and Jan Huisken. "Image quality guided smart rotation improves coverage in microscopy". In: *Nature Communications* 11.1 (2020), pp. 1–9. DOI: 10.1038/s41467-019-13821-y.

[425] Mark Alber et al. "Integrating machine learning and multiscale modeling—perspectives, challenges, and opportunities in the biological, biomedical, and behavioral sciences". In: *npj Digital Medicine* 2.1 (2019), pp. 1–11. DOI: 10.1038/s41746-019-0193-y.

[426] Mahdi Imani and Seyede Fatemeh Ghoreishi. "Bayesian Optimization Objective-Based Experimental Design". In: *Proceedings of the American Control Conference*. Vol. 2020-July. Denver, CO, USA: Institute of Electrical and Electronics Engineers Inc., 2020, pp. 3405–3411. ISBN: 9781538682661. DOI: 10.23919/ACC45564.2020.9147824.

[427] Georgios Karagiannis, Bledar A. Konomi, and Guang Lin. "On the Bayesian calibration of expensive computer models with input dependent parameters". In: *Spatial Statistics* 34 (2019), p. 100258. DOI: 10.1016/j.spasta.2017.08.002.

[428] Christoph Mark et al. "Bayesian model selection for complex dynamic systems". In: *Nature Communications* 9.1 (2018), p. 1803. DOI: 10.1038/s41467-018-04241-5.

[429] Aleix Boquet-Pujadas, Jean Christophe Olivo-Marin, and Nancy Guillén. "Bioimage Analysis and Cell Motility". In: *Patterns* 2.1 (2021), p. 100170. DOI: 10.1016/j.patter.2020.100170.

[430] Lucas von Chamier et al. "Democratising deep learning for microscopy with ZeroCostDL4Mic". In: *Nature Communications* 12.1 (2021), p. 2276. DOI: 10.1038/s41467-021-22518-0.

[431] Guillaume Jacquemet et al. "The cell biologist's guide to super-resolution microscopy". In: *Journal of Cell Science* 133.11 (2020). DOI: 10.1242/jcs.240713.

[432] Erik Meijering. "A bird's-eye view of deep learning in bioimage analysis". In: *Computational and Structural Biotechnology Journal* 18 (2020), pp. 2312–2325. DOI: 10.1016/j.csbj.2020.08.003.

[433] Donald R. Jones, Matthias Schonlau, and William J. Welch. "Efficient Global Optimization of Expensive Black-Box Functions". In: *Journal of Global Optimization* 13.4 (1998), pp. 455–492. DOI: 10.1023/A:1008306431147.

[434] Peter I. Frazier. "Bayesian Optimization". In: *Recent Advances in Optimization and Modeling of Contemporary Problems*. Ed. by Douglas R. Shier. INFORMS, 2018, pp. 255–278. DOI: 10.1287/educ.2018.0188.

[435] Bobak Shahriari et al. "Taking the human out of the loop: A review of Bayesian optimization". In: *Proceedings of the IEEE* 104.1 (2016), pp. 148–175. DOI: 10.1109/JPROC.2015.2494218.

[436] J. Kennedy and R. Eberhart. "Particle swarm optimization". In: *Proceedings of IEEE International Conference on Neural Networks (ICNN)*. Vol. 4. IEEE, 1995, pp. 1942–1948. ISBN: 0-7803-2768-3. DOI: 10.1109/ICNN.1995.488968.

[437] Nikolaus Hansen, Sibylle D. Müller, and Petros Koumoutsakos. "Reducing the Time Complexity of the Derandomized Evolution Strategy with Covariance Matrix Adaptation (CMA-ES)". In: *Evolutionary Computation* 11.1 (2003), pp. 1–18. DOI: 10.1162/106365603321828970.

[438] Jorge Nocedal. "Updating quasi-Newton matrices with limited storage". In: *Mathematics of Computation* 35.151 (1980), pp. 773–773. DOI: 10.1090/S0025-5718-1980-0572855-7.

[439] Benjamin J. Shields et al. "Bayesian reaction optimization as a tool for chemical synthesis". In: *Nature* 590.7844 (2021), pp. 89–96. DOI: 10.1038/s41586-021-03213-y.

[440] Ryan Rhys Griffiths and José Miguel Hernández-Lobato. "Constrained Bayesian optimization for automatic chemical design using variational autoencoders". In: *Chemical Science* 11.2 (2020), pp. 577–586. DOI: 10.1039/c9sc04026a.

[441] Prashant Singh and Andreas Hellander. "Hyperparameter optimization for approximate Bayesian computation". In: *Proceedings - Winter Simulation Conference*. Vol. 2018-Decem. Gothenburg, Sweden: Institute of Electrical and Electronics Engineers Inc., 2019, pp. 1718–1729. ISBN: 9781538665725. DOI: 10.1109/WSC.2018.8632304.

[442] J. Knowles. "ParEGO: a hybrid algorithm with on-line landscape approximation for expensive multiobjective optimization problems". In: *IEEE Transactions on Evolutionary Computation* 10.1 (2006), pp. 50–66. DOI: 10.1109/TEVC.2005.851274.

[443] Matthew W Hoffman and Bobak Shahriari. "Modular mechanisms for Bayesian optimization". In: *NIPS workshop on Bayesian optimization*. 2014, pp. 1–5.

[444] Eric Brochu, Vlad M. Cora, and Nando de Freitas. "A Tutorial on Bayesian Optimization of Expensive Cost Functions, with Application to Active User Modeling and Hierarchical Reinforcement Learning". In: *arXiv preprint* (2010). arXiv: 1012.2599.

[445] Ravikumar Meghana, Harvey Cheng, and Michael McCourt. *Bayesian Optimization 101 | SigOpt*. URL: https://sigopt.com/blog/bayesian-optimization-101/ (visited on 06/28/2021).

[446] Michael Litzkow, Miron Livny, and Matthew Mutka. "Condor–a hunter of idle workstations." In: *8th International Conference on Distributed Computing Systems*. 1988, pp. 104–111. DOI: 10.1109/DCS.1988.12507.

[447] Ruben Martinez-Cantin. "BayesOpt: A Bayesian Optimization Library for Nonlinear Optimization, Experimental Design and Bandits". In: *Journal of Machine Learning Research* 15 (2014), pp. 3915–3919.

[448] Ruben Martinez-Cantin, Kevin Tee, and Michael McCourt. "Practical Bayesian optimization in the presence of outliers". In: *Proceedings of the Twenty-First International Conference on Artificial Intelligence and Statistics*. Ed. by Amos Storkey and Fernando Perez-Cruz. Vol. 84. Proceedings of Machine Learning Research. Banff, Alberta, Canada: PMLR, 2018, pp. 1722–1731.

[449] Andrea Saltelli. "Sensitivity Analysis for Importance Assessment". In: *Risk Analysis* 22.3 (2002), pp. 579–590. DOI: 10.1111/0272-4332.00040.

[450] Jasper Snoek, Hugo Larochelle, and Ryan P. Adams. "Practical Bayesian Optimization of Machine Learning Algorithms". In: *Conference on Neural Information Processing Systems (NIPS)*. Ed. by F. Pereira et al. Lake Tahoe, Nevada, USA: Curran Associates, Inc., 2012.

[451] Ruben Martinez-Cantin et al. "A Bayesian exploration-exploitation approach for optimal online sensing and planning with a visually guided mobile robot". In: *Autonomous Robots* 27.2 (2009), pp. 93–103. DOI: 10.1007/s10514-009-9130-2.

[452] Eric Brochu, Tyson Brochu, and Nando de Freitas. "A Bayesian Interactive Optimization Approach to Procedural Animation Design". In: *Proceedings of the 2010 ACM SIGGRAPH/Eurographics Symposium on Computer Animation*. SCA '10. Madrid, Spain: Eurographics Association, 2010, pp. 103–112. DOI: 10.5555/1921427.1921443.

[453] Wojciech M Czarnecki, Sabina Podlewska, and Andrzej J Bojarski. "Robust optimization of SVM hyperparameters in the classification of bioactive compounds". In: *Journal of Cheminformatics* 7.1 (2015), p. 38. DOI: 10.1186/s13321-015-0088-0.

[454] Peter I. Frazier and Jialei Wang. "Bayesian Optimization for Materials Design". In: *Information Science for Materials Discovery and Design. Springer Series in Materials Science*. Vol. 225. Springer, Cham, 2016. Chap. 3, pp. 45–75. ISBN: 9783319238708. DOI: 10.1007/978-3-319-23871-5_3.

[455] Doniyor Ulmasov et al. "Bayesian Optimization with Dimension Scheduling: Application to Biological Systems". In: *Computer Aided Chemical Engineering* 38 (2016), pp. 1051–1056. DOI: 10.1016/B978-0-444-63428-3.50180-6.

[456] Stewart Greenhill et al. "Bayesian Optimization for Adaptive Experimental Design: A Review". In: *IEEE Access* 8 (2020), pp. 13937–13948. DOI: 10.1109/ACCESS.2020.2966228.

[457] Paul Martin, Susan M Parkhurst, and M Peifer. "Parallels between tissue repair and embryo morphogenesis." In: *Development* 131.13 (2004), pp. 3021–34. DOI: 10.1242/dev.01253.

[458] Anne K. Knecht and Marianne Bronner-Fraser. "Induction of the neural crest: a multigene process". In: *Nature Reviews Genetics* 3.6 (2002), pp. 453–461. DOI: 10.1038/nrg819.

[459] F. Spill et al. "Mesoscopic and continuum modelling of angiogenesis". In: *Journal of Mathematical Biology* 70.3 (2015), pp. 485–532. DOI: 10.1007/s00285-014-0771-1.

[460] Laurent Lamalice, Fabrice Le Boeuf, and Jacques Huot. "Endothelial cell migration during angiogenesis." In: *Circulation research* 100.6 (2007), pp. 782–94. DOI: 10.1161/01.RES.0000259593.07661.1e.

[461] E Reina-Romo et al. “A lattice-based approach to model distraction osteogenesis.” In: *Journal of Biomechanics* 45.16 (2012), pp. 2736–42. DOI: 10.1016/j.jbiomech.2012.09.004.

[462] C. Valero et al. “Nonlinear finite element simulations of injuries with free boundaries: Application to surgical wounds”. In: *International Journal for Numerical Methods in Biomedical Engineering* 30.6 (2014), pp. 616–633. DOI: 10.1002/cnm.2621.

[463] Tanya J. Shaw and Paul Martin. “Wound repair at a glance”. In: *Journal of Cell Science* 122.18 (2009), pp. 3209–3213. DOI: 10.1242/jcs.031187.

[464] John Condeelis and Jeffrey W. Pollard. “Macrophages: Obligate Partners for Tumor Cell Migration, Invasion, and Metastasis”. In: *Cell* 124.2 (2006), pp. 263–266. DOI: 10.1016/J.CELL.2006.01.007.

[465] John Condeelis, Robert H. Singer, and Jeffrey E. Segall. “THE GREAT ESCAPE: When Cancer Cells Hijack the Genes for Chemotaxis and Motility”. In: *Annual Review of Cell and Developmental Biology* 21.1 (2005), pp. 695–718. DOI: 10.1146/annurev.cellbio.21.122303.120306.

[466] Clemens M. Franz, Gareth E. Jones, and Anne J. Ridley. “Cell Migration in Development and Disease”. In: *Developmental Cell* 2.2 (2002), pp. 153–158. DOI: 10.1016/S1534-5807(02)00120-X.

[467] Héctor Vicente Ramírez-Gómez et al. “Sperm chemotaxis is driven by the slope of the chemoattractant concentration field”. In: *eLife* 9 (2020). DOI: 10.7554/ELIFE.50532.

[468] Jeffrey A. Riffell, Patrick J. Krug, and Richard K. Zimmer. “The ecological and evolutionary consequences of sperm chemoattraction”. In: *Proceedings of the National Academy of Sciences* 101.13 (2004), pp. 4501–4506. DOI: 10.1073/PNAS.0304594101.

[469] Fei Sun et al. “Lack of species-specificity in mammalian sperm chemotaxis”. In: *Developmental Biology* 255.2 (2003), pp. 423–427. DOI: 10.1016/S0012-1606(02)00090-8.

[470] Valentina Sasselli, Vassilis Pachnis, and Alan J. Burns. “The enteric nervous system”. In: *Developmental Biology* 366.1 (2012), pp. 64–73. DOI: 10.1016/J.YDBIO.2012.01.012.

[471] Jennifer C. Kasemeier-Kulesa et al. “CXCR4 Controls Ventral Migration of Sympathetic Precursor Cells”. In: *Journal of Neuroscience* 30.39 (2010), pp. 13078–13088. DOI: 10.1523/JNEUROSCI.0892-10.2010.

[472] Eric Theveneau et al. “Collective Chemotaxis Requires Contact-Dependent Cell Polarity”. In: *Developmental Cell* 19.1 (2010), pp. 39–53. DOI: 10.1016/J.DEVCEL.2010.06.012.

[473] Joannie Roy et al. “A Haptotaxis Assay for Neutrophils using Optical Patterning and a High-content Approach”. In: *Scientific Reports* 7.1 (2017), pp. 1–13. DOI: 10.1038/s41598-017-02993-6.

[474] Mieke Metzemaekers, Mieke Gouwy, and Paul Proost. “Neutrophil chemoattractant receptors in health and disease: double-edged swords”. In: *Cellular & Molecular Immunology* 17.5 (2020), pp. 433–450. DOI: 10.1038/s41423-020-0412-0.

[475] Wilhelm Pfeffer. *Locomotorische Richtungsbewegungen durch chemische Reize*. Tübingen, Germany, 1884.

[476] J. Adler. "Chemotaxis in Escherichia coli". In: *Cold Spring Harbor Symposia on Quantitative Biology* 30 (1965), pp. 289–292. DOI: 10.1101/SQB.1965.030.01.030.

[477] Julius Adler. "Chemotaxis in Bacteria". In: *Science* 153.3737 (1966), pp. 708–716. DOI: 10.1126/SCIENCE.153.3737.708.

[478] J. Adler and M. M. Dahl. "A method for measuring the motility of bacteria and for comparing random and non-random motility." In: *Journal of general microbiology* 46.2 (1967), pp. 161–173. DOI: 10.1099/00221287-46-2-161.

[479] Julius Adler. "Chemoreceptors in bacteria". In: *Science* 166.3913 (1969), pp. 1588–1597. DOI: 10.1126/science.166.3913.1588.

[480] Kristen F. Swaney, Chuan-Hsiang Huang, and Peter N. Devreotes. "Eukaryotic Chemotaxis: A Network of Signaling Pathways Controls Motility, Directional Sensing, and Polarity". In: *Annual Review of Biophysics* 39.1 (2010), pp. 265–289. DOI: 10.1146/annurev.biophys.093008.131228.

[481] Tim Lämmermann et al. "Rapid leukocyte migration by integrin-independent flowing and squeezing". In: *Nature* 453.7191 (2008), pp. 51–55. DOI: 10.1038/nature06887.

[482] Catherine Beauchemin, Narendra M. Dixit, and Alan S. Perelson. "Characterizing T Cell Movement within Lymph Nodes in the Absence of Antigen". In: *The Journal of Immunology* 178.9 (2007), pp. 5505–5512. DOI: 10.4049/jimmunol.178.9.5505.

[483] Ryan J. Petrie et al. "Activating the nuclear piston mechanism of 3D migration in tumor cells". In: *Journal of Cell Biology* 216.1 (2017), pp. 93–100. DOI: 10.1083/jcb.201605097.

[484] O. Moreno-Arotzena et al. "Fibroblast Migration in 3D is Controlled by Haptotaxis in a Non-muscle Myosin II-Dependent Manner". In: *Annals of Biomedical Engineering* 43.12 (2015), pp. 3025–3039. DOI: 10.1007/s10439-015-1343-2.

[485] Yu-Ren Liou et al. "Substrate Stiffness Regulates Filopodial Activities in Lung Cancer Cells". In: *PLoS ONE* 9.2 (2014). Ed. by Chih-Hsin Tang, e89767. DOI: 10.1371/journal.pone.0089767.

[486] Michael C. Weiger et al. "Directional Persistence of Cell Migration Coincides with Stability of Asymmetric Intracellular Signaling". In: *Biophysical Journal* 98.1 (2010), pp. 67–75. DOI: 10.1016/J.BPJ.2009.09.051.

[487] O. Moreno-Arotzena et al. "Inducing chemotactic and haptotactic cues in microfluidic devices for three- dimensional in vitro assays". In: *Biomicrofluidics* 8.6 (2014), p. 064122. DOI: 10.1063/1.4903948.

[488] Josefine Starke et al. "Mechanotransduction of mesenchymal melanoma cell invasion into 3D collagen lattices: Filopod-mediated extension–relaxation cycles and force anisotropy". In: *Experimental Cell Research* 319.16 (2013), pp. 2424–2433. DOI: 10.1016/J.YEXCR.2013.04.003.

[489] Kenneth G. Campellone and Matthew D. Welch. "A nucleator arms race: cellular control of actin assembly". In: *Nature Reviews Molecular Cell Biology* 11.4 (2010), pp. 237–251. DOI: 10.1038/nrm2867.

[490] Jiqing Sai et al. "Parallel phosphatidylinositol 3-kinase (PI3K)-dependent and Src-dependent pathways lead to CXCL8-mediated Rac2 activation and chemotaxis". In: *Journal of Biological Chemistry* 283.39 (2008), pp. 26538–26547. DOI: 10.1074/jbc.M805611200.

[491] Lingfeng Chen et al. “PLA2 and PI3K/PTEN Pathways Act in Parallel to Mediate Chemotaxis”. In: *Developmental Cell* 12.4 (2007), pp. 603–614. DOI: 10.1016/J.DEVCEL.2007.03.005.

[492] Satheesh Elangovan et al. “The enhancement of bone regeneration by gene activated matrix encoding for platelet derived growth factor”. In: *Biomaterials* 35.2 (2014), pp. 737–747. DOI: 10.1016/J.BIOMATERIALS.2013.10.021.

[493] Prasun Shah, Louise Keppler, and James Rutkowski. “A Review of Platelet Derived Growth Factor Playing Pivotal Role in Bone Regeneration”. In: *Journal of Oral Implantology* 40.3 (2014), pp. 330–340. DOI: 10.1563/AAID-JOI-D-11-00173.

[494] Gary E Friedlaender et al. “The role of recombinant human platelet-derived growth factor-BB (rhPDGF-BB) in orthopaedic bone repair and regeneration.” In: *Current Pharmaceutical Design* 19.19 (2013), pp. 3384–90. DOI: 10.2174/1381612811319190005.

[495] Ruth R. Chen et al. “Spatio–temporal VEGF and PDGF Delivery Patterns Blood Vessel Formation and Maturation”. In: *Pharmaceutical Research* 24.2 (2007), pp. 258–264. DOI: 10.1007/s11095-006-9173-4.

[496] Masahiro Ueda and Tatsuo Shibata. “Stochastic Signal Processing and Transduction in Chemotactic Response of Eukaryotic Cells”. In: *Biophysical Journal* 93.1 (2007), pp. 11–20. DOI: 10.1529/BIOPHYSJ.106.100263.

[497] Roshanak Irannejad et al. “Effects of endocytosis on receptor-mediated signaling”. In: *Current Opinion in Cell Biology* 35 (2015), pp. 137–143. DOI: 10.1016/J.CEB.2015.05.005.

[498] Alexander Sorkin and Mark von Zastrow. “Endocytosis and signalling: intertwining molecular networks”. In: *Nature Reviews Molecular Cell Biology* 10.9 (2009), pp. 609–622. DOI: 10.1038/nrm2748.

[499] Evan A. Saltzman et al. “Simulating Multivariate Nonhomogeneous Poisson Processes Using Projections”. In: *ACM Transactions on Modeling and Computer Simulation* 22.3 (2012), pp. 1–13. DOI: 10.1145/2331140.2331143.

[500] Sandra Pérez-Rodríguez, Esther Tomás-González, and José García-Aznar. “3D Cell Migration Studies for Chemotaxis on Microfluidic-Based Chips: A Comparison between Cardiac and Dermal Fibroblasts”. In: *Bioengineering* 5.2 (2018), p. 45. DOI: 10.3390/bioengineering5020045.

[501] Erik S. Welf et al. “Migrating fibroblasts reorient directionality: By a metastable, PI3K-dependent mechanism”. In: *Journal of Cell Biology* 197.1 (2012), pp. 105–114. DOI: 10.1083/jcb.201108152.

[502] Ryan J. Petrie, Andrew D. Doyle, and Kenneth M. Yamada. “Random versus directionally persistent cell migration”. In: *Nature Reviews Molecular Cell Biology* 10.8 (2009), pp. 538–549. DOI: 10.1038/nrm2729.

[503] Anne J. Ridley et al. “Cell Migration: Integrating Signals from Front to Back”. In: *Science* 302.5651 (2003), pp. 1704–1709. DOI: 10.1126/science.1092053.

[504] Jiao Chen, Daphne Weihs, and Fred J. Vermolen. “A model for cell migration in non-isotropic fibrin networks with an application to pancreatic tumor islets”. In: *Biomechanics and Modeling in Mechanobiology* (2017), pp. 1–20. DOI: 10.1007/s10237-017-0966-7.

[505] Alexandra Jilkine and Leah Edelstein-Keshet. “A Comparison of Mathematical Models for Polarization of Single Eukaryotic Cells in Response to Guided Cues”. In: *PLoS Computational Biology* 7.4 (2011). Ed. by Jason M. Haugh, e1001121. DOI: 10.1371/journal.pcbi.1001121.

[506] J. D. Eshelby. "The Determination of the Elastic Field of an Ellipsoidal Inclusion, and Related Problems". In: *Proceedings of the Royal Society A: Mathematical, Physical and Engineering Sciences* 241.1226 (1957), pp. 376–396. DOI: 10.1098/rspa.1957.0133.

[507] C. Del Amo et al. "Quantifying 3D chemotaxis in microfluidic-based chips with step gradients of collagen hydrogel concentrations". In: *Integrative Biology* 9.4 (2017), pp. 339–349. DOI: 10.1039/C7IB00022G.

[508] C. Borau, R. D. Kamm, and J. M. García-Aznar. "Mechano-sensing and cell migration: A 3D model approach". In: *Physical Biology* 8.6 (2011), pp. 66008–13. DOI: 10.1088/1478-3975/8/6/066008.

[509] Charles R. Harris et al. "Array programming with NumPy". In: *Nature* 585.7825 (2020), pp. 357–362. DOI: 10.1038/s41586-020-2649-2.

[510] Pauli Virtanen et al. "SciPy 1.0: fundamental algorithms for scientific computing in Python". In: *Nature Methods* 17.3 (2020), pp. 261–272. DOI: 10.1038/s41592-019-0686-2.

[511] Daniel T Gillespie. "A general method for numerically simulating the stochastic time evolution of coupled chemical reactions". In: *Journal of Computational Physics* 22.4 (1976), pp. 403–434. DOI: 10.1016/0021-9991(76)90041-3.

[512] Daniel T. Gillespie. "Exact stochastic simulation of coupled chemical reactions". In: *The Journal of Physical Chemistry* 81.25 (1977), pp. 2340–2361. DOI: 10.1021/j100540a008.

[513] Yang Cao, Daniel T. Gillespie, and Linda R. Petzold. "Efficient step size selection for the tau-leaping simulation method". In: *The Journal of Chemical Physics* 124.4 (2006), p. 044109. DOI: 10.1063/1.2159468.

[514] Daniel T. Gillespie. "Approximate accelerated stochastic simulation of chemically reacting systems". In: *The Journal of Chemical Physics* 115.4 (2001), pp. 1716–1733. DOI: 10.1063/1.1378322.

[515] Larry Lok. "The need for speed in stochastic simulation". In: *Nature Biotechnology* 22.8 (2004), pp. 964–965. DOI: 10.1038/nbt0804-964.

[516] Paolo Cazzaniga et al. "Tau Leaping Stochastic Simulation Method in P Systems". In: *International Workshop on Membrane Computing*. Springer, Berlin, Heidelberg, 2006, pp. 298–313. DOI: 10.1007/11963516_19.

[517] David F. Anderson, Arnab Ganguly, and Thomas G. Kurtz. "Error analysis of tau-leap simulation methods". In: *The Annals of Applied Probability* 21.6 (2011), pp. 2226–2262. DOI: 10.1214/10-AAP756.

[518] Vishwas M. Paralkar et al. "Recombinant human bone morphogenetic protein 2B stimulates PC12 cell differentiation: Potentiation and binding to type IV collagen". In: *Journal of Cell Biology* 119.6 (1992), pp. 1721–1728. DOI: 10.1083/jcb.119.6.1721.

[519] Mariko Hatakeyama et al. "A computational model on the modulation of mitogen-activated protein kinase (MAPK) and Akt pathways in heregulin-induced ErbB signalling." In: *The Biochemical journal* 373.Pt 2 (2003), pp. 451–63. DOI: 10.1042/BJ20021824.

[520] Kai Heinecke et al. "Receptor oligomerization and beyond: a case study in bone morphogenetic proteins". In: *BMC Biology* 7.1 (2009), p. 59. DOI: 10.1186/1741-7007-7-59.

[521] Stephanie I. I. Fraley et al. “A distinctive role for focal adhesion proteins in three-dimensional cell motility”. In: *Nature Cell Biology* 12.6 (2010), pp. 598–604. DOI: 10.1038/ncb2062.

[522] Dorin Comaniciu, Visvanathan Ramesh, and Peter Meer. “Real-time tracking of non-rigid objects using mean shift”. In: *Proceedings of the IEEE Computer Society Conference on Computer Vision and Pattern Recognition*. Vol. 2. IEEE Comput. Soc, 2000, pp. 142–149. ISBN: 0-7695-0662-3. DOI: 10.1109/CVPR.2000.854761.

[523] Frank Nielsen. “Generalized Bhattacharyya and Chernoff upper bounds on Bayes error using quasi-arithmetic means”. In: *Pattern Recognition Letters* 42 (2014), pp. 25–34. DOI: 10.1016/J.PATREC.2014.01.002.

[524] Robert E. Kass and Adrian E. Raftery. “Bayes Factors”. In: *Journal of the American Statistical Association* 90.430 (1995), p. 773. DOI: 10.2307/2291091.

[525] Leonard Bosgraaf and Peter J. M. Van Haastert. “Navigation of Chemotactic Cells by Parallel Signaling to Pseudopod Persistence and Orientation”. In: *PLoS ONE* 4.8 (2009). Ed. by Terry Means, e6842. DOI: 10.1371/journal.pone.0006842.

[526] Loling Song et al. “Dictyostelium discoideum chemotaxis: Threshold for directed motion”. In: *European Journal of Cell Biology* 85.9-10 (2006), pp. 981–989. DOI: 10.1016/J.EJCB.2006.01.012.

[527] Tong Li et al. “Molecular investigation of the mechanical properties of single actin filaments based on vibration analyses”. In: *Computer Methods in Biomechanics and Biomedical Engineering* 17.6 (2014), pp. 616–622. DOI: 10.1080/10255842.2012.706279.

[528] Mohammad R. K. Mofrad and Roger D. Kamm, eds. *Cytoskeletal Mechanics : Models and Measurements in Cell Mechanics*. Cambridge University Press, 2006, p. 256. ISBN: 9780511607318. DOI: 10.1017/CBO9780511607318.

[529] Alina De Donatis et al. “Proliferation versus migration in platelet-derived growth factor signaling: The key role of endocytosis”. In: *Journal of Biological Chemistry* 283.29 (2008), pp. 19948–19956. DOI: 10.1074/jbc.M709428200.

[530] Rajagopal Rangarajan and Muhammad H. Zaman. “Modeling cell migration in 3D”. In: *Cell Adhesion & Migration* 2.2 (2008), pp. 106–109. DOI: 10.4161/cam.2.2.6211.

[531] Daniel T Gillespie. “Stochastic Simulation of Chemical Kinetics”. In: *Annu. Rev. Phys. Chem* 58 (2007), pp. 35–55. DOI: 10.1146/annurev.physchem.58.032806.104637.

[532] Katrin Talkenberger et al. “Amoeboid-mesenchymal migration plasticity promotes invasion only in complex heterogeneous microenvironments”. In: *Scientific Reports* 7.1 (2017), p. 9237. DOI: 10.1038/s41598-017-09300-3.

[533] Josephine T. Daub and Roeland M. H. Merks. “A Cell-Based Model of Extracellular-Matrix-Guided Endothelial Cell Migration During Angiogenesis”. In: *Bulletin of Mathematical Biology* 75.8 (2013), pp. 1377–1399. DOI: 10.1007/s11538-013-9826-5.

[534] F. J. Vermolen and E. Javierre. “A finite-element model for healing of cutaneous wounds combining contraction, angiogenesis and closure”. In: *Journal of Mathematical Biology* 65.5 (2012), pp. 967–996. DOI: 10.1007/s00285-011-0487-4.

[535] Amy L. Bauer, Trachette L. Jackson, and Yi Jiang. "Topography of Extracellular Matrix Mediates Vascular Morphogenesis and Migration Speeds in Angiogenesis". In: *PLoS Computational Biology* 5.7 (2009). Ed. by András Czirók, e1000445. DOI: 10.1371/journal.pcbi.1000445.

[536] Katie Bentley et al. "Tipping the Balance: Robustness of Tip Cell Selection, Migration and Fusion in Angiogenesis". In: *PLoS Computational Biology* 5.10 (2009). Ed. by Rama Ranganathan, e1000549. DOI: 10.1371/journal.pcbi.1000549.

[537] Anna Haeger et al. "Collective cell migration: guidance principles and hierarchies". In: *Trends in Cell Biology* 25.9 (2015), pp. 556–566. DOI: 10.1016/j.tcb.2015.06.003.

[538] Chi-Li Chiu et al. "Nanoimaging of Focal Adhesion Dynamics in 3D". In: *PLoS ONE* 9.6 (2014). Ed. by Maddy Parsons, e99896. DOI: 10.1371/journal.pone.0099896.

[539] William Y. Wang et al. "Actomyosin contractility-dependent matrix stretch and recoil induces rapid cell migration". In: *Nature Communications* 10.1 (2019), p. 1186. DOI: 10.1038/s41467-019-09121-0.

[540] Stefan Hoehme and Dirk Drasdo. "A cell-based simulation software for multi-cellular systems". In: *Bioinformatics* 26.20 (2010), pp. 2641–2642. DOI: 10.1093/bioinformatics/btq437.

[541] Daniela K. Schlüter, Ignacio Ramis-Conde, and Mark A.J. Chaplain. "Computational Modeling of Single-Cell Migration: The Leading Role of Extracellular Matrix Fibers". In: *Biophysical Journal* 103.6 (2012), pp. 1141–1151. DOI: 10.1016/J.BPJ.2012.07.048.

[542] Fong Yin Lim, Yen Ling Koon, and Keng-Hwee Chiam. "A computational model of amoeboid cell migration". In: *Computer Methods in Biomechanics and Biomedical Engineering* 16.10 (2013), pp. 1085–1095. DOI: 10.1080/10255842.2012.757598.

[543] Amit Singh et al. "Boolean approach to signalling pathway modelling in HGF-induced keratinocyte migration". In: *Bioinformatics* 28.18 (2012), pp. i495–i501. DOI: 10.1093/bioinformatics/bts410.

[544] Zhihui Wang et al. "Cross-scale, cross-pathway evaluation using an agent-based non-small cell lung cancer model". In: *Bioinformatics* 25.18 (2009), pp. 2389–2396. DOI: 10.1093/bioinformatics/btp416.

[545] Jorge Escribano et al. "Balance of mechanical forces drives endothelial gap formation and may facilitate cancer and immune-cell extravasation". In: *PLOS Computational Biology* 15.5 (2019). Ed. by Andrew D. McCulloch, e1006395. DOI: 10.1371/journal.pcbi.1006395.

[546] Miquel Marin-Riera et al. "Computational modeling of development by epithelia, mesenchyme and their interactions: A unified model". In: *Bioinformatics* 32.2 (2016), pp. 219–225. DOI: 10.1093/bioinformatics/btv527.

[547] Marco Scianna, Luigi Preziosi, and Katarina Wolf. "A Cellular Potts model simulating cell migration on and in matrix environments". In: *Mathematical Biosciences and Engineering* 10.1 (2012), pp. 235–261. DOI: 10.3934/mbe.2013.10.235.

[548] P. Van Liedekerke et al. "Simulating tissue mechanics with agent-based models: concepts, perspectives and some novel results". In: *Computational Particle Mechanics* 2.4 (2015), pp. 401–444. DOI: 10.1007/s40571-015-0082-3.

[549] Florian Milde et al. “SEM++: A particle model of cellular growth, signaling and migration”. In: *Computational Particle Mechanics* 1.2 (2014), pp. 211–227. DOI: 10.1007/s40571-014-0017-4.

[550] Nieves Movilla. “Análisis del efecto de la matriz extracelular en la migración 3D de fibroblastos y osteoblastos humanos. / Nieves Movilla Meno”. PhD thesis. University of Zaragoza, 2021.

[551] Achilleas D. Theocharis et al. “Extracellular matrix structure”. In: *Advanced Drug Delivery Reviews* 97 (2016), pp. 4–27. DOI: 10.1016/j.addr.2015.11.001.

[552] Carlos F. Guimarães et al. “The stiffness of living tissues and its implications for tissue engineering”. In: *Nature Reviews Materials* 5.5 (2020), pp. 351–370. DOI: 10.1038/s41578-019-0169-1.

[553] Kaeuis A. Faraj, Toin H. Van Kuppevelt, and Willeke F. Daamen. “Construction of collagen scaffolds that mimic the three-dimensional architecture of specific tissues”. In: *Tissue Engineering* 13.10 (2007), pp. 2387–2394. DOI: 10.1089/ten.2006.0320.

[554] Pia Ringer et al. “Sensing the mechano-chemical properties of the extracellular matrix”. In: *Matrix Biology* 64 (2017), pp. 6–16. DOI: 10.1016/J.MATBIO.2017.03.004.

[555] Matthew G Rubashkin et al. “Force engages vinculin and promotes tumor progression by enhancing PI3K activation of phosphatidylinositol (3,4,5)-triphosphate.” In: *Cancer research* 74.17 (2014), pp. 4597–611. DOI: 10.1158/0008-5472.CAN-13-3698.

[556] Katarina Wolf et al. “Multi-step pericellular proteolysis controls the transition from individual to collective cancer cell invasion”. In: *Nature Cell Biology* 9.8 (2007), pp. 893–904. DOI: 10.1038/ncb1616.

[557] Tony Fischer, Alexander Hayn, and Claudia Tanja Mierke. “Effect of Nuclear Stiffness on Cell Mechanics and Migration of Human Breast Cancer Cells”. In: *Frontiers in Cell and Developmental Biology* 8 (2020), p. 393. DOI: 10.3389/FCELL.2020.00393/BIBTEX.

[558] Katarina Wolf et al. “Physical limits of cell migration: Control by ECM space and nuclear deformation and tuning by proteolysis and traction force”. In: *Journal of Cell Biology* 201.7 (2013), pp. 1069–1084. DOI: 10.1083/jcb.201210152.

[559] Carmela Rianna and Manfred Radmacher. “Comparison of viscoelastic properties of cancer and normal thyroid cells on different stiffness substrates”. In: *European Biophysics Journal* 46.4 (2017), pp. 309–324. DOI: 10.1007/s00249-016-1168-4.

[560] Haijiao Liu, Yu Sun, and Craig A. Simmons. “Determination of local and global elastic moduli of valve interstitial cells cultured on soft substrates”. In: *Journal of Biomechanics* 46.11 (2013), pp. 1967–1971. DOI: 10.1016/J.JBIOMECH.2013.05.001.

[561] Anant Chopra et al. “Cardiac myocyte remodeling mediated by N-cadherin-dependent mechanosensing”. In: *American Journal of Physiology-Heart and Circulatory Physiology* 300.4 (2011), pp. 1252–1266. DOI: 10.1152/AJPHEART.00515.2010.

[562] Shang You Tee et al. “Cell Shape and Substrate Rigidity Both Regulate Cell Stiffness”. In: *Biophysical Journal* 100.5 (2011), pp. L25–L27. DOI: 10.1016/J.BPJ.2010.12.3744.

[563] Jérôme Solon et al. “Fibroblast Adaptation and Stiffness Matching to Soft Elastic Substrates”. In: *Biophysical Journal* 93.12 (2007), pp. 4453–4461. DOI: 10.1529/BIOPHYSJ.106.101386.

[564] Fabian Pedregosa et al. "Scikit-learn: Machine learning in Python". In: *Journal of Machine Learning Research* 12 (2011), pp. 2825–2830.

[565] A. A. Malik, B. Wennberg, and P. Gerlee. "The Impact of Elastic Deformations of the Extracellular Matrix on Cell Migration". In: *Bulletin of Mathematical Biology* 82.4 (2020), pp. 1–19. DOI: 10.1007/s11538-020-00721-2.

[566] Chun Min Lo et al. "Cell Movement Is Guided by the Rigidity of the Substrate". In: *Biophysical Journal* 79.1 (2000), pp. 144–152. DOI: 10.1016/S0006-3495(00)76279-5.

[567] Shawn P. Carey, Karen E. Martin, and Cynthia A. Reinhart-King. "Three-dimensional collagen matrix induces a mechanosensitive invasive epithelial phenotype". In: *Scientific Reports* 7.1 (2017), p. 42088. DOI: 10.1038/srep42088.

[568] Weijing Han et al. "Oriented collagen fibers direct tumor cell intravasation". In: *Proceedings of the National Academy of Sciences of the United States of America* 113.40 (2016). DOI: 10.1073/pnas.1610347113.

[569] Carmela Rianna, Manfred Radmacher, and Sanjay Kumar. "Direct evidence that tumor cells soften when navigating confined spaces". In: *Molecular Biology of the Cell* 31.16 (2020), pp. 1726–1734. DOI: 10.1091/MBC.E19-10-0588/ASSET/IMAGES/LARGE/MBC-31-1726-G007.JPEG.

[570] Johannes Rheinlaender et al. "Cortical cell stiffness is independent of substrate mechanics". In: *Nature Materials* 19.9 (2020), pp. 1019–1025. DOI: 10.1038/s41563-020-0684-x.

[571] Léa Trichet et al. "Evidence of a large-scale mechanosensing mechanism for cellular adaptation to substrate stiffness." In: *Proceedings of the National Academy of Sciences of the United States of America* 109.18 (2012), pp. 6933–8. DOI: 10.1073/pnas.1117810109.

[572] Daoxiang Huang et al. "Characterization of 3D matrix conditions for cancer cell migration with elasticity/porosity-independent tunable microfiber gels". In: *Polymer Journal* 52.3 (2019), pp. 333–344. DOI: 10.1038/s41428-019-0283-3.

[573] Lingling Liu et al. "Nucleus and nucleus-cytoskeleton connections in 3D cell migration". In: *Experimental Cell Research* 348.1 (2016), pp. 56–65. DOI: 10.1016/J.YEXCR.2016.09.001.

[574] Patrizia Romani et al. "Crosstalk between mechanotransduction and metabolism". In: *Nature Reviews Molecular Cell Biology* 22.1 (2021), pp. 22–38. DOI: 10.1038/s41580-020-00306-w.

[575] Fei Wang. "The Signaling Mechanisms Underlying Cell Polarity and Chemotaxis". In: *Cold Spring Harbor Perspectives in Biology* 1.4 (2009), a002980. DOI: 10.1101/CSHPERSPECT.A002980.

[576] M. Ehrbar et al. "Elucidating the role of matrix stiffness in 3D cell migration and remodeling". In: *Biophysical Journal* 100.2 (2011), pp. 284–293. DOI: 10.1016/j.bpj.2010.11.082.

[577] Muhammad H. Zaman et al. "Migration of tumor cells in 3D matrices is governed by matrix stiffness along with cell-matrix adhesion and proteolysis". In: *Proceedings of the National Academy of Sciences of the United States of America* 103.29 (2006), pp. 10889–10894. DOI: 10.1073/pnas.0604460103.

[578] Yanyan Han. "Analysis of the role of the Hippo pathway in cancer". In: *Journal of Translational Medicine 2019 17:1* 17.1 (2019), pp. 1–17. DOI: 10.1186/S12967-019-1869-4.

[579] Xianjue Ma et al. “Hippo signaling promotes JNK-dependent cell migration”. In: *Proceedings of the National Academy of Sciences of the United States of America* 114.8 (2017), pp. 1934–1939. DOI: 10.1073/PNAS.1621359114.

[580] Wan Jiao Gao et al. “Suppression of macrophage migration by down-regulating Src/FAK/P130Cas activation contributed to the anti-inflammatory activity of sinomenine”. In: *Pharmacological Research* 167 (2021), p. 105513. DOI: 10.1016/J.PHRS.2021.105513.

[581] Yu Sen Peng et al. “BSA-bounded p-cresyl sulfate potentiates the malignancy of bladder carcinoma by triggering cell migration and EMT through the ROS/Src/FAK signaling pathway”. In: *Cell Biology and Toxicology* 36.4 (2020), pp. 287–300. DOI: 10.1007/s10565-019-09509-0.

[582] Wangmi Liu et al. “CX3CL1 promotes lung cancer cell migration and invasion via the Src/focal adhesion kinase signaling pathway”. In: *Oncology Reports* 41.3 (2019), pp. 1911–1917. DOI: 10.3892/or.2019.6957.

[583] Peng Liu et al. “CX3CL1/fractalkine enhances prostate cancer spinal metastasis by activating the Src/FAK pathway”. In: *International Journal of Oncology* 53.4 (2018), pp. 1544–1556. DOI: 10.3892/ijo.2018.4487.

[584] Zong Lin Chen et al. “INHBA gene silencing inhibits gastric cancer cell migration and invasion by impeding activation of the TGF-β signaling pathway”. In: *Journal of Cellular Physiology* 234.10 (2019), pp. 18065–18074. DOI: 10.1002/JCP.28439.

[585] Norelia Torrealba et al. “TGF-β/PI3K/AKT/mTOR/NF-kB pathway. Clinicopathological features in prostate cancer”. In: *https://doi.org/10.1080/13685538.2019.1597840* 23.5 (2019), pp. 801–811. DOI: 10.1080/13685538.2019.1597840.

[586] Anahita Hamidi et al. “TGF-β promotes PI3K-AKT signaling and prostate cancer cell migration through the TRAF6-mediated ubiquitylation of p85α”. In: *Science Signaling* 10.486 (2017). DOI: 10.1126/scisignal.aal4186.

[587] Zane R Thornburg et al. “Fundamental behaviors emerge from simulations of a living minimal cell”. In: *Cell* 185.2 (2022), 345–360.e28. DOI: 10.1016/J.CELL.2021.12.025.

[588] Adrien Coulier, Stefan Hellander, and Andreas Hellander. “A multiscale compartment-based model of stochastic gene regulatory networks using hitting-time analysis”. In: *The Journal of Chemical Physics* 154.18 (2021), p. 184105. DOI: 10.1063/5.0010764.

[589] Stefan Hellander and Andreas Hellander. “Hierarchical algorithm for the reaction-diffusion master equation”. In: *Journal of Chemical Physics* 152.3 (2020), p. 034104. DOI: 10.1063/1.5095075.

[590] Ossama Moujaber and Ursula Stochaj. “The Cytoskeleton as Regulator of Cell Signaling Pathways”. In: *Trends in Biochemical Sciences* 45.2 (2020), pp. 96–107. DOI: 10.1016/j.tibs.2019.11.003.

[591] Hugo Lavoie, Jessica Gagnon, and Marc Therrien. “ERK signalling: a master regulator of cell behaviour, life and fate”. In: *Nature Reviews Molecular Cell Biology* 21.10 (2020), pp. 607–632. DOI: 10.1038/s41580-020-0255-7.

[592] Naoya Hino et al. “ERK-Mediated Mechanochemical Waves Direct Collective Cell Polarization”. In: *Developmental Cell* 53.6 (2020), 646–660.e8. DOI: 10.1016/j.devcel.2020.05.011.

[593] Amine Mehidi et al. "Forces generated by lamellipodial actin filament elongation regulate the WAVE complex during cell migration". In: *Nature Cell Biology* 23.11 (2021), pp. 1148–1162. DOI: 10.1038/s41556-021-00786-8.

[594] Shashi Prakash Singh, Peter A. Thomason, and Robert H. Insall. "Extracellular Signalling Modulates Scar/WAVE Complex Activity through Abi Phosphorylation". In: *Cells* 10.12 (2021), p. 3485. DOI: 10.3390/CELLS10123485.

[595] Jamie A. Whitelaw et al. "The WAVE Regulatory Complex Is Required to Balance Protrusion and Adhesion in Migration". In: *Cells* 9.7 (2020), p. 1635. DOI: 10.3390/cells9071635.

[596] Hui Guo et al. "Cancer Physical Hallmarks as New Targets for Improved Immunotherapy". In: *Trends in Cell Biology* 31.7 (2021), pp. 520–524. DOI: 10.1016/J.TCB.2021.03.011.

[597] Emma Wrenn, Yin Huang, and Kevin Cheung. "Collective metastasis: coordinating the multicellular voyage". In: *Clinical & Experimental Metastasis* 38.4 (2021), pp. 373–399. DOI: 10.1007/S10585-021-10111-0.

[598] Vanesa L. Silvestri et al. "A Tissue-Engineered 3D Microvessel Model Reveals the Dynamics of Mosaic Vessel Formation in Breast Cancer". In: *Cancer Research* 80.19 (2020), pp. 4288–4301. DOI: 10.1158/0008-5472.CAN-19-1564.

[599] Peter Friedl et al. "Classifying collective cancer cell invasion". In: *Nature Cell Biology* 14.8 (2012), pp. 777–783. DOI: 10.1038/ncb2548.

[600] Yelena Y Bernadskaya et al. "Supracellular organization confers directionality and mechanical potency to migrating pairs of cardiopharyngeal progenitor cells". In: *eLife* 10 (2021). DOI: 10.7554/ELIFE.70977.

[601] Gema Malet-Engra et al. "Collective Cell Motility Promotes Chemotactic Prowess and Resistance to Chemorepulsion". In: *Current Biology* 25.2 (2015), pp. 242–250. DOI: 10.1016/J.CUB.2014.11.030.

[602] Elizabeth Pauline Wolf. "EXPERIMENTAL STUDIES ON INFLAMMATION I. THE INFLUENCE OF CHEMICALS UPON THE CHEMOTAXIS OF LEUCOCYTES IN VITRO." In: *Journal of Experimental Medicine* 34.4 (1921), pp. 375–396. DOI: 10.1084/JEM.34.4.375.

[603] S J Holmes. "The behavior of the epidermis of amphibians when cultivated outside the body". In: *Journal of Experimental Zoology* 17.2 (1914), pp. 281–295.

[604] Eduard Uhlenhuth. "CULTIVATION OF THE SKIN EPITHELIUM OF THE ADULT FROG, RANA PIPIENS". In: *Journal of Experimental Medicine* 20.6 (1914), pp. 614–634. DOI: 10.1084/JEM.20.6.614.

[605] Ross Granville Harrison. "The outgrowth of the nerve fiber as a mode of protoplasmic movement". In: *Journal of Experimental Zoology* 9.4 (1910), pp. 787–846.

[606] Dietrich Barfurth. "Zur regeneration der gewebe". In: *Archiv für mikroskopische Anatomie* 37.1 (1891), pp. 406–491.

[607] Alexander S. Hauser et al. "GPCR activation mechanisms across classes and macro/microscales". In: *Nature Structural & Molecular Biology* 28.11 (2021), pp. 879–888. DOI: 10.1038/s41594-021-00674-7.

[608] Halil Bagci et al. "Mapping the proximity interaction network of the Rho-family GTPases reveals signalling pathways and regulatory mechanisms". In: *Nature Cell Biology* 22.1 (2020), pp. 120–134. DOI: 10.1038/s41556-019-0438-7.

[609] Madison A. Rogers and Katherine A. Fantauzzo. "The emerging complexity of PDGFRs: activation, internalization and signal attenuation". In: *Biochemical Society Transactions* 48.3 (2020), pp. 1167–1176. DOI: 10.1042/BST20200004.

[610] Claudia Loebel, Robert L. Mauck, and Jason A. Burdick. "Local nascent protein deposition and remodelling guide mesenchymal stromal cell mechanosensing and fate in three-dimensional hydrogels". In: *Nature Materials* 18.8 (2019), pp. 883–891. DOI: 10.1038/s41563-019-0307-6.

[611] Ivan de Curtis. "Biomolecular Condensates at the Front: Cell Migration Meets Phase Separation". In: *Trends in Cell Biology* 31.3 (2021), pp. 145–148. DOI: 10.1016/j.tcb.2020.12.002.

[612] Vinay Swaminathan and Martijn Gloerich. "Decoding mechanical cues by molecular mechanotransduction". In: *Current Opinion in Cell Biology* 72 (2021), pp. 72–80. DOI: 10.1016/J.CEB.2021.05.006.

[613] Heming Ge et al. "Extracellular Matrix Stiffness: New Areas Affecting Cell Metabolism". In: *Frontiers in Oncology* 11 (2021), p. 8. DOI: 10.3389/fonc.2021.631991.

[614] Jing Xie et al. "Energy expenditure during cell spreading influences the cellular response to matrix stiffness". In: *Biomaterials* 267 (2021), p. 120494. DOI: 10.1016/J.BIOMATERIALS.2020.120494.

[615] Jack R. Staunton et al. "High-frequency microrheology in 3D reveals mismatch between cytoskeletal and extracellular matrix mechanics". In: *Proceedings of the National Academy of Sciences of the United States of America* 116.29 (2019), pp. 14448–14455. DOI: 10.1073/pnas.1814271116.

[616] Alberto Elosegui-Artola and Roger Oria. "Cell Migration: Deconstructing the Matrix". In: *Current Biology* 30.20 (2020), R1266–R1268. DOI: 10.1016/j.cub.2020.08.013.

[617] Michael J Lawson et al. "A positive feedback loop involving the Spa2 SHD domain contributes to focal polarization". In: *PLOS ONE* 17.2 (2022). Ed. by Robert Alan Arkowitz, e0263347. DOI: 10.1371/JOURNAL.PONE.0263347.

[618] Greg M. Allen et al. "Cell Mechanics at the Rear Act to Steer the Direction of Cell Migration". In: *Cell Systems* 11.3 (2020), 286–299.e4. DOI: 10.1016/j.cels.2020.08.008.

[619] Edouard Hannezo and Carl-Philipp Heisenberg. "Mechanochemical Feedback Loops in Development and Disease." In: *Cell* 178.1 (2019), pp. 12–25. DOI: 10.1016/j.cell.2019.05.052.

[620] Lauren A Hapach et al. "Phenotypic Heterogeneity and Metastasis of Breast Cancer Cells". In: *Cancer Research* 81.13 (2021), pp. 3649–3663. DOI: 10.1158/0008-5472.CAN-20-1799.

[621] Jude M. Phillip et al. "Fractional re-distribution among cell motility states during ageing". In: *Communications Biology* 4.1 (2021), p. 81. DOI: 10.1038/s42003-020-01605-w.

[622] Siiri I. Salomaa et al. "SHANK3 conformation regulates direct actin binding and crosstalk with Rap1 signaling". In: *Current Biology* 31.22 (2021), 4956–4970.e9. DOI: 10.1016/J.CUB.2021.09.022.

[623] Nils C. Gauthier and Pere Roca-Cusachs. "Mechanosensing at integrin-mediated cell–matrix adhesions: from molecular to integrated mechanisms". In: *Current Opinion in Cell Biology* 50 (2018), pp. 20–26. DOI: 10.1016/J.CEB.2017.12.014.

[624] Valentin Laplaud et al. “Pinching the cortex of live cells reveals thickness instabilities caused by myosin II motors”. In: *Science Advances* 7.27 (2021). DOI: 10.1126/sciadv.abe3640.

[625] Kamen P. Simeonov et al. “Single-cell lineage tracing of metastatic cancer reveals selection of hybrid EMT states”. In: *Cancer Cell* 39.8 (2021), 1150–1162.e9. DOI: 10.1016/J.CCELL.2021.05.005.

[626] Valentin Gensbittel et al. “Mechanical Adaptability of Tumor Cells in Metastasis”. In: *Developmental Cell* 56.2 (2021), pp. 164–179. DOI: 10.1016/j.devcel.2020.10.011.

[627] S. G. Gilbert et al. “CASTLE: Cell adhesion with supervised training and learning environment”. In: *Journal of Physics D: Applied Physics* 53.42 (2020), p. 16. DOI: 10.1088/1361-6463/ab9e35.

[628] Robert Prevedel et al. “Brillouin microscopy: an emerging tool for mechanobiology”. In: *Nature Methods* 16.10 (2019), pp. 969–977. DOI: 10.1038/s41592-019-0543-3.

[629] Adai Colom et al. “A fluorescent membrane tension probe”. In: *Nature Chemistry* 10.11 (2018), pp. 1118–1125. DOI: 10.1038/s41557-018-0127-3.

[630] Jing Bai et al. “A novel 3D vascular assay for evaluating angiogenesis across porous membranes”. In: *Biomaterials* 268 (2021), p. 120592. DOI: 10.1016/j.biomaterials.2020.120592.

[631] Adrian A. Shimpi and Claudia Fischbach. “Engineered ECM models: Opportunities to advance understanding of tumor heterogeneity”. In: *Current Opinion in Cell Biology* 72 (2021), pp. 1–9. DOI: 10.1016/j.ceb.2021.04.001.

Main contributions

Articles in peer-review journals

Published work:

- **Francisco Merino-Casallo**, Maria Jose Gomez-Benito, Yago Juste-Lanas, Ruben Martinez-Cantin, and Jose Manuel Garcia-Aznar. *Integration of in vitro and in silico models using Bayesian optimization with an application to stochastic modeling of mesenchymal 3D cell migration* Frontiers in Physiology, Vol. 9, 1246, September (2018).

Accepted work for publication:

- **Francisco Merino-Casallo**, Maria Jose Gomez-Benito, Silvia Hervas-Raluy, and Jose Manuel Garcia-Aznar. *Unravelling cell migration: defining movement from the cell surface* Cell Adhesion & Migration (2022).

Submitted work under review:

- **Francisco Merino-Casallo**, Maria Jose Gomez-Benito, Ruben Martinez-Cantin, and Jose Manuel Garcia-Aznar. *A mechanistic protrusive-based model for 3D cell migration: an integrative approach* European Journal of Cell Biology.

Communications in conferences

The work presented in this PhD thesis has been presented in the following international conferences:

- Oral presentations:
  - *Stochastic modeling of mesenchymal 3D cell migration guided by chemotaxis.* VII International Conference on Computational Bioengineering. ICCB 2017 Compiègne

- *Calibrating a stochastic model of cell migration using image-based in vitro analysis and Bayesian optimization* Virtual Physiological Human. VPH 2018 Zaragoza
- *In silico models of cancer cell metastasis: from local invasion to extravasation* Cancer Modeling Meeting 2018 Santiago de Compostela *
- *Mechanobiology of cell migration: mathematical modeling and microfluidics-based experiments go hand-in-hand* Computational Biology Seminars 2019 Oxford *
- *Cell migration in complex environments: combination of microfluidic-based experiments and numerical models* Spanish Network of Mechanobiology Symposium 2019 Madrid *
- *Tuning micro-environment to understand tumor metastasis: combination of microfluidic-based experiments and numerical models* Invited Talk for the Biomechanics Department 2019 Leuven *
- *Integration of mathematical models & cell culture experiments to unravel cell migration mechanobiology* Applied Mathematics Seminar Series 2019 Birmingham *
- *Computational models of 3D cell migration* Applied Mathematics Seminar Series 2019 Birmingham
- *Mechanobiology of tumor metastasis: integration of modeling, simulation and microfluidic-based experiments* CMTM Kickoff Symposium 2020 Boston *

- Poster presentations:
  - *Three-dimensional cell migration: an integrative approach.* Virtual Physiological Human. VPH 2020 Paris

---

* José Manuel García Aznar presented the work in these sessions.

Collaborations

The PhD candidate initiated a long-term collaboration with Ruben Martinez-Cantin during the initial stage of his doctoral studies. The first results of this collaboration are already tangible with a couple of joint publications. that present an integrative methodology to combine experimental data with theoretical studies based on Bayesian optimization. The suitability for such methodology in this endeavor has been clearly demonstrated. Moreover, future works expanding this methodology with novel features are already in the pipeline.

The PhD candidate also collaborated with Fabian Spill during his research stay at the School of Mathematics of the University of Birmingham (United Kingdom). We did an in-depth study of how biophysical cues from the surrounding matrix influence cell migration. This work was considered the seed of a literature review about cell migration that is currently under review. We also defined an extended signaling pathway to include biophysical cues as additional initiators triggering signaling cascades. Despite this work not being included in this PhD thesis, it is considered the basis for future works that would expand our current *in silico* model of 3D cell migration. As a result, other biophysical factors, such as the alignment of ECM fibers would also regulate cell migratory behavior.